USE OF SOFT COMPUTING PATTERN RECOGNITION TECHNIQUES TO ANALYSE TROPICAL CYCLONES FROM METEOROLOGICAL SATELLITE DATA

By

FAKHAR KHALID [BSc. (Hons), MSc]

A thesis submitted in partial fulfilment of the requirement of the University of Greenwich for the Degree of Doctor of Philosophy

August 2013

School of Science
University of Greenwich, Medway Campus
Chatham Maritime
Kent ME4 4TB, UK

UNIVERSITY
of
GREENWICH

DECLARATION

"I certify that this work has not been accepted in substance for any degree, and is not concurrently being submitted for any degree other than that of Doctor of Philosophy being studied at the University of Greenwich. I also declare that this work is the result of my own investigations except where otherwise identified by references and that I have not plagiarised the work of others".

Fakhar Khalid (Candidate)

....

<u>PhD Supervisors</u>

Professor Martin Snowden
(University of Greenwich)

Dr. Clare Power
(Bath Spa University)

ACKNOWLEDGMENTS

There are many that I would like to acknowledge who have helped me throughout the long period. Firstly I would like to acknowledge my parents who with their selfless beings supported me right the way through my education. Secondly, I would like to thank my supervisor Dr Clare Power, without her advice and exemplary knowledge of the subject, I would not have been able to survive the world of meteorology. I have achieved a respectable academic position which wouldn't have been possible without her mentoring. My very close friends and colleagues, Dr Mike McGibbon, Dr Richie Simon and Dr Tim Acott has always kept me on track to finish and pushed me whenever it was utterly needed; especial thanks to Mike and Richie for proof reading the thesis, their abilities to put thought onto paper are second to none.

A special thanks to Dr Esam Shehab, whose temporary supervision of the project helped algorithm development and two conference presentations.

I would like to acknowledge, School of Science at University of Greenwich for their continuing support, even though when at times things were hard. Also, without Professor Babur Chowdhry’s persuasive language this thesis will not have made it to print.

I would like to show my sincere gratefulness to the NOAA’s National Climatic Data Center and National Hurricane Center for providing HURSAT, IBTrACS and HURDAT databases.

Last but not least I would like to thank my family, my lovely wife and my angelic daughter, for putting up with my extremely busy schedule. As a wise man once said that there is a woman behind every successful man! I just happened to have two.

This research is dedicated to my parents, Shahida and Khalid. Their personal sacrifices towards my education will never be forgotten. May Allah rest their soul in peace.

"***The wind blew a perfect hurricane; ..., one after another, until nothing remained.***"

(from a testimony of a hurricane survivor on Last Island Louisiana in 1856)

ABSTRACT

Tropical cyclones are potentially the most destructive of all natural meteorological hazards. When these cloud systems make landfall, they cause significant amounts of human death and injury as well as extensive damage to property, therefore reliable cyclone detection and classification form important weather forecasting activities.

The work carried out in this research has focused on developing a unique fuzzy logic based patter recognition algorithm for identifying key recognisable structural elements of North Atlantic basin hurricanes. Due to vaguely defined boundaries and cloud patterns associated to cyclones and hurricanes, existing hurricane detection and classification techniques such as Advanced Dvorak's T-classification technique and Objective Dvorak's techniques fail to deal with the pattern uncertainties. Therefore, a fuzzy logic pattern recognition model was developed and implemented to overcome the shortcomings of manual and subjective algorithms for tropical cyclone detection and intensity classification.

Three key storm patterns are recognised during the cyclogenesis of any hurricane: Central Dense Overcast (CDO); the eye of the storm; and the spiral rain bands. A cognitive linguistic grammar based approach was used to semantically arrange the key structural components of hurricanes. A fuzzy rule based model was developed to recognise these features in satellite imagery in order to analyse the geometrical uncertain shapes of clouds associated with tropical storms and classify the detected storms' intensity. The algorithms were trained using NOAA AVHRR, GOES, and Meteosat satellite data at spatial resolution of ~4km and ~8km. The training data resulted in fuzzy membership function which allowed the vagueness of cloud patterns to be classified objectively. The algorithms were validated by detecting and classifying the storm cloud patterns in both visible and infrared satellite imagery to confirm the existence of the storm features. Gradual growth of hurricanes was monitored and mapped based on 3 hourly satellite image dataset of ~8km spatial resolution, which provided a complete temporal profile of the region. 375 North Atlantic storms were processed comprising of a period of 31 years with over 112,000 satellite images of cloud patterns to validate the accuracies of detection and intensity classification of tropical cyclones and hurricanes.

The evidence from this research suggests that the fusion of fuzzy logic with traditional pattern recognition techniques and introduction of fuzzy rules to T-classification provides a

promising technique for automated detection of tropical cyclones. The system developed displayed detection accuracy of 81.23%, while the intensity classification accuracy was measured at 78.05% with an RMSE of 0.028 T number. The 78.05% intensity classification accuracy was based on storm being recognised from a preliminary stage of tropical storms. The accuracy of hurricane or tropical cyclone intensity estimation from T1 onwards was recorded as 97.12%. While the storms were recognised, their central locations were also estimated because of their importance in tracking the hurricane. Validation process resulted in an RMSE of 0.466 degrees in longitude and RMSE of 0.715 degrees in latitude. The high RMSE which averages 38.4 km suggests that the estimated centre of the storms were around 38.4 km away from the actual centre measured by NOAA. This was an anomalous figure caused by 9 wrongly georeferenced images. Correcting this error resulted in an RMSE of 0.339 degrees in longitude and RMSE of 0.282 degrees in latitude, approximating an average shift of 19km. In 1990s these forecasting errors hovered around 100km area, while according to NOAA the current research averages the track accuracies around 50km, making this research a valuable contribution to the research domain.

This research has demonstrated that subjective and manual hurricane recognition techniques can be successfully automated using soft computing based pattern recognition algorithms in order to process a diverse range of meteorological satellite imagery. This can be essential in the understanding of the detection of cloud patterns occurring in natural disasters such as tropical cyclones, assisting their accurate prediction.

CONTENTS

LIST OF FIGURES

LIST OF TABLES

LIST OF ABBREVIATIONS

Abbreviations	Meaning
AFGWC	Air Force Global Weather Central
AVHRR	Advanced Very High Resolution Radiometer
BF	Banding Feature
CDO	Central Dense Overcast
CF	Central Feature
CI	Current Intensity
DAFF	Department of Agriculture, Fisheries and Forestry
EMR	Electro Magnetic Radiation
ESRI	Environmental Systems Research Institute
FY2	Feng Yun 2
GIS	Geographical Information System
GMS	Geostationary Meteorological Satellite
GOES	Geostationary Operational Environmental Satellites
GUI	Graphical User Interface
HHI	Harvard Humanitarian Initiative
HURDAT	Hurricane Database
HURSAT	Hurricane Satellite Image Database
HRIR	High Resolution InfraRed
IBTraCS	International Best Track Archive for Climate Stewardship
IC	Intensity Classifier
IDAPS	Image Data Processing System
IMD	Indian Meteorological Department

Abbreviations	**Meaning**
IR	InfraRed
MTSAT	Multifunctional Transport Satellites
NASA	National Aeronautics and Space Administration
NCDC	National Climatic Data Center
NERC	Natural Environment Research Council
NHC	National Hurricane Center
NOAA	National Oceanic and Atmospheric Administration
NWP	Numerical Weather Prediction
PRM	Pattern Recognition Module
RADAR	Radio Detection And Ranging
RS	Remote Sensing
SSM/I	Special Sensor Microwave/Imager
TIROS	Total Internal Reflection Optical System
TIR	Thermal InfraRed
VIS	Visible
WMO	World Meteorological Organisation
μ (mu)	Fuzzy Membership Function

CONFERENCE PRESENTATIONS/PUBLICATIONS

CONFERENCES

Title:	Designing a fuzzy logic pattern recognition system for tropical cyclones.
Date:	September 2003
Type:	Abstract/Poster/Oral
Co-Authors:	Clare Power, Esam Shehab
Details:	Annual conference of Remote Sensing and Photogrammetry Society Nottingham, UK

Title:	Evaluation of a fuzzy pattern recognition algorithm for tropical cyclone monitoring and assessment.
Date:	September 2005
Type:	Abstract/Oral Presentation
Co-Author:	Clare Power, Esam Shehab
Details:	Annual conference of the Remote Sensing and Photogrammetry Society with NERC Earth Observation Conference. Portsmouth, UK

PUBLICATIONS

Publication Type:	Journal Manuscript
Title:	An automated fuzzy pattern recognition system to detect cyclones using meteorological satellite imagery.
Year:	2013
Journal:	To be submitted to: International Journal of Remote Sensing.

Publication Type:	Journal Manuscript
Title:	Modelling hurricane wind damage impact using friction surface analysis.
Year:	2013
Journal:	To be submitted to: Geomatics, Natural Hazards and Risk

CHAPTER 1. INTRODUCTION

1.1 General Introduction

Weather has always affected life on Earth. The evolution of human behaviour and lifestyles have been strongly influenced by weather regimes in different parts of the world, Records indicate that weather events are the biggest contributor to natural disasters, claiming millions of lives every year (NOAA, 2008a; Kousky, 2012). The Mesopotamian civilisation is among the oldest in the world and was characterised by domesticated agriculture and settlement in groups. Residing in settlements rendered the population more vulnerable to natural disasters by increasing densities. The early urban societies in the region between the Tigris and Euphrates rivers are believed to be among the first in the world regularly swept away by violent weather related events such as floods caused by storms (National History Museum, 2011). Despite the technological sophistication of contemporary society, weather continues to play an important part in creating stable or destructive living environments (Gibilisco, 1984; Upgren and Stock, 2000; Anderson, 2011). Every year various seemingly unstoppable meteorological events cause nations financial, environmental and human losses. It is therefore important to be capable of anticipating accurately the location and timing of potentially disastrous weather events in order to minimise destruction and loss of life. The weather phenomenon that forms the focus of this research project is the tropical cyclone, characterised in the following section.

1.2 Tropical Cyclones or Hurricanes

Tropical cyclones are well known to be among the most destructive of atmospheric phenomena and are the most frequent cause of natural disasters. (Pielke and Pielke, 1997; Eugene, 2012). The floods on the Yangtze River in 1931 killed nearly 3.5 million people (NOAA, 2008b). These floods were credited to 7 cyclones that affected China in July of that year (Pietz, 2002). Tropical storms normally bring high winds and intense rain, which cause extreme damage. Ludlum (1963), pp 166-167) reports the testimony of a hurricane survivor on Last Island Louisiana in 1856, illustrating the ferocity of such storms:

"The wind blew a perfect hurricane; every house on the island giving way, one after another, until nothing remained. Every one sought the most elevated point on the island. Many persons were wounded; some mortally. The water commenced rising so rapidly from the bay side, that there could no longer be any doubt that the island would be submerged. The scene at this moment forbids description. The violence of the wind, together with the rain, which fell like hail and the sand, blinded the eyes. Many were drowned from being stunned by scattered fragments of the buildings, which had been blown asunder by the storm".

On average 46.9 hurricanes occur globally every year. Regionally most are recorded in the NW Pacific which averages 16.9 storms. In the Atlantic and Indian Oceans an average of 6.4 and 10.1 storms respectively are recorded each year. Globally, 21 storms every year, on average, are classified as intense and are certain to cause severe damage to property and human life (Landsea and Goldenberg, 2011). One of the deadliest tropical cyclones, recorded on 13th November 1970, made landfall in the densely populated region of East Pakistan, now Bangladesh, killing around 300,000 people (Landsea and Goldenberg, 2011). Less developed countries like Bangladesh have been prone to greater loss of life when a cyclone makes landfall. This is generally due to higher population density and lack of preparedness for the storm. The effect of high population and development density are illustrated by the case of hurricane Katrina which caused nearly twice the damage of hurricane Andrew in 1992, despite the latter being twice as strong when it made landfall (NHC, 2012; Landsea and Goldenberg, 2011). In addition to direct effects from the cyclones, these storms are also associated with high winds, storm surges, flash floods, landslides due to extreme rainfall and spread of disease in the aftermath (World Meteorological Organisation, 1983). Given the range of destructive impacts, early storm detection and observation play vital roles in disaster management programmes to avoid loss of life and property (Reilly, 2009).

Hurricane is the most destructive and structurally strong stage of a cyclone. The terms hurricane, typhoon and tropical cyclone are interchangeably used, depending on their geographical origin. In the North Atlantic Ocean, the Northeast Pacific Ocean and the South Pacific Ocean the strong cyclonic storm are referred to as 'hurricanes', while 'typhoons' originate in the Northwest Pacific Ocean. Similarly, the high intensity cyclonic storms originating in the Indian Ocean are termed as 'tropical cyclones' (Landsea and Goldenberg, 2011; Neumann et al., 1993). Nonetheless, the term tropical cyclone can be used to generically identify all rotating storm systems with a low pressure centre, originating in the tropics.

1.3 Cyclone Detection and Prediction

Accurate prediction, detection and warning of the formation of tropical cyclones have been subjects of much research (Raju et al., 2011a; Johnson and Watson, 2011; NHC, 2011; Goni et al., 2009; Liu et al., 2009; Olander and Velden, 2007; Camargo and Zebiak, 2002; Goerss, 2000; Neumann, 1972). Due to the complicated and unpredictable nature of this phenomenon, forecasters face unique problems compared to more traditional weather forecasting (NHC, 2009). Cyclones can be influenced by the external steering currents of the wind as well as by their own internal large-scale circulation. This dynamic environment makes it difficult for the forecasters to predict the movement and intensity of the storm.

The earliest methods for forecasting cyclones were based on observations of cloud movements and sea swells. Vines (1898), a Jesuit priest in Havana, Cuba, studied hurricanes during late 1800s. He developed a hurricane warning system which consisted of a pony express between isolated villages and a group of observers around the coastline. He made his predictions based on cirrus cloud movements and sea swells. Conventional methods of using buoys and ships to record the existence of cyclones are still in use in various countries (IMD, 2005). These dated methods rely on a ship or a buoy encountering a storm, otherwise the cyclone stays undetected. With the advent of new technology, developing countries have started to use better and more accurate methods of storm detection and tracking to improve predictability (Raju et al., 2011b; Liu et al., 2009; Bongirwar et al., 2011; Rath and Pradhan, 2011; Raju et al., 2011a; Prasad, 2006). Track prediction is an important part of monitoring and numeric prediction and modelling of the detected storms (Pattanaik and Rama Rao, 2009; Murthy et al., 2008; Leslie et al., 1998). The National Oceanic and Atmospheric Administration (NOAA) in the US and the Meteorological Office in UK have various Numerical Weather Prediction (NWP) models predicting a range of weather conditions including dedicated sections to monitor and predict storms (World Meteorological Organisation, 1983; World Meteorological Organisation, 1976; Skidmore, 2002; Elsner et al., 1998; Johnson and Watson, 2011). Vidal et al. (2010) describe the international collaborative work of the UK Meteorological Office Hadley Centre and Japan Agency for Marine-Earth Science and Technology, which discusses a class of global climate models working at ground breaking spatial and temporal resolutions. High spatial resolution and temporal frequency of data are processed using supercomputers by hypervariate modelling techniques, emphasising the importance of development of cyclone prediction models and cross border knowledge exchange.

1.4 Satellite Imagery and its Importance in Cyclone Detection

During meteorological storms, conventional communications can be disrupted, rendering surface based weather observation equipment ineffective. Efficacious monitoring has become possible over the past 30 years with the use of satellites to monitor meteorological events (Ohring, 1973; Elsner et al., 1998). Satellites give a broader and superior overview compared to previous observation systems. Moreover, the satellites can provide data from the remotest part of the ocean where storms can otherwise develop without detection by surface based weather stations.

Satellites gather data using electromagnetic radiation (EMR) responses from the target objects. These data can provide information beyond general human observation capabilities by working within a wider range of captured EMR. Use of space-borne satellite sensors are crucial for weather prediction. However, conventional meteorological and geophysical data are essential for validating the satellite observations (Carleton, 1991; Bongirwar et al., 2011; Lewis et al., 2010). Satellite climatology has rapidly developed within the last two decades and dedicated weather satellites have become a key source of atmospheric information (Zhang et al., 2006; Chuai-Aree et al., 2008; Wylie and Menzel, 1989; Spencer and Christry, 1990; Woodbury and McCormick, 1986).

Operational weather satellites assist in meteorological analysis such as high-frequency surveillance of cloud patterns, temperature and moisture profiles, precipitation estimation and weather forecasting (Carleton, 1991). The use of satellite images in tropical cyclone monitoring has been so successful that no tropical storm or hurricane of significant size has gone undetected since the first operational polar-orbiting weather satellite system was inaugurated in 1966 (Barrett and Curtis, 1999; Potter et al., 2005). However, satellite images have always been used in conjunction with various other meteorological datasets, captured either by physical sensors on the sea surface or via aerial reconnaissance (Sanford et al., 2007), to validate their forecasts.

Within the domain of storm prediction and understanding its effects, satellites are mostly used for monitoring tropical storm tracks, to assess storm intensity, to estimate maximum wind speed, to identify area of influence and to calculate the estimated rainfall (Potter et al., 2005; Thies et al., 2010; Kuciauskas et al., 1998). Although satellites aid the detection and monitoring of tropical storms, an expert input is always required to identify these cyclones, classify their intensity and suggest their movement (NHC, 2011). With increasing use of artificial intelligence, ample resources have been dedicated to devise automated and machine intelligent algorithms to predict and detect these weather phenomena (Kuciauskas et al., 1998; Yip and Wong, 2004; Rodionov and Martin, 1996; Johnson and Watson, 2011; Wehner et al., 2010; Forbes and Rhome, 2012; Ho and Talukder, 2008).

Since the launch of early meteorological satellites, researchers have been developing methods to detect hurricanes and cyclones solely from satellite images (Conover, 1962; Blankenship, 1962; Dvorak, 1975; Dvorak, 1984; Zehr, 1989; Olander and Velden, 2007). However, the vague and uncertain geometric cloud patterns in cyclogenesis have always caused accuracy issues, bringing in experts' subjectivity in storm identification. Dvorak (1975) developed a technique that exclusively required satellite images to identify hurricanes and classify their intensity. However, the manual technique required expert knowledge to distinguish between key cloud patterns. Dvorak's T classification technique was updated in mid 1980s (Dvorak, 1984) add pattern identification methods and rules to ascertain hurricane intensity. It was only later (Olander et al. (2002); Olander and Velden (2007); Velden et al., 1998a) that an element of objectivity to Dvorak's successful but highly subjective approach was introduced. Although objective, Velden et al. (1998a) required analyst evaluation of infrared imagery to identify various hurricane features and Olander and Velden (2007) cited a continuously developing automated algorithm to classify hurricane intensity. However in 2011 they suggested that detection of a storm centre in the absence of a storm eye requires further research.

1.5 Aim

The main aim of this research is to develop an algorithm for fully automated detection and classification of tropical cyclones from satellite imagery using soft computing techniques.

1.6 Objectives

Achievement of the research aim depends, in turn, on consideration of four specific research objectives:

1. To investigate and identify the principal detectable features of tropical cyclones and hurricanes from satellite images. (Chapter 2 & 4)
2. To devise pattern recognition algorithms for the detection of vital features of tropical cyclones and hurricanes, taking into consideration their vague and imprecise shapes. (Chapter 3 & 4)
3. To develop an algorithm that can automatically detect tropical cyclones from satellite imagery and classify their intensity. (Chapter 3, 4, & 5)
4. To validate the developed system with existing meteorological records. (Chapter 6)
5. To investigate the efficiency and efficacy of soft computing algorithms for the purpose of storm detection systems. (Chapter 7)

1.7 Conceptual Framework of the Research

The key research themes in the research are unpinned by three topics (Figure 1): understanding of storm dynamics; soft computing algorithms for pattern recognition and intensity classification; and validation of the results against a database of observed hurricanes. To develop an algorithm for automated detection of storms, it is essential to understand and comprehend the dynamics of the storms, including their physical structure and meteorological characteristics. Identification of the vital components of any storm is essential before application of pattern recognition and classification algorithms. Review and evaluation of a range of algorithms is then required to assist in the development of a new algorithm with higher accuracy and reliability.

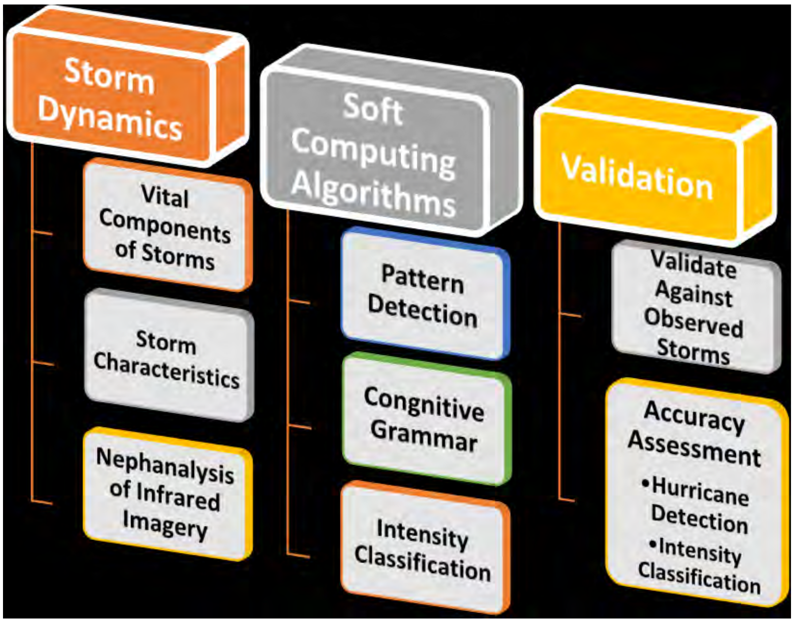

Figure 1.1 The conceptual research framework

1.8 Study Area

Due to the investigative nature of the research two main study areas were chosen to ensure examination of a wide range of cyclonic cloud patterns. The Atlantic basin and Indian Ocean regions were chosen to form the basis of cognition training and validation. The choice of these regions ensured comparative analyses with previous studies and access to available data.

Figure 1.2: Map showing North and South Atlantic Ocean.

1.9 Structure of the Thesis

The central focus of this research is aimed at evaluating the capability of intelligent computer algorithms to detect and classify tropical cyclones and hurricanes accurately using satellite data with minimal human expert knowledge using fuzzy logic (Zadeh, 1993; Zadeh, 1965).

The aim of this thesis is to answer the following research questions:

- What is the feasibility of using fuzzy logic to recognise hurricanes in the North Atlantic basin?
- How accurately can fuzzy membership functions classify hurricane intensity?
- Is it possible to detect and classify hurricanes solely from satellite imagery?

To address the research focus, the thesis is organised into eight chapters. Following the introduction, chapter two provides a review of recent literature relevant to cloud dynamics, behaviour of cyclonic cloud patterns, mechanisms of cyclones and the factors that influence these phenomena. Chapter two also examines methods currently used in the detection of storms, as well as the general principles of storm dynamics and intelligent algorithms used in their prediction. Chapter three describes and discusses the structure of the developed system including various processing stages. This chapter also provides justification of the methods used in this research. Chapters four, five and six discuss the results of the research and are presented as three major parts of the developed software prototype. Chapter seven discusses the evaluation methods used to validate the results, while chapter eight presents conclusions on the accuracy of results, critical evaluation of the efficiency of the developed system and reflective discussion of potential future research.

Even though the validation region selected is the North Atlantic Basin, the methods discussed in this thesis can be applied to any cyclones developing in the northern hemisphere. The algorithms will need to be modified to detect a reverse spiral because of the clockwise rotation of the cyclone in the southern hemisphere. For the ease of reference, hurricane, cyclones and typhoons will be referred to as tropical cyclones

CHAPTER 2. LITERATURE REVIEW

2.1 Introduction

This chapter reviews the current and previous work carried out in the field of tropical cyclone monitoring and intensity classification, image based automated pattern recognition and fuzzy logic systems to tackle the uncertainty in ambiguous cloud structures.

From section 2.2 to section 2.8, tropical cyclones are discussed in general initially while the later sections discuss the anatomy of tropical cyclones. Anatomy of the tropical storms plays an important role in the algorithm development for pattern recognition. These sections will define and discuss various natures of tropical cyclones and how they are currently monitored and forecasted. Section 2.8 specifically analyses the literature available in the field of monitoring tropical cyclones with the help of satellite remote sensing. Section 2.9 outlines the various approaches available for forecasting tropical cyclones with the help of satellite imagery. This section also discusses available computer models for forecasting cyclone tracks and estimating cyclone intensity.

Section 2.13 explores and overview of various techniques and models available for image based pattern recognition. While section 2.15 and 2.16 review the soft computing approaches towards detection and intensity estimation of tropical cyclones. These sections particularly focus on rule based fuzzy models for storm cloud pattern recognition. Finally a summary of literature is provided highlighting the gaps that will be dealt with in this research.

2.2 Hurricanes and Cyclones

Tropical cyclones are amongst the most powerful and destructive meteorological phenomena on Earth. Every year, hundreds of cyclones develop over tropical oceans many of which make landfall to cause extensive damage to property and life. These tropical cyclones bring high winds, heavy rain and storm surges with them, which are the main cause of damage (MetOffice, 2011).

2.2.1 Origin of the words Hurricane and Cyclone

Hurricanes are known to be the strongest forms of tropical cyclones. According to Emanuel (2005) the term "hurricane" comes from the Spanish word *huracan,* which in turn is thought to have originated from words in use amongst some of the Caribbean tribes. In the Mayan dialect "Hunraken" is the storm god. In Taino, an extinct tribe of the Greater Antilles and the Bahamas and especially Haiti, the word for hurricane was also *huracan,* meaning evil spirit. The Galibi Indians of Dutch and French Guiana used the word *hyoracan,* or devil, and the Quiche of southern Guatemala spoke of "Hurakan" the thunder and lightning god. Other Carib Indian words for hurricane were *iaracan*, *urican*, and *huiranvucan*, which have been translated as "Big Wind," and similar terms. Dunn and Miller (1964) described it as the "meteorological monster of the sea".

While the word hurricane has its Spanish origins, the word cyclone refers to a Greek word 'kyklon' meaning coil of the snake (Forrester, 1982), with the word 'typhoon' originating from ancient Arabic word 'toofan' (Hirth, 1880).

2.2.2 Naming the Storms

Several hundred years ago hurricanes in the Spanish islands of the Caribbean were named after the particular saint's day on which the hurricane occurred. Earlier in this century the forecasters in Australia named hurricanes after political figures (Dunn and Miller, 1964). One technique of naming tropical storms and hurricanes started in 1950 with the simple phonetic alphabets used by military services such as Alpha, Bravo, Charlie, Delta etc. In 1953 meteorologists started naming storms after alphabetically ordered female names. The first written mention of female hurricanes or storms may have been in the novel *Storm*, by George R. Stewart, Random House 1941 (Dunn and Miller, 1964). This female-naming approach was abolished in 1979 with the introduction of alternating male and female names in a season. More recently the names selected for Atlantic and Caribbean storms have included French and Spanish, reflecting all the languages spoken in the region (Reynolds and Ogley, 1989).

2.3 Geography of Tropical Cyclones

Tropical cyclones all over the world form near the tropical regions of the world and almost all of them form following similar meteorological processes in the known seasons of the year. The frequent areas of hurricane and tropical cyclone occurrence are shown in figure 2.1.

Hurricanes originate only in the tropical trade winds where the ocean temperatures are quite warm. The tropical trade winds are affected by large high pressure areas that are present most of the time over the oceans at about 30^{o} latitude. In the Northern Hemisphere these are called the Hawaiian and Bermuda highs (Eagleman, 1990). The winds blowing around the high pressure travel anticyclonically in the Northern Hemisphere and create persistent Northeast winds on the southern side of the high-pressure areas that are known as the trade winds. It is within these trade winds where a cloud mass may be transformed into one of the most devastating storms on earth.

Hurricanes typically originate over the South of North Atlantic Ocean, including the Gulf of Mexico and the Caribbean Sea. The common hurricane seasons last from June through to October. However infrequently they can develop in May and November and very rarely during other months of the year (Dunn and Miller, 1964), while typhoons form in the Northwest Pacific Ocean west of the dateline. According to records from 1951 to 2009 the average typhoon season starts in March-April and ends in May-June (Zhao et al., 2011). In the Indian Ocean a typical cyclone season will start in December and last until March, with 4 to 5 storms forming every year on average. In the Arabian sea, cyclones normally occur in May and June (NGIA, 2012).

Due to the confusing nature of the naming of these storms, this thesis will refer to all storms generically as ‘tropical cyclones’, specifically referring to their geographical titles, i.e. hurricane, cyclones and typhoons, when required.

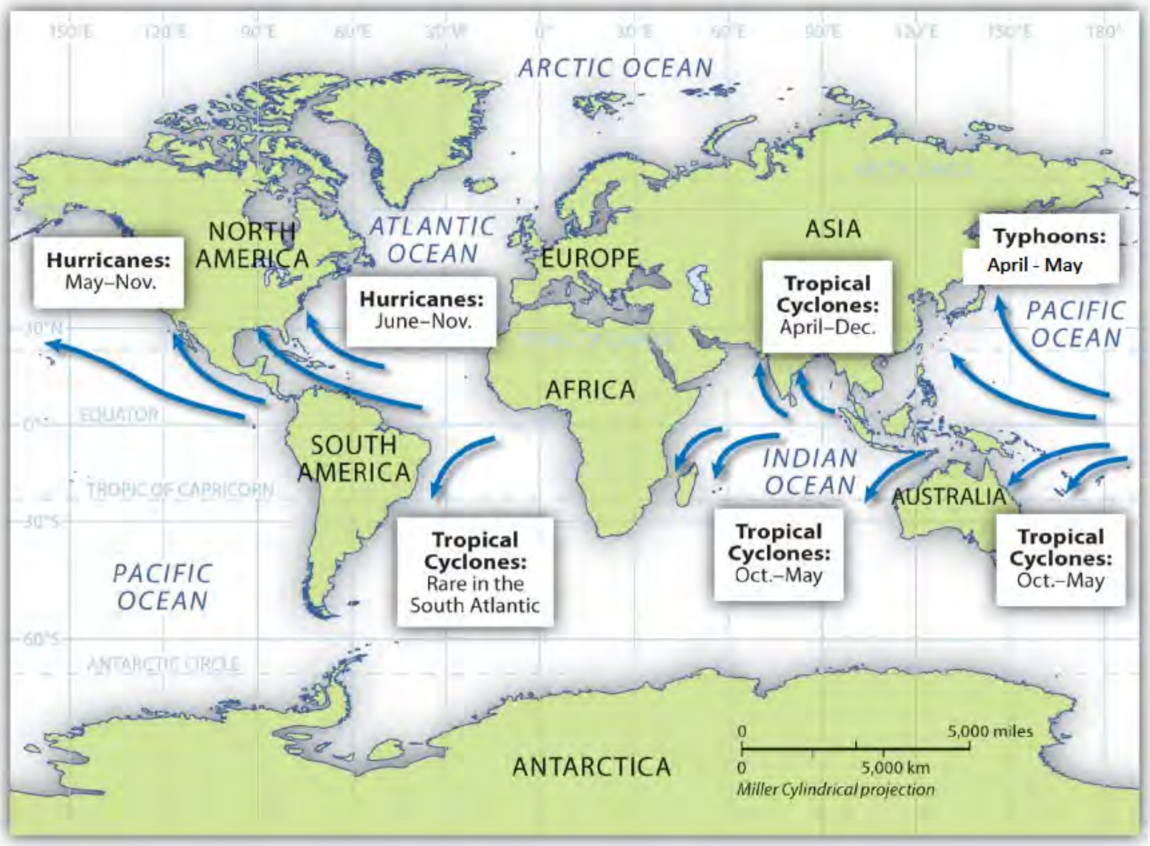

Figure 2.1: Hurricanes, typhoons, and tropical cyclones form around the warm tropics (Berglee, 2012).

Tropical cyclones are more devastating during summer seasons, while most of the winter season tropical cyclones develop in the southern part of the North Atlantic, but almost none of these ever reach hurricane intensity. One such storm passed near Puerto Rico during January 1951, and another developed in the western Gulf of Mexico and crossed Florida, near Miami, on February 2, 1952 (Dunn and Miller, 1964; Norton, 1952; Moore and Davis, 1951).

More tropical cyclones originate in the Southwest portion of the North Pacific Ocean, than anywhere else in the world - on average more than twenty tropical cyclones per year. In contrast, off the West Coast of Central America or Mexico on average six tropical cyclones per year develop, but fewer than half of this number reach hurricane intensity (Dunn and Miller, 1964; Knapp et al., 2010; Evan and Camargo, 2011; Weinkle et al., 2012).

2.4 Cyclogenesis

To be able to identify and warn of the threat caused by tropical cyclones, it is necessary to appreciate the structure of cyclones. According to an older definition by Dunn (1964) a weather system that covers an approximately circular or elliptical area of at least 50 miles and has a circulation can be classified as a cyclone. Thus, a cyclone can be any system of rotating winds, except a tornado, which is rarely greater than one mile wide, or a whirlwind, which is hardly ever more than a few yards in diameter. Over recent years the definition and classification of cyclonic storms has been tightened and a cyclone is now defined as a storm with a warm-centred non-frontal low-pressure system, which originates over specific areas of tropical and sometimes subtropical waters, and has an organised circulation and associated wind patterns (BoM, 2008). The organised circulation in a cyclone is caused by atmospheric pressure changes and the Earth's coriolis force, which is counter clockwise in the northern hemisphere and clockwise in the southern hemisphere due to the Earth's rotation.

Elsberry (1985) defines the term 'tropical cyclone' as being comprised of three kinds of tropical synoptic weather system. Firstly, a tropical depression with a weak tropical weather system characterised by wind speeds of no more than 34 knots; secondly, a tropical storm with wind speeds higher than the speeds of a depression but no higher than 63 knots; and, third, a hurricane or a tropical cyclone with sustained wind speeds of 64 knots and above. Figure 2.2 shows the process of cyclogenesis in the North Atlantic Ocean.

The geographic origin of a tropical cyclone determines whether it should be labelled as a hurricane, tropical cyclone or a typhoon. Tropical cyclones originating in the North Atlantic Ocean, the Northeast Pacific Ocean or the South Pacific Ocean are called 'hurricanes', while 'typhoons' originate in the Northwest Pacific Ocean west of the dateline. The name 'tropical cyclone' is associated with storms originating in the Indian Ocean, specifically around the Bay of Bengal and Australia (Landsea and Goldenberg, 2011; Musk, 1988; Neumann, 1993).

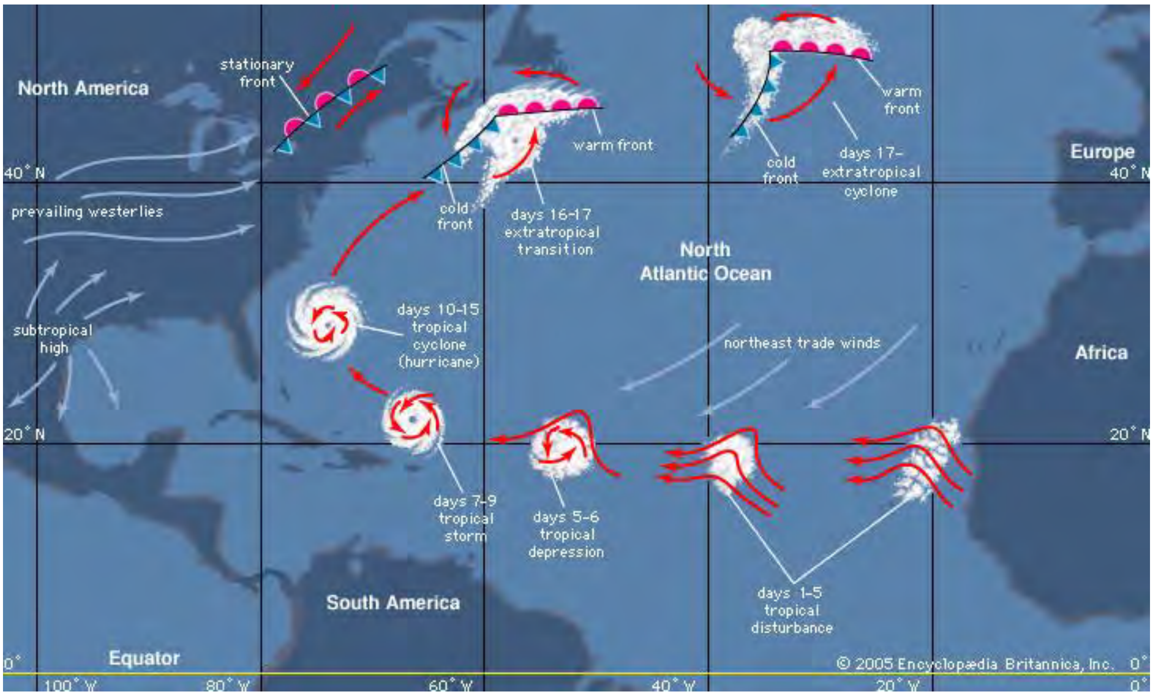

Figure 2.2: Cyclogenesis in the North Atlantic Ocean (Britannica, 2013)

Based on various structural and geographical variables, cyclones can also be categorised as tropical, extratropical or subtropical, depending upon characteristics of the surrounding air masses. It is important to differentiate between these three categories of storm because it is the tropical weather systems that normally have the potential to become a cyclone, while the extratropical and subtropical do not. The three categories are defined below.

2.4.1 Tropical Cyclone

A tropical cyclone is a non-frontal synoptic scale, low pressure system specifically developing over tropical or subtropical waters, in the presence of warm moist air and sea surface temperature of at least 26^{o}C. It can have a diameter in the range of 160 to 956 km and normally has a very warm central core. The wind speeds are normally strongest near the centre of the storm where the pressure gradients are highest. Within such a storm winds can exceed 241 km per hour (Anthes, 1982a).

2.4.2 Extratropical cyclones

A tropical cyclone that loses its tropical characteristics as it moves into non-tropical regions is called an extratropical cyclone. Extratropical storms normally have a cold core. The strongest winds are usually located 321 to 804 km from the centre of the storm. However, it is mainly dependant on the location of the strong pressure gradient and stability of the low pressure system. The formation of an extratropical cyclone depends on temperature contrasts in its surroundings (Neumann, 1993; Houze, 1993)

2.4.3 Subtropical Cyclone

A subtropical cyclone is defined as a non-frontal low-pressure system with a cold core. Wind speeds in a subtropical cyclone normally range from 48 to 115 km per hour. A subtropical storm primarily depends on warm water temperatures for its survival (Musk, 1988).

Apart from various geographical and structural categories tropical cyclones are also classified into stages according to their intensity and severity. Some systems use the stages of system development as well as the intensity factors for classifying cyclones, although it is mostly the wind speed that is used to determine the intensity of a cyclone. A standard intensity measurement unit is used to give an estimate of the potential property damage and flooding expected along the coast from a hurricane landfall. This scale is known as Saffir-Simpson Hurricane Scale. It is a 1-5 rating scale based on a hurricane's present intensity. Figure 2.3 describes the Saffir-Simpson scale. This scale will be discussed later in detail in this chapter.

2.5 Formation of Cyclones

All tropical cyclones originate over warm oceanic waters in regions of low level convergence of the wind. The surrounding atmosphere requires a rapid temperature decrease, which makes the air rapidly turbulent and saturated. The saturated air is buoyant compared to its surroundings and creates uplift in the region forming cumulus clouds, as shown in figure 2.4.

If the middle and upper troposphere are sufficiently moist, these cumulus clouds can rise to the top of the troposphere. These deep cumulus clouds, called cumulonimbus, are effective transporters of heat and moisture to the upper level of the atmosphere.

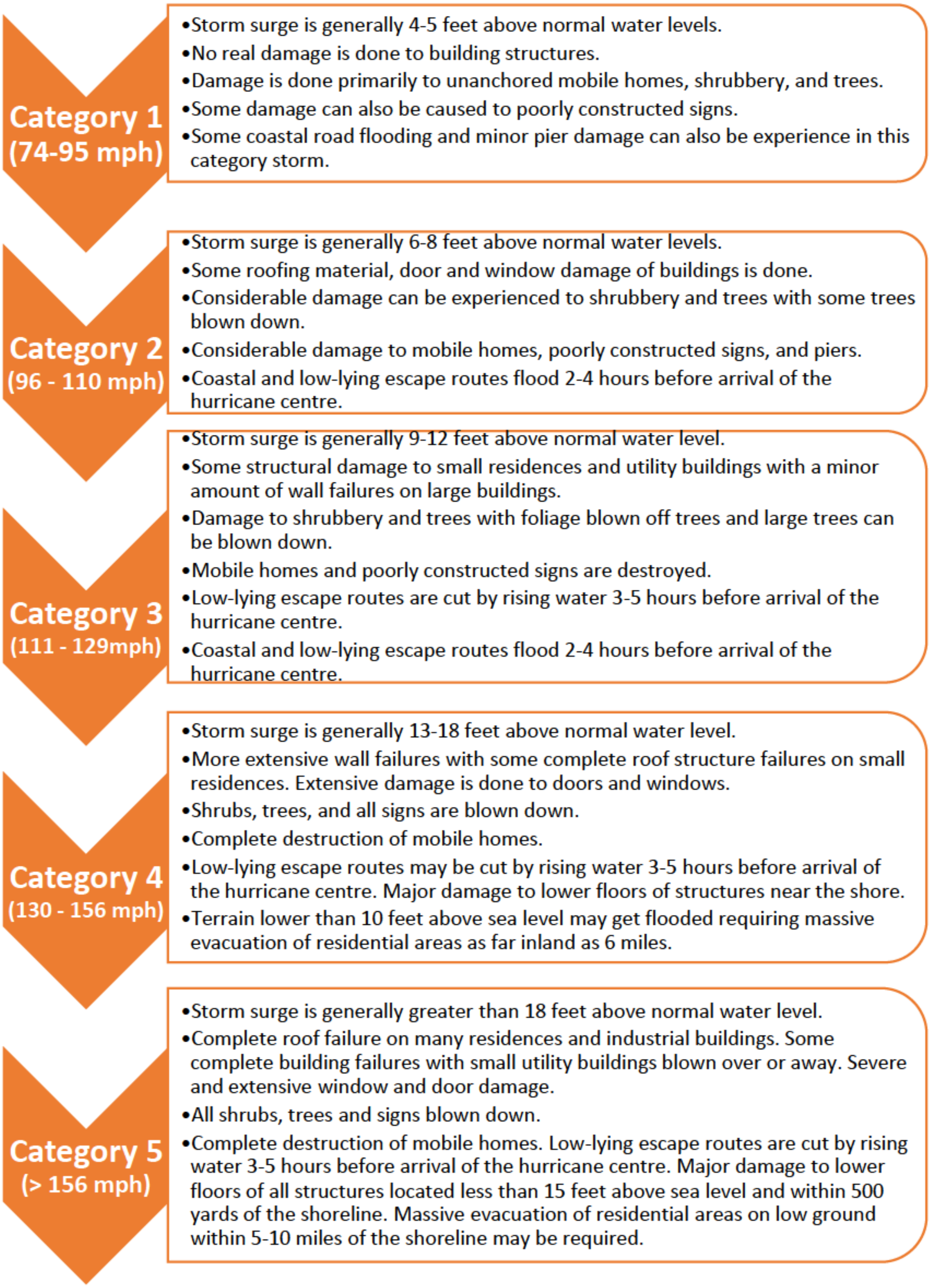

Figure 2.3: Saffir Simpson Hurricane Scale. Adapted from (Neumann et al., 1993; NOAA, 2012).

Due to the strong thermodynamic stability of the stratosphere the cumulus clouds that are transported upwards spread out horizontally, thereby lowering pressure near the surface. The fall in pressure near the surface results in a stronger low level convergence, hence forming a heat engine for additional cumulonimbus development. Pressure in the centre of the system continues to fall at the surface as long as the divergence at the upper atmosphere is greater than the convergence at low levels (Pielke, 1990; Merrill, 1985). This process is illustrated schematically in figure 2.4 and summarised in figure 2.5.

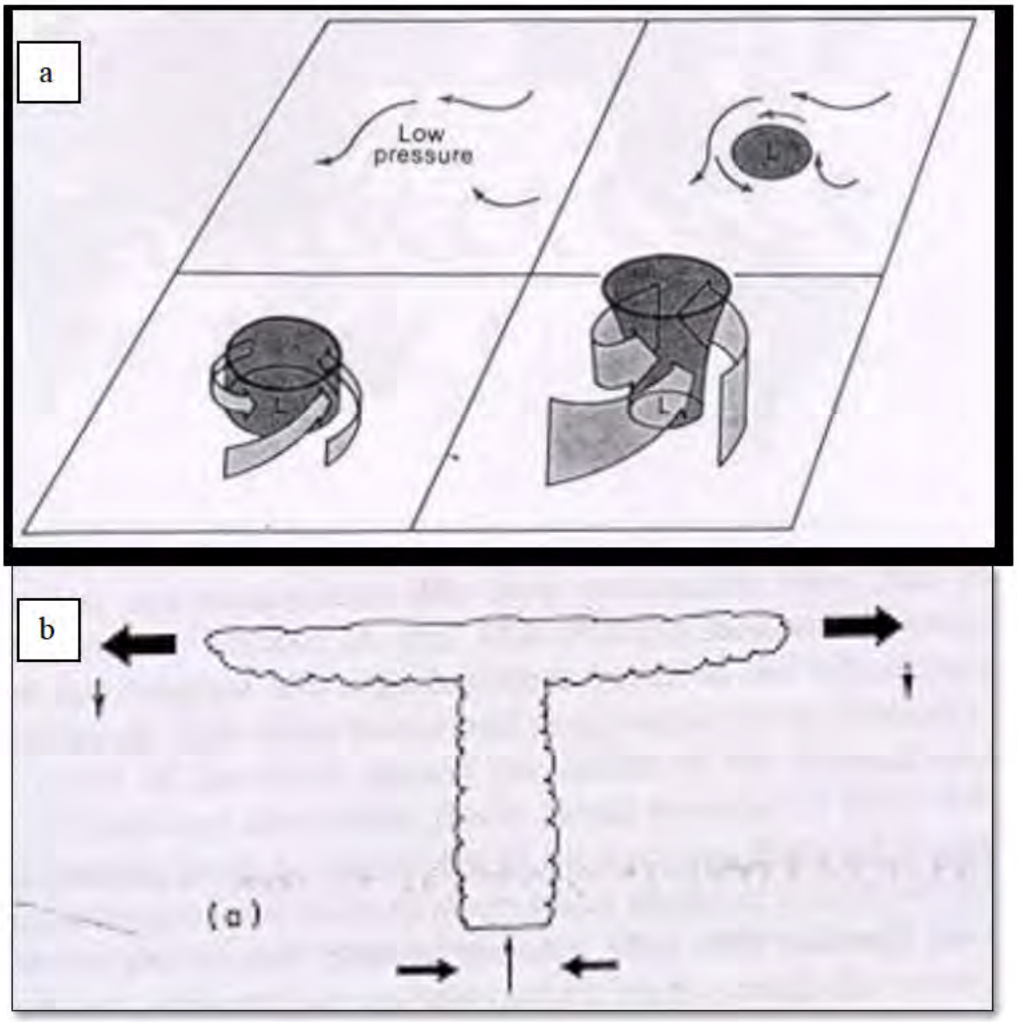

Figure 2.4: [a] The formation of a hurricane involves the combined effects of pressure and circular winds. (Eagleman, 1990). [b] Development of cumulonimbus cloud from low level convergence (Pielke, 1990).

Generally, surface pressure does not fall very far because the air that diverges in the upper atmosphere sinks at the edges of the cumulonimbus cloud system and is recycled into the storm. This results in slowing down the rate of pressure drop. In addition, the subsiding air warms and dries the region surrounding the cloud system. The central cumulonimbus column strengthens and broadens if more mass is removed from the upper atmosphere than is replaced at low level (Merrill, 1985). The coriolis force is then required to spin the emerging cumulonimbus system and create a cyclonic vortex. The coriolis force, fuelled by the rotation of the earth, introduces a spin to the rising air eventually forming the spiral bands, which are a significant part of a cyclonic vortex. Due to an absence of coriolis force cyclones tend not to form within 5° of the equator (O'Hare et al., 2005) as shown in figure 2.6.

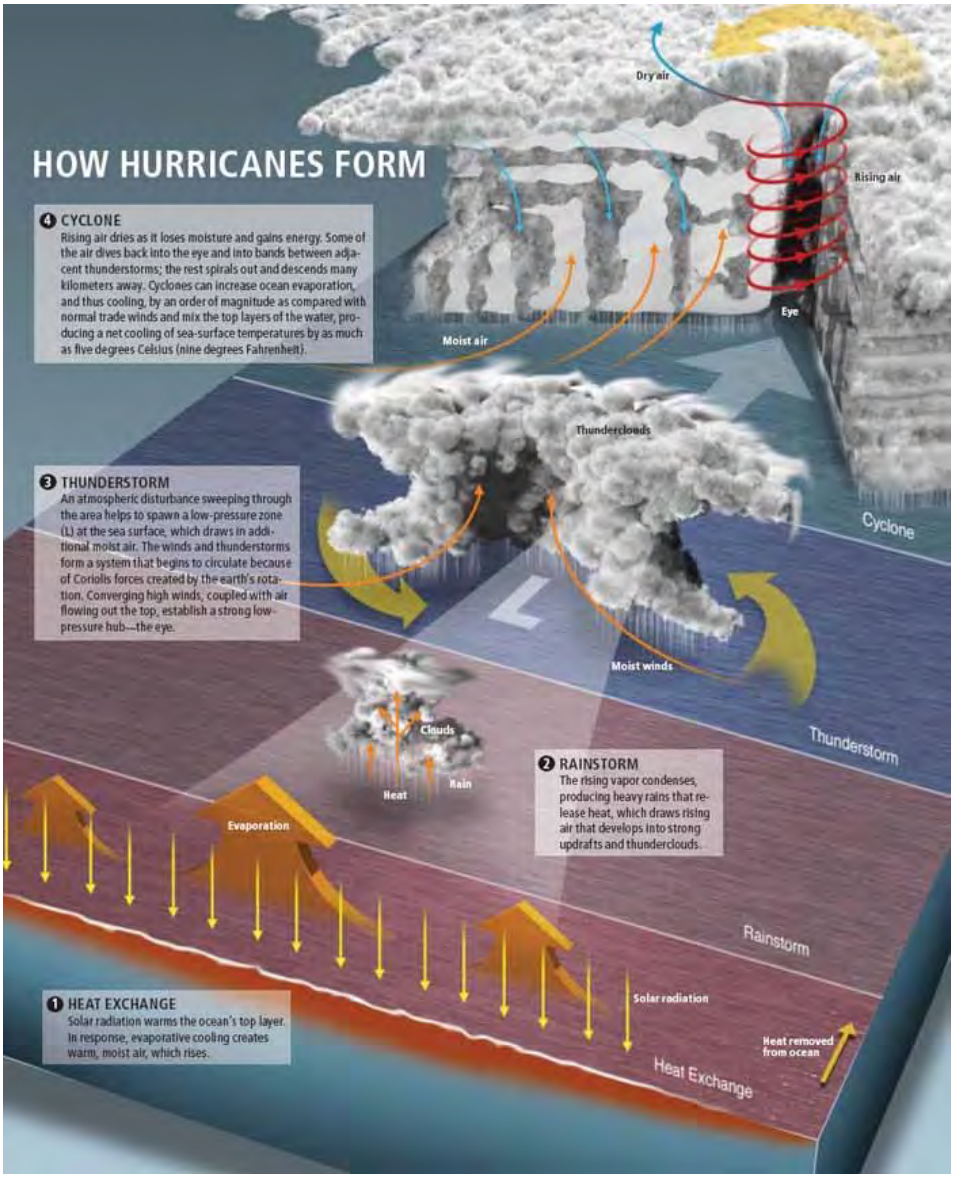

Figure 2.5: How hurricanes form (Biello, 2007).

Palmen (1948) found that cyclones will develop only over comparatively warm water, approximately 26^{o} C and higher, although there have been a few exceptions. Palmen (1948) also identified the environmental conditions that should be present for a cyclone to develop. In addition, formation of an unstable thunderstorm environment is required to transfer the heat stored in warm waters into the atmosphere.

Relatively moist mid-troposphere conditions are also necessary because a drier mid atmosphere will not be favourable for the required thunderstorm formation. Proximity to the equator is important as, due to the lack of coriolis force, low pressure of disturbance cannot be maintained.

Minimal vertical wind shear between the surface and the upper troposphere is essential for the genesis of any tropical cyclone (Gray, 1968; Gray, 1979).

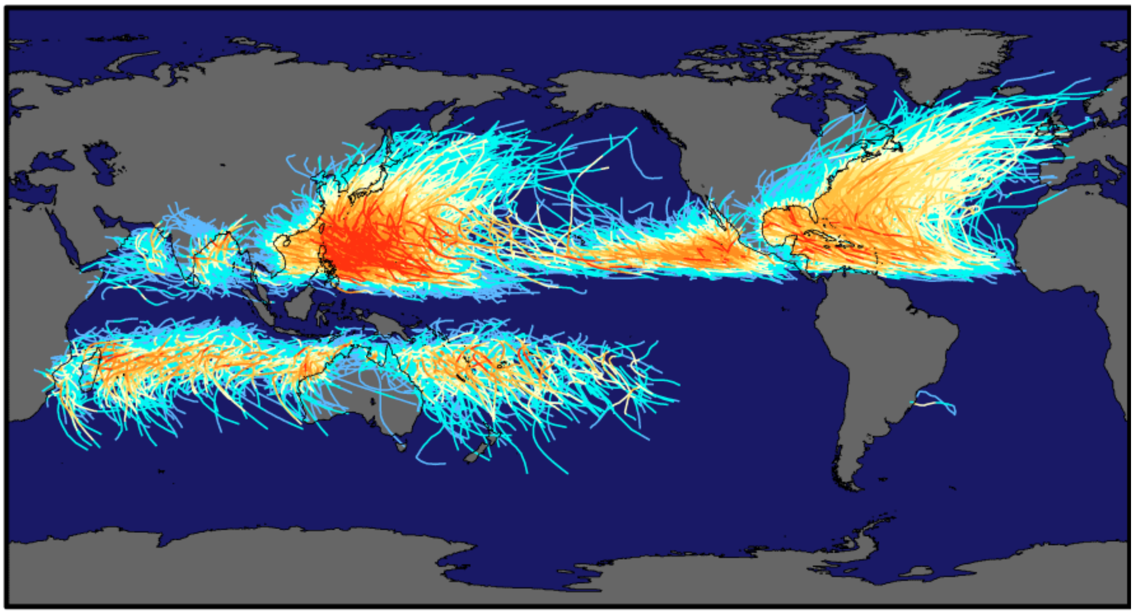

Figure 2.6 : Tropical cyclone density worldwide (Laing and Evans, 2011).

Although the conditions described above are necessary to form a cyclone, many systems that appear to meet these conditions do not develop into cyclones. Riehl (1954) developed a comparison of a tropical cyclone development procedure to a man-made engine and listed five stages of development. Gray (1968; 1979) and Palmen (1948) stated the importance of the tropospheric current providing the cooling system to carry away the excess heat from the cyclonic regions.

As the storm intensifies, the lowered atmospheric pressure in a tropical cyclone can cause the local sea level to rise to an average of 4m (Harris, 1963), thus accumulating the water at the centre of the storm. The storm surge, in addition to extreme spiralling winds, eventually causes most of the damage to property and life.

2.6 Intensification of Cyclones

The low-level convergence inflow does not accelerate with time unless more mass is removed upward than converges at low levels. In addition, the constant evaporation of warm water ensures moisture enrichment of the middle and upper troposphere subsequently growing the bulk of cumulonimbus cloud near the tropopause level, resulting in a greater percentage coverage of the disturbed area with deep cumulus clouds. This provides an effective linkage between the lower and upper troposphere. Providing that a mechanism exists to exhaust this mass to regions far removed from the disturbance, surface pressure will continue to fall and the low-level cyclonic circulation will intensify.

2.7 Anatomy of Cyclones

Three cloud decks can be identified in the outer circulation of a hurricane. The lowest layer, consisting of nimbostratus clouds, produces rain. The middle layer consists of altocumulus and altostratus clouds, and the upper cloud layer is composed of cirrus and cirrocumulus. (Gibilisco, 1984). It is mainly the upper cloud layer that is used for monitoring the storm using satellite data. Due to unpredictable and dangerous conditions within a tropical cyclone, physical instruments to monitor the intensity of the storm are generally not cost effective, hence the importance of using remote sensing to monitor the visible development of a storm. The anatomy of a cyclone plays a vital role in its detection and monitoring using satellite data. There has been more than 50 years of research into reliable detection and monitoring of tropical cyclones from space (Conover, 1962; Blankenship, 1962; Maykut, 1964; Greaves and Chang, 1970; Miller, 1971; Reynolds and Haar, 1977; Spencer and Christry, 1990; Neumann, 1993; Chuai-Aree et al., 2008; Vidale et al., 2010; Bongirwar et al., 2011; Johnson and Watson, 2011).

2.7.1 Eye Wall

Merrill (1985) concluded that divergent upper-level winds, at and beyond the periphery of the storm outflow region, are required to remove the mass from the storm environment, and thus to prevent a re-circulation of the air back into the storm at low levels. As the low-level convergence becomes stronger it becomes increasingly difficult for air to reach the centre of the storm. Due to centrifugal spiral forces it is difficult for the air to spiral inwards, causing the air flow to be minimal in the centre of the storm (Pielke and Pielke, 1997). However winds blow tangentially to lines of constant pressure. This newly developed region of contrasting wind is known as the eye of the storm as seen in figure 2.7 & figure 2.8. The rate of change of barometric pressure is steepest in this region. The eye wall contains the maximum inward penetration of the inward spiralling air and is the region of strongest winds, while the eye itself is one of the calmest parts of the storm. At the surface, the eye wall of the storm produces torrential rains and 'hurricane force' winds.

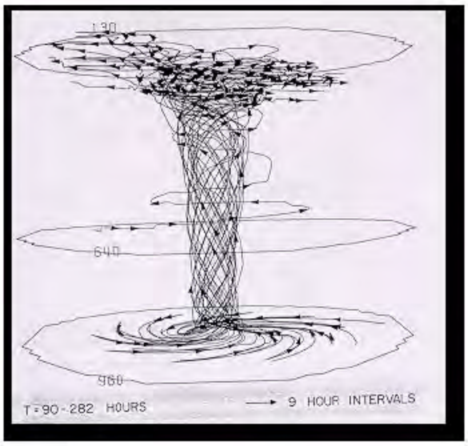

Figure 2.7: [left] The eye wall: cloud starting to swirl up at the top, usually means that the clouds at that altitude are starting to spin like the clouds below, a sign of storm intensification. (Dommin, 2010); [right] A computer simulation of flow into, upward, and out from the eye wall.(Pielke, 1990)

2.7.2 Eye of the storm

At the core of the hurricane, the winds and rains decrease and a becalmed area called the eye of the storm is found. The eye may range from 5 to 120 miles in diameter, but is usually between 20 to 40 miles across (Weatherford and Gray, 1988). The barometric pressure is lowest within the eye, which forms the basis for determining the intensity of the hurricane. Inside the eye, the compressional warming of the air causes it to hold more moisture while the relative humidity decreases, forcing the clouds to dissipate ensuring lack of cumulus formation. In an intensifying tropical cyclone, the eye region can be completely cloud free. This phenomenon is also known as the 'lull'.

Due to this aspect of storm behaviour, ordinary people think that the hurricane approaches from the same direction as the wind blows and when the eye passes over it gives an impression that the storm has "blown itself out"; but when the winds from the other side of the eye wall return with nearly the opposite direction and intense force, such people will often say that the storm "came back". The eye of a hurricane can mislead people into thinking that the storm is over, but the remaining portion of the storm arrives with sudden and surprising violence. As the eye of the violent hurricane of September, 1926, passed over downtown Miami, the wind decreased to about 10 mph, but at the same time Allison Hospital, now St. Francis, on Miami Beach just over six miles away was reporting the wind at 80mph (Gibilisco, 1984). Figure 2.8 (below) illustrates the contrasting wind speeds and pressure in a tropical cyclone.

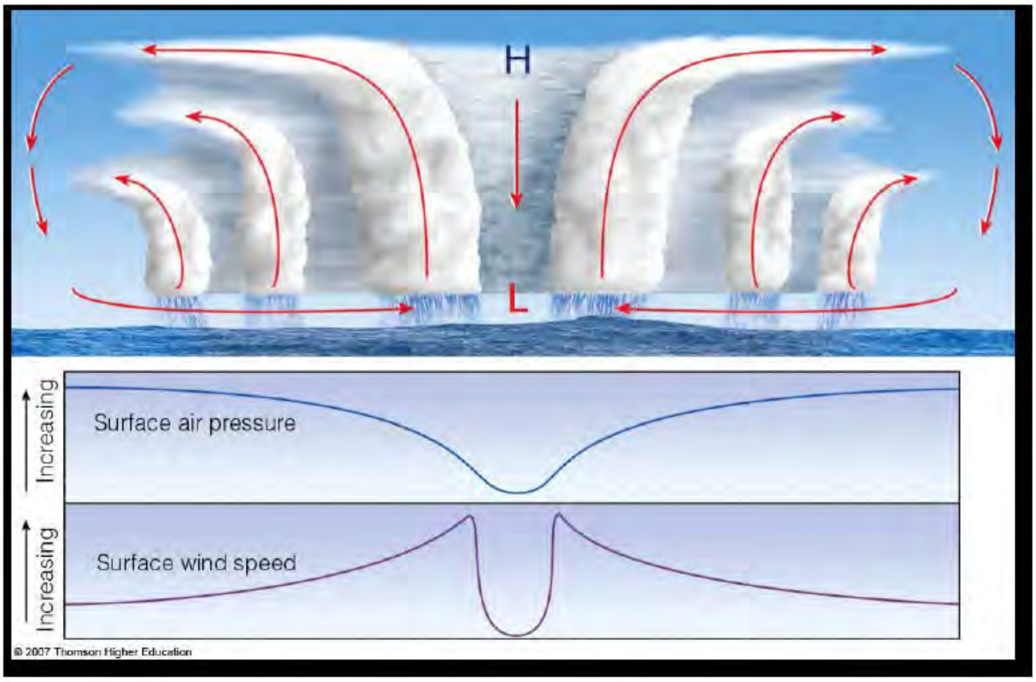

Figure 2.8: Cross section of a typical tropical cyclone.(College, 2010)

According to NOAA (2010) many observers have described conditions in the eye as "oppressive", "sultry", "suffocating" and full of strange odours. Some have described the odours to be "like escaping gas". This reaction is apparently largely psychological and due to the rapid transition from hurricane winds to the relatively calm conditions.

2.7.3 Rain bands

A tropical cyclone is composed of numerous bands of thunderstorm clouds. These are also known as rain bands (figure 2.9). They spiral around the centre of the hurricane whilst holding vast amounts of rainwater, because they feed off evaporated moisture from warm ocean waters. These thunderstorm rain bands can range from few to tens of miles wide and 50 to 300 miles long (NOAA, 1999).

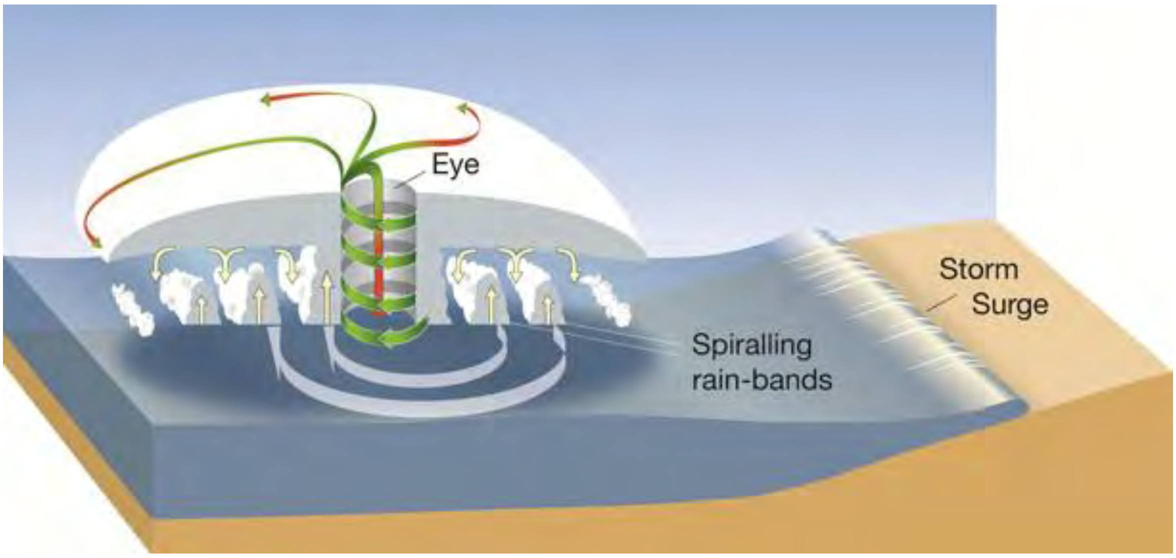

Figure 2.9: Cross-section of a typical cyclone with its spiralling rain bands (BoM, 2013a).

2.7.4 Storm Surge

Due to high pressure winds swirling inwards, the oceanic waters tend to gather towards the centre of the storm. The low-pressure eye of the storm normally does not have enough force to push down the water causing an excessive build-up of water just under the eye wall. This build-up of water is called a storm surge. It has also been referred to as the ocean swell or a hurricane tsunami; however the behaviour has been reported to be very unlike tsunamis.

When a storm surge makes landfall, it behaves more like fast flowing floodwaters than a tidal wave. A less powerful storm surge can reach a height of 4 to 5 feet and causes minimal damage to coastal areas. However a mature storm's surge can rise as high as 18 feet and cause severe flooding with disastrous consequences. It has been calculated that a hurricane with a pressure of 900mb will have an increase in ocean level of more than 1m because of the lower atmospheric pressure (Eagleman, 1990).

Hurricane Camille at the Gulf of Mexico in 1969 brought a storm surge of more than 7m (Eagleman, 1990). In the Bay of Bengal off the coast of India, Pakistan and Bangladesh, even higher waves were recorded. The configuration of the bay allowed water to be driven into the narrowing portions to cause increases in ocean swells of up to 12m or more. The largest storm surge recorded in the historical records was caused by the tropical cyclone Mahina, which affected Bathurst Bay in Australia on 5th March 1899. The recorded storm surge measured a height between 43 to 48 feet, or 13 to 15 meters. (Annonymous, 1899; Nott and Hayne, 2000; Whittingham, 1958).

The storm surge can intensify the effects of tidal flooding. The phenomenon known as the storm tide is a combination of the storm surge and the normal astronomical tide. The combination of the storm surge, tidal swell and waves caused by high winds is deadly. More than 6,000 people were killed in the Galveston Hurricane of 1900 mainly due to the storm tide. Similarly, Hurricane Camille in 1969 produced a 25-foot storm tide in the Mississippi and infamous Hurricane Hugo in 1989 generated a 20-foot storm tide in South Carolina (Delaware, 2009; Schwarzbach, 1963).

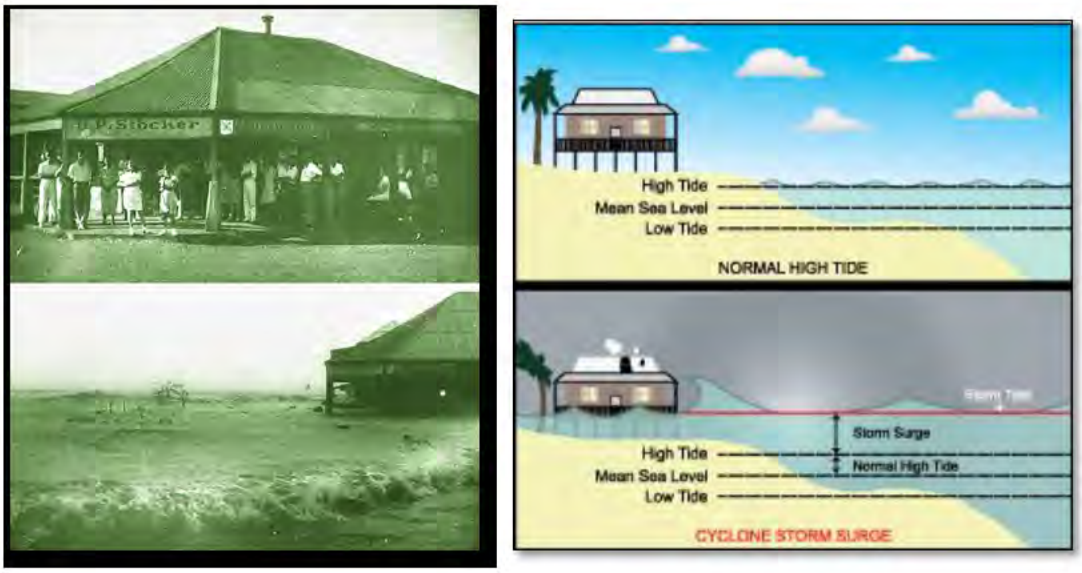

Figure 2.10: A typical storm surge (BoM, 2009).

2.7.5 Size of tropical cyclones

The size of a cyclone is usually measured either by the diameter of the hurricane or gale force winds. In the past, the size was measured by the diameter of the outer closed isobar, however, that approach is not practised anymore. Using the outermost closed isobar approach, a composite of 100 storms gave an average size of 500 km in diameter. Whereas, if only those with winds greater than hurricane velocity are considered, the average cyclones are about 250 km in diameter (Eagleman, 1990).

In the early stages of tropical cyclone development and even for the first few days after the storm reaches its full intensity, the diameter of the storm can remain quite small; as it becomes older it also becomes larger. One of the most intense hurricanes on record, the Labour Day storm on the Florida Keys in 1935, had a path of destruction no more that thirty-five to forty miles wide (McDonald, 1935).

2.7.6 Life Span of cyclones

A hurricane must eventually face either death by landfall or death by cold water. There are four major reasons for the inability of these storms to maintain their intensity near the surface after landfall (Houze, 1993; Pielke, 1990). As tropical cyclones are a form of heat engine, they require the warmest temperatures to be located near the centre of the storm. However, as air spirals into a hurricane, it expands as a result of the lower pressure closer to the eye resulting in cooling of the system. Moreover, when cyclones make landfall there is no heat source to counteract this cooling. Due to this break in the heat transfer, the deep cumulonimbus convection over land becomes inhibited and the divergent winds in the upper levels of the tropical cyclone weaken in strength as the storms deform and lose their strength.

The development of sea spray in strong winds, and its subsequent evaporation, is an additional source of water vapour over the oceans. Over land, the availability of water is limited to the amount that may be extracted from the ground and plants through evaporation and evapo-traspiration, and the re-evaporation of rainfall on the ground. This evaporation over land also further contributes to cooling of the lower levels of the atmosphere since heat is required in the conversion of liquid water-to-water vapour (Gibilisco, 1984; Merrill, 1985; Pielke and Pielke, 1997; NOAA, 2010).

Another substantial difference between the ocean and land areas is the generally larger aerodynamic roughness of the land. Trees, buildings, and even grasslands tend to be relatively rougher surfaces than water. Due to friction caused by these land features the air movement decelerates more than it normally would over an ocean. Even with large amplitude sea waves during windy conditions, the ocean remains relatively aerodynamically efficient (Pielke, 1990).

The shape of the hurricane also changes as it crosses a coastline or enters the cool temperate part of the world. The intense, symmetrical circulation gives way to a more elongated and distorted shape (Gibilisco, 1984).

A storm of tropical origin may appear on the weather charts for a period of three weeks or more. During this whole time storm is never static and its characteristics are constantly changing from day to day and even from hour to hour. The physical processes of the storm itself and its environment are continually affecting its development, structure, shape, and intensity. McDonald (1942) first described the four stages in the normal cycle of development and decay:

- Preliminary or Incipient stage
- Deepening stage
- Expanding stage
- Decline or Decaying phase

However, Dunn and Miller (1964) used different terms in dividing the life cycle of tropical cyclones, also into four similar stages:

- The formative stage
- The stage of immaturity
- The stage of maturity
- The stage of decay

The average life span of a hurricane is about nine days, although August storms normally live the longest, with an average span of twelve days. July and November storms last about eight days (NOAA, 2008b; NOAA, 2010; Landsea and Goldenberg, 2011).

Location of the origin of the tropical cyclones, time of the year and various other meteorological and atmospheric factors determine the lifetime of any cyclone. Very few storms dissipate as long as they remain over tropical or subtropical waters unless some abnormal features of the wind-flow patterns surrounding the storms act to bring cold and dry air into the hurricane circulation.

After leaving the tropics some hurricanes encounter moist and active troughs of low pressure. These supply new energy that may keep the hurricane alive for long periods of time. This is illustrated by the Galveston hurricane of 1900. The storm was tracked from the middle of the tropical Atlantic Ocean into the Gulf of Mexico and to the Texas coast. From there it changed its course and became an active storm in the Great Lakes region. It then crossed the Atlantic Ocean and moved across northern Europe into Siberia (Dunn, 1964). Many hurricanes cross the Atlantic in the trade-wind belt, moving from east to west, and then re-cross the Atlantic from west to east in the prevailing westerlies north of the Azores-Bermuda High. Once these storms leave the tropics, however, they lose their earlier characteristics rapidly and can no longer be considered true tropical cyclones (Landsea and Goldenberg, 2011; Dunn, 1964).

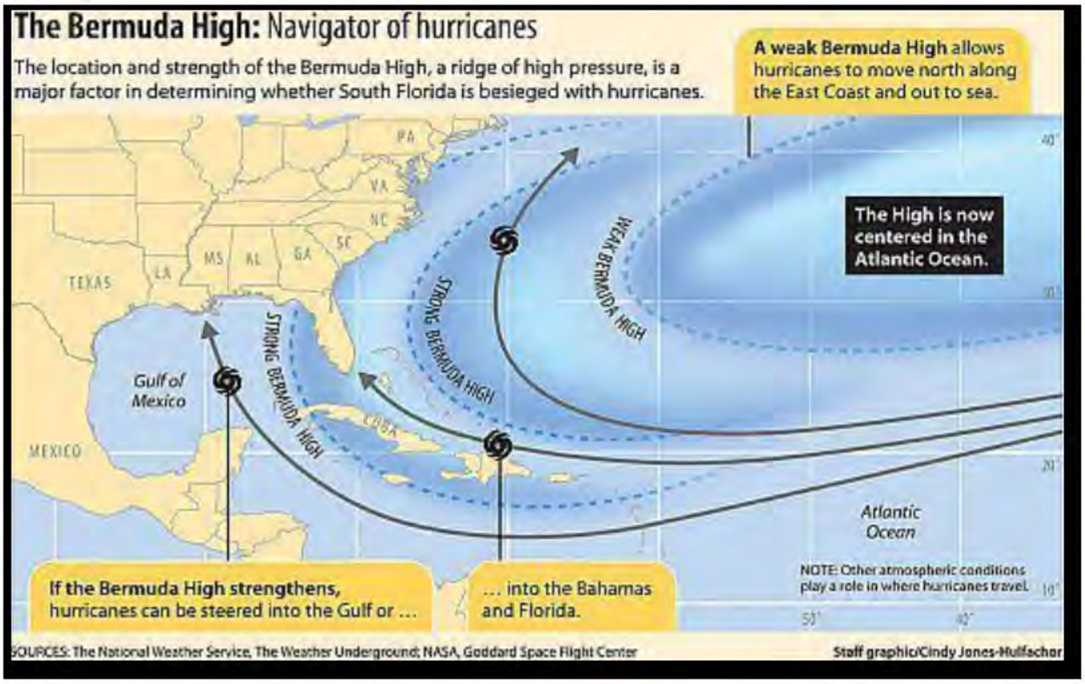

Figure 2.11: The Bermuda High and its effect on hurricanes (GSFC, 2009).

2.7.7 Tropical Cyclone Path Prediction

Some storms move faster than others; sometimes a Northern Hemisphere hurricane with its origins in Atlantic will head out to the North Atlantic and die harmlessly over cold ocean waters. But in most instances, it will linger over humid tropical waters for days before riding the wind and shifting toward coastal cities and towns. In the Atlantic, the "Bermuda High" often dictates whether a hurricane will hit the Eastern United States. If a large Bermuda High catches up to a storm, it will push the storm toward the U.S. coast whilst a smaller Bermuda High will swing a storm out to open sea. When these steering winds aren't present, a hurricane can still move slowly under its own momentum but has trouble staying on any one course. This makes a hurricane's path nearly impossible for weather experts to predict.

To maintain itself, a hurricane needs a steady supply of heat, humidity and warm ocean waters. As a storm moves across the open sea, the bands of thunderstorms that form a hurricane draw up evaporated moisture and gain strength. A hurricane can grow quickly if it keeps moving from one warm stretch of water to another. An encounter with cool currents can mean death for a hurricane. Without the humidity and evaporation, a storm can start to weaken (Landsea and Goldenberg, 2011). When strong steering winds sweep the hurricane onto the shore, the havoc the storm brings also marks the beginning of the end. Over land, a hurricane loses its main fuel source. The storm begins to weaken and its winds start to diminish.

Throughout any tropical cyclone’s life span, experts monitor growth and decay to minimise the impact. Many methods and techniques have been developed over centuries to monitor and predict this phenomenon (Vines, 1898; McDonald, 1942; Elsberry, 1985; Vigh, 2000; Johnson and Watson, 2011; Khalid et al., 2003). In recent decades, the use of satellite imagery and ground based remote sensing to monitor tropical cyclones has increased considerably.

2.7.8 Tropical Cyclone Modification

There have been attempts to modify tropical cyclones. Project Stormfury was one of the notable efforts to destroy hurricane related weather systems. This procedure for attempting to stop or weakening the hurricane is called seeding. Seeding a hurricane consists of adding silver iodide or dry ice to it by means of an aeroplane (Eagleman, 1990). Dry ice crystals have a very low temperature and can generate ice crystals in the atmosphere. The concept of seeding a hurricane is to spray the eye wall with Silver iodide that can cause the generation of extra ice crystals, transforming the water vapour in the cumulous cloud system into ice particles. This change of form causes the eye wall to expand inadvertently in turn causing it to reduce the winds forming in the hurricane. The breakage in the heat engine due to lack of winds causes the storm to break itself. This can be seen in figure 2.12

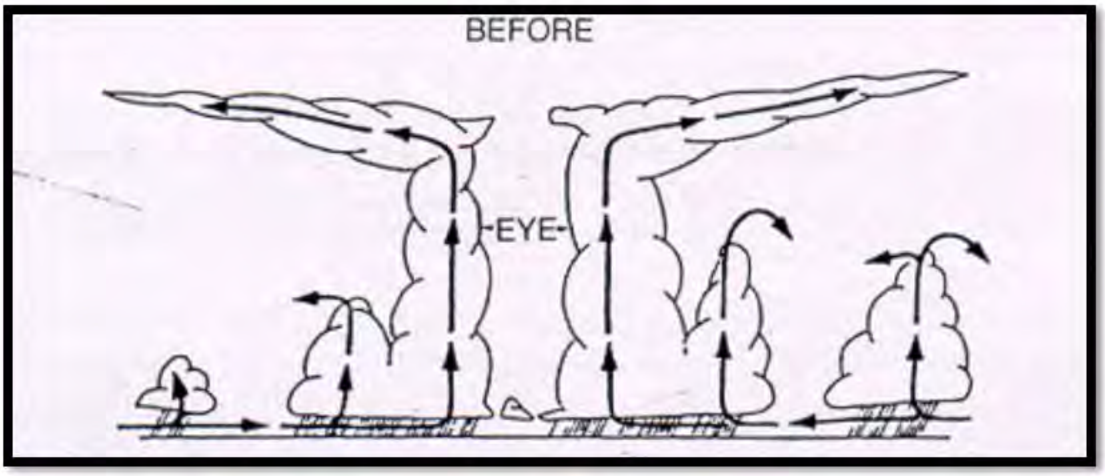

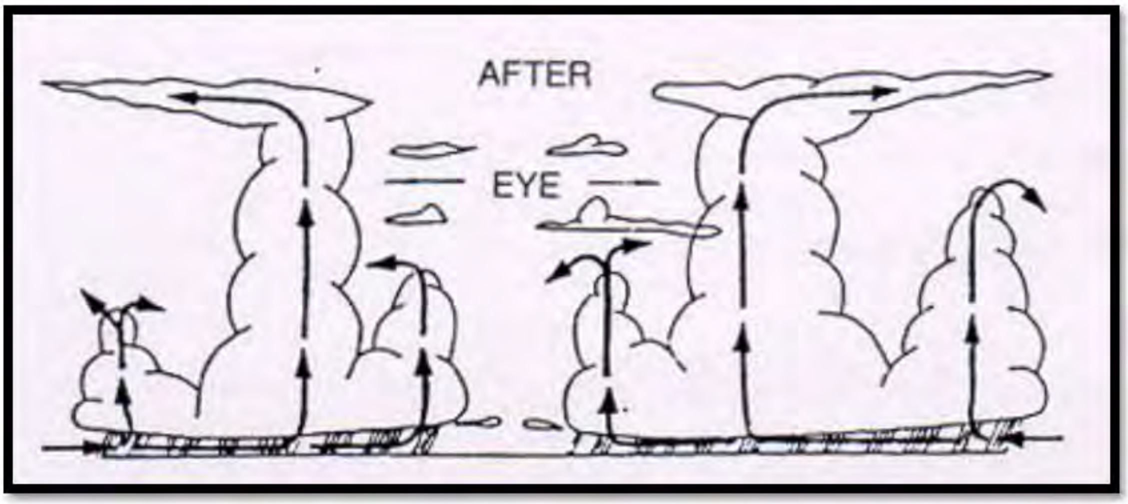

Figure 2.12: Vertical cross-section of a hurricane eye wall and rain bands before and after seeding (Pielke, 1990).

Tropical cyclones can be seeded at different locations to break the systematic processes taking place in this organised weather system (figure 2.13). There are normally two different locations that can be seeded, the eye wall and rain band surrounding the storm. The seeding of the rain bands can cause the warm air to cool rapidly breaking the flow of the heat engine. This cuts down the amount of moisture that can be carried into the most intense region of the hurricane.

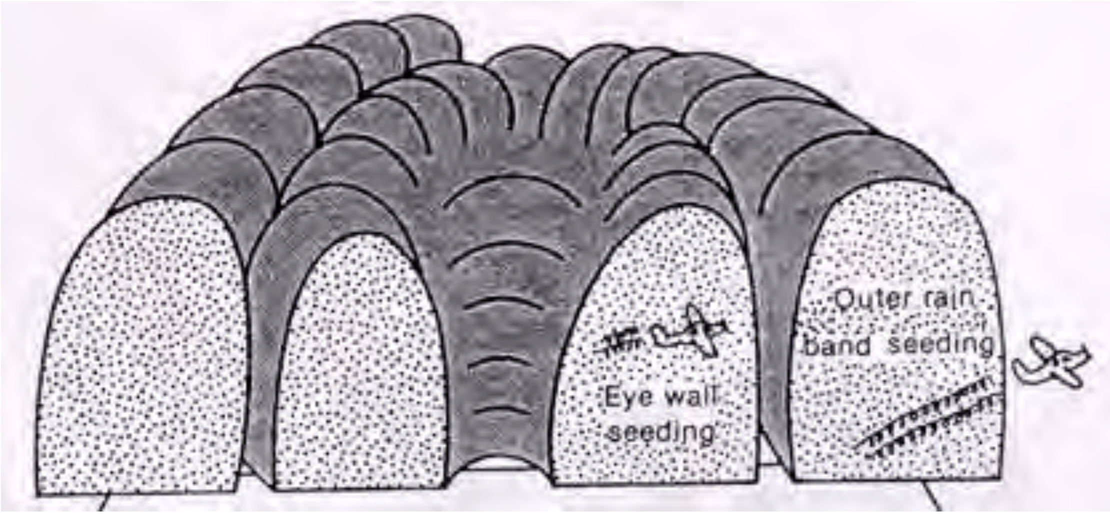

Figure 2.13: Different locations where a hurricane can be seeded (Eagleman, 1990).

Four hurricanes were seeded in the period from the early 1960s to the mid-1970s. The first was hurricane Esther in 1961, followed by hurricane Beulah in 1963. After the former had passed, seeding measurements indicated that the ice crystals were produced as expected. However the hurricane began to follow a looping path and made landfall in the US. There was no direct evidence, however, that seeding was the cause of the change in direction. In fact, none of the other hurricanes that had been seeded showed any change in direction. However, when Esther made landfall, new rules were created around the seeding procedure such that a minimum distance requirement was sanctioned (Eagleman, 1990). When hurricane Beulah was seeded in 1963 there were some indications of weakening winds; however, it was only noted after the second seeding effort.

Hurricane Debbie was seeded in 1969 (Ahrens et al., 2011) and showed an immediate 31% reduction in winds. Debbie was left to its own course considering the reduction in power; however, the winds returned to their original intensity. After another seeding effort the winds dropped again approximately 16%, thus proving for the first time the impact of seeding theory in practice (Eagleman, 1990). Some further efforts were made in the 1970s to seed hurricanes, but they did not show any variation or reduction in wind greater that the natural variations. After this, hurricane seeding was stopped as it was deemed to be ineffective.

Studies of natural storm variability, exploratory seeding experiments, and numerical and theoretical simulations indicate that the implementation of the Stormfury hypothesis could result in a reduction of 10%-15% in the maximum wind speed, with associated damage reductions of 20%-60% (Sheets, 1981). Currently, further seeding experiments are not being performed, although detailed observational sampling of tropical storms is continuing as part of the Stormfury project.

Other modification methods have included the introduction of a sheet material over the sea surface to avoid evaporation of warm waters and breaking the heat transfer mechanism. Various compounds such as Ether and Alcohol have been tested to create a thin film over the sea surface. However, experiments have shown that wave action rapidly breaks up the film layer making this method impractical. Another technique discussed was to spread carbon dust in the air around and within the tropical cyclone. This will create a heated effect disrupting the heat transfer. This technique was never tested due to the unknown environmental effects of carbon dust.

2.8 Monitoring Cyclones

As discussed in the previous sections hurricane development requires the presence of certain geographical and environmental variables. These variables can be measured and monitored with relative ease using either ground based instruments or space borne sensors. However, developing an algorithm to accurately predict the genesis of tropical cyclones is close to impossible. Due to their dynamic and evolutionary nature, it is extremely difficult to distinguish between a severe tropical thunderstorm and one that will develop into a fully blown tropical cyclone. In contrast, thunderstorms can be predicted and monitored with relative ease and confidence. It is the uncertainty surrounding thunderstorms and tropical disturbances turning into tropical cyclones that is problematic. Therefore, most of the tropical depressions and disturbances are monitored, especially in appropriate seasons, to catch the chance of one developing into a cyclone. Prediction of the cyclone can be classified into two categories: first, seasonal probabilities; and, second, track prediction. Seasonal probabilities estimate the number of tropical cyclones at the beginning of each peak season. It is difficult to estimate the numbers due to the complicated and unpredictable nature of the phenomenon; moreover numerical predictions can take a long time to process and produce results sometimes rendering them out of date. In addition, the accuracy of these predictions is always questionable. The errors are inversely proportional to the amount of time between the prediction and the actual occurrence of the storm. Despite advances in numerical and computing techniques, errors can range between 200 miles for 5 days before landfall to 50 miles for 1 day before landfall (Jovanovic, 2011; NHC, 2011), see figure 2.14.

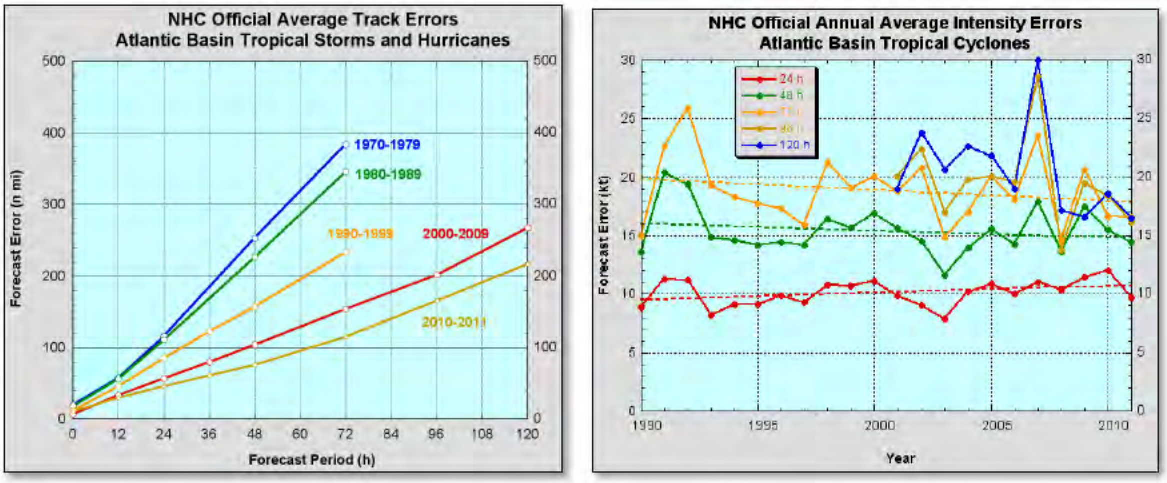

Figure 2.14: Errors in tropical cyclone prediction (NHC, 2011)

However, track predictions made by relatively simpler algorithms have better accuracy. These algorithms produce better results because track monitoring requires a cyclone to exist already. Once a cyclone is being tracked all the surrounding environmental variables can help estimate a path that any tropical cyclone could follow.

A number of tropical cyclones in the past went undetected merely because of the absence of physical instruments or lack of human observation records (Power, 1989). In recent decades, use of satellite imagery has not only provided organisations with close to real time data but also ensured availability of data on demand. Many organisations exist with their sole purpose being the monitoring and prediction of tropical cyclones (Neumann, 1993; NOAA, 2010; Landsea and Goldenberg, 2011). The National Hurricane Center (NHC) (NHC, 2011)) in Miami, Florida, for example, has the responsibility for predicting the path and intensity of hurricanes originating in both the Atlantic basin and eastern Pacific Ocean.

2.8.1 Satellites Remote Sensing

Satellites are instruments used for the purpose of observing the Earth's terrain and atmosphere at work. Over many years satellites have provided meteorologists with a comprehensive view of the world’s weather. Satellites are helpful in locating developing hurricanes and in charting their path after they have formed. The earth’s weather is monitored constantly by hundreds of specially designed satellites. However, use of the data from these satellites for forecasts and weather monitoring requires special expertise in image processing and analysis. Various intelligent algorithms have been developed over decades to make the weather forecast more reliable and accurate.

There are various types of satellites orbiting the Earth taking images at time intervals ranging from every few minutes to few days. Geostationary satellites orbit the earth at an approximate altitude of 22,000 miles above the equator providing imagery of multiple weather systems, both at day and night. Satellite imagery has helped provide experts with data that can estimate the location, size and intensity of any storm and its surrounding environment.

The first weather satellite, Television Infrared Observation Satellite (TIROS), launched from Cape Canaveral in 1960, provided essential imagery for the purpose of weather predictions and forecasts. It also provided one of the first satellite images to be broadcast on a television weather channel (figure 2.15)

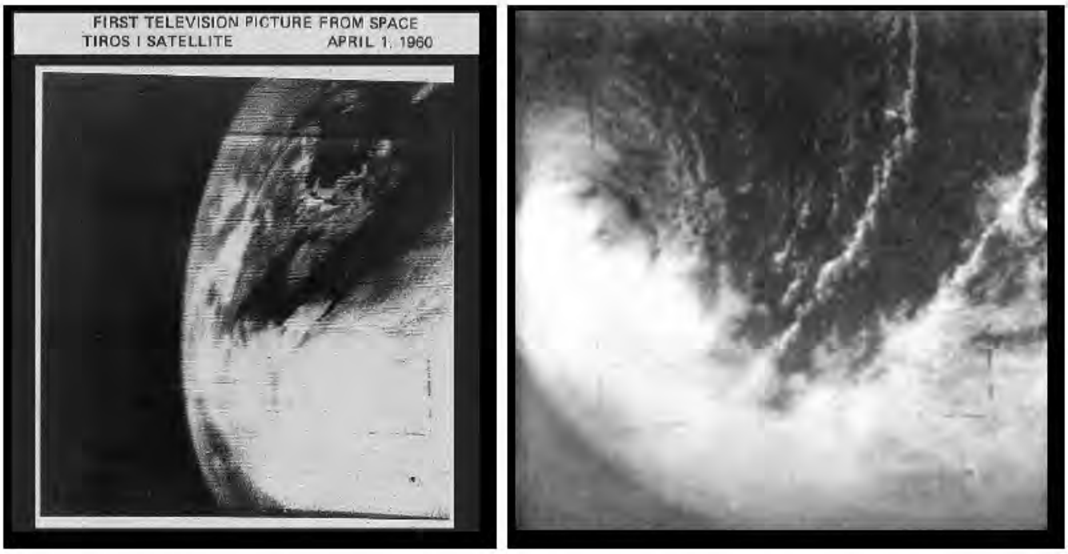

Figure 2.15: Image of a tropical storm by satellite TIROS (a) first televised image (b) first cyclone captured via a satellite.(NOAA, 2011)

Images sent back from the satellite were not the first or only observations from space assisting weather forecasters. Movie cameras mounted on rockets provided essential images of weather systems before TIROS was launched. Regular earth orbits meant that experts had access to a more sophisticated and consistent global view of the atmosphere thus improving scientific outputs.

There are many other satellites that have dedicated sensors for atmospheric and weather monitoring. The Geostationary Operational Environmental Satellite (GOES) is a geostationary orbit satellite with an imaging sensor and a sounder to analyse various layers of the atmosphere. This satellite is capable of providing data related to temperature, wind movements and cloud heights. The GOES plays a vital role in statistical and imaging analyses of global weather patterns (NASA, 2010).

Earth orbiting satellites and the data they provide have helped start a revolution in the sciences of meteorology and climatology over the past four decades. With effective global views captured using space borne and air borne sensors, and high-speed computers, forecasters have produced efficient weather models for more accurate predictions (Lehmiller et al., 1997; Han et al., 2009). Meteorological satellite information has enhanced our understanding of synoptic systems and provided insights into previously little known mesoscale circulation systems, particularly as higher spatial and temporal resolution has become available (Businger and Reed, 1989).

All of the data collected by satellites around the Earth coupled with ground based instrumental data are fed into numerical weather models. Meteorologists then read and use the models to create weather predictions, as well as hurricane forecasts. This is not only a lengthy process, but it is less efficient compared to automated detection of cyclones (Ho and Talukder, 2008; Khalid et al., 2003). The overwhelming amount of data and complexity of numerical modelling makes human interaction in the forecasting process unfeasible and less productive. Instead, automated cyclone detection algorithms can improve the detection of any tropical cyclone.

Meteorological satellites can capture data at various wavelengths, but the most widely used products are visible, thermal infrared and water vapour imagery. A major problem with visible images is that half the Earth is in darkness at any moment and therefore cannot be seen in visible light. In contrast to the radiation that has come from the sun and has been reflected, the Earth and its atmosphere emit their own radiation to space. This ‘terrestrial’ infrared radiation is emitted by the continents, oceans, glaciers, clouds and other physical objects. The strength of the outgoing signal depends on the temperature of the emitting surface. Thermal infrared images are essential in tropical cyclone monitoring as they are not hindered by the lack of sun’s energy reflecting off the targets, hence providing round the clock imagery of our atmosphere.

2.8.2 Reconnaissance Aircraft

Aircraft reconnaissance is a complementary data gathering effort executed by the US Air Force. Pilots fly aircraft into the cores of tropical cyclones to measure wind speed, pressure, temperature, and humidity as well as to provide an accurate location of the centre of the hurricanes. Apart from US Air Force Reserve 53rd Weather Reconnaissance Squadron, who are the major body in operational reconnaissance, the National Oceanic and Atmospheric Administration (NOAA) also flies aircraft into hurricanes to help scientists improve their modelling and understanding of these storms and to improve forecast capabilities (HHA, 2011).

The variables measured and recorded by these flights can be combined with satellite images to assist weather forecasts. The nature of the eye and surrounding cloud bands are used to make predictions about the intensity of hurricanes. If the central dense overcast (CDO) and cloud bands completely enclose the eye, a stronger storm is indicated (Riehl, 1954; BoM, 2008; Ahrens et al., 2011; Dvorak, 1975).

2.8.3 RADAR

Ground based RADAR sensors are widely used to monitor tropical storms when they are approaching land. A network of Doppler RADAR stations can be used to obtain an effective and real time feed of a developing and approaching cyclone. These RADAR stations provide detailed information on hurricane wind fields and their changes. Using RADAR it is also possible to present more accurate flood and tornado warnings.

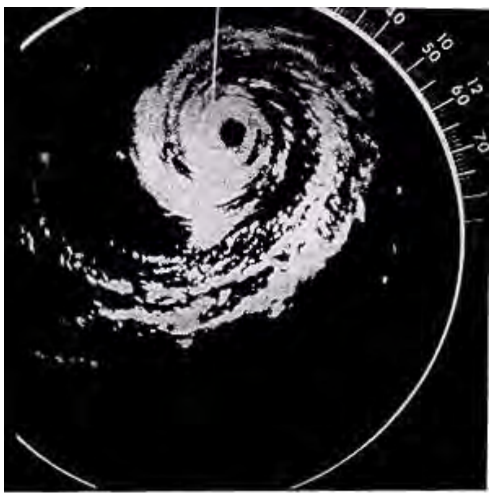

Figure 2.16: 1960 Radar image of Hurricane Donna taken by the WSR-57 RADAR (Pielke, 1990).

2.9 Computer Models

Various organisations around the world are responsible for forecasting tropical cyclones. Normally forecasts are generated by complex numerical models that rely on a combination of satellite images, historical storm information, current weather data from within a storm, as well as results from other predictive models.

Due to the complex nature of atmospheric interactions, these models make varying predictions, especially in forecast periods beyond twenty-four hours (NHC, 2011; World Meteorological Organisation, 1976; Neumann, 1993; Aberson, 1998; Johnson and Watson, 2011). Human expertise is required to monitor the outputs from different models (Dvorak, 1975; Dvorak, 1984). Ultimately, a forecast is a product of varying amounts of human intuition mixed with the results of one or more models, which could be relatively subjective and tedious.

Experts regularly use outputs from various computer models to accurately forecast any tropical cyclone movement. Statistical models are used to relate the hurricane's motion to experience with past storms, while dynamic models address atmospheric changes (Houze, 1993; Goerss, 2000; Murthy et al., 2008). Numerical models are normally considered to be a combination of the statistical and dynamic models. Numerical Weather Prediction (NWP) requires computers with vast processing power to compute the outputs within appropriate times. The use of satellite images to assist NWPs has become widespread in recent decades (Leslie et al., 1998; Bongirwar et al., 2011; Olander et al., 2002; Olander and Velden, 2007; Olander and Velden, 2011). However, before the advent of NWPs, nephanalysis was used to monitor cloud behaviour. This has led to researchers investigating automated cloud analyses for weather prediction, not just hurricane analyses. Though automated processes produce results with an acceptable accuracy, continuing research suggests that there is further need for accuracy improvement. This research engages in such models to address uncertainty and improve accuracy in automated recognition of tropical cyclones by using soft computing techniques such as fuzzy logic and heuristic models.

2.9.1 Nephanalysis

The term nephanalysis refers to the making of cloud charts. The concept and the use of nephanalysis pre-dates the satellite era (Berry et al., 1945), but since the availability of satellite data nephanalysis has become almost wholly associated with meteorological satellite imagery. The pioneering work in interpreting satellite imagery was performed by Conover (1962; 1963). When nephanalysis adopted computer technology, the process became objective, consistent and in many cases faster. Most computer assisted nephanalysis procedures use traditional and standardised cloud categories (Conover, 1963; Conover, 1962; Dvorak, 1975; Dvorak, 1984). This has the advantage that the products of various procedures are standardised. From the early 1960s till the late 1980s, satellite based nephanalysis' introduction of impartiality in predictive model remained limited due to lack to confidence in automated procedures, requiring experts to confirm the results at all time.

2.9.2 Interpreting cloud patterns in satellite imagery

Conover (1963; 1962) suggested six criteria for successful cloud identification from satellite imagery: brightness, texture, size, shape, organisation and shadow effects. The principal feature of the cloud cover is the cloud amount, as this affects energy exchanges at the earth's surface and in the atmosphere. In the past few decades, many experiments have been taken up to examine computerised methods of cloud amount estimation (Arnold, 1977; Reynolds and Haar, 1977; Houze, 1993; Chuai-Aree et al., 2008).

An early paper by Blankenship (1962) suggested a scheme using 3.7 - 4.2μm wavelength data to determine cloud amount at 700, 500 and 300mb in the atmosphere, and Maykut (1964) used a similar technique with TIROS HRIR (High Resolution Infra-red) data. Miller (1971) used a brightness-weighting scheme to estimate cloud amount and a technique similar to this has been used in the US Air Force Global Weather Central (AFGWC) 3DNEPH procedure (Coburn, 1971). The progress in cloud amount estimation has proceeded from simple linear spatial summaries to more sophisticated histogram weighting procedures (Reynolds and Haar, 1977; Woodbury and McCormick, 1986) and 3D reconstruction of real time atmospheric data (Chuai-Aree et al., 2008; Liu et al., 2011).

The first two criteria in Conover's list for interpreting satellite cloud imagery are cloud brightness and cloud texture, and it is these two variables which have attracted the most attention over recent years. Cloud brightness in Visible, Water Vapour and Thermal IR wavebands has been used both singly and jointly in cloud type classification (Barnes and Chang, 1968; Greaves and Chang, 1970; Shenk et al., 1976; Liu et al., 2011; Khalid et al., 2003; Toldalagi and Lebow, 1982; Dvorak, 1984; Olander and Velden, 2011)

Having characterised spatial and textual variables in cloud based satellite imagery, the pixel values are classified into groups ensuring categories of various types of clouds. The procedures follow the two classical remote sensing approaches known as supervised and unsupervised classification. Given the variation in cloud type concepts a variety of classification routines have been examined, many of which are summarised by Toldalagi and Lebow (1982) and Baum *et al.* (1995; 1997). Clustering methodologies have also been used in cloud classification procedures (Ambroise et al., 2000; Desbois et al., 1982; Talbot et al., 1999; Bezdek, 1998; Chiu, 1994).

Desbois et al (1982) used a dynamic clustering method, which iteratively defines cloud clusters. Once identified, clusters then have to be given names, and this gives a route by which new classification of cloud types might emerge, although to date clusters have been named with traditional cloud type categories. Multispectral analyses are also used to distinguish between various cloud densities (Talbot et al., 1999; Liu et al., 2011; Yingying et al., 2011). An Image Data Processing System (IDAPS) was developed by NASA/Marshall Space Flight Center in 1975 to process high-resolution satellite images, both visible and infrared, to study cloud to height variability, temperature distribution, and the growth and collapse rates of the clouds (NASA, 1975).

2.9.3 Forecasting Tropical Cyclones

As mentioned in the earlier sections tropical cyclone monitoring can involve generating seasonal forecasts or cyclone track prediction. These forecasts are produced before the existence of any storm. However, once the storm has developed it is important to monitor its growth or decay, and to estimate its track and intensity. Cyclone monitoring mainly involves tracking its path and measuring its intensity.

2.10 Path tracking

The typical movement of Atlantic hurricanes involves initial travel from the Southeast. As they move into more northerly latitudes, they generally start to curve with a more northward movement, followed by movement from the Southwest (Vega, 1991). A hurricane may suddenly change directions as it follows a looping path or it may strike land when its path encounters appropriate winds. About 70% of the hurricanes behave in a typical fashion by travelling in paths that are predictable. It is the other 30%, which help build up databases of current and past hurricane paths to assist predictions of future paths of tropical cyclones.

The National Hurricane Center (NHC) in Miami uses a variety of different track prediction models in an effort to pinpoint the location of landfall for hurricanes reaching the United States. Four of the major types are listed in figure 2.17. Figure 2.18 shows a modern track prediction output.

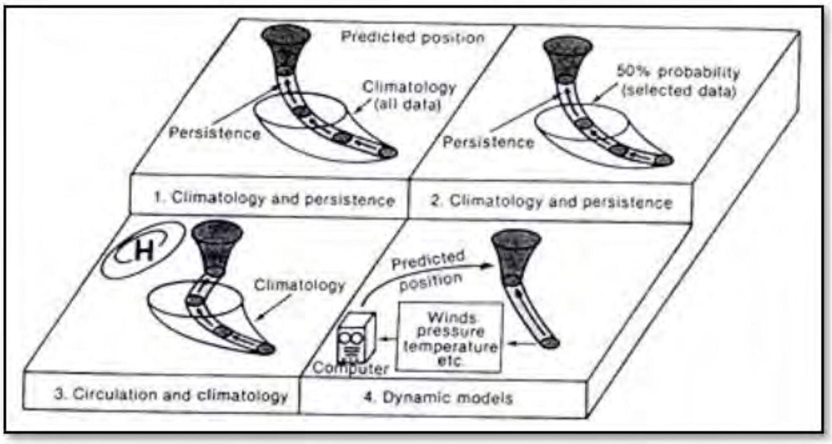

Figure 2.17: Hurricane track prediction techniques include the four different methods (Joe 1983)

Figure 2.18: Hurricane Dean track forecast by the National Hurricane Center (NHC, 2012)

One of these is purely dynamic; the others are statistical or climatological. If the location of landfall can be predicted, it makes a tremendous difference in warning people of the approaching danger. The accuracy of predicting the exact location of the centre of the hurricane at landfall is only about 175 km (NHC, 2011). This distance may mean that one particular city is affected instead of another. None of the techniques predict the hurricane path perfectly (DeMaria, 2005). This is the reason for having different prediction models to locate as specifically as possible where the hurricane is going to make landfall. NHC executes as many as 44 models to produce an official track and intensity forecast (NHC, 2009). A combination of statistical, dynamic and persistence models are used to generate a forecast report that is agreed by various experts at NHC. Persistence models simply refer to the behaviour of the storms in the past. This includes speed of travel and their direction during their existence. These past records are then used to project the hurricane speed and direction for all the current and predicted hurricanes. The combination of various models can provide a prediction, path or intensity, for any specific location in the Atlantic and East Pacific Oceans within the range of 12 hours to 5 days in advance (Sorenson, 2000; Goerss, 2000).

In addition to global prediction, which covers the whole of the Atlantic basin and East Pacific Ocean, NHC also produces localised forecasts, which means that only past records nearer to a particular location of a current hurricane are used. All models can utilise persistence data, past records of climatological variables or any combination of these to predict the path of a hurricane. The climatology of past hurricanes considers factors such as the surrounding pressure systems, upper air flow patterns, direction of the trade winds, and other environmental variables (Vigh, 2000; NHC, 2009).

The dynamic models are intelligent computer algorithms that process various data at several atmospheric levels of a hurricane (Lehmiller et al., 1997; Elsner et al., 1998; Jovanovic, 2011). Dynamic NWP models are the most complicated algorithms and require a lengthier processing time. As they are reliant on the most current data available, their outputs can be delayed and do not include the most up to date forecast. However, once the algorithms have completed processing, their outputs can, in turn, be input into other models to produce more accurate predictions.

None of these hurricane path prediction methods are consistently more accurate than the others. All are used for every hurricane that forms in their respective regions (Jovanovic, 2011; NHC, 2011). The results of one method may be considered more reliable than the others for a particular hurricane from past experience, but no one method is better under all conditions.

Figure 2.19 illustrates an example of prediction of the movement of hurricane Frederic in 1979, from its initial position, at 7am on 11th September, north of the coast of Cuba. The models listed in figure 2.19 are statistical models, which form the prediction using a combination of observed and predicted atmospheric conditions. Statistical analysis of historic tropical cyclones permits the currently used numerical models to be more accurate; these are normally reliant on a given set of current and forecasted meteorological variables (Pielke, 1990; Murthy et al., 2008; Aberson, 1998).

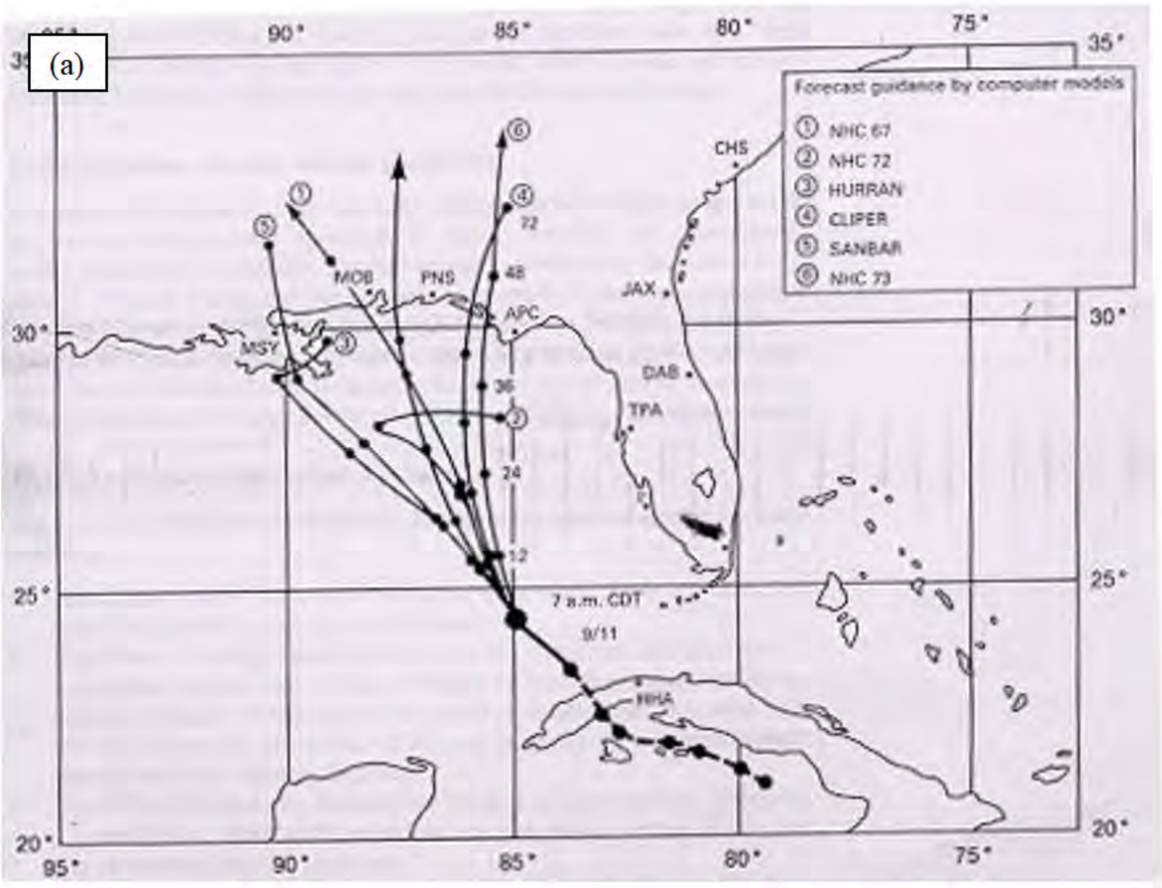

Figure 2.19: (a) Forecast positions, generated by six compute models for Hurricane Fredric, September 1979.(Pielke, 1990; NWS, 2009)

Characteristically comprehensive three-dimensional numerical models of tropical cyclone prediction, using observed and modelled atmospheric conditions, were widely used during the late eighties to improve the accuracy of the predictions. These models included the

National Meteorological Center's Moveable Fine-mesh Model (Kerlin, 1979; Kurihara and Bender, 1980), two US Navy models at Fleet Numerical Oceanography Center called The One-way Tropical Cyclone Model and the Nested Tropical Model (Goerss, 2000; Goerss and Jeffries, 1994) and the Multiple-Nested Grid Model of the Japan Meteorological Center. The European Centre for Medium-range Weather Forecasts has also been widely used to predict tropical cyclone paths (Pielke, 1990).

2.11 Tropical Cyclone Detection

Tropical cyclone detection algorithms differ from predictive algorithms in the sense that they are detecting existing tropical storms, hence removing the uncertainty caused by stochastic algorithms. Cyclone detection is an important phase of hazard management associated with tropical storms. It is understood that not every tropical depression eventually takes on tropical cyclone status (Dunn and Miller, 1964; Pielke and Pielke, 1997; Aberson, 1998; Anthes, 1982b; Anthes, 1982a). The storm has to hold its shape and intensity for at least two days before it can be classified as a tropical cyclone. This means that the warning associated with cyclones can be relatively abrupt (Aberson, 1998), but nonetheless more accurate.

Detection of a developing tropical cyclone and its path monitoring are more important than some vaguely produced seasonal prediction of these storms. The importance of this is emphasised by the impact of present day cyclones making landfall and the logistics involved in issuing warnings and evacuation calls. Many algorithms are used for the detection of cyclones throughout the various tropical regions (Ho and Talukder, 2008; Camargo and Zebiak, 2002; Fitzpatrick, 1997). These techniques involve various hybrid methods of combining many statistical and dynamic algorithms. Many of the techniques rely on a best match technique using various environmental data collected via physical instruments. Once a cyclone is born various techniques are used to monitor its growth over a period of time until experts are assured that it is going to make landfall hence affecting the environment. Figure 2.21 present an example of a decision tree used by the National Hurricane Center to determine whether a suspected weather system will develop into a tropical storm, while figure 2.22 illustrates a decision tree used by experts to conclude whether an existing tropical cyclone will intensify over its remaining life (Pielke, 1990).

In the decision trees, illustrated in figure 2.21 & figure 2.22, there is a significant reliance on data captured in real time using physical instruments. Satellite imagery has been widely used in early cyclone detection algorithms (Conover, 1962; Blankenship, 1962; Conover, 1963; Maykut, 1964; Greaves and Chang, 1970; Miller, 1971) but it always had to be combined with other ancillary data. Dvorak (1975) established one of the first techniques to estimate tropical cyclone intensity that solely relied on satellite images. Since then Dvorak's technique has been extended by many experts (Dvorak, 1984; Olander et al., 2002; Olander and Velden, 2007; Olander and Velden, 2011). Originally Dvorak's technique for intensity estimation was extremely subjective and all analyses and identifications were performed manually with the help of flow charts similar to the one illustrated in figure 2.20. This placed a huge responsibility on the experts applying these techniques to satellite images and classifying the storms. Dvorak's technique was further developed in mid-1980s by many others (Olander et al., 2002; Olander and Velden, 2007; Olander and Velden, 2011) including Dvorak himself (Dvorak, 1984). He revisited his own algorithm and improved its accuracy by removing some of the subjective aspects. Initially Zehr (1989) attempted to objectify Dvorak's techniques, but there were still subjective aspects left within the newly developed algorithms, mainly associated with locating the centre of the storm. Identification of the centre of tropical cyclones was still a manual and error prone job. In addition to the detection algorithms Dvorak also introduced a new intensity classification technique, known as the T classification. As compared to the Saffir Simpson Scale, the T classification had 8 categories of storm intensity, further to which each class could also be split into half classes creating further distinction between storm categories (table 2.1)

In the nineties various other researchers built upon the Dvorak's revised technique of 1984 to further introduce objectivity into the algorithms (Velden et al., 1998b), but it was not until the start of the 21st century that an Advanced Objective Dvorak Technique (AODT) was developed (Olander et al., 2002). AODT was capable of identifying earlier storm stages of tropical depressions and various other storm stages with an acceptable margin of accuracy. It also had an automated centre determination algorithm to identify the centre of the storm. Although accurate identification of centre of the storm is still considered to be a difficult task and required further research (Olander and Velden, 2011).

Table 2.1: Comparison of Dvorak's T-classification and Saffir Simpson Scale (NOAA, 2012).

CI Number	MWS (Knots)	MSLP (Atlantic)	MSLP (Davolio)	Saffir-Simpson Category (Approximate)
1	25 Knots			
1.5	25 Knots			
2	30 Knots	1009 mb	1000 mb	
2.5	35 Knots	1005 mb	997 mb	
3	45 Knots	1000 mb	991 mb	
3.5	55 Knots	994 mb	984 mb	
4	65 Knots	987 mb	976 mb	1 (64-83 KTS)
4.5	77 Knots	979 mb	966 mb	1 (64-83 KTS); 2 (84-96 KTS)
5	90 Knots	970 mb	954 mb	2 (84-96 KTS); 3 (97-113 KTS)
5.5	102 Knots	960 mb	941 mb	3 (97-113 KTS)
6	115 Knots	948 mb	927 mb	4 (114-135 KTS)
6.5	127 Knots	935 mb	914 mb	4 (114-135 KTS)
7	140 Knots	921 mb	898 mb	5 (136+ KTS)
7.5	155 Knots	906 mb	879 mb	5 (136+ KTS)
8	170 Knots	890 mb	858 mb	5 (136+ KTS)

With accuracies still not close to the original manual technique, Olander and Velden (2007) worked on the algorithms further (Olander and Velden, 2011) to revise the Advanced Dvorak Technique (ADT). ADT was capable of implementing nearly all of the scenarios described in the original publication. In addition, it used regression functions to deal with the detection of the centre of the storm and relied on the long wave infrared measurements to estimate the intensity. There were obvious similarities between ADT and Dvorak's original technique as they tend to identify the same physical feature of a cyclone, i.e. Central Dense Overcast (CDO), eye and banding around the CDO. The revised versions of ADT introduced various analytical techniques to identify the storm centre and are heavily reliant on the fact that the storm centre needs to be identified accurately. Moreover the algorithms are heavily reliant on the presence of the eye to classify the intensity.

In the past decade there has been a rapid increase in the advent of algorithms similar to Dvorak's (Olander and Velden, 2007; Zehr, 1989; Velden et al., 1998a; Bankert and Tag, 2002a; Wimmers and Velden, 2004), trying to estimate intensity of tropical cyclones from the satellite imagery, but none of them have managed to create a seamlessly automated procedure. Even AODT (Olander et al., 2002; Olander and Velden, 2007), the most objective of them all, still requires certain manual input under particular scenarios as seen in figure 2.20.

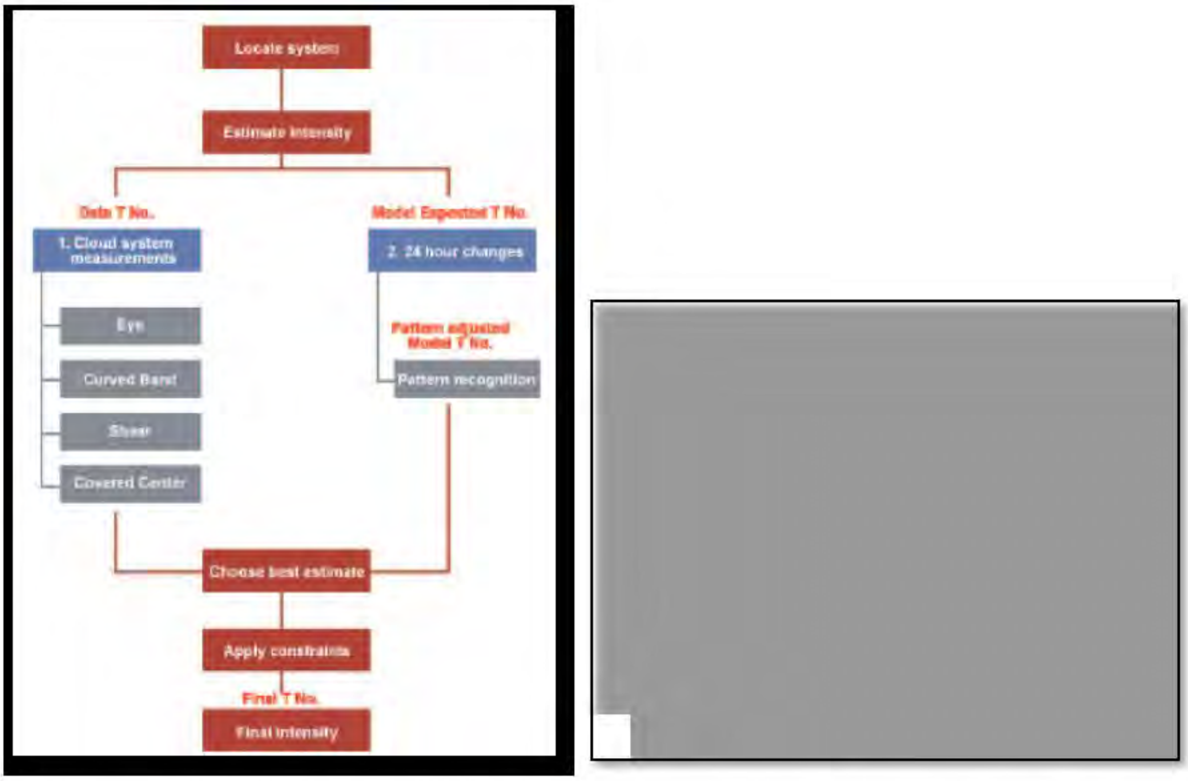

Figure 2.20: (left) Basic Dvorak technique (Dvorak, 1984) (right) Advanced Dvorak technique (Olander and Velden, 2007)

Another drawback with the existing techniques is that algorithms such as ADT, AODT and other evolved Dvorak's techniques do not take into consideration the uncertainty associated with the feature shape and sizes. Working with traditional logical (crisp) methods, the identification of the features and their measurements tend to be biased.

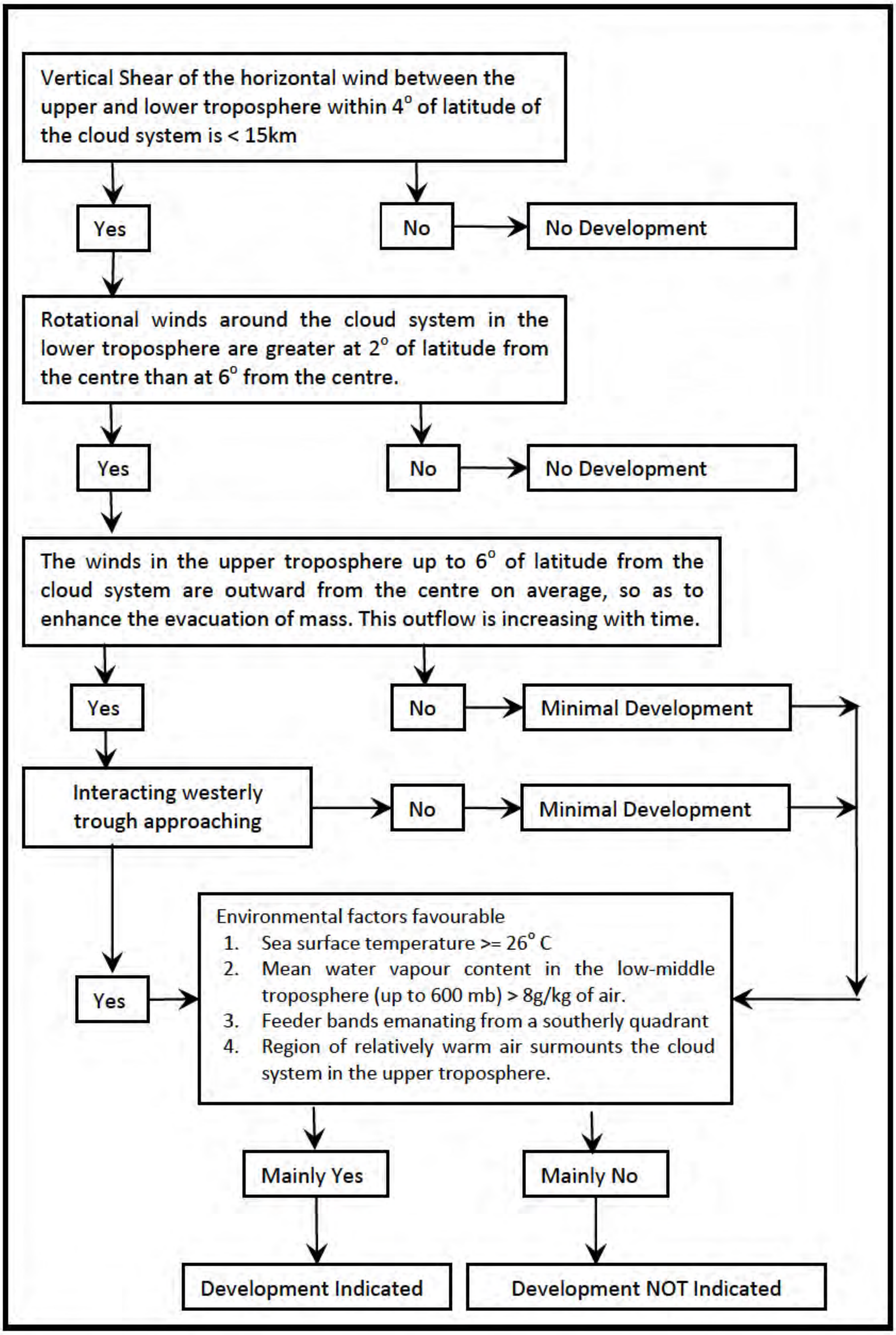

Figure 2.21: Decision trees to estimate tropical cyclone development (Pielke, 1990; Simpson, 1971)

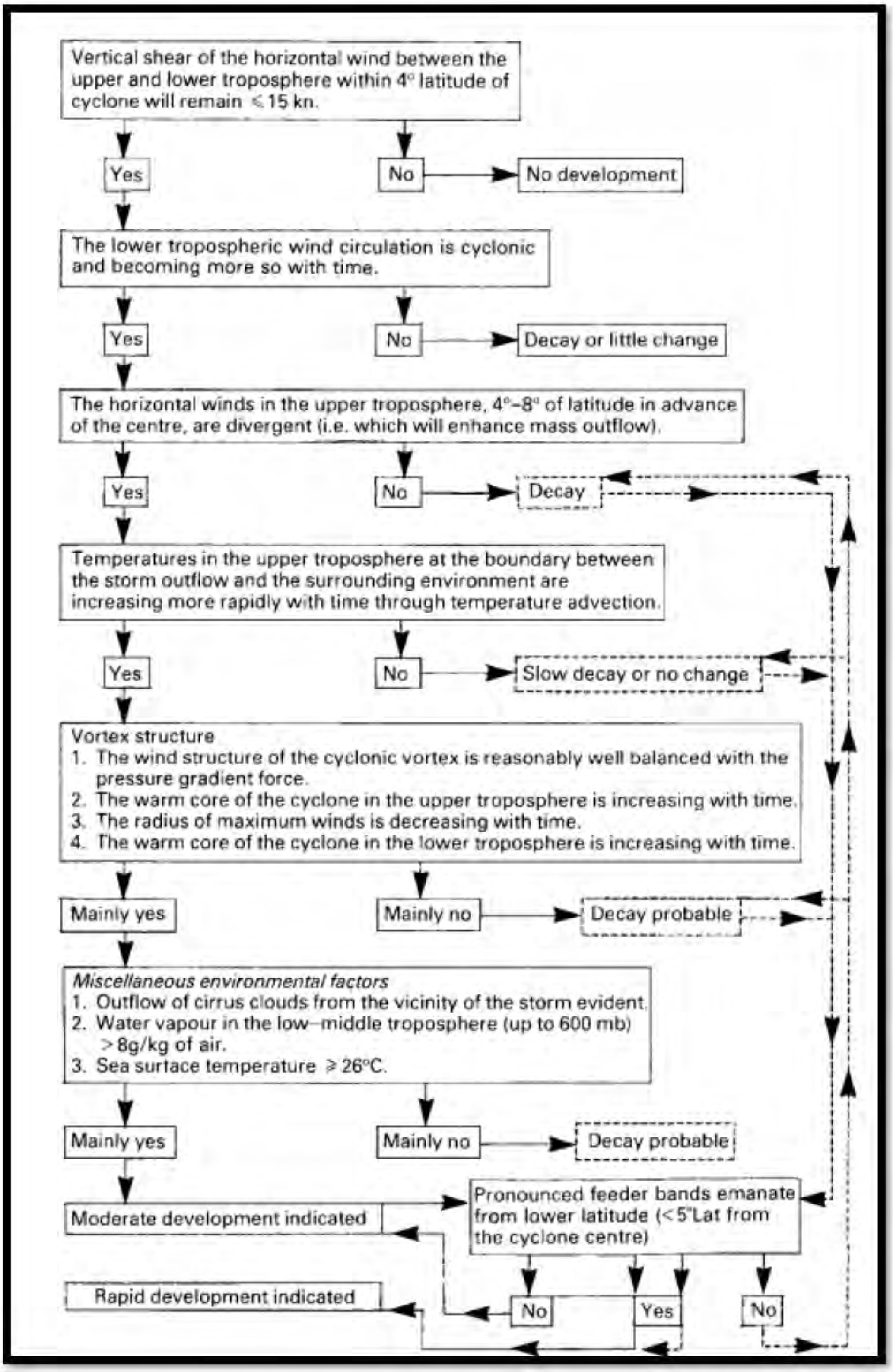

Figure 2.22: A decision tree to estimate if an existing tropical cyclone would intensify (Pielke, 1990; Simpson, 1971)

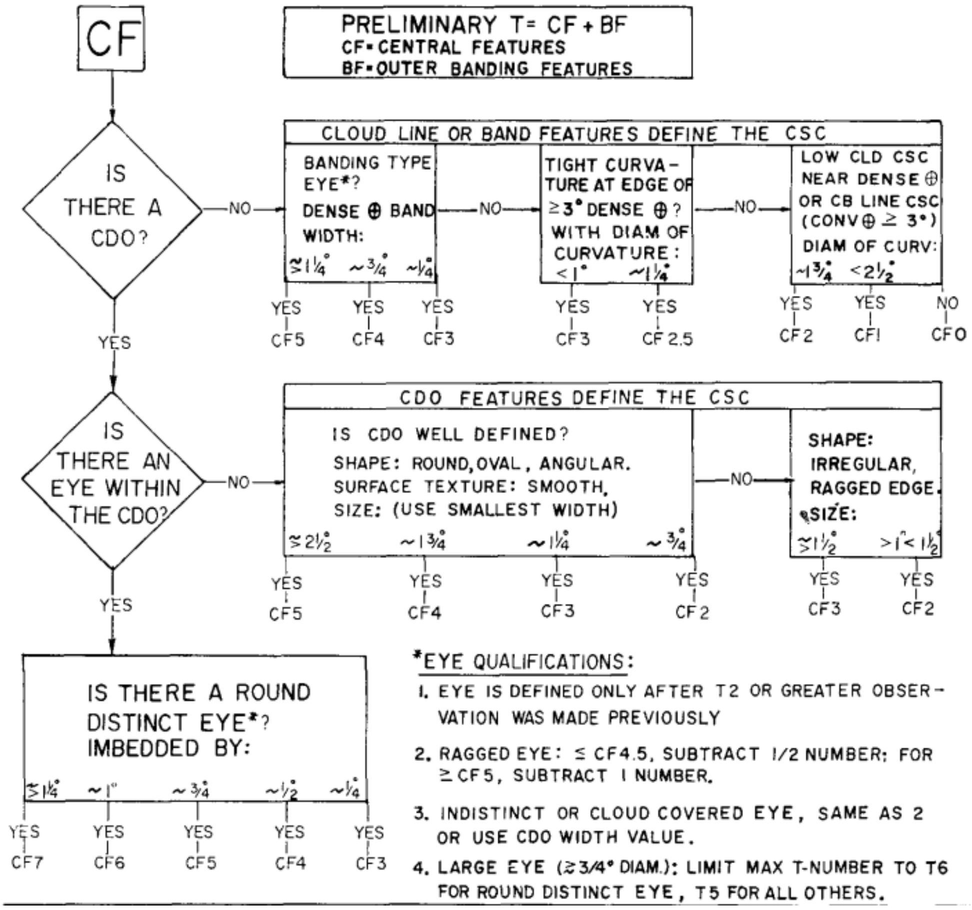

Figure 2.23. Dvorak's diagram for determining storm intensity (Dvorak, 1984; Dvorak, 1975).

In order to address issues of uncertainty and vagueness associated with shape identification and intensity classification, a fuzzy logic rule based approach is chosen in this research to provide much more accurate and realistic results. Chapters 4 and 5 respectively discuss various pattern recognition and soft computing techniques.

One of the more stale developments in cyclone detection and their size determination is in the field of intelligent pattern recognition algorithms using satellite images (Hossain et al., 1999; Lee and Liu, 2001; Conover, 1963; Khalid et al., 2003). Though pattern recognition has been a widely and actively researched area in many applied fields of science and engineering, in recent years it has hardly been appropriately exploited for the detection of hurricanes and tropical cyclones.

2.12 Pattern Recognition of Storm Clouds

One of the essential human brain functionalities is recognition of everyday patterns. A pattern is merely a systematic description of any target object. Humans perform the act of pattern recognition every hour of their lives, making decisions based on the analysis of pattern recognition outputs. Ability to read handwriting and analyse sounds are all part of pattern recognition. Dependant on the nature of patterns to be recognised, the process of recognition can be categorised into two major types; firstly, the recognition of exact items; and, secondly, the recognition of abstract items. Humans have the ability to recognise characters, pictures, sound, music, and other objects in their proximate environment. This is referred to as sensory recognition, which includes visual and aural pattern recognition. This recognition process involves the classification and segmentation of spatial and temporal patterns. On the other hand, a solution to a problem can be recognised without certain sensory abilities. This process involves the recognition of abstract items and can be termed conceptual recognition.

Recognition of exact patterns by human beings is considered as a psycho-physiological issue, which involves a relationship between a person and a physical stimulus. On perception of a pattern, an inductive inference and association is typically made, which is derived from past experience of learning, i.e. cognition. Human recognition as an estimation of patterns is typically associated with a set of known statistical populations, which depend on past experience of individuals. Thus, the problem of pattern recognition is regarded as one of discrimination, not between individual patterns but between populations. This is done through a search for features or primitive attributes amongst the members of a population (Sternberg, 2006; Biederman, 1987).

Pattern recognition can also be defined as "the categorisation of input data into identifiable classes via the extraction of significant features or attributes of the data from a background of irrelevant detail" (Annadurai, 2007, p. 318). Patterns are the means by which we interpret the world (Pal and Mitra, 1999). Bezdek (1981) and Rutkowska (2002) define pattern recognition as a search for structure in data. Another definition by Fukunaga (1972) states that pattern recognition consists of feature selection and classifier design, while Schalkoff (1992) defines pattern recognition as the science that concerns the description or classification of measurements. Easily described, pattern recognition is about feature analysis, clustering, and classifier design. Pattern recognition is frequently associated with identification of relevant classes that are usually characterised by patterns derived from past experience (Peeva and Kyosev, 2004). To be able to recognise and classify patterns is one of the primary characteristics of human intelligence. The science of pattern recognition has been thoroughly researched since the early 1950s (Pal et al., 1986; Pal and Pal, 2001). With the advancement in technology automated pattern recognition has achieved nearly impossible heights (Myagmarbayar et al., 2013).

Generally, the process of pattern recognition can be visualised as a sequence of three phases: data acquisition, feature extraction and classification. The data acquisition step involves obtaining data via a set of sensors, also known as sensing. The second process in pattern recognition consists of extraction of characteristic features from the input data in order to reduce the number of variables within the data. This feature extraction process involves enhancing features which should be the characterising attributes of any given pattern class. Finally a set of decision rules are defined to recognise or classify the required patterns. These rules are also known as the discrimination functions (Peeva and Kyosev, 2004; Duda et al., 2001).

Pattern recognition algorithms can be numerical or contextual (Kitler and Pairman, 1985; Jain et al., 2000; data, 1982; Li, 1995; Li and Jain, 2011). A well-designed pattern recognition algorithm can be applicable to a large variety of problems.

In order to extract significant features from the image pattern, a pre-processing stage in pattern recognition can involve filtering, edge enhancement, skeleton identification, object segmentation, contour extraction and other techniques (Rosenfeld and Kak, 1982; Gonzalez and Wintz, 1987). A complete image recognition/interpretation system is also known in the literature as a vision system (Marr, 1982; Ballard and Brown, 1982).

In any pattern recognition system, uncertainties can arise at any phase introducing ambiguity or vagueness in input images. These ambiguities and uncertainties can propagate errors through all stages of pattern recognition. It is therefore important for a pattern recognition system to have sufficient provision for representing the uncertainties involved (Pal et al., 1986; Pal, 2003).

2.13 Pattern Recognition Principles

There are various key principles in the study of patterns.

2.13.1 Membership-roster concept

When a pattern class is characterised by a list of its members, the design of a pattern recognition system may be based on the membership-roster concept. Characterisation of a known target class by a membership-roster concept also can be seen as pattern recognition by template matching. The set of patterns belonging to the same pattern class is stored in the pattern recognition system. For efficient pattern recognition, an appropriate set of patterns must be stored for each pattern class to capture its pattern variety. When an unknown pattern or shape is shown to the system, it is geometrically and texturally compared with the stored patterns one by one. The pattern recognition system then identifies the input patterns as members of a pattern class. For instance, if letters of different fonts are stored in the pattern recognition system, such letters may be recognised by the membership-roster approach as long as they are not distorted by noise. However, this concept can lead to the design of inexpensive recognition schemes, which serve the purpose in certain applications. The membership-roster approach's results are only acceptable when the condition of input pattern samples are in near-perfect match with the training data (Aziz et al., 2001).

2.13.2 Common-property concept

This particular pattern recognition ideology requires the features in a single target pattern class to share well defined properties. The common properties, for example, can be stored in the pattern recognition system. When an unknown pattern is encountered by the system, its features are extracted and sometimes coded and then are compared with the stored features. The algorithm classifies the new pattern as a member of a class with similar features. Thus the main problem in this approach is to determine common properties from a finite set of sample patterns known to belong to the pattern class to be recognised. However, it is extremely difficult, if not impossible, to find the complete set of discriminating features for a pattern class due to imperfect geometric nature of the shapes. Utilisation of this concept, therefore, often necessitates the development of feature selection techniques, which are optimum (Aziz et al., 2001; Ballard and Brown, 1982; Schalkoff, 1992; Jesan, 2004).

2.13.3 Clustering concept

Clustering refers to a task of grouping a set of homogenous features together. Several clustering algorithms exist which aim to characterise pattern classes by computationally simple recognition approaches, such as the minimum-distance classifiers. When the clusters overlap, however, it becomes necessary to utilise more sophisticated techniques for partitioning the pattern space. Overlapping clusters represent problems in observed information and presence of measurement noise. Hence, the degree of overlapping can often be minimised by increasing the number and the quality of measurements performed on the pattern of a class.

2.13.4 Heuristic Methods

Heuristic methods tend to use an existing knowledge base and can utilise the membership-roster and common-property concepts to process the knowledge base. A system designed using this principle generally consists of a set of ad hoc procedures developed for specialised recognition tasks (Fukunaga, 1972). Although the heuristic approach is an important pattern recognition concept, each problem requires a set of specifically tailored design rules. Therefore the success of heuristic models largely depends on the good understanding of the pattern being detected.

2.13.5 Mathematical methods

The mathematical approach is based on classification rules utilising common-property and clustering approaches. Unlike heuristic approaches, mathematical models tend not to be single problem specific and can be applied to a wide range of variables (Schalkoff, 1992). The mathematical approach can either be deterministic or statistical. The statistical approach is normally based on mathematical classification rules, which are formulated and derived in a statistical structure. However, the deterministic approach tends to be based on statistics free linguistic methods (Anderson, 1971).

2.13.6 Bayes Decision Theory

Over the past three decades, statistical methods have played a vital role in the development of pattern recognition techniques (Berger, 1985; Shafer, 1976; Bishop, 2006; Duda et al., 2001; Devroye, 1996; Bishop, 1995). Statistical decision theory and related fields has seen significant theoretical advances and innovations over the years. Statistical methods provide a framework for understanding pattern recognition problems when the underlying pattern generating algorithms can be satisfactorily represented by statistical models.

Bayes Decision theory belongs to the category of statistical decision theories for pattern classification. The role of this theory is mainly to provide a framework for modelling the pattern-generating mechanism. This theory is a probabilistic approach where all relevant probabilities are known. The aim of the Bayesian decisions is to assign the target objects to their probable pattern class (Robert and Tourneret, 1994).

2.13.7 Linguistic Methods (Syntactical Approach)

In a linguistic or syntactical approach for recognising embedded patterns, the target is categorised in its primitive elements, also known as sub-patterns and lexicon (Wu and Sun, 1996). These sub-patterns are then logically structured so that their relationships suggest automatic pattern recognition, often defined by their shared characteristics as suggested in common-property concept (Anderson, 1971; Tou and Gonzalez, 1974; Kitler and Pairman, 1985). These related sub-patterns are then logically placed in a hierarchical structure, very similar to a language grammar. This logical grammatical structure can be classed as pattern grammar. A pattern grammar consists of a set of variables, primitives and production rules. The most common type of grammars are regular grammars, context-free grammars, and context-sensitive grammars. The production rules define the type of a grammar (Chomsky, 1956a; Chomsky, 1956b).

Linguistic methods are useful at identifying patterns where numerical and mathematical methods fail. At times it is difficult to define a mathematical structure for an unrecognisable object, where a global linguistic approach can arrange loosely connected patterns in a hierarchical structure (Andras, 2008; Uhr, 1971; Hong, 2013)

2.13.8 Formal language theory (FLT)

The origin of formal language theory may be traced to the mid-1950s with the development by Noam Chomsky (1956a; 1956b) of mathematical models of grammars related to his work in natural languages.

According to FLT an alphabet is any finite set of symbols, while a sentence over an alphabet is any string of finite length composed of symbols. For example, given the alphabet {d, t, 0,1}, the following are valid sentences: {dd0,td1,00,0d1,1t0…}. A sentence without any symbol is called an empty sentence and is demoted by S_0. For any alphabet V, V* can be used to denote the set of all sentences composed of symbols from V, including the empty sentence. The symbol V^+ then denotes the full set of sentences without any empty sentences, i.e. V* - S_0.

Hence given the alphabet V = {a,b}, we have V* = {S_0, a, b, aa, ab, ba, bb, aaa, …} and V^+ = {a,b,aa,ab, ba, bb, aaa, … }. A language can then be defined as any set of sentences over an alphabet.

Regardless of the advances in the pattern recognition techniques and rapid developments in the field of syntactic and numerical methods to construct artificial cognition, these theories have hardly been applied to automate the detection of tropical cyclones and hurricanes (Lee and Liu, 2001; Khalid et al., 2003; Wei and Jing, 2010; Wei et al., 2011). There have been other researchers that have focused on one or two parts of a hurricane's anatomy to be detected or classified, rather than detection of the storm as a whole (Wong and Yip, 2009; Wei and Jing, 2010; Wei et al., 2011).

The following chapters will discuss a holistic approach to detect and classify hurricanes using linguistic pattern recognition algorithms.

2.14 Uncertainty and Vagueness of Storm Clouds

According to the conventional positivist view, science should strive for certainty in all its manifestations, such as precision, specificity, sharpness, consistency; hence uncertainty that could lead to imprecision, non-specifically, vagueness, inconsistency has mostly been regarded as unscientific. More recently, scientific thought has come to regard uncertainty as central to science (Johnston, 1945; Funtowicz and Ravetz, 1990; van Asselt, 2000; Lemons, 1996; Goodchild and Zhang, 2002).

2.15 Fuzzy Logic

The traditional hard computing paradigm is often not suitable for many real life problems Sankar (1996). Precise models for solving simple real life problems under the conventional computing paradigm become not only very difficult but also expensive. Hence problems with embedded uncertainty require imprecise solutions. The first stage of the transition from the traditional approach to the modern approach of tackling uncertainty began in the late 19th century (Charles, 1878). Black (1937) contributed to ideas of uncertainty by publishing a paper entitled 'Vagueness: an exercise in logical analysis". In this paper he introduced the concept of vague sets as compared to the traditional crisp or hard logic sets. This ideology was later known as Soft Computing, according to which a computer provides results using an imprecise logical system. However, recognition of the importance of uncertainty emerged strongly in the 1960s when Zadeh (1965), introduced a theory known as fuzzy sets. The theory of fuzzy logic describes sets with boundaries that are not precise. Unlike traditional sets, an object's membership in a fuzzy set is not a matter of yes or no but rather a matter of degree. Fuzzy sets became the new way to represent vagueness in analysis of everyday problems; they attempt to model human reasoning/thinking processes.

Fuzzy sets, also known as membership functions, tend to map real numbers from a universe of discourse to [0,1]. In other words the membership values range from 0 to 1 (Zadeh, 1993; Zadeh, 1996b; Zadeh, 1997; Chi et al., 1996). These membership functions cannot be confused with probability. Membership functions possesses elasticity; the higher the value of membership of an object to a class, the less the imprecisely defined concept of the fuzzy set must be stretched to accommodate the object (Sankar, 1996; Pal, 2003). Fuzzy logic provides a conceptual framework to model the world inundated by uncertainty and imprecision (Zadeh, 1996a).

Since fuzzy sets help characterise imprecise properties of any known or unknown patterns, they can be used effectively to model vagueness associated with simulated real world problems. Fuzzy logic is based on the theory of fuzzy sets and approximate reasoning. It defines logic based on approximate reasoning, which is more similar to real world problems than the traditional logical system and thus helps fuzzy logic develop better and effective solutions for the inexact and imprecise issues (Bezdek and Castelaz, 1977; Cox, 1992; Zadeh, 1993; Peeva and Kyosev, 2004; Wadhawan et al., 2013).

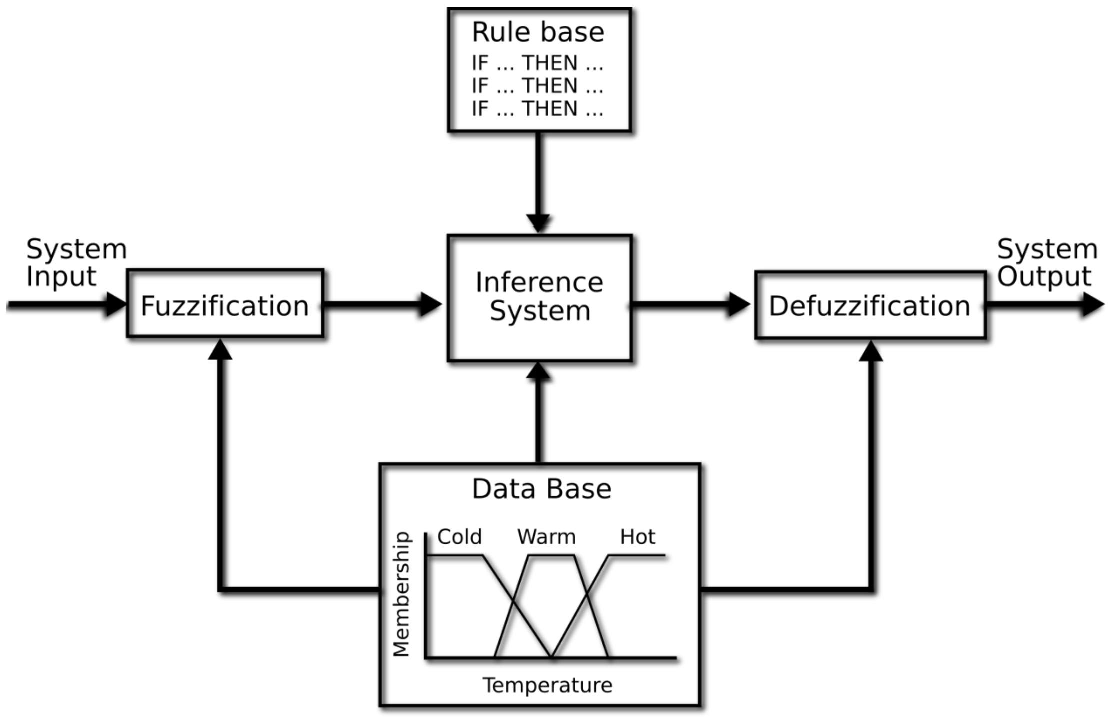

Figure 2.24: A typical Fuzzy System with its individual components (Kovacs, 2011).

The importance of fuzzy logic derives from the fact that most modes of human reasoning are approximate in nature. In fuzzy logic using approximate reasoning maps everything as a matter of a degree of membership. Any real world problem can be fuzzified with inference of knowledge based rules implemented as fuzzy membership functions. In fuzzy logic inference is a process of propagation of input values to an approximate output based on fuzzy functions (Zadeh, 1992). Like traditional crisp sets, fuzzy sets can also be mathematically manipulated.

2.15.1 Fuzzy systems

A fuzzy system usually has three components: fuzzification; inferencing; and defuzzification as shown in figure 2.24 above. The fuzzification step provides a fuzzy set representation of a crisp input by which a fuzzy degree of membership can be obtained. Membership functions are used to define fuzzy inputs and outputs required to characterise the fuzzy model of a system. The inference process can also utilise a bank of fuzzy rules that assist in fuzzifying the inputs. The type of processing depends on the fuzzy model being used. If a fuzzy clustering model is used, then the processing may be an iterative optimisation of an objective function (Bezdek, 1981); while for a fuzzy controller the processing means the use of some reasoning scheme to compute a fuzzy consequent (Driankov et. al, 1993).

The defuzzification phase produces crisp action from a fuzzy conclusion. Depending on the type of fuzzy system, the defuzzification scheme may be different. For example, in the case of a fuzzy classifier, the defuzzification scheme can be to find the class with highest membership value. On the other hand, for a fuzzy control system, the defuzzification is obtained by aggregating several output fuzzy sets using one of several schemes, like centre of mass, height method (Driankov et. al, 1993). Fuzzy rules help define the membership functions deduce the final crisp output as shown in figure 2.25.

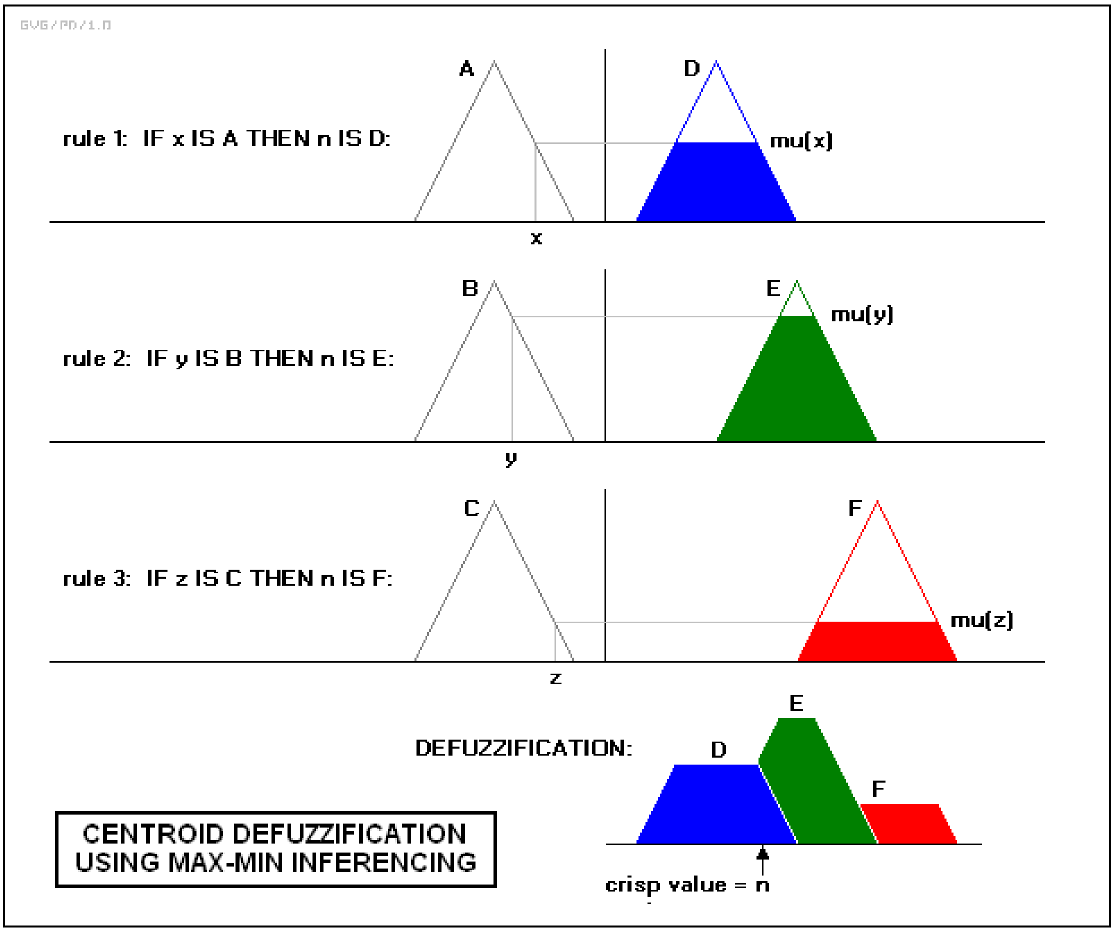

Figure 2.25 Defuzzification with the help of rule-based approach (Cox, 1992)

A fuzzy system can be an iterative process; the input values are passed on to a fuzzifier where they are converted into suitable fuzzy functions or fuzzy sets in order to tackle the uncertainty associated. The fuzzified measurements are then passed on to the inference engine which, with the help of a knowledge rule base, evaluates the fuzzified set and generates the approximate results. The fuzzified results must then be converted back into an applicable crisp results (figure 2.24).

There have been many attempts investigating the application of fuzzy set theoretic approaches to real life pattern recognition problems. Some of these have been used (Pal et al., 1986; Bezdek and Pal, 1992; Laface and De-Mori, 1992; Melin, 2012) for recognising speech patterns that are biological in origin, indicating a considerable amount of fuzziness. Pathak and Pal (1987) demonstrated an application of fuzzy and fractionally fuzzy grammars in syntactic recognition of ages of different bones from X-ray image patterns.

2.15.2 Fuzzy Pattern Recognition

The mid-1960s noticed the recognition of fuzzy logic in the pattern recognition field. Research on the application of fuzzy set theory to supervise pattern recognition by Bellman et al. (1966) was received successfully. Bellman et al. (1966) proposed two phases of pattern recognition—abstraction and generalisation. The process of abstraction was synonym to the modern process of fuzzification, while generalisation was performed when the fuzzy membership functions were used to devise the values of μ for patterns that were originally not present in the training samples. Zadeh (Bellman et al., 1966; Zadeh, 1996b) also suggested consideration of linguistic features and fuzzy relations in representing a class. Sankar (1977) and Majumder (1977) outlined an early application of fuzzy sets for decision theoretic classification, where a pattern is considered as an array of linguistically phrased features denoting certain properties and where each of these features is a fuzzy set. The variation of the recognition score with the change of fuzziness in the linguistically phrased feature values has subsequently been investigated (Pal et al., 1986). These classifiers have also been used for designing a self-supervised recognition system (Pathak and Pal, 1987). Nath et al. (1983, 1985) proposed a classification model applicable in the soft sciences where enough a priori knowledge about the classifier is available from the expert in linguistic form.

Literature dealing with fuzzy pattern recognition and fuzzy clustering is now quite extensive. Recently Nagalakshmi and Jyothi (2013) reviewed a fuzzy clustering approach to highlight the importance of edge detection for image segmentation. The main aim of fuzzy set theory is to manage uncertainties in various applications to a reasonable extent, particularly in decision making models under different kinds of risk, subjective judgement, vagueness, and ambiguity. Since this theory is a generalisation of the classical set theory, it has greater flexibility to capture various aspects of incompleteness or imperfection in information about a situation (Zadeh, 1965).

Although the task of feature selection plays an important role in designing a pattern recognition system, the research in this area using fuzzy set theory, for hazard identification particularly in hurricane analyses, has not been significant. Bezdek and Castelaz (1977) showed an application of the fuzzy c-means clustering algorithm to select an optimum feature subset from the available features to avoid appreciable loss of classifier performance with the reduced set of features. Pal and Chakraborty (1986) explained an application of fuzziness measures of a set in selecting features without going through classification. This has then been extended to evaluate the importance of any subset of features to provide an average quantitative index of goodness (Pal, 1992). Pedrycz (1990) also stressed the importance of the use of fuzzy and probabilistic methods in the field of pattern recognition. Pedrycz (1990) clearly states the use of fuzzy measures and fuzzy clustering techniques in various classification hybrid methods, especially for feature selection.

Recent years have highlighted an increased importance of linguistic, knowledge and rule based decision support algorithms and their incorporation in traditional fuzzy logic (Ishibuchi and Nakashima, 2001; Duda et al., 2001; Ho et al., 2012; Wei et al., 2012; Laha and Das, 2011; Cordón et al., 1999). However, a gap still exists in successful application of the rule based fuzzy systems in the field of hurricane and tropical cyclone detection (Olander and Velden, 2011; Duong et al., 2013; Shah et al., 2012).

2.15.3 Fuzzy Rule Based Systems

Rule based systems have also gained popularity in pattern recognition activities. By modelling the rules, facts and expert knowledge in terms of fuzzy sets, it is possible to make interfaces using the concept of approximate reasoning. Such a system has been designed for automatic target recognition using 40 rules (Nafarieh and Keller, 1991). Nozaki et al. (1996) proposed an adaptive fuzzy rule based pattern recognition system that could adjust the grade of uncertainty associated with fuzzy sets. A system such as this assisted Abebe et al. (2000) to estimate precipitation levels for a weather station based on the knowledge base from the other stations in the region.

With conventional probabilistic and deterministic classifiers, the features characterising the input patterns are considered to be quantitative in nature. The pattern vectors having imprecise or incomplete specification are usually ignored or discarded from the design and test sets. For this reason, it may become convenient to use the linguistic variables and hedges in order to describe the feature information. In such case, it is not appropriate to give exact representation to uncertain feature data. Rather, it is reasonable to represent uncertain feature information by fuzzy subsets.

The uncertainty in classification or clustering of patterns may arise from the overlapping nature of the various classes. This overlapping may result from fuzziness or randomness. In conventional classification techniques, it is usually assumed that a pattern belongs to only one class. This is not necessarily realistic physically, and certainly not mathematically. A pattern can and should be allowed to have degrees of membership in more than one class. It is therefore necessary to convey this information while classifying a pattern or clustering a data set. Another problem is that of determining the boundary or shape of a class from a set of sampled points. There are various approaches by Pathak (Pathak and Pal, 1987; Pathak et al., 1984; Pathak and Pal, 1986) that attempt to estimate an exact shape for the area in question by determining a boundary that contains some or all of the sample points. It may be necessary to extend the boundaries to represent the possible uncovered portions by the sampled points. The extended portions should have lower membership values to belong to the class than the portions explicitly highlighted by these points. The size of the extrapolated boundary should also decrease with an increase in the number of sample points. Similar techniques can be utilised to estimate a fuzzy boundary, provided only sample data are in existence. Conventional approaches to image analysis and recognition (Gonzalez and Wintz; Rosenfeld and Kak; Marr; Ross, 2009; Li et al., 1994; Ahmed et al., 2002) consist of segmenting the image into meaningful regions, extracting their edges and skeletons, computing various features and primitives of, and relationships among, the regions, and finally, developing decision rules and grammars for describing, interpreting and/or classifying the image and its sub-regions. Since the regions in an image are not always sharply defined, uncertainty can arise within every phase of the image segmentation. Ignoring the uncertainty in analyses at an early stage of image classification can cause it to feed through the system in to the results. According to Pal (2003), it is essential for any image based pattern recognition system to provide representation of uncertainties at all processing stages involved. If this is achieved appropriately, the ultimate output of the system will possess minimal uncertainty.

It is also important to take into consideration the processing and recognition of greyscale image patterns (Peters et al., 2007). A greyscale image possesses ambiguity within each pixel because of the possible multi-valued levels of brightness. This pattern uncertainty is due to inherent vagueness rather than randomness. If the grey levels are scaled to lie in the range [0,1], the grey level of a pixel can be regarded as its degree of belonging in the set of high-valued (bright) pixels; thus a grey tone image can be viewed as a fuzzy set. Other classified aspects of a digital image such regions and features that are normally not crisply defined can similarly be regarded as fuzzy subsets (Ghosh and Ghosh, 2002; Rosenfeld and Kak, 1982; Pal, 1992). Basic principles and operation of image processing and recognition in the light of fuzzy set theory can be distinguishably seen in Sankar and Majumder (1986).

The Australian government's Department of Agriculture, Fisheries and Forestry has clearly highlighted a research gap in clear understanding of the threats caused by tropical cyclones (DAFF, 2012). There has been significant resources dedicated to the hazard management of cyclone related events. However there is still an urgent need to improve the accuracy of cyclone detection techniques especially with assistance from remotely sensed data (Sampson and Schrader, 2000b; Sampson et al., 2012; Yu et al., 2012; Cossuth et al., 2012; Gombos et al., 2012; Belanger et al., 2012; Brennan and Majumdar, 2011; Galarneau and Davis, 2012).

2.16 Fuzzy Logic and Storm Clouds Pattern Detection

As previously mentioned in section 2.8.1, nephanalysis based on satellite imagery has been around since the early 1960s (Conover, 1962). However, at present only limited systems can fully automate the process. Likes of (Dvorak (1975); Olander and Velden (2007)) have attempted to eliminate human involvement in the process of storm detection with limited success. Even multivariate and multi sensor tropical cyclone forecasts are not free from error. Errors in recognising the centre of the storm of a tropical cyclone can impact the accuracy forecasts (Rappaport et al., 2009). Moreover, research towards tackling uncertainty in tropical cyclone forecasting from satellite imagery has always been limited (FMS, 2013; Torn and Snyder, 2012; Dvorak, 1975; Tsai and Elsberry; Iman et al., 2002; Poroseva et al., 2007). Errors can also occur due to mismatch of cloud boundaries in the detection phase, and also from the forecasting techniques themselves (Kovordányi and Roy, 2009).

Many pattern recognition algorithms analyse cloud features' patterns to estimate the intensity of tropical cyclones. These algorithms use adaptive patterns segmentation and feature extraction techniques to identify various regions of tropical cyclones in the satellite imagery (Abebe et al., 2000; Duong et al., 2013; Nozaki et al., 1996). Tropical cyclone recognition is a multilevel process requiring a sequence of algorithms to detect various nephanalysis parameters present in satellite imagery of suspected hurricanes. The multilevel and multivariate approaches make the algorithms complex and at times biased. Complex relationships between various environmental variables required for hurricane track forecasting and monitoring require organisations around the world to invest in automated systems (Sampson and Schrader, 2000a; NRL, 2011; Talukder et al., 2008; NHC, 2009). These automated algorithms provide a means of tracking the storms and classifying their intensities without any manual expert knowledge input. However, all of them require certain levels of human interaction for accurate assessments. A range of algorithms have been developed in the past four decades for systematic analysis and forecasting of tropical cyclone intensity. Though some of these procedures are currently being used by forecasting agencies, some difficulties and technical complexities make them error prone. To avoid uncertainty and biased errors caused due to complex detection of numerically and geometrically complicated cloud features, vagueness of cloud parameters needs to be embedded in the algorithms. Techniques such as fuzzy logic can reduce the levels of uncertainty feeding in to the final output.

Application of fuzzy logic has been in practice since the late 1980s (Bezdek and Pal, 1992). In a fuzzy rule based system experts define a knowledge base that sets the fuzzy membership functions. Defining the fuzzy rules can be an iterative process, where training data can be used to define the sets, while after validation the mismatch results can be used to retrain the fuzzy knowledge base. Once these fuzzy rules have been agreed, the image is processed either at a pixel level or segment level depending on the application and methods identified. Careful consideration needs to be given when constructing fuzzy rules from training data (Wang and Mendel, 1991; Wang and Mendel, 1992). Fuzzy rules are merely "if-then" conditional structures which allow the relationships in the data to be modelled. Many researchers in the past two decades have devised methods to efficiently generate fuzzy rules (Bentley, 2000; Dehzangi et al., 2007; Finn, 1999; Mallinson and Bentley, 1999; Wu and Chen, 1999; Klir and Yuan, 1995). Chiu (Chiu (1994); 1997) specifically discusses the fuzzy rule generation for pattern classification. According to Chiu, training data sets are classified into the required patterns; a subtractive clustering technique is applied to the input space of each identified class from which the rules are extracted. While Dehzangi et al. (2007) describes algorithms for finding appropriate thresholds when moving from input space to the output space.

Researchers since the 1990s have been suggesting techniques for using fuzzy logic approaches in the application of automated cloud classification using satellite imagery. Baum et al. (1997) proposed fuzzy logic based cloud classification methods to distinguish between clear skies and single and multilayered clouds. Pal et al. (2006) and Lizarazo and Elsner (2009) used a fuzzy rule-based system to segment segments in RADAR imagery and confidently used a linguistic approach to define the fuzzy rules used. Moreover, several researchers have used fuzzy rule based systems or fuzzy c-mean clustering approaches to distinguish between clouds and land surfaces (Key et al., 1989; Lizarazo and Elsner, 2009).

2.17 Summary of Literature Reviewed

This chapter has reviewed and analysed work related to a versatile range of field of expertise associated with this research. Due to the complexity of the subject area, the literature review was categorised into three clear fields; climatology of cyclones, pattern recognition and fuzzy logic.

Anthes (1982a) described tropical cyclones as a non-frontal synoptic scale, low pressure system which originates in the tropics and enjoys warm sea surface temperature of at least 26^{o}C. According to NOAA (2012; 2010) globally tropical cyclones intensities are classified using either the Saffir Simpson Scale or Dvorak's T-Classification. The Saffir Simpson Scale has 5 intensity categories based on the sustained wind within the storm, while Dvorak's T-Classification (Dvorak, 1975) classifies a tropical cyclone by its T number ranging from 1 to 8. Dvorak also provides half intensity grades for more accurate estimation. Dvorak's T classification technique has been widely used by cyclone forecasting agencies around the world. One reason for its popularity is the level of objectivity it provides for the detection of cyclones and the estimation of their intensity detected from satellite imagery. However, Dvorak has updated his algorithms (Dvorak, 1984) to eliminate the subjective manual interpretation, although he did not achieve a fully objective model for an unbiased estimation. Olander and Velden (2007), Velden et al. (1998a) and Zehr (1989) have since proposed advances to Dvorak's original methodology, but still could not achieve high accuracy. Moreover, Olander and Velden (2011) both concentrate on the intensity estimation, disregarding the actual detection of the existence of tropical cyclones.

Before the launch of first meteorological satellite, forecasting and estimation of storm tracks and intensity was mainly carried out using data gathered via ground based observations, which made the forecasts heavily dependent on landfall. With the availability of satellite imagery researchers have used remotely sensed data to forecast the emerging storms. However reliance on ground based sensors is still extremely common. During the 1980s, forecasting of the track and intensity of tropical cyclones was mainly based on statistical methods incorporating satellite images and observed meteorological datasets. It was in the early 1990s, remote sensing techniques emerged and were used successfully for cyclone forecasting and track prediction (Le Marshall et al., 2002; Fitzpatrick, 1997; Leslie et al., 1998). In addition, Bankert and Tag (2002b) measured the intensity of tropical cyclones based on satellite images and data from a Special Sensor Microwaver Imager (SSM/I), successfully incorporating different remotely sensed data into forecasting. Although, the Dvorak model for intensity estimation was successfully received, it involved human expert decisions which make it subjective and unreliable by introducing uncertainty. Even though Olander and Velden (2007) improved Dvorak's algorithm by introducing objectivity, they failed to introduce the capability of the algorithm to tackle uncertainty.

Meteorological satellites captured imagery of cyclone bearing oceans either via polar orbiting platforms or geostationary satellites. Geostationary satellites can provide data at a much higher temporal resolution than polar orbiting satellites. Cloud classification from satellite images required expert algorithms to intelligently detect known patterns associated with tropical cyclones. These ambiguous cloud patterns needed to go through logical pattern recognition systems to identify the existence of tropical storms. Linguistic methods and formal language theories can resolve all issues associated with constructing pattern hierarchies for the detection of tropical cyclones solely from remote sensing. However this is still an area that requires further research. Li et al. (1994) and Bezdek et al. (2005) defined pattern recognition systems that could cater for uncertainties in complex objects. Lee and Liu (2001), Demirci et al. (2004) and Kim et al. (2010) devised fuzzy logic based pattern recognition systems to predict tropical cyclone intensity and track. However, the detection of hurricane and tropical cyclone centres remained a complex and erroneous procedure (Wei et al., 2011; Olander and Velden, 2007).

Olander and Velden (2011; 2007) stressed that there is still need for a more objective approach to identify the centre of the detected storms. Moreover, the accuracy of storm detection and intensity estimation obtained solely from satellite imagery needs to improve.

The literature review in this area of fuzzy rule based pattern recognition of tropical cyclones from satellite data has revealed that:

- Storm centres need to be identified more accurately,
- The accuracy of automated intensity estimation needs to improve, and
- The successful algorithms need to be less computing intensive so that they are able to handle high temporal resolution imagery.

CHAPTER 3. THE DEVELOPED FUZZY LOGIC SYSTEM FOR TROPICAL CYCLONE DETECTION

3.1 Introduction

This chapter details the structure of the developed fuzzy logic pattern recognition system to detect and classify intensity based on the WMO T-Classification scale. The aim of this research as highlighted in section 1.5 is to develop a fully automated system that can detect tropical cyclone using satellite imagery and classify the intensity of the detected cyclone using a soft computing approach. The aim was achieved by designing, developing and evaluating the algorithms proposed in this research. These algorithms are classed into four categories; pattern classification and recognition, syntactical language engine, fuzzy controller and intensity classifier. The system has a modular structure where independent modules representing key algorithms integrate seamlessly to create a fully automated cyclone detection system. The structure of the developed system is discussed and illustrated in the following section.

3.2 The Developed System

Tropical cyclone detection, tracking and monitoring techniques can be automated using digital analysis of satellite data. However, their severity assessment has traditionally relied on expert interactive interpretation by hurricane meteorologists using well-established hurricane classification systems such as the WMO 'T' Classification (Dvorak, 1975; Dvorak, 1984) and the Saffir Simpson Scale (NOAA, 2012), to determine their intensity and force. The subjective nature of T-classification techniques makes it difficult to automate the process. Additionally, the T-classification technique fails to deal with the uncertainty in the shape definition of the cloud patterns belonging to cyclones as these features do not have clearly defined boundaries. In the past, attempts (Olander and Velden, 2007; Cossuth et al., 2012; Velden et al., 1998a) have been made to objectively automate Dvorak's technique, although there still remains the issue of uncertainty and accuracy of storm detection (Olander and Velden, 2011). T classification reference chart can be seen in figure 3.1. Due to complex numerical algorithms used in current forecasting techniques, it is essential that the developed system uses cost and time effective models in order for its application to be possible in parts of the world that need it, such as the developing countries.

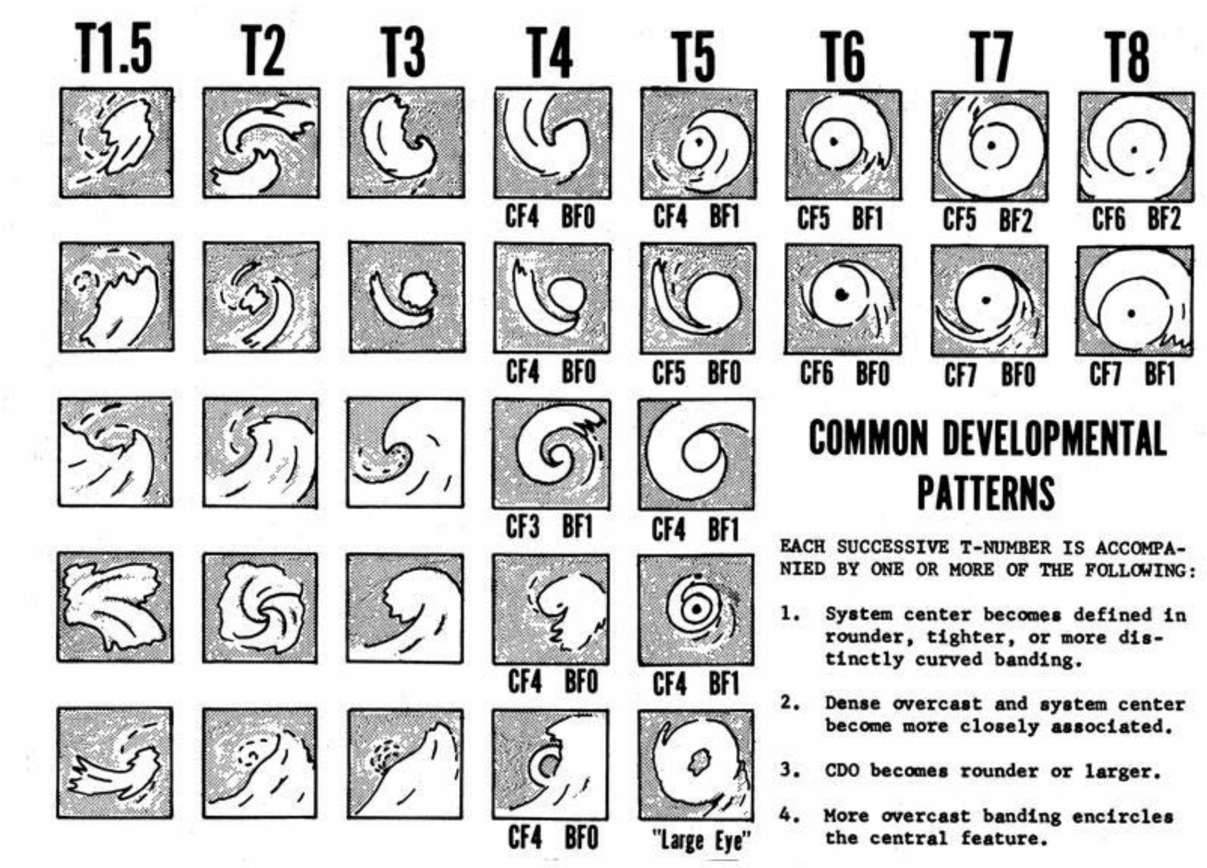

Figure 3.1: Dvorak's T classificaiton reference chart.

As part of this research, a fuzzy logic rule based model was developed and implemented to overcome these shortcomings and to fully automate the process in order to eliminate the subjectivity involved. Moreover, the introduction of fuzzy logic meant that uncertainty was addressed during the intermediate stages of the system, hence reducing its occurrence in the final output.

According to (1977) it is the patterns formed by tropical cyclone cloud canopies that are related to the storm intensity and not the cloud density. Therefore the model has been created by developing a 'syntactical grammar' of primitives identifies as the building blocks typically associated with cyclones. The model generates a set of rules by which a tropical cyclone or a hurricane can first be discriminated from other weather systems. Once a tropical cyclone is detected the model examines the shape, form and the presence of other characteristics of the cloud canopy in order to determine its intensity (Dvorak, 1975; Dvorak, 1984; Khalid et al., 2005). The overall structure of the proposed system is illustrated in figure 3.1.

The proposed system is composed of four main modules: a Pattern Classification Module, a Grammar Engine, a Fuzzy Engine and the Intensity Classifier. The system also has a user interface module, a knowledge base and a central database, known as 'storm database', to store the final results. The dotted boundary indicates the developed system, while the entities outside the dotted line are independent of the functionality of the developed modules. Typically, a user, via the GUI module, inputs a set of satellite imagery from an image database and feeds them to the Pattern Classification and Recognition (PCR) module. The PCR module individually processes these images, by applying multiple algorithms and with the help of the Fuzzy Engine (FE), to extract and segment the required features. After a set of known cloud features are recognised, the PCR module passes the data to the Grammar Module (Myagmarbayar et al.), which applies linguistic rules on the detected primitives to identify the existence or absence of a tropical cyclone. Once a cyclone is detected, it is stored in the Storm database and subsequently passed on to the Intensity Classifier (IC) module. The IC module uses the FE to classify the detected storm's intensity. FE has a bank of knowledge base which it uses to apply the appropriate rules to the input dataset.

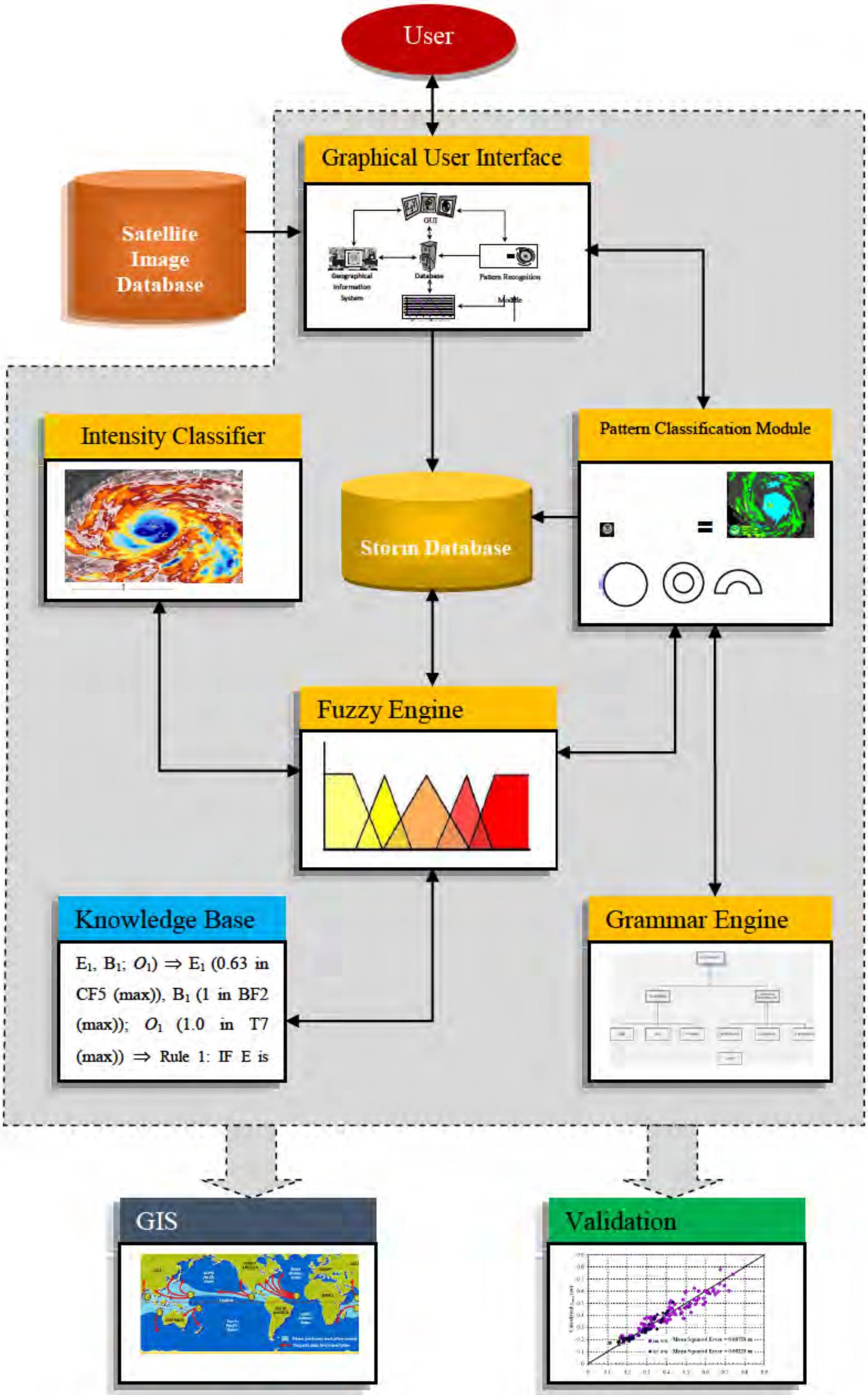

Figure 3.2: Structure of the proposed system.

The proposed system was developed in a Visual C++ environment; this allowed the algorithms to execute faster and use less memory to process. One of the drawbacks of using a standalone C++ environment was its inability to recognise georeferenced coordinate system. Hence the satellite images were converted to Tiff files with their world file (*.tfw) stripped before processing. The world files were associated back to all the corresponding resulting images after processing. This ensured that the resulting images had the same spatial resolution and pixel dimension as their predecessors; otherwise the world file wouldn't match the GeoTiff data coordinates.

3.3 Geostationary Satellite data

Geostationary Operational Environmental Satellites (GOES) is a suite of satellites which are placed in geosynchronous orbits around the Earth. The geostationary or geosynchronous orbits are located in the equatorial plane and the satellites orbit at the speed of the rotation of the Earth so that they are stationary relative to the location on Earth. This allows them to constantly monitor a particular region. GOES has been used in meteorological monitoring since its first launch in 1975 (OSPO, 2013). Since then there has been 15 satellites in this series successfully launched. However, currently there are only 4 in operation, i.e. GOES 12, GOES 13, GOES 14 and GOES 15. GOES is operated by the US National Environmental Satellite, Data and Information Services (NESDIS).

Meteosat is another suite of geostationary satellites with similar characteristics as GOES. Unlike GOES, Meteosat is operated by the European Organisation for the Exploitation of Meteorological Satellites (EUMETSAR), an intergovernmental organisation composed of 27 EU member states. Meteosat’s second generation satellites are currently in operation over Asia and Africa (EUMETSAT, 2013). Figure 3.2 shows an example of full disk images from both GOES and Meteosat.

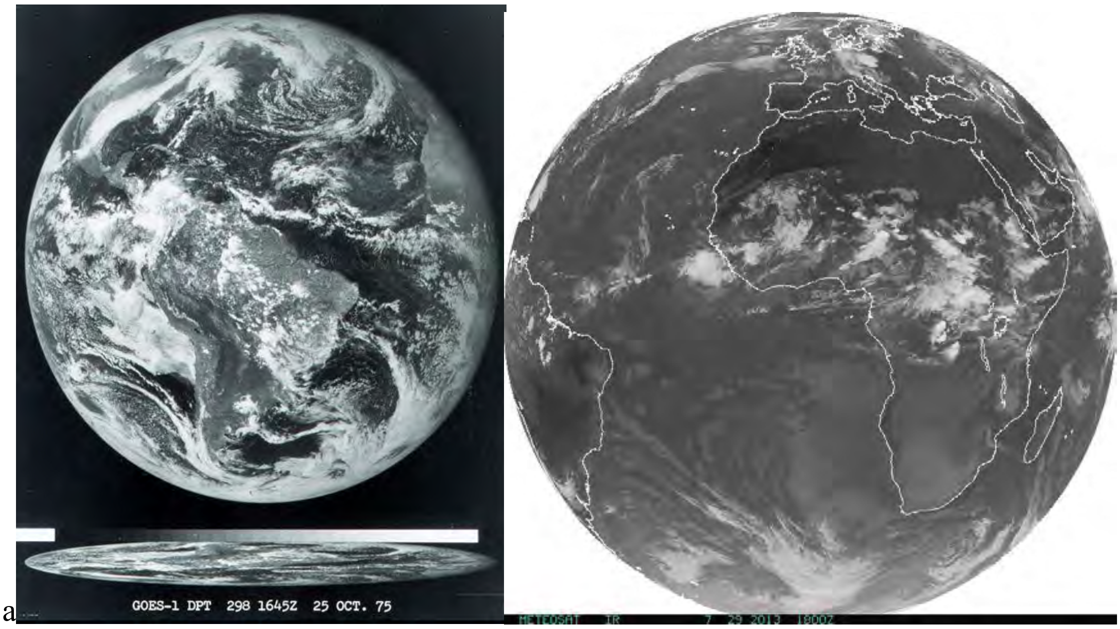

a

Figure 3.3: [left] First image captured by GOES-1 in 1975; [right] An IR image captured by Meteosat July 2013

Both these satellites, amongst other geostationary satellites, play a vital role in daily forecasting of weather and tropical storms. These satellites have multiple sensors on board that allow researchers to have a multispectral view of the atmosphere from space. The most common range of wavelengths used for meteorology are Thermal Infrared (Pal et al.), Visible and Water Vapour. A combination of Meteosat and GOES has had global coverage since the early 1970s. Figure 3.3 provides a good understanding of the coverage of these geostationary satellites in the equatorial place.

3.4 Training and Validation data set

The National Climate Data Center (NCDC) at NOAA hosts an historical archive of GOES and Meteosat images covering all known tropical cyclones and hurricanes. This archive is known as the Hurricane Satellite dataset (HURSAT). The temporal coverage of HURSAT offers satellite data from May 30 1978 to Dec 15, 2009 with a 3 hourly global image cover of 3321 tropical cyclones and 299,260 satellite images. The archive covers a range of satellite platforms, such as SMS-2, GOES -1 to 13, Meteosat-2 to 19, GMS-1 to 5, MTSAT-1R, MTS-2 and FY2-C/E at an approximate resolution of 8km (Knapp and Kossin, 2007). The spatial resolution decreases to around 10km near the equator. The TIR channels imagery in this archive are calibrated and tested for long term stability (Knapp, 2008), with the calibrated archive known as HURSAT-B1. This archive is a unique database due to its complete coverage of calibrated TIR imagery for all tropical cyclones and hurricanes since 1978. Hence this archive was used to validate the developed system. A combination of HURSAT-B1 TIR imagery and HURSAT-AVHRR data were used to train the fuzzy pattern recognition algorithms. HURSAT-B1 orginates from the GOES satellites while HURSAT-AVHRR is an archive of AVHRR satellite data. Even though only the North Atlantic basin was used for validation, cyclones from the Indian Ocean were also used for training purposes, due to their similarity in nature.

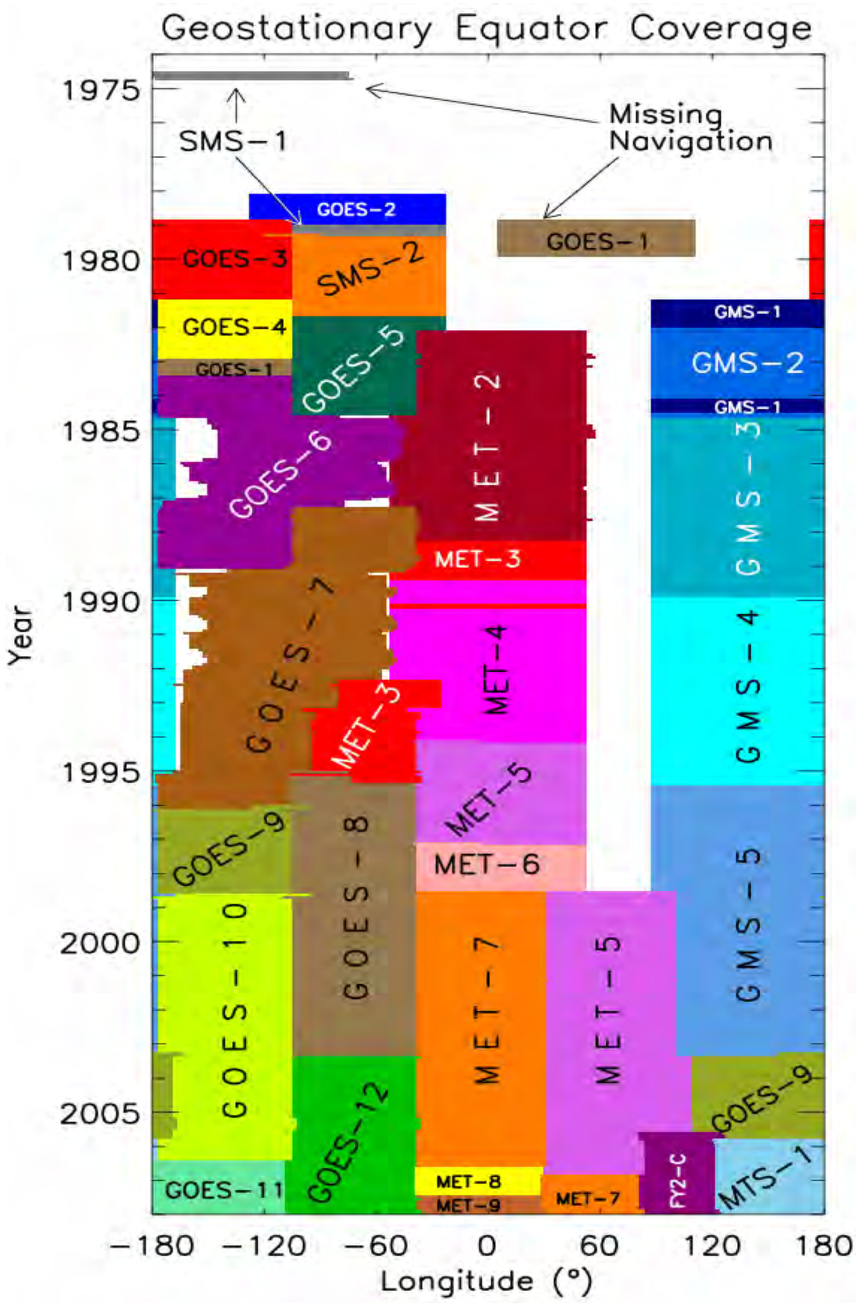

Figure 3.4: Spatial coverage of geostationary satellites since 1975.

NOAA's Advanced Very High Resolution Radiometer (AVHRR) offers the coverage of imagery at a higher spatial resolution of 1.1km, which in this study is resampled at 4km for consistency with other datasets. A combination of AVHRR, GOES and Meteosat data were used to train the pattern recognition algorithms. However, only GOES and Meteosat were used to test the developed system due to low temporal resolution of AVHRR data set. Temporal resolution of the AVHRR is limited to 2 to 8 images per day, making it relatively inconsistent. The lower spatial resolution as compared to the original data, allowed the whole period from 1978 to 2009 to be processed seamlessly, due to relatively lower amounts of data. Moreover, the North Atlantic was chosen as the study area due to its complete coverage of GOES and Meteosat images (figure 3.4). In addition, the existence of comprehensive forecast databases such as International Best Track Archive for Climate Stewardship (IBTrACS) and Hurricane Data (HURDAT) for North Atlantic provides a justified platform for the validation process. These databases are the National Hurricane Center's (NHC) official post storm analyses, while the latter are considered as the best track data and intensity estimates for the North Atlantic basin (Landsea et al., 2004a; Landsea et al., 2004b; Landsea et al., 2008; Landsea et al., 2012). Figure 3.5 shows the study area with example satellite images of an emerging hurricane GUSTAV 2008, with the HURDAT storm locations plotted for density estimation.

For consistency 6 hourly images were processed, instead of 3 hourly imagery available via HURSAT, resulting in 4 images per day, i.e. 0000hrs, 0600hrs, 1200hrs, 1800hrs. This allowed a reasonable number of images to process to validate the system, while keeping it consistent with the temporal resolution of HURDAT. HURSAT-B1 version v05 was used with the temporal resolution reduced to 6 hours to match HURDAT. Though HURSAT-B1 v05 is a complete record of all storm satellite images in the North Atlantic Basin, many storms never reached the stage to be categorised as tropical storms; only 375 storms in the region were named for the period from 1978 to 2009. All 375 storms were processed using the developed system, starting at a low depression stage all the way up to their highest intensity and then back to a deteriorating tropical depression stage, covering a complete cyclogenesis of each storm. 11717 images were processed in total, encompassing 8311 images with tropical storms and 3037 images with hurricanes. Table 3.1 and table 3.2 summarises the details of the data used for training and validation.

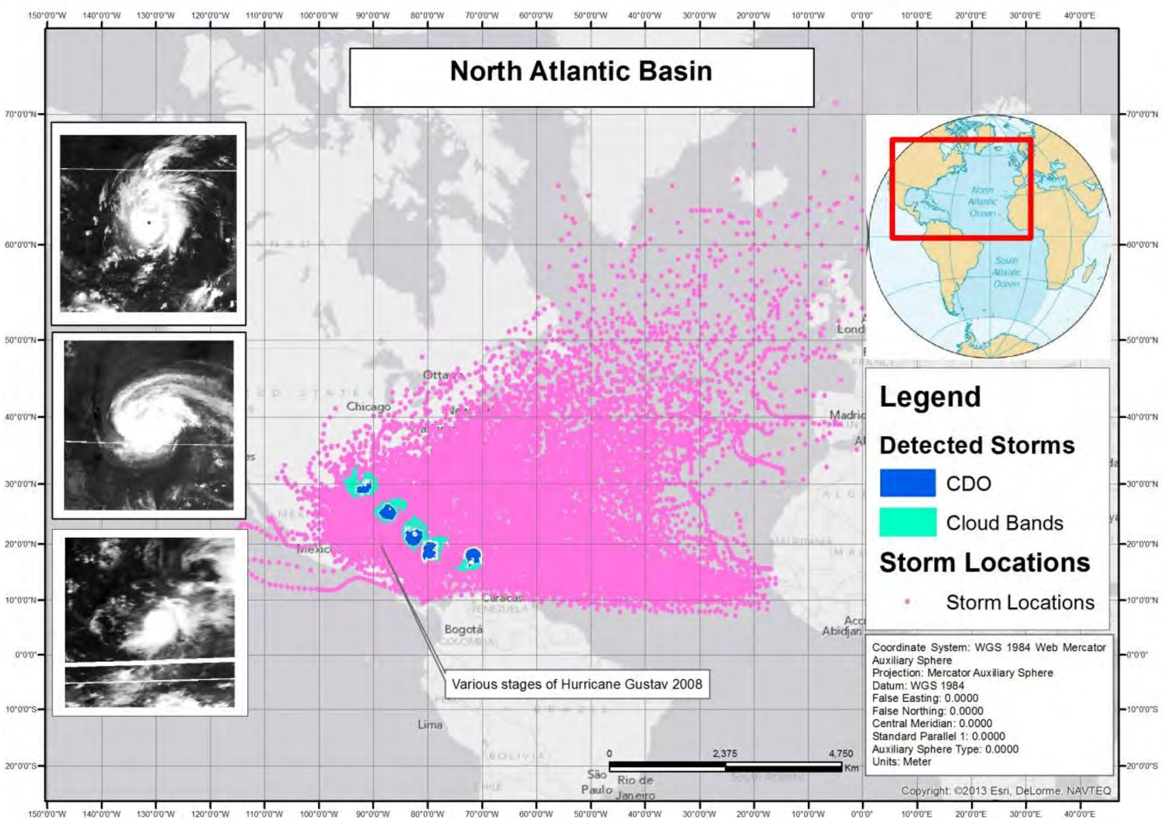

Figure 3.5: North Atlantic Hurricane Tracks of 2008

Table 3.1: Summary of data used in training of the developed system using HURSAT data.

Satellites	NOAA	GOES	Meteosat
Spatial Resolution	Interpolated to ~4Km	~8Km	~8km
Temporal Resolution	Varies: 2 – 8 images/day	3 hourly	3 hourly
Number of storms processed	35	40	25
Number of Images processed	500	500	500
Range of years	1978-2009	1978-2009	1978-009

Table 3.2: Summary of data processed and used in validation of the developed system

Satellites	IBTrACS & HURDAT	GOES	Meteosat
Spatial Resolution	-	~8Km	~8km
Temporal Resolution	6 hourly	6 hourly	6 hourly
Number of storms processed	375	375	
Images with storms	-	8311	
Images with hurricanes	-	3037	
Number of Images processed	11717	11717	
Range of years	1978-2009	1978-2009	1978-009

3.5 Graphical User Interface (GUI)

The user interface plays a vital role in the ease of operation of the system. A user-friendly graphical interface was developed in order to access the system easily and efficiently. The GUI is based on a standard Windows environment. Users can interact with the system by providing satellite images as inputs and commencing the pattern recognition phase. Moreover, the system is designed to provide the users with the option of either running the entire integrated system or operating the individual modules separately. In addition, the GUI allows the user to interact with the embedded relational database to extract the results of processing in a standardised and structured format.

3.6 Database – The Storm Database

A relational database was developed to record extracted information from the PRM and FE. The storm database stores the measurements of the storm features, area of influence, dimensions of the area covered, temporal information of the storm, and the intensity of the storm. The storm database is a dynamic database and is updated automatically by the system during the pattern detection and intensity classification phases. The Microsoft Access database management system was used to develop the required database. Appendix 1 illustrates the entity relationship schema of the database.

3.7 Geographical Information System (GIS)

The processed images and intensity data were analysed through to a standard GIS application to investigate the spatial trends within the data. Moreover, storm centre distances were also calculated using GIS. Due to incompatibility of the developed system with spatial referencing, the processed image files were associated with their world files to ensure spatial analyses could be performed. Analyses such as area of influence, distance root mean square errors for storm centres, geographical variable regression and ordinary least square regression were applied to examine relationships between the observed and predicted intensity and storm centre location.

3.8 Knowledge Base

A knowledge base is a distinctive form of a repository of formal description of meaningful information with symbolic encoding in a conditional logical structure. In the artificial intelligence domain, in addition to data, knowledge includes abstract information, logical rules and criteria. A knowledge base is commonly used in the reasoning process with the help of logical expert rules that define a solution to a complex problem. The knowledge base in the developed system consists of a hybrid of fuzzy and crisp rules that were employed to classify and segment satellite imagery, detect cyclone associated patterns, and estimate the storm intensity. Originally 153 rules were suggested (Khalid et al., 2005), however recent updates in literature (Dvorak et al., 1990; Chiu, 1997; Bentley, 2000; Laha and Das, 2011; BoM, 2013b; Olander and Velden, 2007; Knaff et al., 2010; Olander and Velden, 2011) and the introduction of TIR imagery, have increased the number of rules to 673. The rules were generated based on Alcalá et al. (1999) learning techniques for linguistic models. All the fuzzy and crisp rules formulated and implemented in the developed system follow the following format:

IF <antecedent$_{(1)}$*>...<antecedent*$_{(n)}$*>*

THEN <consequent$_{(1)}$*>...<consequent*$_{(m)}$*>*

The format above illustrates a commonly used conditional rule format, however some of the rules used a nested format as below:

IF <antecedent$_{(1)}$*>...<antecedent*$_{(k)}$*>*

ELSE IF <antecedent$_{(1)}$*>...<antecedent*$_{(n)}$*>*

THEN <consequent$_{(1)}$*>...<consequent*$_{(m)}$*>*

In the above statements any number of antecedents could be combined together with the help of logical connectives such as AND, OR and NOT, while consequents defined an action to be taken if a particular rule was applied. The careful choice of 71 rules allowed the system to be stringent in nature to perform expert criteria based tasks, while at the same time the rules allowed flexibility in the system to adapt to future change.

3.9 Summary

Regardless of the current developments in the field of tropical cyclone forecasting and automation of the procedure (Ho and Talukder, 2008; NRL, 2011; Kovordányi and Roy, 2009; Knaff et al., 2010; Shah et al., 2012; Sampson et al., 2012; Galarneau and Davis, 2012; BoM, 2013b; Dvorak et al., 1990), the developed system described in this chapter provides a unique modular approach to tackle uncertainty by adopting a fuzzy rule based approach. Moreover, the developed system addresses all phases in tropical cyclone monitoring starting from detection and identification of the storms, classifying their physical characteristics and estimating their intensity in a fully automated manner.

The following chapter 4 discusses image segmentation and pattern detection of the tropical cyclone structures; in addition, it reviews the fuzzy rule based approach adopted in this research. Chapter 5 investigates the intensity classification procedure employed in the developed system.

CHAPTER 4. PATTERN DETECTION OF TROPICAL CYCLONES

4.1 Introduction

Early manual meteorological analyses based on satellite imagery were attempted in 1960s and 70s. However, the availability of decadal satellite data and improved image quality has excited research into automated methods for storm forecasting using artificially intelligent algorithms, as seen in chapter 2. One of the main aims of automated algorithms is to understand climatology of tropical cyclones, which has important implications for the future compilation of improved regional forecasts for hazard management. Many researchers in the recent past have attempted to address the issues involved in the automated pattern recognition of tropical storms from satellite imagery, however their approaches have been ineffective in focusing on a more holistic approach (Kim et al., 2010; Laha and Das, 2011; Shah et al., 2012<Lee, 2001 #216; Demirci et al., 2004).

Fuzzy logic plays an important role in the field of pattern recognition, albeit the original methods have not evolved much since its emergence in 1960s. Many researchers provide evidence that fuzzy logic is still one of the most valuable techniques to partner pattern recognition, especially due to its capability of representing real world knowledge base and tackling uncertainty and vagueness (Melin, 2012; Wadhawan et al., 2013; Kamat, 2004; Schmalzel and Johnson, 1993; Melin et al., 2011; Melin and Castillo, 2013). One of the objectives of this research, as highlighted in section 1.6, was to design and implement a soft computing based pattern recognition system that could classify and identify key structural patterns associated with tropical cyclones. Due to the geometric vagueness of the cloud features forming tropical storms, it is vital to introduce techniques that are capable of dealing with uncertainties. The developed system does that by using a fuzzy rule based system that uses syntactical grammar linguistics to detect tropical storms originating in the North Atlantic basin.

This chapter describes the developed methodology for the pattern recognition module and explains the fuzzy rule based approach implemented in the system. The knowledge based approach to image segmentation is discussed in section 4.2. Section 4.3 presents the linguistic methodology used to detect the existence of a tropical storm in the satellite imagery. Finally, fuzzy rule based approach is detailed in section 4.4.

4.2 Key Components of Tropical Cyclones

Before discussing the methodology employed for this research it is important to define the key structural components of a tropical cyclone. As defined in chapter 2, a tropical cyclone is a low pressure system that induces gale force winds and heavy rainfall that cause severe damage to property and life. Tropical cyclones and hurricanes have also been defined as nature's perfect heat engine that feed themselves from warm sea surface temperatures, promoting rapid evaporation (Biello, 2007; Anthes, 1982a). Due to rapid change in atmospheric pressure in the system and the coriolis force, the storm typically takes the shape of a spiral, sometimes also known as a 'comma' shape (World Meteorological Organisation, 1976; Houze, 1993). According to a number of researchers (Dunn and Miller, 1964; Gibilisco, 1984; Anthes, 1982b; Emanuel, 2005) tropical cyclones can be sub-divided into three root primitives. These are:

- Central Dense Overcast (CDO);
- Eye of the Storm; and
- Spiral shaped cloud bands.

4.2.1 Central Dense Overcast (CDO)

A CDO is a relatively uniform cirrus cloud structure, typically located at the centre of the storm. It is a large region of thunderstorms towards the centre of the spiralling cloud mass. Figure 4.1 show the CDO of a cyclone in red colour. This is also considered to be the coldest part of the storm, which eventually will surround the eye, in case of strengthening of any storm. A cyclone's strength can be associated with the uniformity and tightly packed curvatures of a CDO. Dvorak in his intensity estimation algorithms, referred to CDO's size as an important variable in the intensification of any storm. (Dvorak, 1975; Dvorak, 1984). Velden et al. (1998a) and Olander and Velden (2007) also use the presence of CDO to estimate the intensity of a cyclone. Since the developed system establishes its main intensity algorithm on CDO's size, it is vital that the pattern recognition module is able to extract and detect this cold cirrus cloud structure.

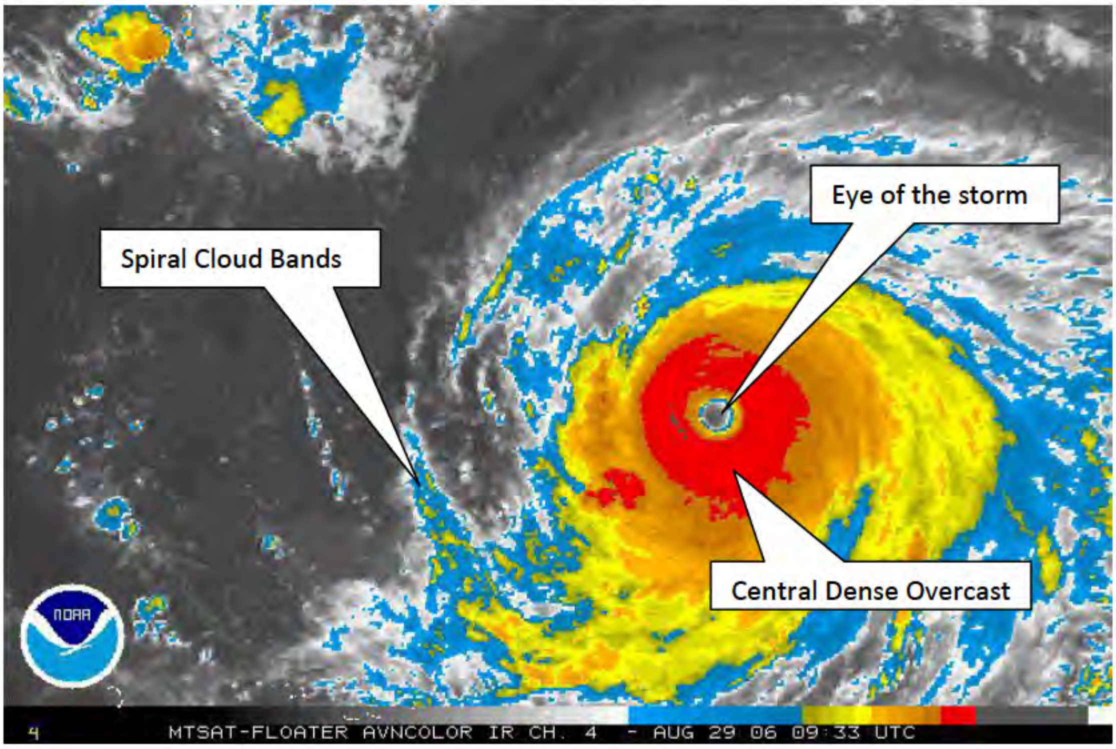

Figure 4.1: CDO is classified and displayed in the red colour indicating coldest part of the storm (NHC, 2011).

4.2.2 Eye of the Storm

If present, the eye of the storm is the distinct feature of any tropical cyclone. Contrary to the CDO the eye has limited or no cloud at all due to a high pressure environment. It is also the warmest part of the storm's anatomy. Due to various reasons, i.e. partial cloud coverage or viewing angle of the satellite platform, sometimes the storm eye is hidden. Hence a thermal TIR imagery is the most suitable data to use for the eye's detection, due to its contrasting temperatures in relation to its surroundings. Moreover, TIR imagery can also be utilised during night time image acquisition, whereas visible imagery would not be able to identify any features of the storm due to the lack of visible light. Figure 4.1 shows a perfectly formed circular eye in the centre of the CDO.

4.2.3 Spiral Cloud Bands

These cloud bands are associated with heavy rain and the heavy wind bearing localised part of the storm. They also occur towards the outer regions of the storm, spiralling inwards towards the eye of the storm. Typically there are gaps between these rain bands, making them very distinct in both visible and TIR imagery. Figure 4.1 depicts much compacted bands of spiral clouds, while figure 4.2 clearly shows the visual distinction of these bands as vital components of any tropical cyclone.

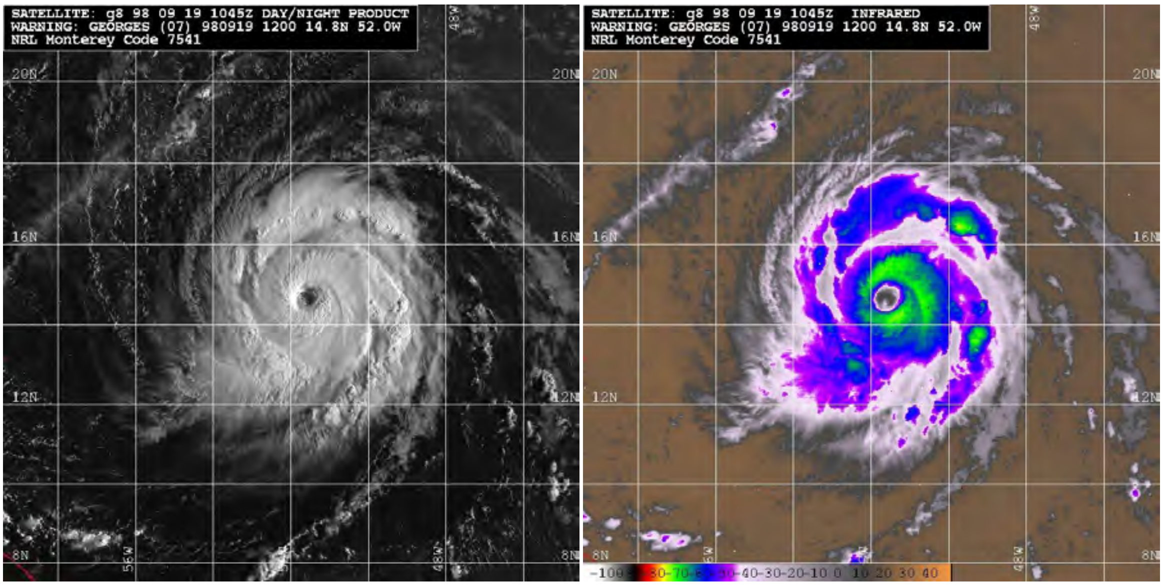

Figure 4.2: Hurricane GEORGES and its prominent spiral bands. [left] Visible image, [right] TIR image (NOAA, 2009).

4.3 Pattern Recognition Module (PRM)

A combination of NOAA, GOES and Meteosat satellite images were used to train the PRM. The temporal range of these images ranged from 1978 to 2009, dependent on the coverage provided by HURSAT. These images were analysed for predefined cloud patterns described in earlier sections. Algorithms in PRM detected cloud features in the meteorological data and classified them as the ‘recognised’ patterns to identify the presence of a storm. A linguistic method was then used to put together these recognised features, or lexicons, and processed through a grammar to identify the existence or absence of tropical cyclones in the satellite imagery. The output of the grammar module was a hierarchical structure of sub-patterns which was processed through an intensity classification algorithm. The process of pattern recognition in the developed system can be divided into three phases namely, Classification, Feature Extraction and Pattern Detection, as shown in Figure 4.3. To assist the pattern recognition procedure and removal of unwanted data, satellite images were pre-processed using traditional image enhancement techniques,

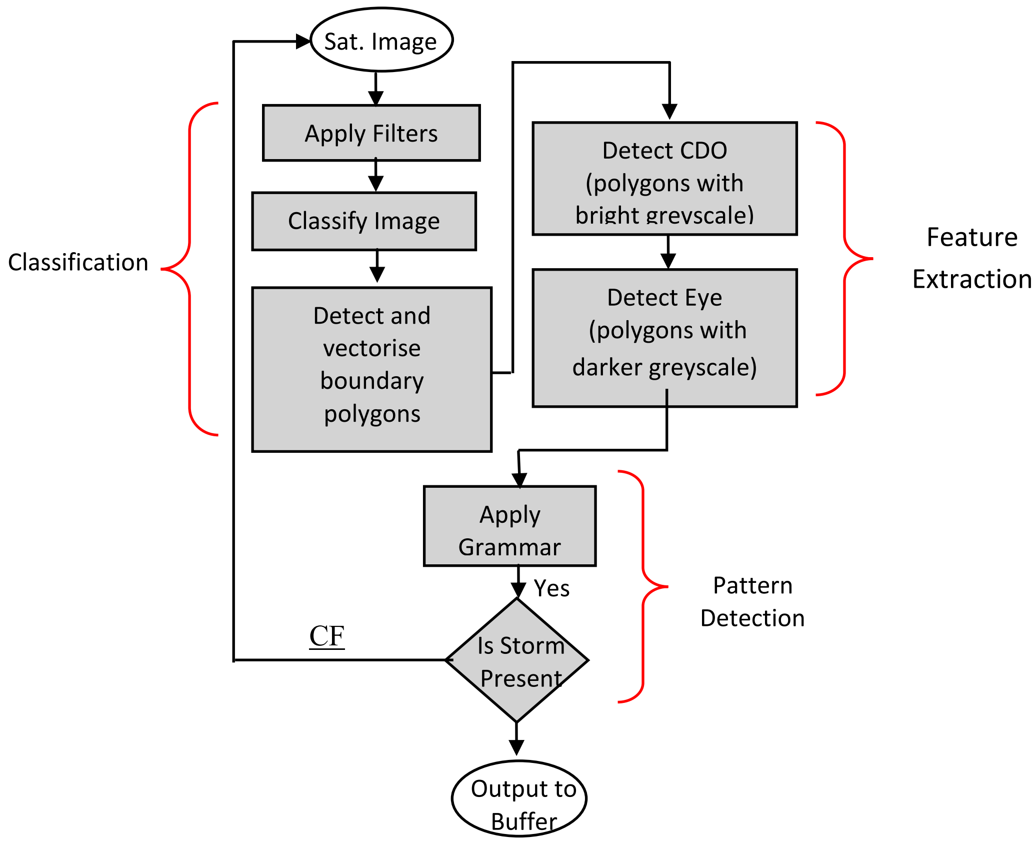

Figure 4.3: Flow diagram of the Pattern Recognition Module

4.3.1 Image classification process

A smoothing filter was applied to the images, which removed any anomalies (Liu, 2000; Kuan et al., 1985). During the validation of the system it was noted that the smoothing filter avoided mis-classification and vectorised polygons were produced with homogenous edges. A stepwise linear classification technique was programmed to accurately segment the cloud features (Bendix et al., 2004). Due to the use of infrared images, a temperature scale was used to differentiate between the three basic patterns associated with a cyclone cloud system recognised via PRM (Dvorak et al., 1990) as:

- *A Central Dense Overcast* (CDO) - a brighter and denser circular or elliptical shape.

- *Eye of the storm* - a dark circular or elliptical shape. The eye of the storm is an optional parameter, as it might not be present in all the stages of development of a tropical cyclone.
- *Cloud bands* as spiral formation – these bands are also known as the rain bands and surround the main structure of a storm.

CDO is very dense and an extremely cold feature in TIR imagery and has bright greyscale. If present, the eye of the storm is the most distinct feature of a tropical cyclone with a darker greyscale value in the TIR imagery, while the rain bands were classified as cold cloud structures that were not CDO or the eye. This method reduced the values to be processed for vectorisation, because certain features were only associated with specific greyscale and temperature value ranges (Dvorak et al., 1990). Once the satellite image was classified, boundaries of all possible classes were highlighted using an edge enhancement filter. After classification of the greyscale values, edges of required classes were detected and then vectorised using an algorithm based on chain coding (Freeman, 1974). This vectorisation algorithm also cleaned up the topology by disregarding any open polygons. The chain coding process generated multiple polygons that could be candidates for either being part of a CDO or an eye as shown in figure 4.4. Spiral band cloud boundaries were also stored for pattern recognition.

4.3.2 Feature extraction

Vectorised polygons from the pre-processing stage were processed to search for elliptical patterns. Due to the Earth’s rotational coriolis force and meteorological systems associated with a cyclone, the CDO and eye of a storm can be assumed to almost form a circle in the early stages of the storm development. However, due to the nature of remote data capture causing oblique incident angles, geometric distortion and tropical cyclone decay, the shapes can appear to be distorted. The pattern recognition system took into consideration the possible distortions that might make a circular cloud feature appear to be of an elliptical shape. Hence all prospective CDOs and eye polygons were assumed to be elliptical. A fuzzy rule based algorithm was designed to identify the membership of each polygon to an ellipse family.

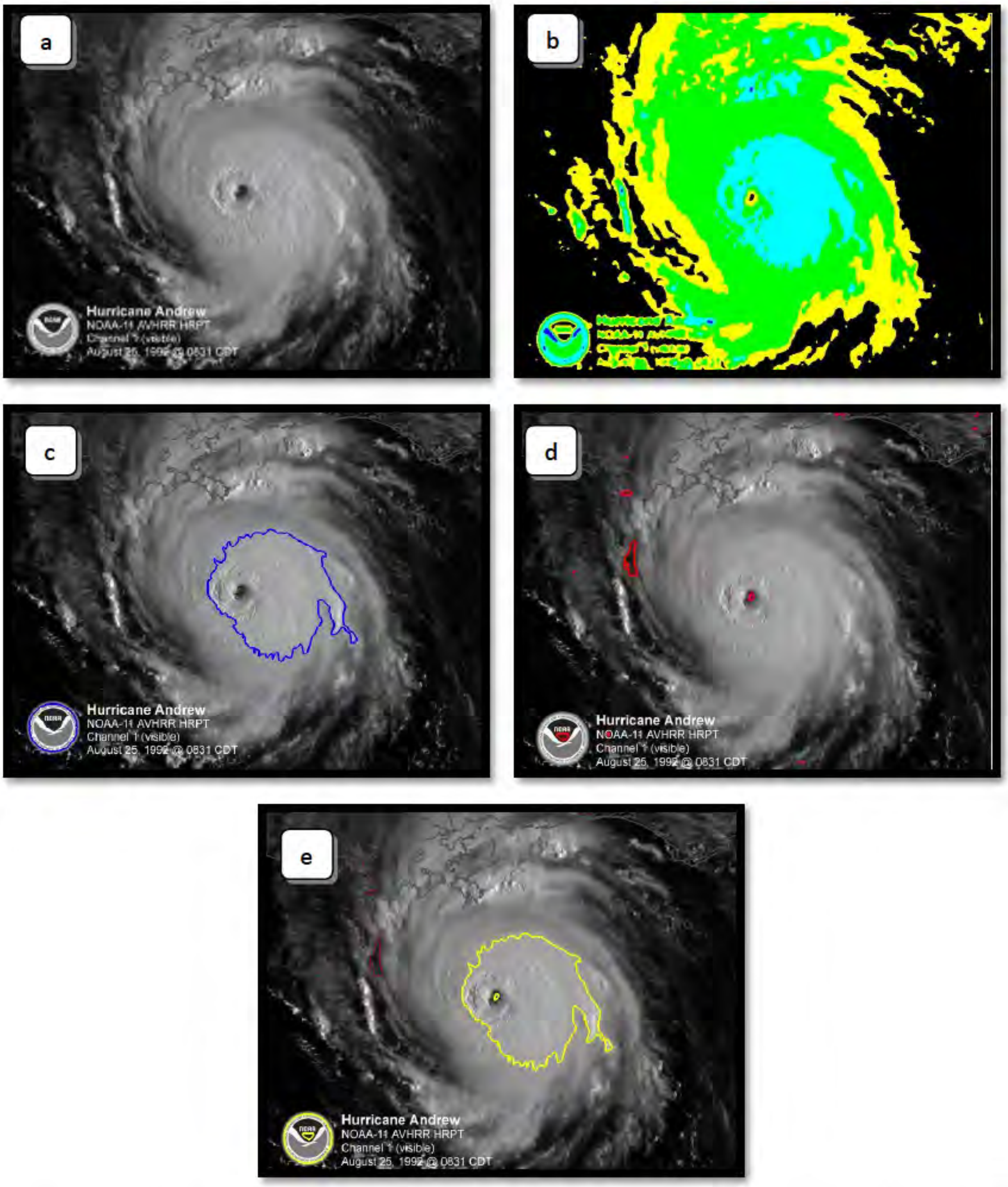

Figure 4.4: (a) Visible NOAA-11 AVHRR image of Hurricane Andrew; (b) Classified image of Hurricane Andrew; (c) Potential CDO polygons detected by the developed system; (d) Potential eye polygons detected by the developed system; (e) Suggested location of the storm

4.3.2.1 Identification of Elliptical Polygons

To evaluate whether polygons were elliptical, each point on the boundary of every polygon was numerically associated with an ellipse function. Fuzzy rule based functions were used to decide if the majority of the points on the boundary of any polygon belonged to an ellipse. To define the membership of polygons, major and minor axes of every polygon were calculated by scanning the distance of the boundaries of clusters from the centre of polygon. Instead of using the maximum distance as the major axis and minimum distance as the minor axis, a median value was estimated. The average distance from median to the boundary of the polygon was computed for major and minor axes. This approach was used to avoid any bias caused by possible spikes in boundaries; a template ellipse is shown in figure 4.5. The following equation 4.1 was employed to check if any point location in the detected polygons belonged to an ellipse:

$$\left(\frac{(x-x_c)\cos\theta-(y-y_c)\sin\theta}{a}\right)^2+\left(\frac{(x-x_c)\sin\theta+(y-y_c)\cos\theta}{b}\right)^2=1 \qquad \text{... Equation 4.1}$$

Where;

x, y = a point on the ellipse

x_c, y_c = estimated centre of ellipse

a = radius of the ellipse along major axis

b = radius of the ellipse along minor axis

θ = the angle ellipse is rotated from the horizontal axis

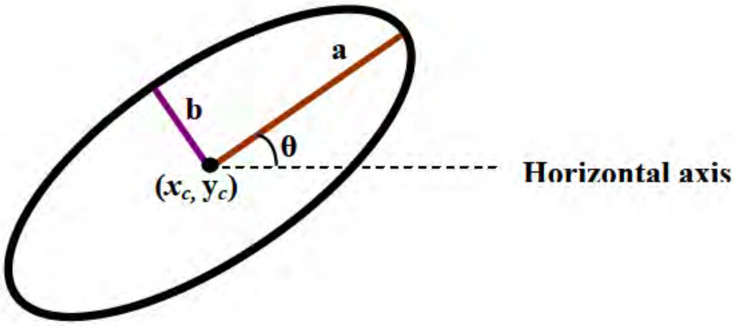

Figure 4.5: A template ellipse.

All the points on the suspected elliptical polygons were examined against equation 4.1. Figure 4.6 illustrates the fuzzy membership function to calculate if a point on the polygon belonged to an ellipse. The sum of the deviation square (SODS), equation 4.2, was calculated from the values generated by this method.

$$SODS = \Sigma(z - z')^2 \qquad \text{...Equation 4.2}$$

Where;

z = a value from equation 4.1 for a point on the polygon,

z' = mean of all the values computed, using equation 4.1, on a polygon

The SODS function was used to separate the tighter curved elliptical shapes from rough edged elliptical or non-elliptical shapes. SODS effectively separated ellipses from non-elliptical shapes. Test patterns were used to measure the efficiency of SODS in separating elliptical shapes from non-ellipses.

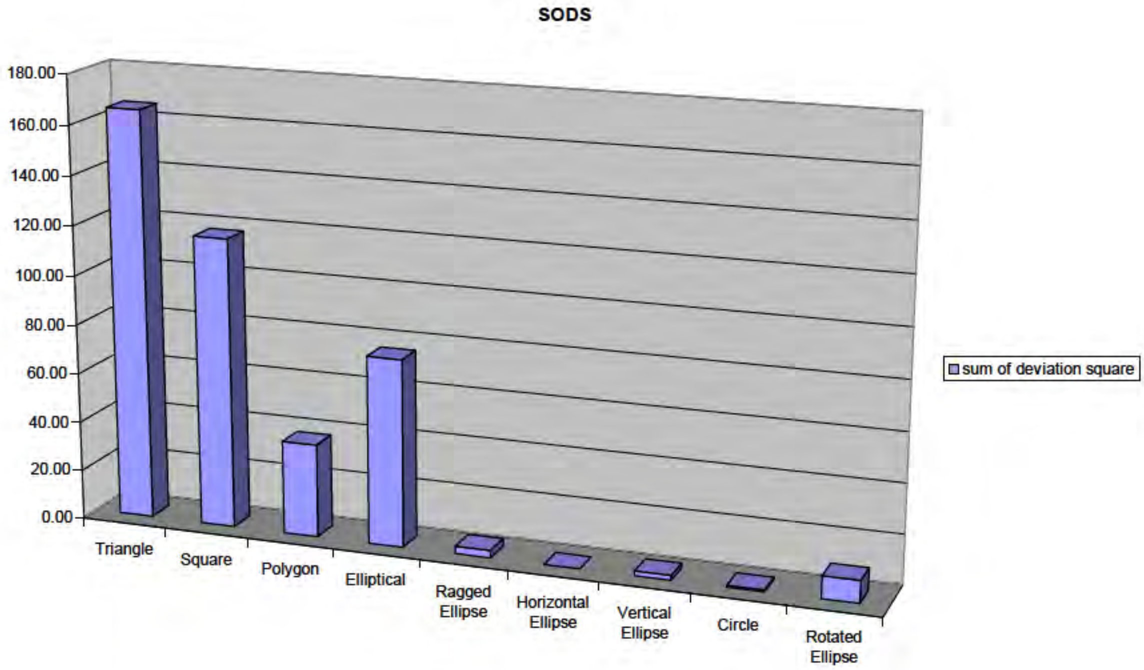

Figure 4.6: Sum of deviation square applied to test objects

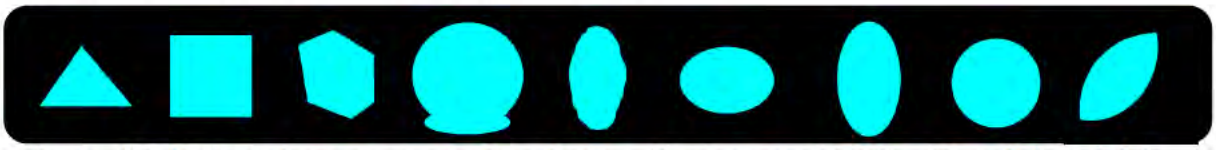

Figure 4.7: Various shapes were tested to observe effectiveness of SODS. (From left to right) Triangle, Square, Polygon, Elliptical, Ragged Ellipse, Horizontal Ellipse, Vertical Ellipse, Circle, Rotated Ellipse.

If an ellipse was detected, it was passed to the Fuzzy Engine to obtain a membership value of an ellipse being a stronger ellipse or even being a circle. The eccentricity (equation 4.3) of an ellipse was used to fuzzify the elliptical polygon. Figure 4.8 illustrates an example of an algorithm that was devised to detect if an eye polygon could be elliptical. This iterative algorithm passes through every point in each polygon and calculate the eccentricity value using the equation of ellipse (4.1). A similar algorithm was used to identify the CDO polygons; colder pixels selected instead of warm temperatures.

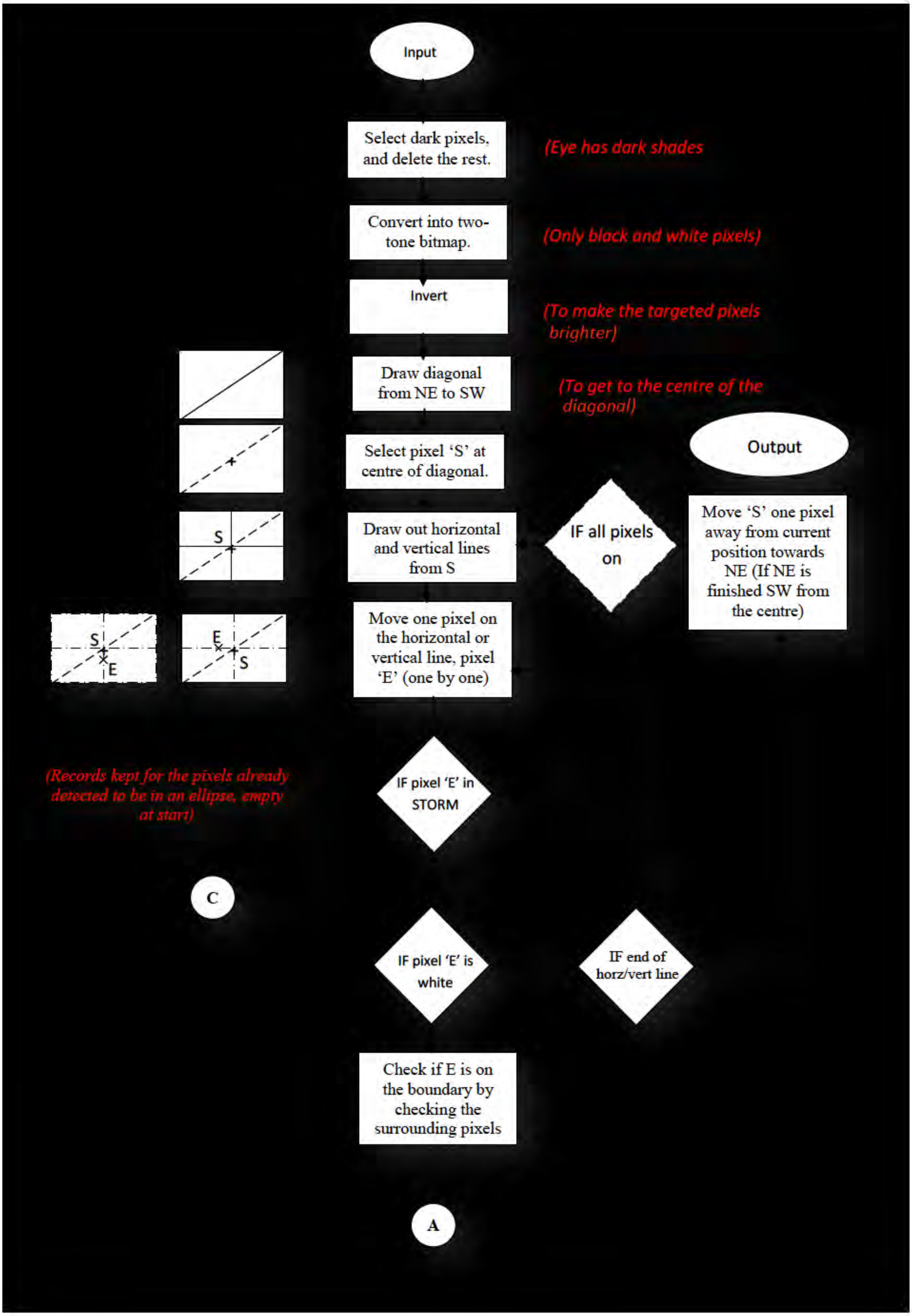
Input
Select dark pixels, and delete the rest.
(Eye has dark shades
Convert into two-tone bitmap.
(Only black and white pixels)
Invert
(To make the targeted pixels brighter)
Draw diagonal from NE to SW
(To get to the centre of the diagonal)
Output
Select pixel 'S' at centre of diagonal.
S
Draw out horizontal and vertical lines from S
IF all pixels on
Move 'S' one pixel away from current position towards NE (If NE is finished SW from the centre)
S
E
E
S
Move one pixel on the horizontal or vertical line, pixel 'E' (one by one)
(Records kept for the pixels already detected to be in an ellipse, empty at start)
IF pixel 'E' in STORM
C
IF pixel 'E' is white
IF end of horz/vert line
Check if E is on the boundary by checking the surrounding pixels
A

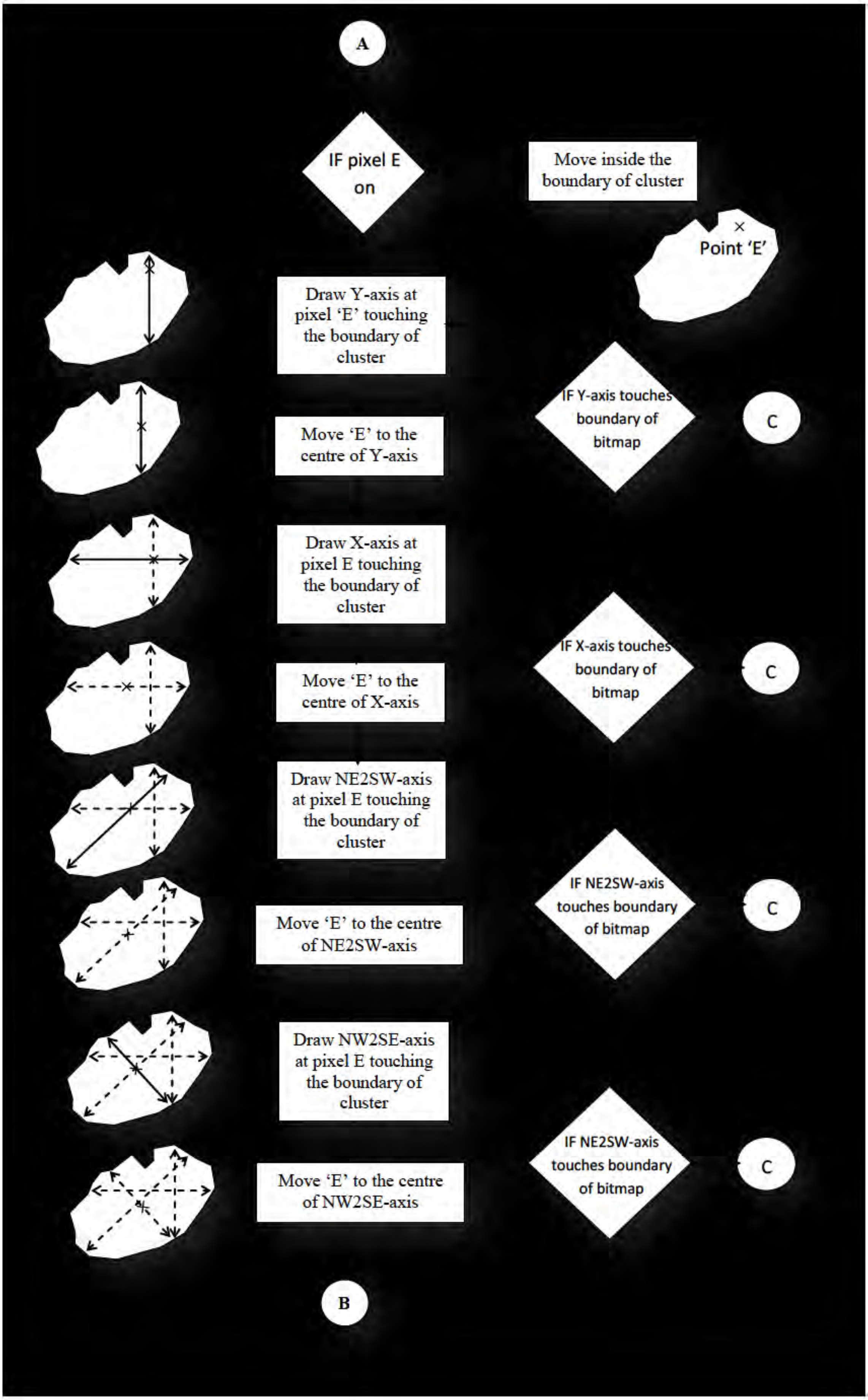
A
IF pixel E on
Move inside the boundary of cluster
Point 'E'
Draw Y-axis at pixel 'E' touching the boundary of cluster
IF Y-axis touches boundary of bitmap
C
Move 'E' to the centre of Y-axis
Draw X-axis at pixel E touching the boundary of cluster
IF X-axis touches boundary of bitmap
C
Move 'E' to the centre of X-axis
Draw NE2SW-axis at pixel E touching the boundary of cluster
IF NE2SW-axis touches boundary of bitmap
C
Move 'E' to the centre of NE2SW-axis
Draw NW2SE-axis at pixel E touching the boundary of cluster
IF NE2SW-axis touches boundary of bitmap
C
Move 'E' to the centre of NW2SE-axis
B

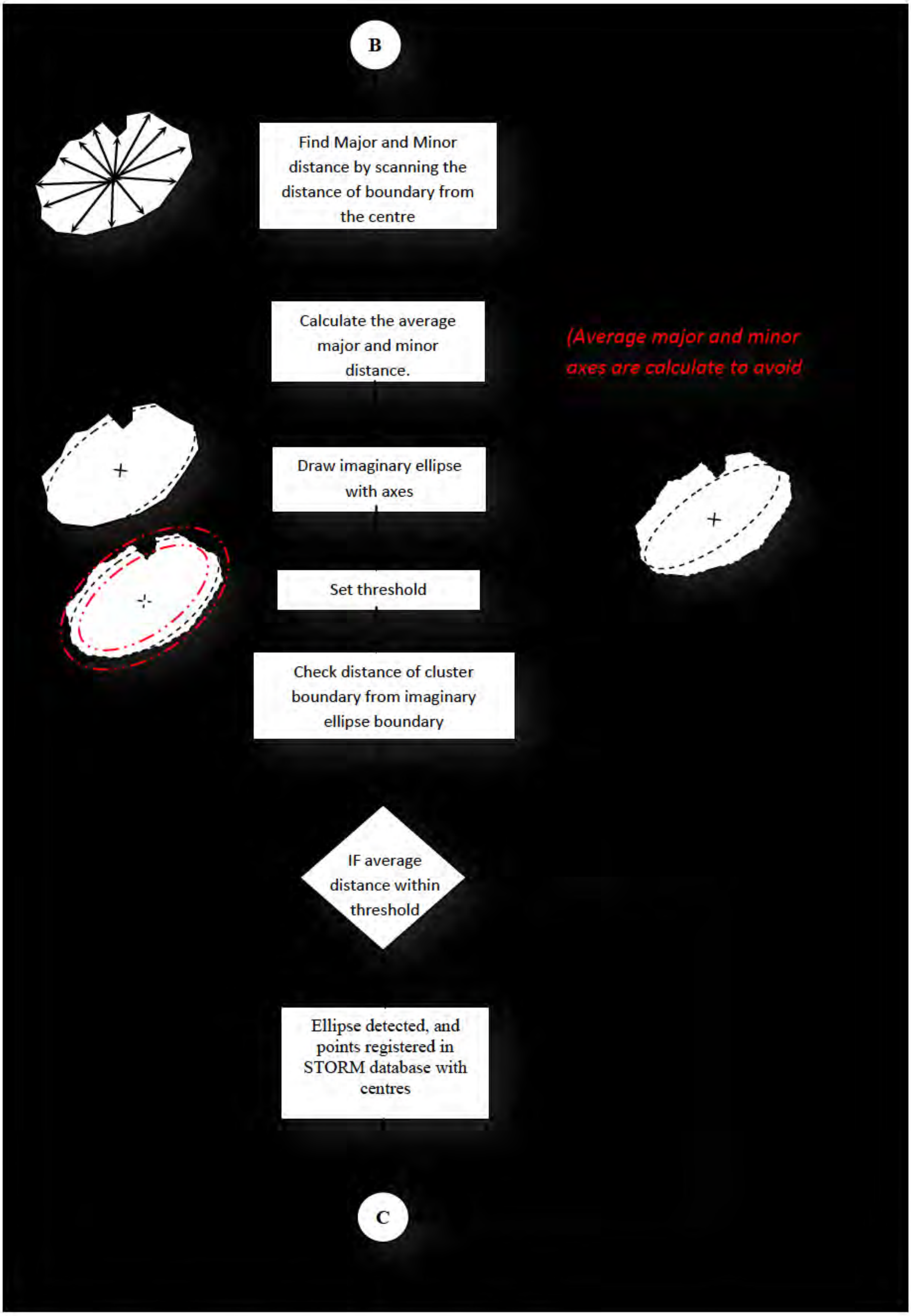

Figure 4.8: Flow diagram of an algorithm to detect eye polygons

During the detection process, if a polygon was suspected to be of elliptical shape, it was passed to the Fuzzy Engine to obtain a membership value to an ellipse group. The Fuzzy engine classified the polygon to be either a stronger ellipse or even a circle. A circle fuzzy function was used to distinguish between a circle and an ellipse. The eccentricity equation (4.3), of an ellipse was used to fuzzify the elliptical polygon.

$$E = \sqrt{1 - \frac{b^2}{a^2}} \qquad \text{...Equation 4.3}$$

Where;

E is the eccentricity,

a is the major and **b** is the minor axis of the ellipse.

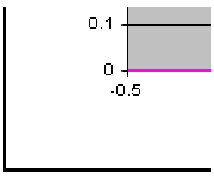

Figure 4.9: Triangular shaped fuzzy membership function using equation 4.3

The process was carried out for polygons belonging to the CDO class and the eye class. After the fuzzy memberships were allocated the resulting data had a set of CDO polygons and eye polygons in their individual images, as seen in figure 4.10. Figure 4.10 displays all the polygons that had a higher fuzzy membership value of eccentricity and were classed as 'elliptical'. The use of fuzzy functions allowed the system to recognise imperfect but oblong shaped polygons as 'elliptical', which cannot be defined in traditional geometrical mathematics.

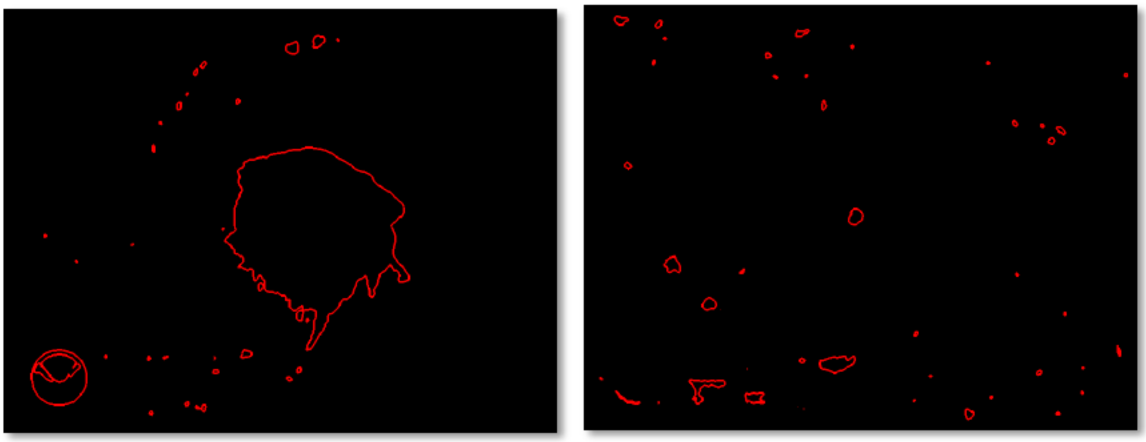

Figure 4.10: [left] Detected potential CDO polygons; [right] Detected potential eye polygons

4.3.2.2 Spiral Bands

Rain bands of clouds around the cyclone play a vital role in classifying the intensity of the storm. Typically, these banding features are clouds circulating around the central feature of the tropical cyclone and are usually in a curved formation, typically identified as spiral bands (Wong and Yip, 2009; Wei et al., 2011; Dvorak et al., 1990). These curved bands of clouds were detected by classifying them using the density slicing approach, targeting the cold clouds. A thinning algorithm (Zhang and Suen, 1984) was used to find the skeleton of the curve cloud bands also known as the curved band axis. The curved band axis is defined as the axis of the coldest overcast grey shade within the cloud band. After identifying the curved band axis, the skeleton was vectorised using the chain coding method (Freeman, 1974). A logarithmic spiral of 10° pitch angle (Dvorak, 1984; Dvorak et al., 1990) was then fitted to the curvature of the vectorised curve band axis using equation 4.5, in polar coordinates (r, θ).

$$r = ae^{b\theta}$$ ...Equation 4.4

where r is the radius of the spiral for a given θ. The radius is calculated from the origin of the spiral assumed to the calculated centre of the storm; 'a' and 'b; are both arbitrary real constants where 'a' defines the rotation of the spiral and 'b' controls the curvature. The calculated skeleton of the cloud bands was then curve fitted to a base 10 logarithmic spiral with the help of equations 4.6 and 4.7 (Daily, 2012).

$$x(\theta) = X_0 + ae^{b\theta}cos\theta$$ ...Equation 4.5

$$y(\theta) = Y_0 + ae^{b\theta}sin\theta$$ ...Equation 4.6

In case of a first attempt mismatch between the skeletal cloud structure and the logarithmic spiral, the equations were used to shift the spiral in an iterative algorithm, until the best match with the skeleton of the cloud features was found. The value of b is changed through the iterations to tighten or loosen the spiral to best fit the skeletal cloud structure. Once a best fit match is found the properties of the spiral are recorded. During the intensity classification stage the arc of the length plays an important part. Arc distance of the spiral, as indicated by Dvorak (1984) and BoM (2013b), was used to calculate the banding features as shown in figure 4.11

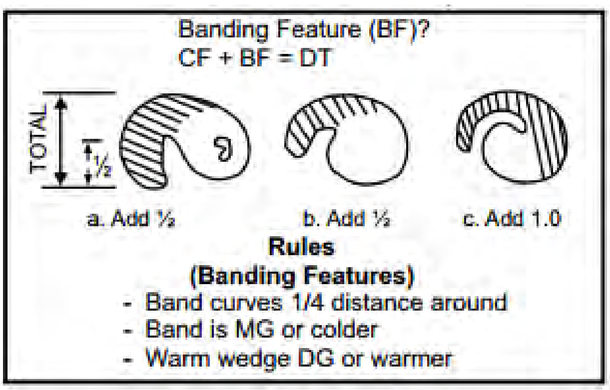

Figure 4.11: Calculating the arc length of the banding features. CF – Central Feature; BF – Banding Feature; DT – Dvorak T number (BoM, 2013b)

Figure 4.12a and 4.12b illustrate an attempt to fit a logarithmic spiral to the cloud band. The algorithm analyses the coordinates of the cloud skeleton and estimates a best fit (black dots in the graph) based on the template logarithmic spiral. It goes through this process iteratively until either it finds a good match or a threshold number of iterations is met. Figure 4.12c show a near perfect fit to the base 10 logarithmic spiral.

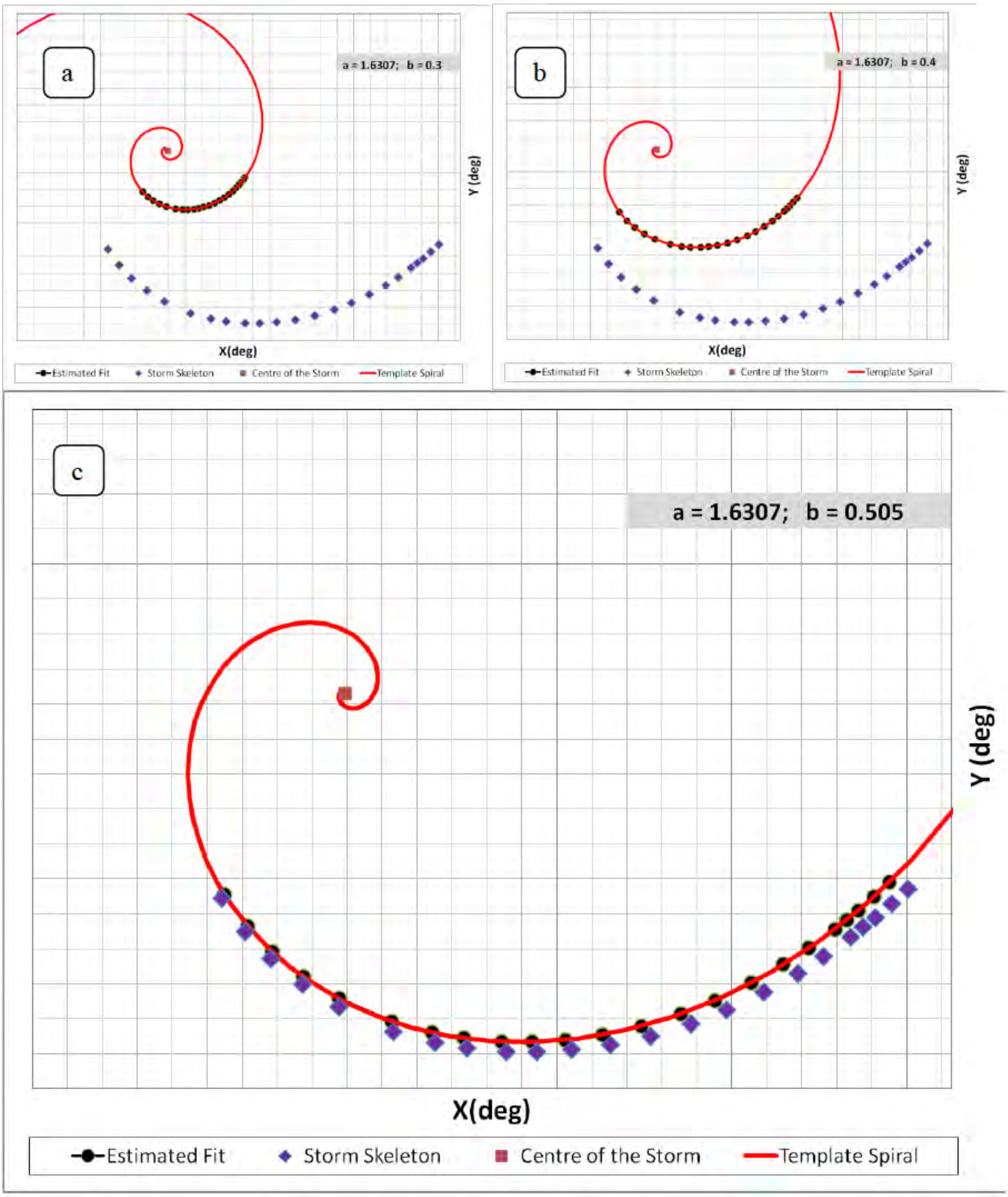

Figure 4.12: [a] misfit hurricane band [b] an unsuccessful attempt to fit the spiral [c] a near perfect curve fit to the hurricane cloud bands.

4.3.3 Syntactical Grammar

Finally, the third stage of pattern recognition involved determination of optimal decision procedures for the detection of the storm from the extracted patterns. Formal Language Theory (Chomsky, 1956a; Chomsky, 1956b) was used to generate a grammar, which consisted of finite sets of elements called variables, primitives, and productions. The production rules were developed and connected to determine the type of grammar. According to Formal Language Theory (Harrison, 1978), alphabets are any finite set of symbols, and a sentence is any string of finite length composed of symbols from the alphabet. A language is any set of sentences. The following algorithm, was employed to create a grammar that could classify the detected primitives as a tropical cyclone (Evans, 1971; Higuera, 2010).

A primitive is an individual entity that can exist independently in a domain, such as the eye of the storm and CDO. Descriptors are functions defined on the primitives to verify the different allowed combination of primitives. An example of the descriptor used in the developed system is I(eye, CDO). I denotes a function 'Inside', which checks to see if an eye is inside a CDO or not, resulting in a Boolean value. The language was developed considering the primitives, positional descriptors, and sample patterns in table 4.1. The sample patterns were a combination of the primitives. Various complex objects were built starting with the primitives and successively applying the descriptors. A complete terminal description of a cyclone can be constructed as a composition of descriptor and primitives. Using the designed descriptors and primitives, a language grammar was built which led to the construction of known cyclonic cloud patterns. A set of production rules were generated using this grammar to successfully identify the presence of cyclones in satellite images.

The sample patterns were used to guide the process until a total description of the pattern was obtained. From simple objects a, b and c much more complex objects were generated. In the above table all three functions generated a new object, stated under column primitive, e.g. CI(a.b) generate Object 1.

Table 4.1: A set of training primitives, descriptors and sample pattern for the grammar; a, band c are the input objects in the function A – around, CI – Completely inside and I-inside.

PRIMITIVES			**Descriptors**	**Training Patterns**
Name	**Description**	**Symbols**		
Eye_set: [Object 1]	A set of a round closed object represented, {Ø, eye}. Ø shows that eye can be absent.		CI(a,b): object a is completely inside object b *e.g. An eye is completely inside a CDO.*	
CDO_set: [Object 2]	Central Dense Overcast, a set of dense circular feature represented {Ø, CDO}. Ø suggests that CDO could also be absent.		A(c,b): object c is around object b *e.g. spiral bands are around a CDO*	
BF: [Object 3]	Spiral Banding Feature		I(b,c): object b is inside object c I(a,3): object a is inside object 3	

This can be denoted as Object 1:CI(a,b). The first set of complex objects are listed below.

Object 4: I(1, 2)	Which is simply Object 1 inside Object 2

This condition was satisfied by the sample pattern. Some more combinations that satisfy the sample pattern are:

Object 5:A(3,1)	Object 6: A(3.2)
Object 7: A(3,3)	Object 8: A(3,4)

Clearly, there are other combinations, which also satisfy the sample pattern. In another pass the required input pattern is obtained by creating an object, such as:

Object 9: A(3,8)

Object 9 is a complete terminal description of the input patterns, i.e. Object 3 around Object 8, which is the 'band of clouds' around Object 8. Object 8 is 'bands of cloud' around Object 4. Object 4, on the other hand is 'eye of the storm' inside the 'CDO'. Thus Object 9 is a tropical cyclone.

A grammar to generate the sample pattern was constructed by considering the steps, which led to the construction of the objects (Chomsky, 1956a; Chomsky, 1956b). Thus, a grammar for this example is as follows:

$$G = \{V_N, V_T, P, S\} \qquad \text{...Equation 4.7}$$

Where

$V_N = \{S, B, C, D\}$, $V_T = \{Eye\_set, CDO\_set, BF\}$
P: $S \rightarrow A(B, C)$
$B \rightarrow A(BF, BF)$
$C \rightarrow I(Eye\_set, D)$
$D \rightarrow A(BF, CDO\_set)$

The set of production is, in effect, a set of rules for constructing the required patterns. If S represents the tropical cyclone, the production rules simply indicate the following. A tropical cyclone is some object B around the object C. Object B is bands of cloud around each other. While object C is an optional eye inside object D and object D is band of cloud features around a CDO. These linguistic rules must be abided by for any tropical cyclone to be recognised in each image processed.

Figure 4.13 illustrates the complete process of an input image being classified, segmented in to regions and classes, fuzzy rules detecting the elliptical closed polygons and finally a grammar constructing a logically legal pattern of a tropical cyclone.

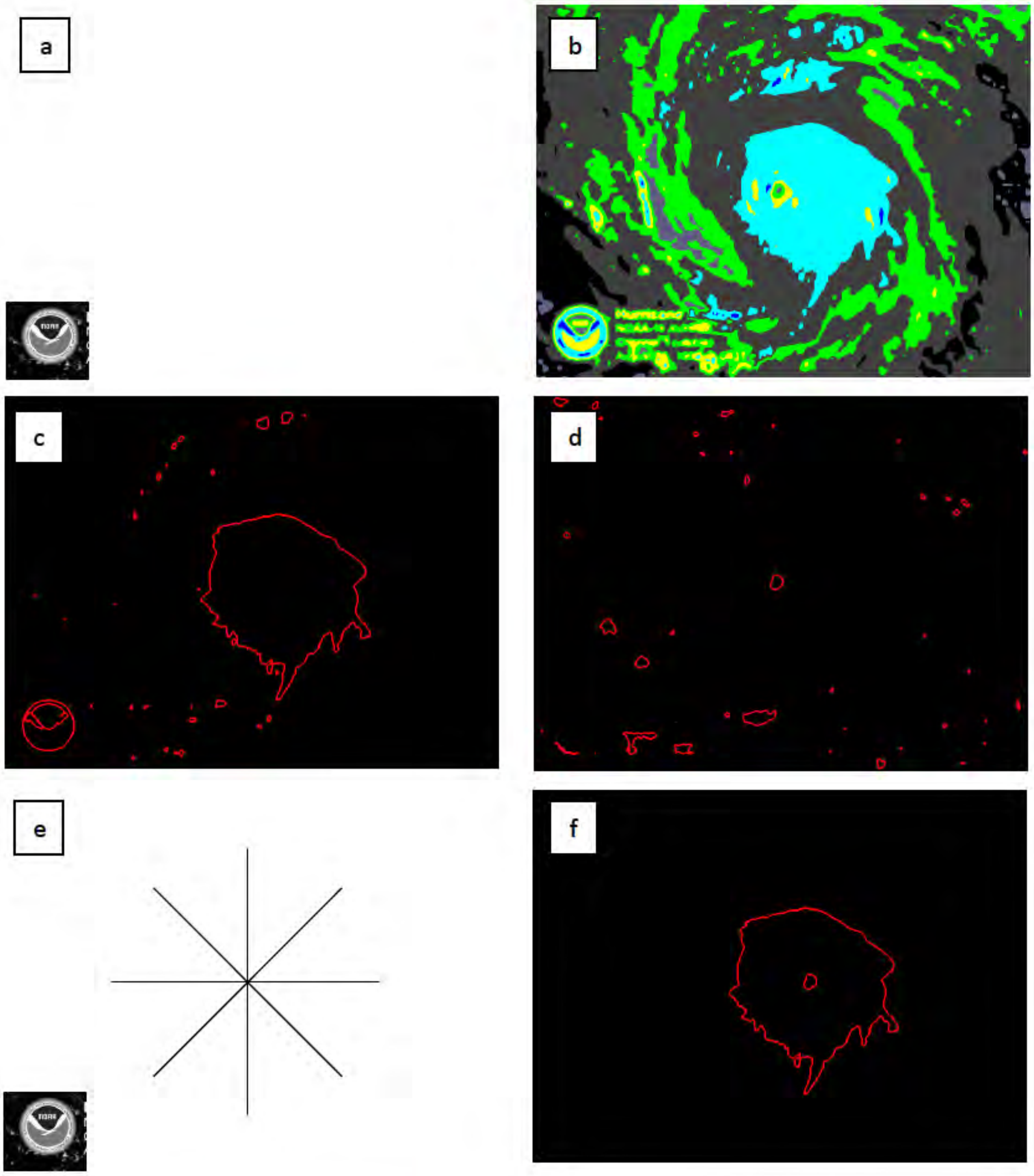

Figure 4.13: [a] Hurricane Andrew visible band image; [b] Classified image of Hurricane Andrew; [c] fuzzy potential CDO polygons; [d] fuzzy potential eye polygons; [e] Logarithmic Spiral fit to the cloud bands; [f] Detected hurricane Andrew after the application of grammar.

Figures 4.14 to 4.17 show examples of other qualified cyclones constructed by the grammatical rules. Moreover, figures 4.18 to 4.22, show hurricanes with only spiral fitting applied. These hurricanes were fully processed after the bands were associated with the logarithmic pitch 10° spirals

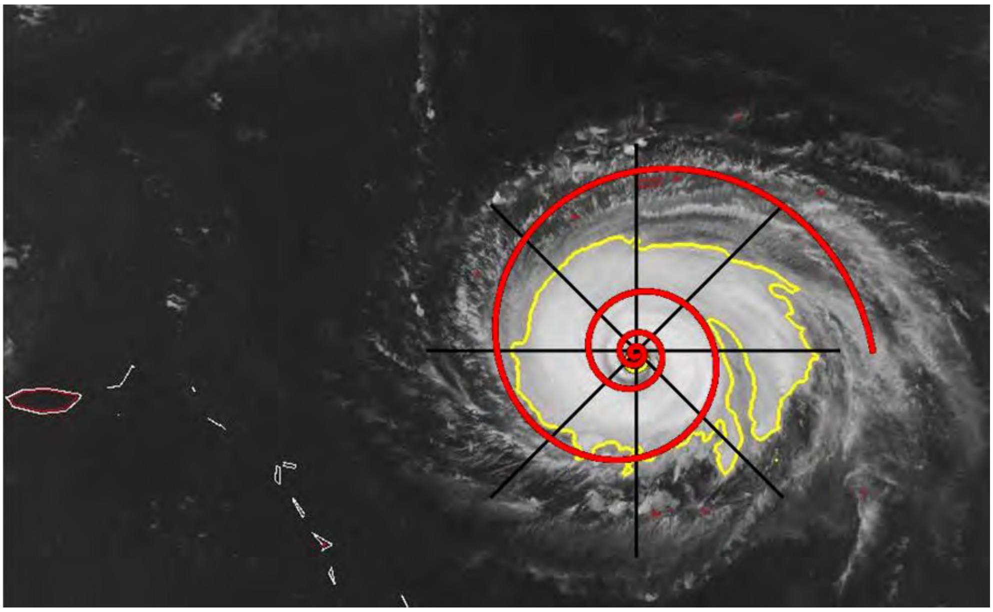

Figure 4.14: Hurricane IRIS; CDO, eye and a reasonable spiral match

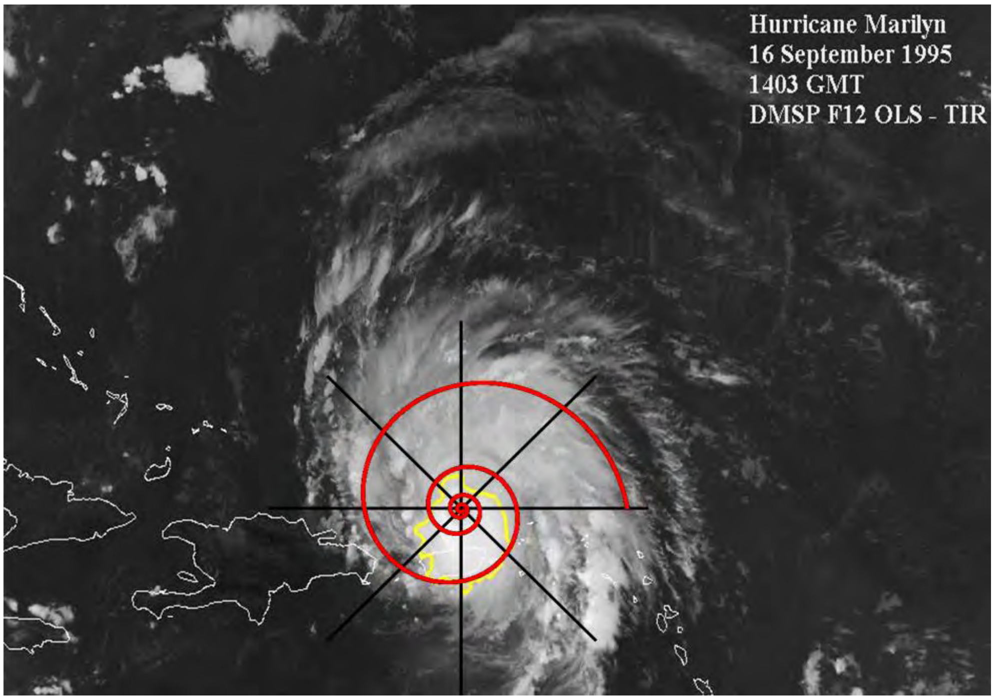

Figure 4.15: Hurricane MARILYN; CDO is ragged and weak, eye is not in the centre, but a good spiral match

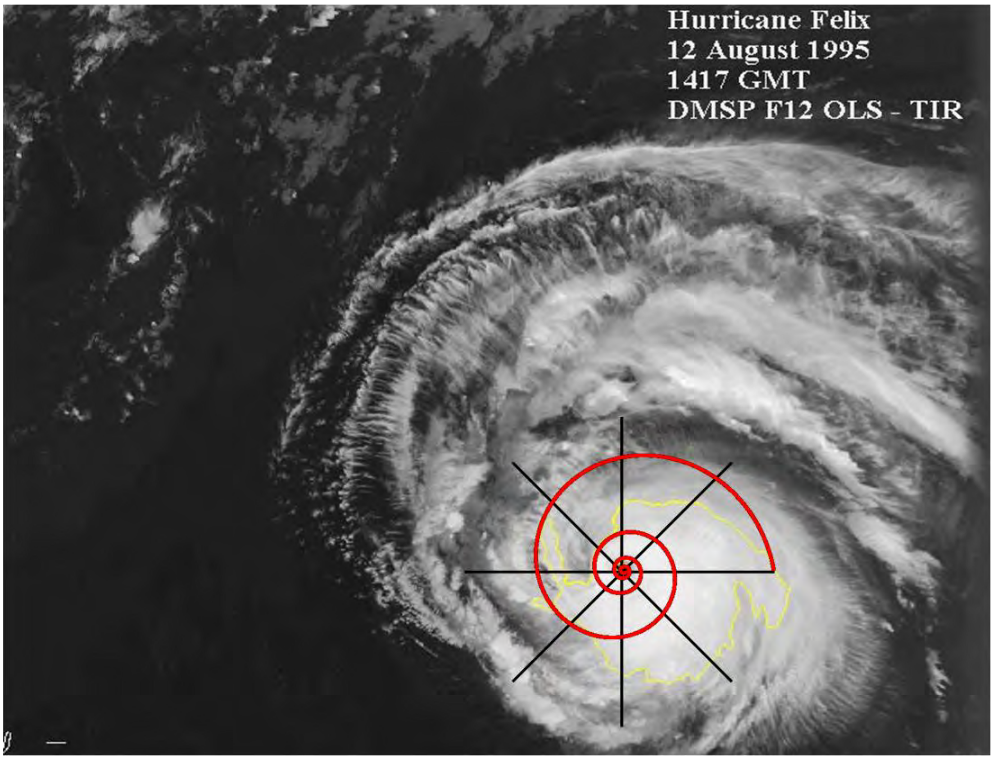

Figure 4.16: Hurricane FELIX: CDO and eye detected, spiral match was partial

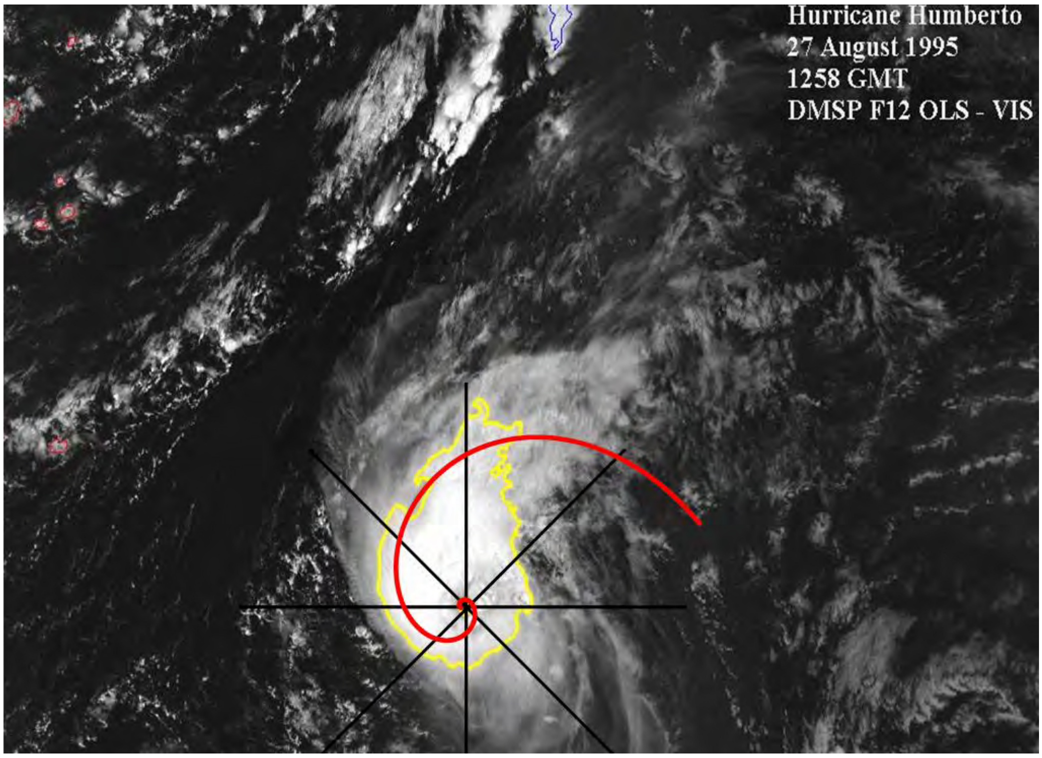

Figure 4.17: Hurricane HUMBERTO; final stages of hurricane, weak CDO, eye is present, the spiral band hardly exist.

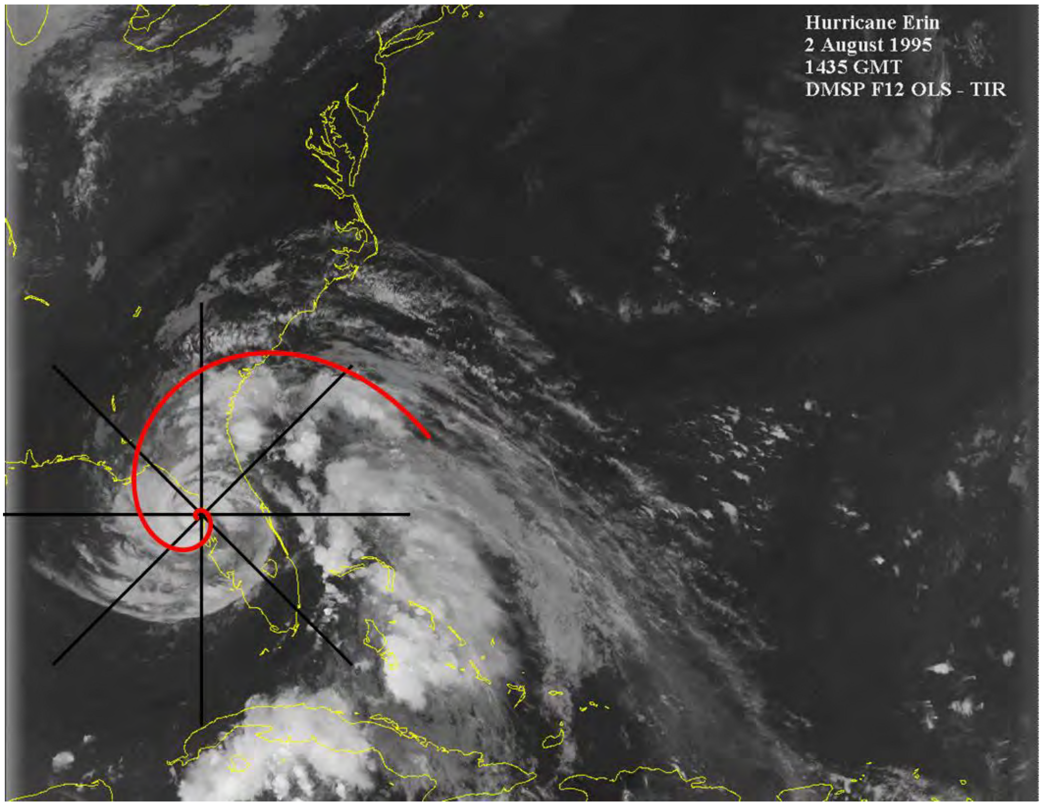

Figure 4.18: Hurricane ERIN with intermittent overlap of spiral, it is still a high match.

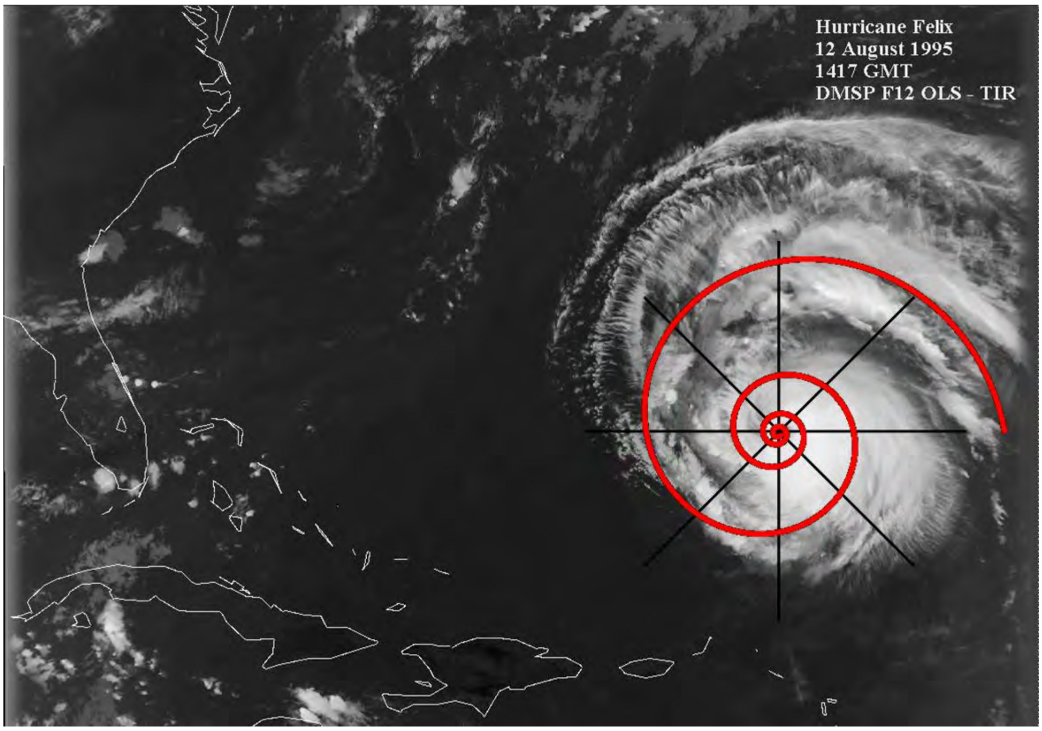

Figure 4.19: Hurricane FELIX: A near perfect spiral match

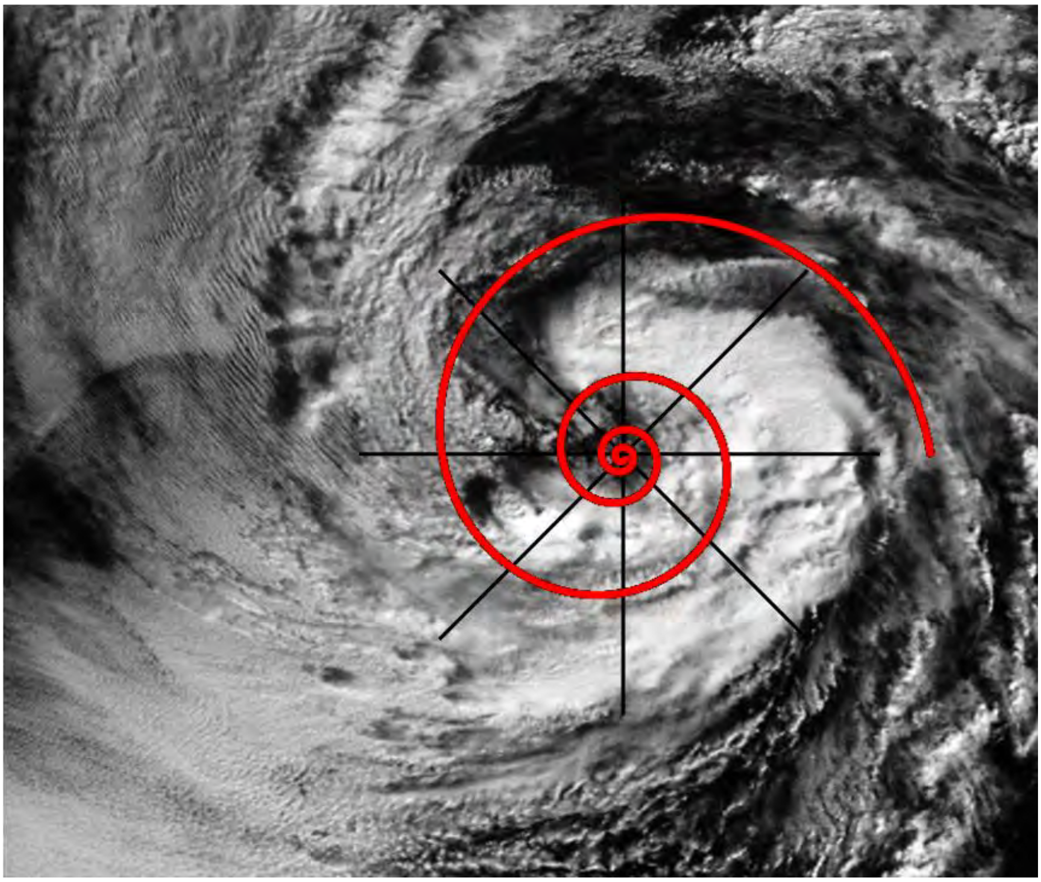

Figure 4.20: Hurricane GORDON: visually it might seem a good match, however only ~200^{o} overlap.

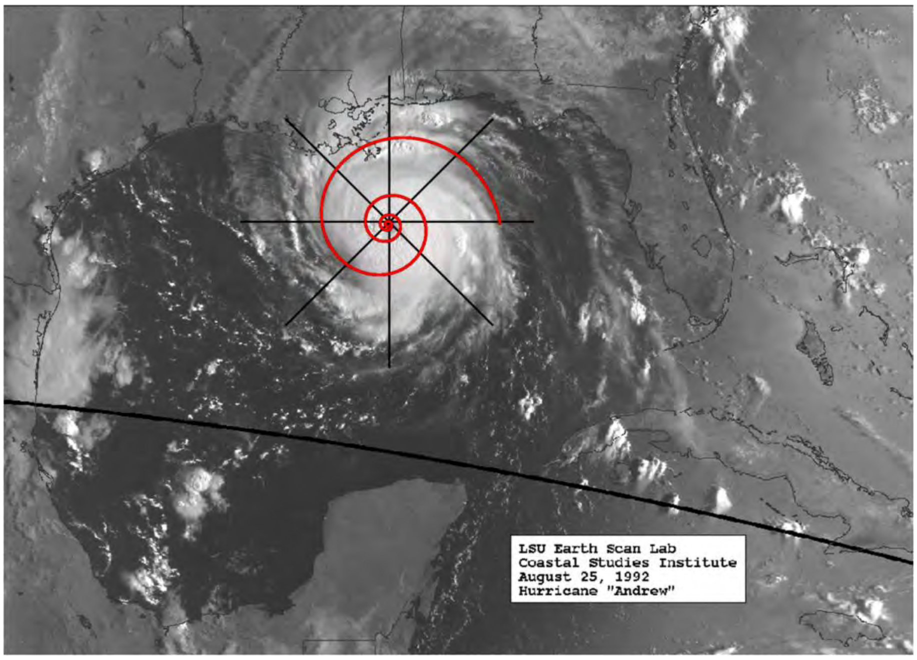

Figure 4.21: Hurricane Andrew; another image of Andrew with a near perfect match.

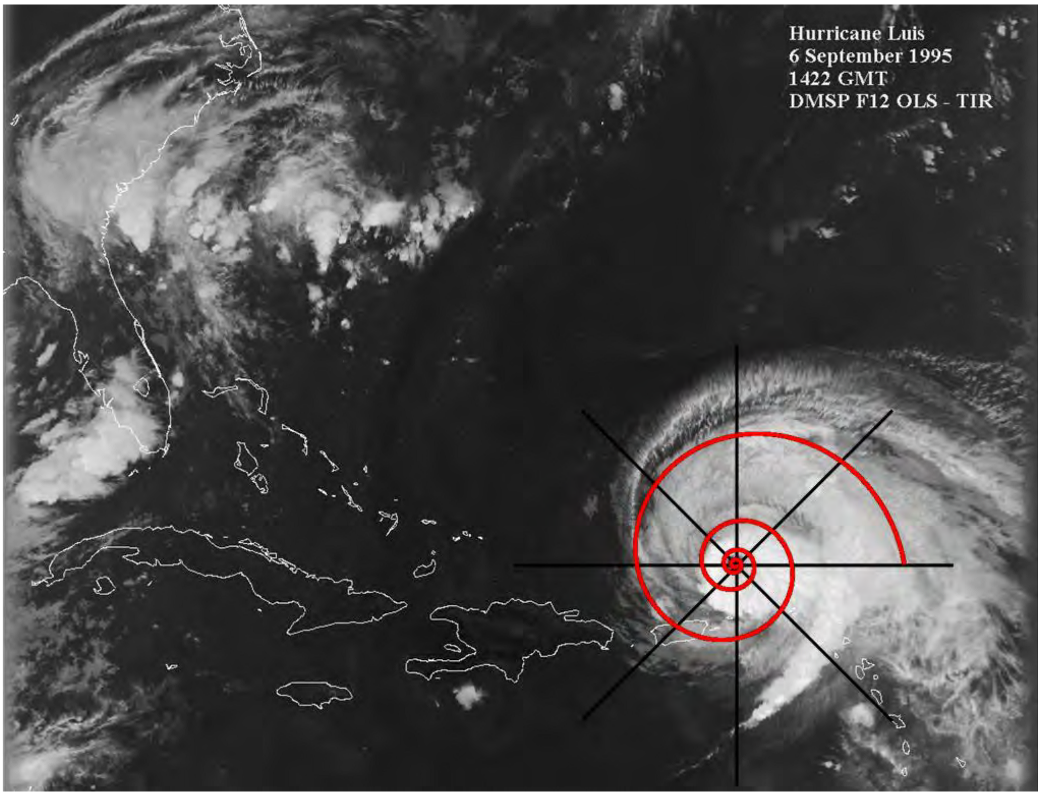

Figure 4.22: Hurricane Luis: excellent spiral match

Once a cyclone was detected, its individual statistics were stored in the STORM database, which included the location of the centre of the storm, dimensions of the eye, dimensions of CDO, best fit curve values, date and time of the image, and all the fuzzy membership values calculated for CDO, eye and spiral bands.

4.4 Summary

A tropical storm can be identified solely from a satellite image by intelligently segmenting it into its primitive components. This chapter has proposed three key structural components to any tropical cyclone, i.e. Central Dense Overcast (CDO), the Eye of the storm, and the Spiral Bands of rain clouds. The chapter also discussed in detail the processes involved in the Pattern Recognition module for successful identification of existing storms using satellite images. The pattern detection of tropical cyclones can be classified into three stages; image classification, feature extractions and application of linguistic grammar. This chapter has exposed that fuzzy logic can be successfully used for the pattern recognition of meteorological phenomenon, more importantly hurricanes and tropical cyclones. Researchers have been using a range of numerical and mathematical approaches to objectively analyse tropical cyclones. However none have holistically looked at the problem of fully automated identification of the tropical cyclone solely from satellite images. Their focus has either emphasised one aspect of storm structure analysis or intensity estimation. The techniques and algorithms described in this chapter provided a comprehensive solution to the detection of tropical cyclones and hurricanes from satellite imagery without any expert knowledge required from the user of the system.

The model described in detail in this chapter, meets the objectives set out in section 1.6. Specifically objective 2 and objective 3 were accomplished. It was noted that a tropical cyclone can be broken down into its structural components that are visually identifiable. Moreover, it is also proven that an automated system can be designed and developed to recognise tropical cyclones' structural components even though the shape and other properties of these structures are fuzzy.

The following chapter 5, investigates and discusses the process of intensity estimation of the detected cyclone. The research discussed in the upcoming chapter proves the importance of fuzzy logic rule based modelling in the intensity estimation of hurricanes and cyclones. This also targets part of objective 3 in section 1.6.

CHAPTER 5. Intensity Estimation using Fuzzy Logic

5.1 Introduction

Fuzzy logic doesn't require complex mathematical models to compute the answers to the majority of problems; it can be extremely cost effective both in terms of time and money. Fuzzy decision support systems and traditional logic expert systems differ from each other mainly because of the reasoning processes used to finalise decisions. However, they both are comparable in the sense that both require a set of logical rule bases to reach the final decisions. These rules are typically described in the form of conditional statements such as;

IF (criteria...) THEN (action...)

However, in the case of fuzzy logic the criteria are replaced with linguistic expressions to which the membership values are assigned. This allows the final output to be expressed in a closer to natural language compared to traditional crisp logic approaches. One of the main advantages of this system is that it allows the results to deal with uncertainties and vagueness, benefiting the models with less induced errors. Since fuzzy logic is providing a solution to how 'the world perceives it' a problem, including the uncertainties, a fuzzy rule-based approach is expected to provide better and realistic results than a crisp rule-based system (Pal et al., 2006; Bentley, 2000; Mallinson and Bentley, 1999; Laha and Das, 2011; Nozaki et al., 1996; Bardossy et al., 1995; Khalid et al., 2003).

5.2 Fuzzy Model

A fuzzy controller requires a set of inputs, and a fuzzy membership function to fuzzify these input into a solution domain, also known as its *universe of discourse* (Cox, 1992; Zadeh, 1996a), and an output flow. The only similarities here between a fuzzy controller and a traditional expert system are the inputs. Once an input is provided to a fuzzy logic controller it needs to be transformed through stages that are only known to fuzzy expert system, i.e. fuzzification, inference, and defuzzification as mentioned earlier in figure 2.24. One of the controversial and debateable aspects of fuzzy logic, as defined by its critics, is the process of defuzzification where a fuzzy output needs to be 'crispened' again for it to be used in other processes (Dubois and Prade, 2005; Opricovic and Tzeng, 2003). However fuzzy logic has been successfully used in many aspects of real life proving many researchers wrong.

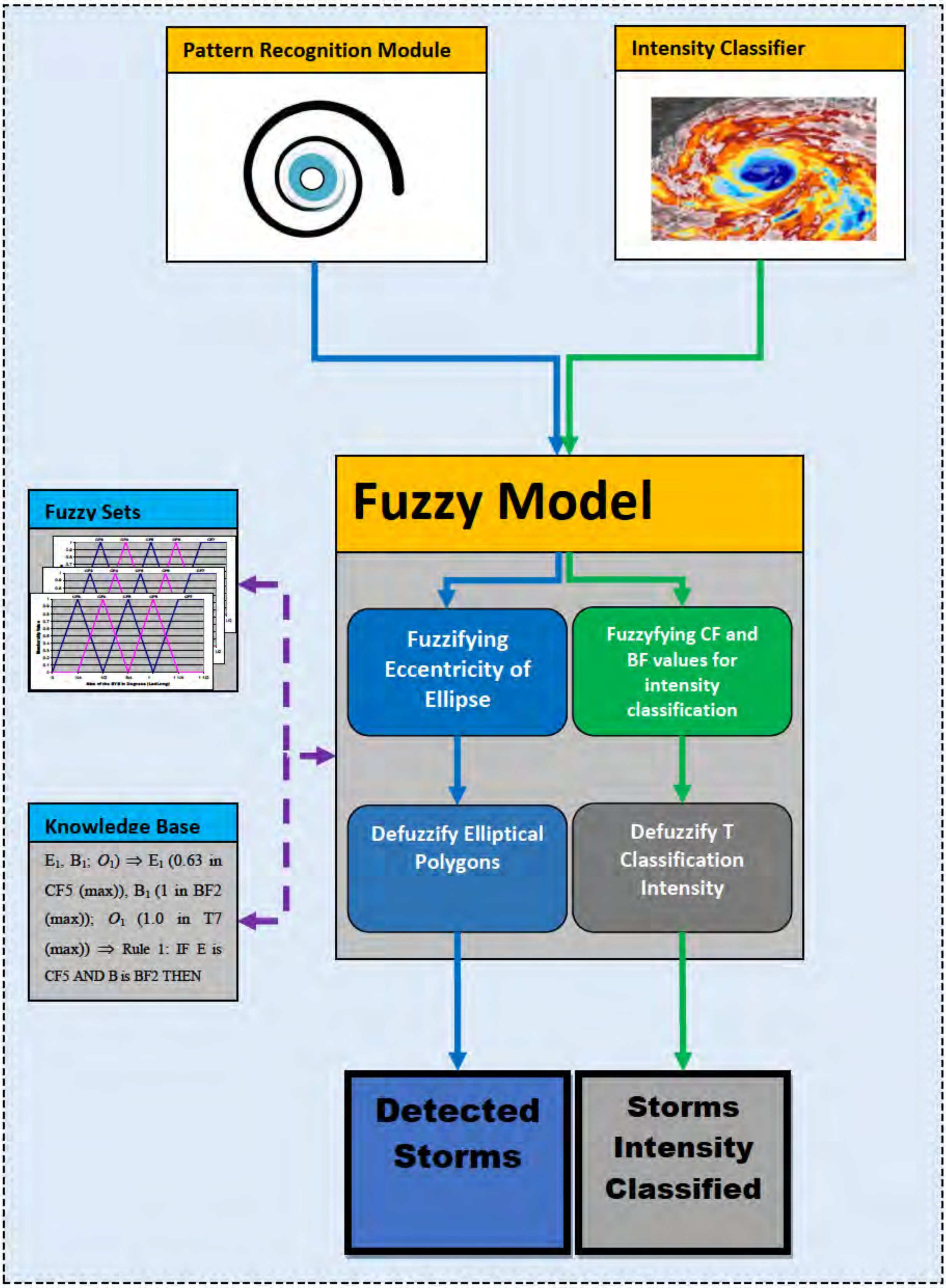

Figure 5.1: The structure of the Fuzzy Engine

Fuzzy expert systems play a vital role in pattern recognition and feature extraction. A fuzzy rule based approach was adopted in the developed system. The main aim of the Fuzzy Engine was to address the issue of vague patterns and uncertainty, which could not be solved by any rigid geometrical equations. Figure 5.1 shows the framework of the developed fuzzy logic system. The Fuzzy Engine in the developed system feeds two specific modules with the services of fuzzification of results. The Pattern Recognition module uses the fuzzy rule base to understand how elliptical either a CDO or an eye of a storm is. The eccentricity of the elliptical shape helps identify the intensity of the storm. It is the Intensity Classifier that utilises the Fuzzy Engine to its full capacity.

5.3 Fuzzy Membership Functions for Intensity Classification

After successfully detecting the cyclonic patterns by using a linguistic approach, Dvorak's technique (1975) for analysing tropical cyclone intensity was adopted to categorise the detected cyclone into one of the eight T numbers. Dvorak's chart deduces two major features in a tropical cyclone and associates a number to each of them. These two main features are Central Features (CF) and Banding Features (BF). Central Features are those which appear within the broad curve of the spiral. The Central Features either surround or cover the storm's centre system. Banding Features are part of the overcast and curves evenly around the Central Features. Once these features have been detected and measured, the T-number can be computed by adding the value of CF and BF. According to Dvorak (1975), the values of CF range from 0.0 to 7.0 while the values for BF range from 0.0 to 2.5. Dvorak updated this technique in 1984 by introducing a variable in the T-number computation called 'rules'. These analytic rules are generally used to adjust the storm intensity measurements. In the Fuzzy Engine of the developed system, these rules were replaced with the fuzzy logic rules introducing a fuzzy factor to the T-classification in order to deal with the uncertainty of feature shapes.

$$\text{T-Number} = (CF + BF) + \text{Fuzzy Rules} \qquad \text{...Equation 5.1}$$

Dvorak introduced another variable to assist in calculating the intensity of a storm, namely temperature measurement. Estimation of temperature was made objectively by using TIR images. These temperatures were deduced from the greyscale value of the CF and BF pixels in the TIR image. Higher the difference between the two temperatures, stronger the recorded intensity. Moreover, an estimate of the storm's intensity can also be determined from the temperature of the eye, called an 'Eye Number'.

The Fuzzy Engine was used to compute the value of CF and BF. Major features of the tropical cyclone, which assist in calculating the CF number and BF number, were plotted against a fuzzy membership graph. These graphs generated a membership value ranging from 0 to 1 for the categories of CF and BF, by calculating the size of the individual features in the detected tropical cyclone. In the membership functions, CF1 refers to the value of CF being 1 and BF2 refers to the value of BF being 2. Figures (5.2) to (5.11) illustrate selected samples of the fuzzy sets that have been implemented in the Fuzzy Engine. The value of the detected category was added to the membership value to get a realistic value of CF and BF features. The greyscale value of the eye was also determined from a TIR image to estimate the temperature of the eye of the storm.

The input parameters of the Fuzzy Engine at this stage are size of the detected eye, temperature of the detected eye, size and temperature of detected CDOs, dimensions of the spiral bands and the location of the centre of the storm; while the output variable is the T-Classification value. A fuzzy set is typically characterised by its membership function, therefore it is essential that the functions are chosen appropriately (Chiu, 1997; Chi et al., 1996). The fuzzy membership functions designed for this research were objectively designed based on the training data mentioned in section 3.4. Strictly depending on the application, membership functions can vary from triangular, trapezoidal, to sigmoid and gaussian. The developed system used a varying range of linear, triangular and trapezoidal membership functions based on the literature suggesting that classification of intensity changes with the size of cloud structures (Dvorak, 1984; Dvorak et al., 1990; Olander and Velden, 2007; Knaff et al., 2010; BoM, 2013b). The intensity computed by the fuzzy membership functions was then validated against the intensity estimates provided and agreed by expert meteorological organisations globally. The results of validation will be discussed in chapter 6.

The fuzzy membership functions are adopted from published literature, but are strongly influenced by Dvorak's (1984) modification to his original work, Olander and Valden's (2007) review of Dvorak's techniques and Knaff et al.'s (2010) evaluation of the techniques, in addition to the expert opinions shared in person with the author by the organisations such as Jet Propulsion Laboratory, which are keenly active in this area of research. The membership functions typically evaluate CDO, eye and spiral dimensions, as well as cloud temperature data. Figures 5.2 to figure 5.11 illustrates examples of the fuzzy membership functions used to classify the intensity of detected hurricanes.

5.3.1 Fuzzy Membership Functions for Calculating CF values

This section lists examples of fuzzy membership functions that were used to define the CF value estimates, using the dimensions of the present eye, regular or irregular shape of the CDO and the geometric characteristics of the spiral banding feature.

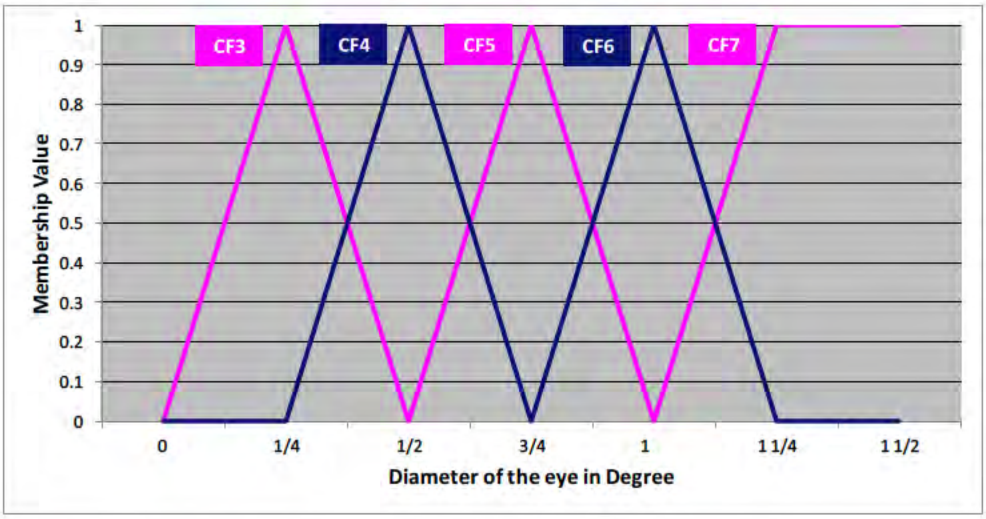

Figure 5.2: Fuzzy membership function to measure CF value when the eye is present

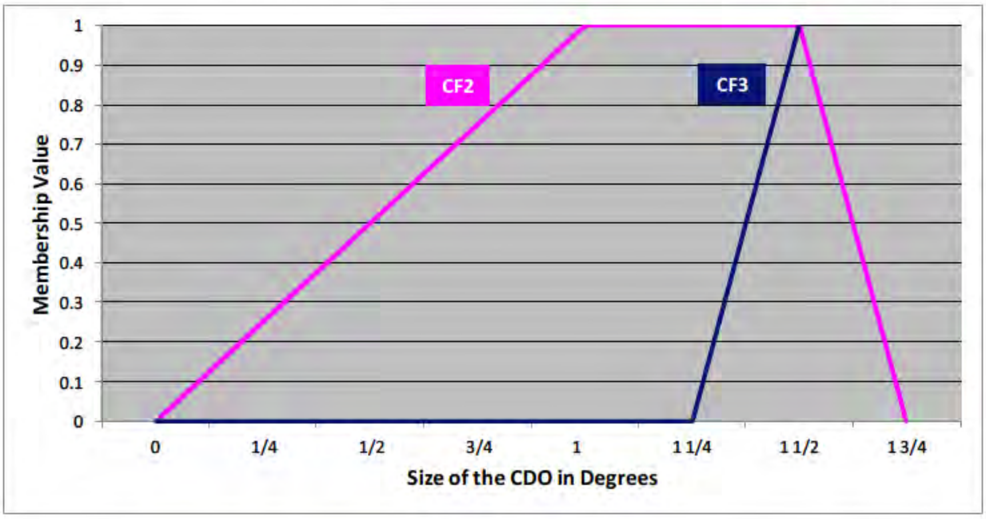

Figure 5.3: Fuzzy membership function to measure CF value when the CDO shape is irregular.

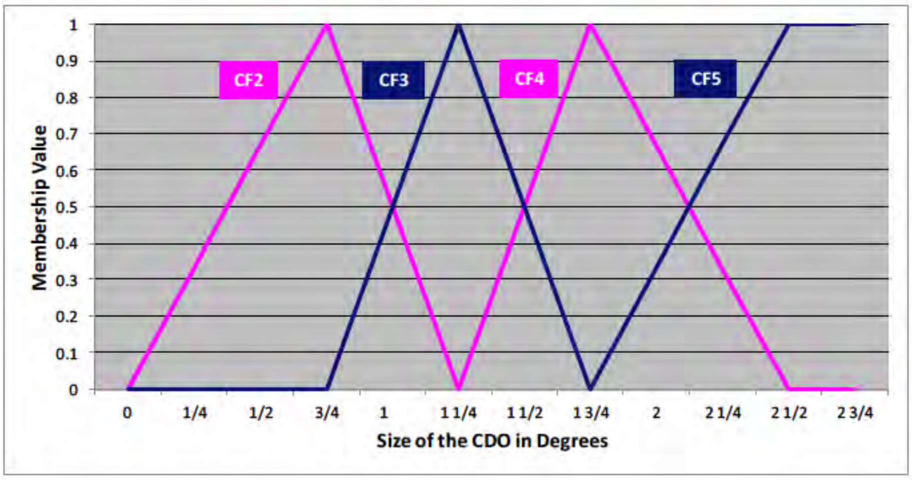

Figure 5.4: CF fuzzy membership function when the shape of the CDO is very well defined.

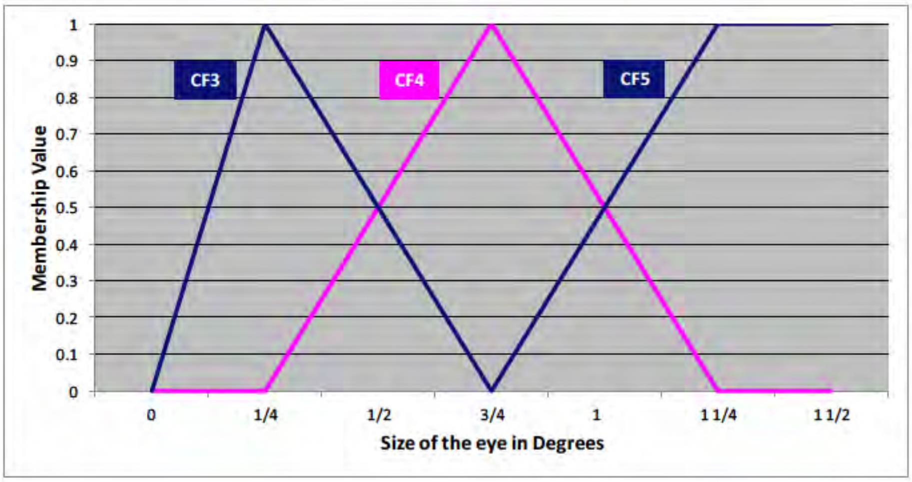

Figure 5.5: CF Fuzzy membership functions when the eye is prominent and well defined.

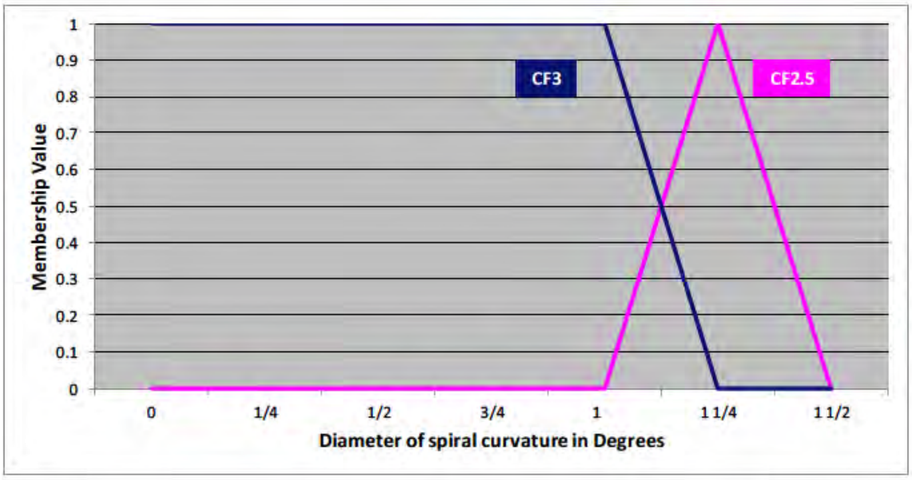

Figure 5.6: CF Fuzzy membership functions calculate from the measurements of spiral Band Features

5.3.2 Fuzzy Membership Functions for Calculating BF values

This section lists examples of fuzzy membership functions that were used to define the BF value estimates, primarily using the dimensions and geometric characteristics of the spiral banding feature.

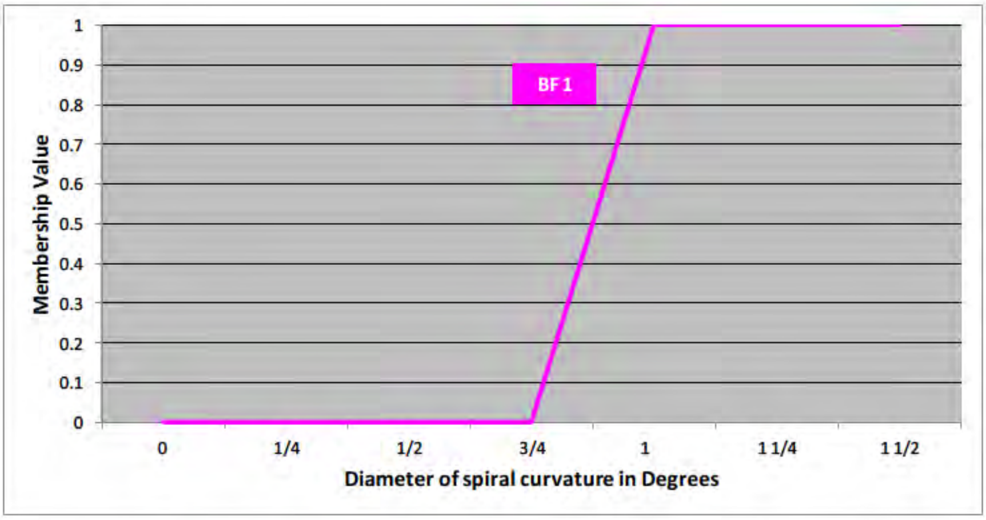

Figure 5.7: BF Fuzzy function when spiral bands encapsulate more than one half of its CDO

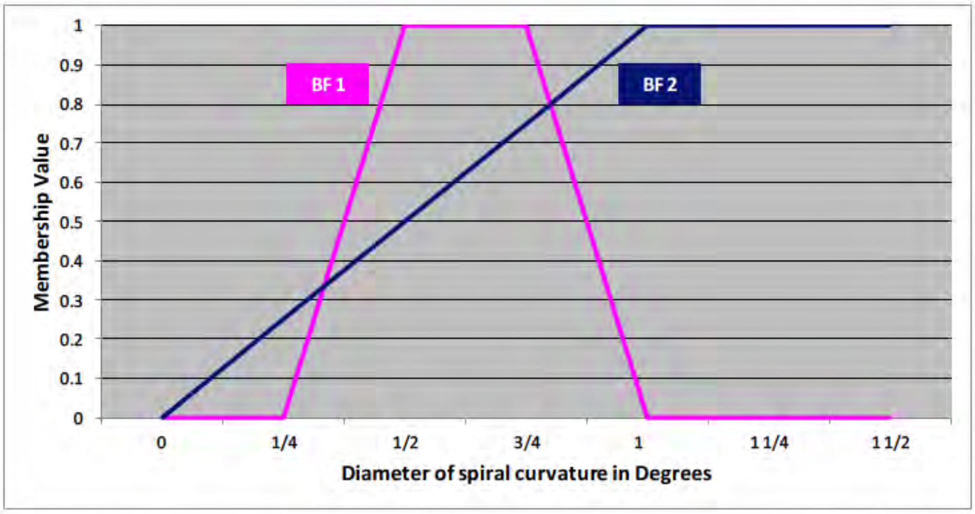

Figure 5.8: BF Fuzzy functions when spiral band completely encircles the CDO once.

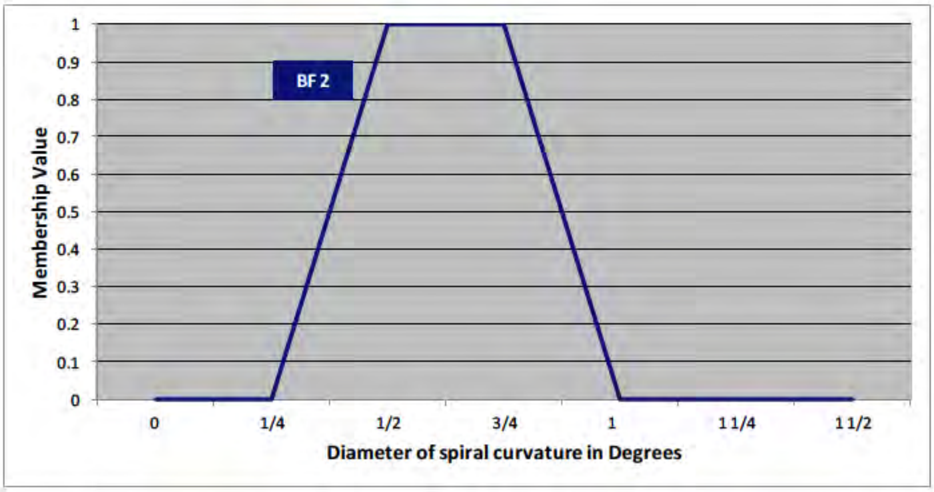

Figure 5.9: BF Fuzzy membership functions when a spiral completely encircles the CDO twice.

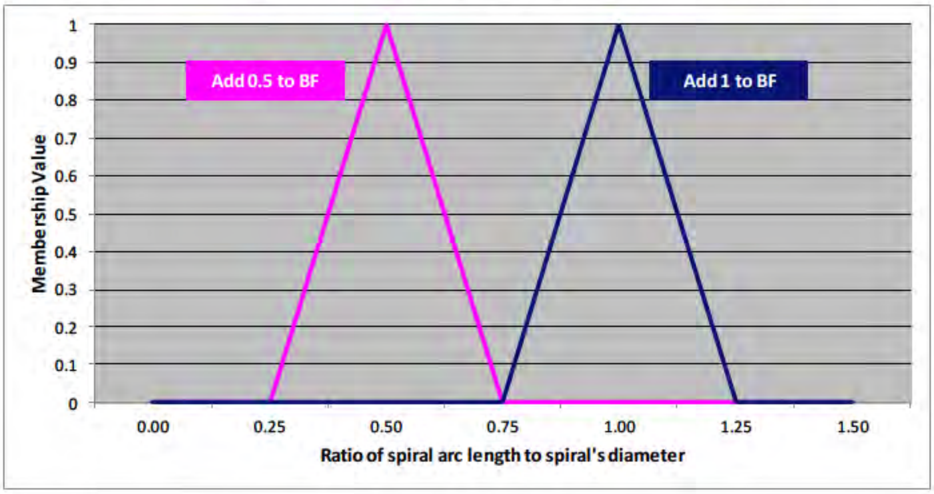

Figure 5.10: BF fuzzy membership functions in the absence of an eye.

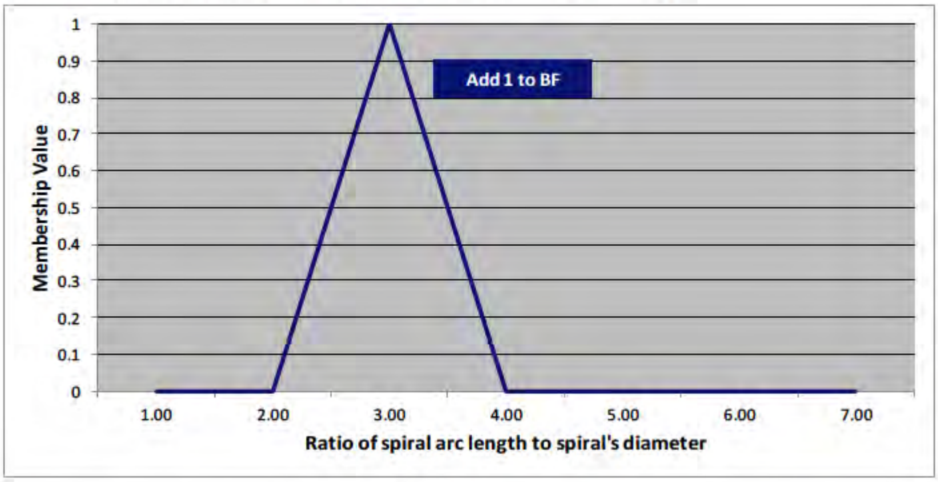

Figure 5.11: BF fuzzy membership function in the presence of an eye

A CF adjustment was performed based on the ratio of eye temperature and the temperature of the its surrounding ring. According to Dvorak et al. (1990), if eye of the storm's temperature was highly contrasting when it was warm then the CF number needs to be adjusted. See figure table 5.1 for a complete list of adjustments performed.

Table 5.1: CF adjustment table based on eye temperature.

		EYE TEMPERATURE °K						
SURROUNDING RING TEMPERATURE °K		**> 282**	**243 - 282**	**232 -242**	**220 - 231**	**210 - 219**	**204 - 209**	**198 - 203**
	> 282	0	-0.5	0	0	0	0	0
	243 - 282	0	0	-0.5	0	0	0	0
	232 -242	0	0	0	-0.5	0	0	0
	220 - 231	0	0	0	-0.5	-0.5	0	0
	210 - 219	0.5	0	0	0	-0.5	-0.5	0
	204 - 209	1	0.5	0	0	0	-1	-1
	198 - 203	1	0.5	0.5	0	0	-0.5	-1
	193 - 197	1	0.5	0.5	0	0	0	0

The new equation for confirming CF values in the presence of an eye is:

E Number + Eye Adjustment = CF ...Equation 5.2

Where E Number is the value contributing towards the intensity of a storm calculated from the characteristics of an eye. The T number equation 5.1 was modified.

T-Number = ([E + adj] + BF) + Fuzzy Rules ...Equation 5.3

5.4 Fuzzy Rules

After calculating the CF and BF values of the tropical cyclone from the fuzzy membership functions, a rule based system was generated using a technique adapted from Wang and Mendel (1991; 1992).

$(E_1, B_1; O_1)$ ...Equation 5.4

E_1 and B_1 are the measurement of CF and BF, respectively. O_1 is the output in T-numbers. The actual task was to generate rules by using this equation (Chi et al., 1996).

After deciding on the membership functions for the data pair, rules were produced accordingly. For instance, if E_1 had a membership value of 0.37 for CF4 and 0.63 for CF5 and zero in all other regions while B_1 had a membership value of 0.9 in BF2 and 0.1 in BF1, two possible rules were generated. One of the rules classified the cyclone's maximum intensity and the other classified the minimum possible intensity. Two example rules generated from the data pair are as follows:

(E_1, B_1; O_1) $\Rightarrow$ E_1 (0.63 in CF5 (max)), B_1 (0.9 in BF2 (max)); O_1 (T7 (max)) $\Rightarrow$

Rule 1: IF E is CF5 AND B is BF2 THEN O_1 is T7

(E_1, B_1; O_1) $\Rightarrow$ E_1 (0.37 in CF4 (min)), B_1 (0.1 in BF1 (min)); O_1 (T5 (min)) $\Rightarrow$

Rule 2: IF E is CF4 AND B is BF1 THEN O_1 is T5

As suggested by Kohavi (1995) and Witlox et al. (2004) decision tables were constructed to indicate the various relationships between features, determining the CF and BF values. Table (5.2) illustrates a decision table with storm eye present and varied values of CF and BF, while table (5.3) shows a decision table for an absent eye, but a well-defined central dense overcast, with the varied value of CF and BF.

Table 5.2: A sample of decision table when the eye is present

Eye is Present	CF3	CF3.5	CF4	CF4.5	CF5	CF5.5	CF6	CF6.5	CF7
BF0	T3	T3.5	T 4	T4.5	T 5	T5.5	T 6	T6.5	T 7
BF0.5	T3.5	T4	T4.5	T5	T5.5	T6	T6.6	T7	T7.5
BF1	T 4	T4.5	T 5	T5.5	T 6	T6.5	T 7	T7.5	T 8
BF1.5	T4.5	T5	T5.5	T6	T6.5	T7	T7.5	T8	
BF2	T 5	T5.5	T 6	T6.5	T 7	T7.5	T 8		

Table 5.3: A sample of the decision table when the CDO is well defined

Eye is Absent	CF2	CF2.5	CF3	CF3.5	CF4	CF4.5	CF5
BF0	T2	T2.5	T 3	T3.5	T 4	T4.5	T 5
BF0.5	T2.5	T3	T3.5	T4	T4.5	T5	T5.5
BF1	T 3	T3.5	T4	T4.5	T 5	5.5	T 6
BF1.5	T3.5	T4	T4.5	T5	T5.5	T6	T6.5
BF2	T 4	T4.5	T 5	T5.5	T 6	T6.5	T 7

The set of example rules generated from the decision table 5.2 are as follows:

Eye Present Rule 1:

IF

(Eye is present) *AND*

(CF is 3) *AND*

(BF is 0)

THEN

(It is a T3 Tropical cyclone)

Eye Present Rule 2:

IF

(Eye is present) *AND*

(CF is 4) *AND*

(BF is 0)

THEN

(It is a T4 Tropical cyclone)

Eye Present Rule 3:

IF

(Eye is present) *AND*

(CF is 5) *AND*

(BF is 0)

THEN

(It is a T5 Tropical cyclone)

After the rules were defined, the fuzzy membership functions and the rule bank was combined together to achieve the best fuzzified output. Figure 5.12 display the copulation of fuzzy membership functions and the rule base.

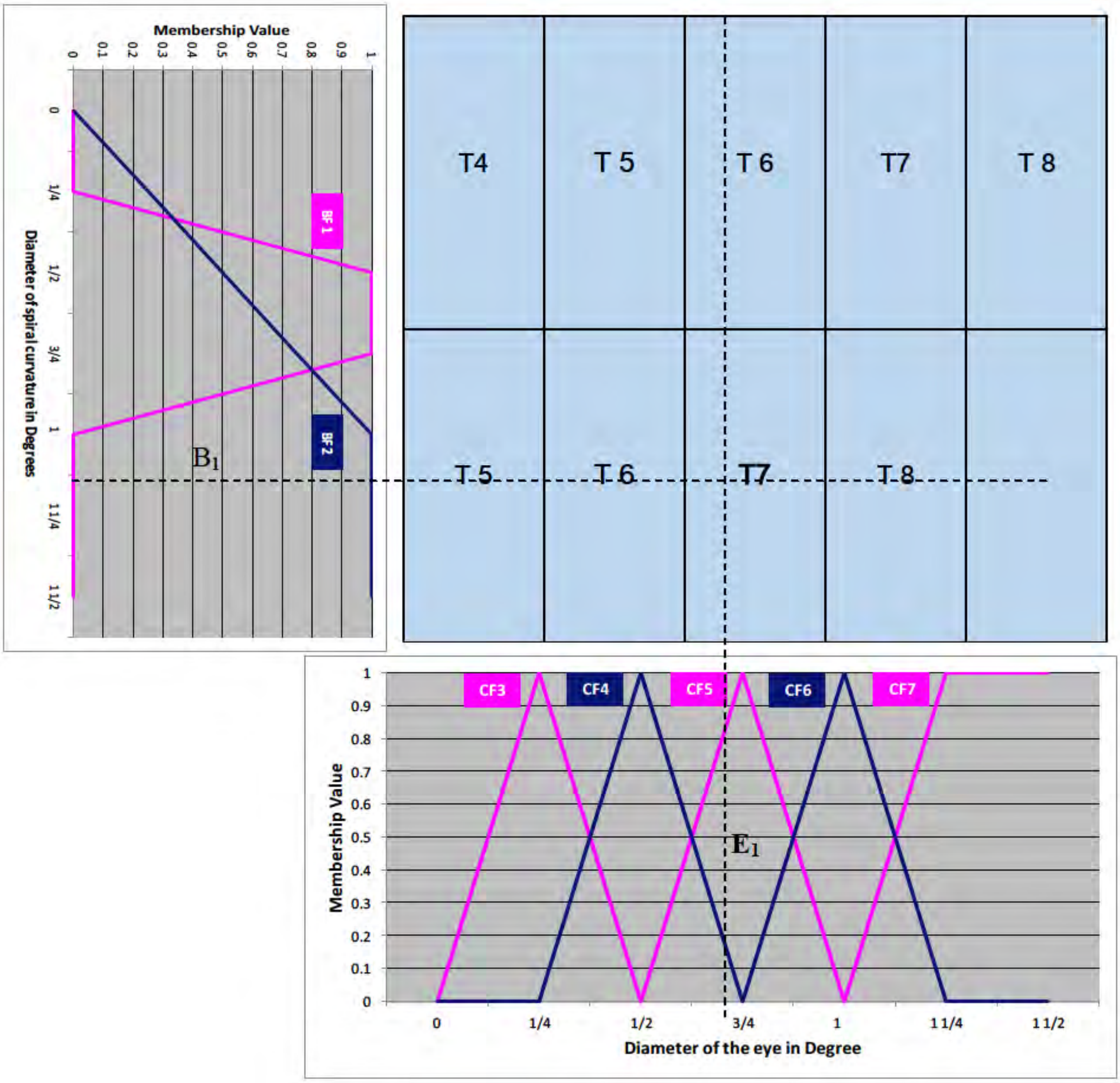

Figure 5.12: Fuzzy partitions and the rule bank for a hurricane Andrew intensity classification problem.

From figure 5.12 Hurricane Andrew now can be classified as a strong T7 (CF5 +BF2) or a weak T6 (CF4 + BF2) or even a weak T5 or a T4. The choice of intensity value is made by implementing a good defuzzifier. Higher membership value should be the criteria for selecting a value for CF or BF.

5.5 Summary

This chapter has described a soft computing pattern recognition and intensity classification tool for automated monitoring of tropical cyclones. The knowledge base tool utilises the power of fuzzy rule based systems to detect amorphous cloud patterns, which could not be defined simply by traditional geometrics. In addition, the fuzzy engine for intensity classification of the detected storm was also presented. The intensity engine uses thirty one fuzzy membership functions generating 673 rules. These rules provide two fuzzy T number values for each tropical cyclone detected; the high fuzzy membership intensity class and the low fuzzy membership intensity class. The high fuzzy membership class was chosen to be the final T number. In the next chapter the estimated T numbers will be validated against the NOAA IBTrACS records to investigate the accuracy and feasibility of the system.

CHAPTER 6. VALIDATION OF THE DEVELOPED SYSTEM

6.1 Introduction

The aim of this chapter is to validate the developed system's ability to detect and classify tropical cyclones. The chapter will also examine the accuracy of the developed system's processed outcomes against an acknowledge database of past hurricane records. In order to produce acceptable validation; data used for training the system will not be assessed or processed, the outputs will be compared against a published source produced by a respectable meteorological organisation and lastly the limitation boundaries of the developed system will be identified.

6.2 Research Context

As described in the chapter 1, the aim of the research was to develop an algorithm for fully automated detection and classification of tropical cyclones from satellite imagery using soft computing techniques. The aim was achieved by first investigating and identifying principal visually recognisable features of tropical cyclones; secondly, by devising intelligent pattern recognition algorithms to detect these features in the satellite images and classify their intensity based on geometric and spectral measurements; and lastly, developing and validating the system to be functional. The developed system calculated intensities of the detected tropical cyclones using rule based fuzzy functions.

Power (1989) originally developed and tested a manual technique for identifying tropical cyclones solely from satellite imagery. This techniques required her to visually inspect satellite images to identify cyclonic patterns. Although subjective, the developed technique was effective and identified a number of new cyclones that were not identified in the historical records. This research exploited the idea of using pattern recognition and artificial intelligence to remove the errors introduced due to subjective nature of storm detection by Power (1989) for full automation of the detection and intensity classification process. Figure (6.1) shows a typical example of the type of outputs manually digitised, making it rather subjective in nature.

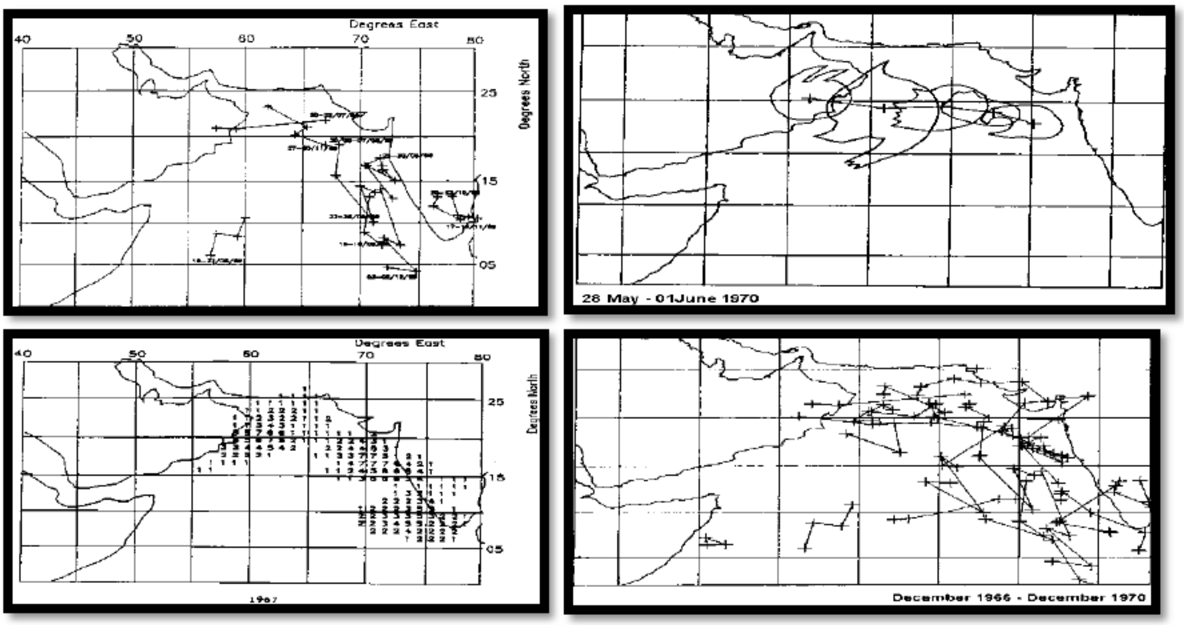

Figure 6.1: Outputs generated by a manual storm detection and digitising technique developed by Power (1989)

In order to replicate Power's successful results in an automated system, pattern recognition and artificially intelligent algorithms were required to incorporate the uncertain and subjective nature of human recognition and decision making process. The system was developed with a modular design in mind; this allowed the system to be updated at a modular scale without affecting other modules in the system. The automated system was trained based on an independent data source using 1500 images consisting of 100 storms; while the algorithms were validated using 11717 and 8311 storm images. This chapter will elaborate the validation process and discuss the results of this process.

The developed system performed the analysis in a rather sequential manner, by first sending the input satellite images to a pattern recognition module, which used image processing techniques to classify the patterns and then segregate these patterns to be recognised as storm clouds. Once appropriate cloud patterns were identified, a grammar based inference model collated these patterns and parsed them to be recognised as tropical cyclones. A set of geometrical and spectral measurements were made to classify the intensity of the detected cyclones. The scale used for intensity calculation was based on Dvorak's T classification, due to its efficiency in recognising cyclones solely from satellite imagery. The subjective nature of Dvorak's algorithm was tackled by adopting a fuzzy rule based approach which allowed the uncertainties in pattern classification to be objectified. A validation regime was adopted to test the accuracy of the detection. The developed system improved hurricane detection accuracies by nearly 11%, managed to detect storm at an earlier stage of their development and improved storm track accuracy to 19km from the published averages of 50km.

Moreover, this study introduced a holistic approach towards solving a problem that has been mostly segmented in literature. Researchers have mainly focused on one aspect of the cyclone anatomy, while this study detects it at an early stage of development and tracks it through its life spans, also classifying the intensity of the cyclone incorporating the uncertain shapes of the composing features. This makes this study a valuable contribution to the research in the area of cyclone detection, pattern recognition, and fuzzy rule development.

6.3 Validation Process

As previously mentioned in section 3.4, 1500 images from three different satellites were used to train the fuzzy pattern recognition system. A total of 100 different storms, from the period of 1978 to 2009, were processed to understand the patterns that needed to be recognised using the automated system. These images were removed from the validation process to remove any bias. At first, over 3000 training images were randomly selected from the full HURSAT archive. These images were then vetted to ensure all stages of the hurricanes were available in the training set. It was also ensured that the time of the day the images were representing did not clash with the validation data, i.e. no images were selected for training with the timestamp of 0000hrs, 0600hrs, 1200hrs and 1800hrs. HURSAT has a three hourly coverage of the North Atlantic basin, which easily allowed a good training dataset without jeopardising the validation data.

The validation data consisted of satellite images from Meteosat and GOES satellites. One hundred seventeen thousand and seventeen images were processed consisting of 375 named storms over a period of 31 years; see table 6.1 for more details. Figure 6.1 provides an example of the nature of images that were processed.

Table 6.1: Data used for validation.

Satellites	IBTrACS & HURDAT	GOES	Meteosat
Spatial Resolution	-	~8Km	~8km
Temporal Resolution	6 hourly	6 hourly	6 hourly
Number of storms processed	375	375	
Images with storms	-	8311*	
Images with hurricanes	-	3037*	
Number of Images processed	11717	11717*	
Range of years	1978-2009	1978-2009	1978-009
*** It was a combination of GOES and Meteosat that makes up the number, depending on the availability of the images.**			

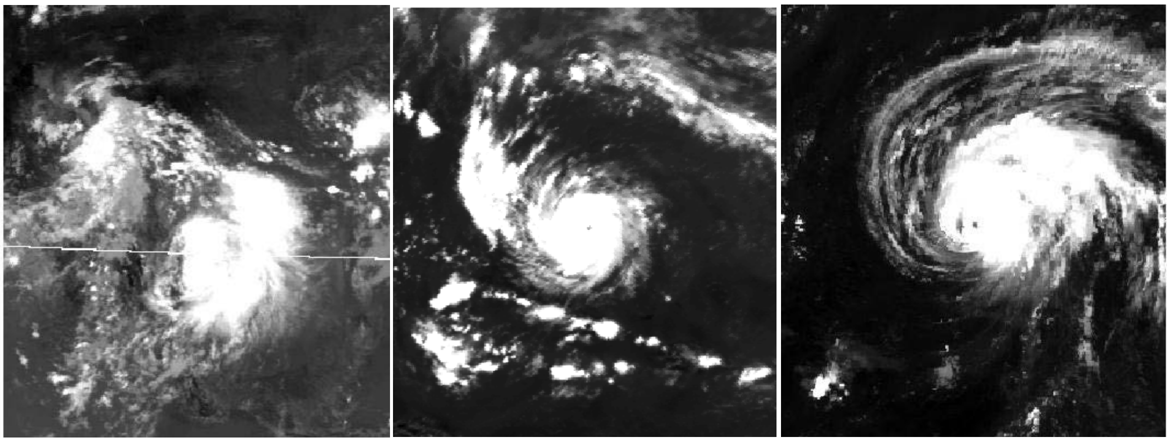

Figure 6.2: [left] Hurricane AMELIA 1978; [middle] Hurricane ANDREW 1992; [right] Hurricane BILL 2009.

For the purpose of validation the procedure is divided into two phases; Validation of the pattern detection module and Validation of the intensity classifier. Each phase includes a series of tests that allows the comparison to be made with the official data obtained from NOAA.

The Pattern Recognition Module was tested for its accurate identification of the storms, and compared with the data from IBTrACS for confirmation. Centre of the storm plays a vital role in its early identification and monitoring, which makes is extremely valuable in disaster management research. The predicted storm centres were analysed against the actual storm centres agreed by official records and storm reports. The intensity classifier was tested by extracting low fuzzy class and the high fuzzy class from the STORM database, for each image that was processed. 11717 records were evaluated against the official 6 hourly storm records. In addition GIS was used to perform spatial statistics and visualise the results and errors.

6.3.1 List of tests performed:

For the Pattern Detection module the following tests were performed:

- Error matrix for hurricane detection
- Accuracy variation by years
- Storm centre RMSE
- Storm centre dimensional regression

For the Intensity Classifier the following tests were performed:

- Cross validation
- Fuzzy membership value statistics

6.4 Pattern Detection (PR) Module

The main aim of the module was to classify, perform object segmentation and pattern recognition using a syntactic approach. Between the years 1978 and 2009 three hundred and seventy five storms were named, although not all of them reached hurricane strength. For the purpose of testing, a distinction between a storm and a hurricane was stressed. Only storms above T2.5 were recognised as tropical storms, any value below that were labelled as low pressure systems of extratropical storms. This section refers to weather systems as storms with a low pressure system and a T-number ranging from 1-8. Hurricanes were classed as storms with T4 and above classification, while all storms with T2.5 and above were classed as tropical storms; see table 6.2

Table 6.2: T numbers and storm categories

T number	1	1.5	2	2.5	3	3.5	4	4.5	5	5.5	6.5	7	7.5	8
Storms														
Tropical Storms														
Hurricanes														
Pre Hurricane Stages														

6.4.1 Storm and Hurricane Detection

According to the official records, from the total of 11711 images chosen, 11001 images had some instance of a storm. The PR module detected 8311 images to have some sort of a low pressure storm, once commission and omission errors were removed. Hence the PR module detected 75.5% of all storms at any stage of their development. However the developed system couldn't identify any storms below the intensity of T2 (figure 6.2). 2007 seemed to be the year with the least accurate detection rate with only 61.1% of the images with storms being recognised during the year via the PR module. On the contrary 1986 and 1999 were the years with highest level of accuracy reaching up to 84.8% and 84.1% respectively. The reason for a large variation between the years with most and least detection was due to the fact that 2007 mainly had storms detected at a T number of 4 or lower, while in 1986 and 1999 majority of the storms were stronger hurricanes.

From the 11001 storm images, official records suggested that 3037 were recorded at hurricane strength. In T number this equates to any storm with a T number of T4 and above. Out of the 3037 images with hurricanes present, the developed system recognised 81.23% of the images with a storm of T4 or higher intensity (figure 6.4). Table 6.3 shows an error matrix to identify any commission or omission errors. The PR module demonstrated a true detection accuracy of 81.23% when storms were present in an image, while false negative accuracy was 92.55%. This meant that apart from detecting cyclones when they were present, the system also rejected the image when there were no cyclones to detect. However small it may be, in 7.44% of the images the system detected a storm when there was nothing there to identify. Figure 6.4 illustrates some of the example of this scenario when the system picked up a false alarm. Figure 6.5 show a graph of how hurricane detection compares every year.

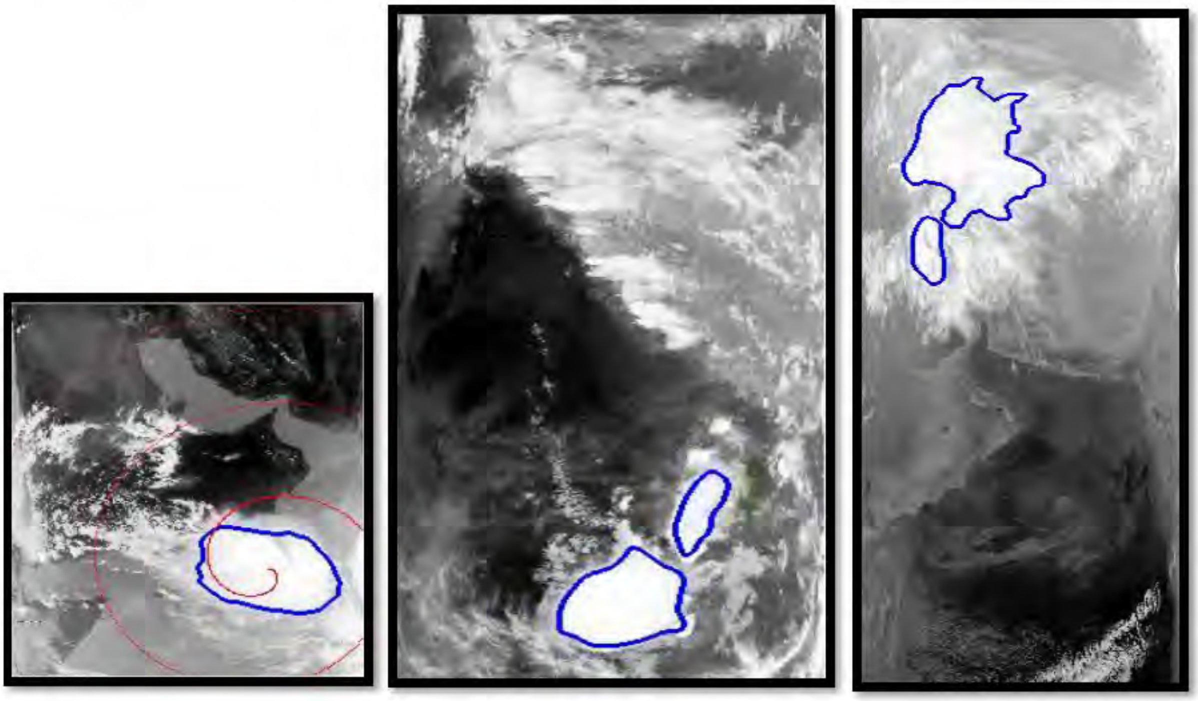

Figure 6.3: Falsely detected storms due their elliptical shapes

With an overall accuracy of 81.23% the automated pattern recognition system utilised the fuzzy logic control appropriately and has managed to detect patterns that otherwise would not be possible to identify due to their rugged and irregular shapes. However, the fuzzy membership function of eccentricity of any ellipse provides every closed polygon a membership to an ellipse, later discarding it if the membership value was too low. Hence recognising patterns that wouldn't have been possible if traditional geometry was used.

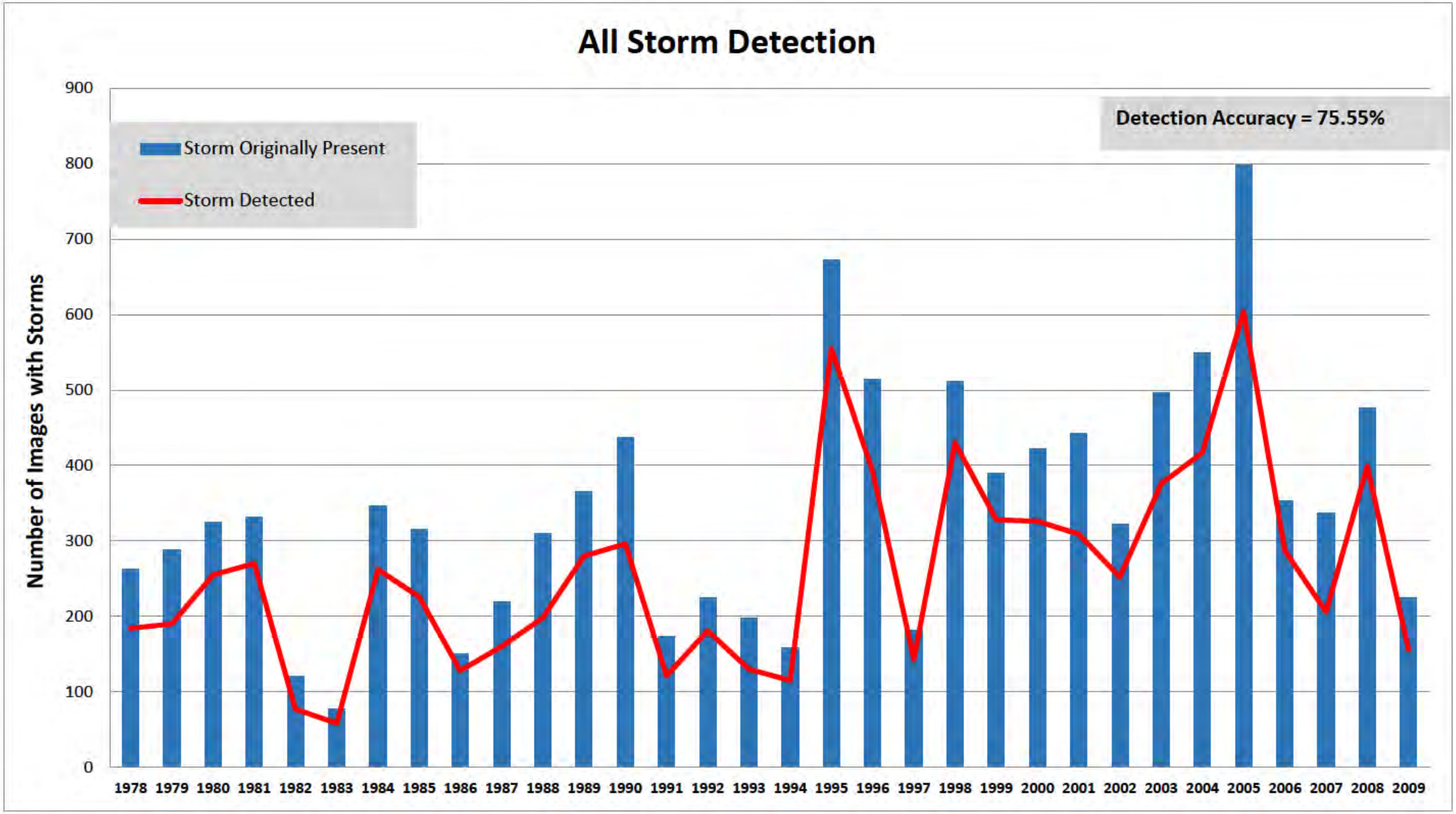

Figure 6.4: Graph showing yearly storm detection accuracy.

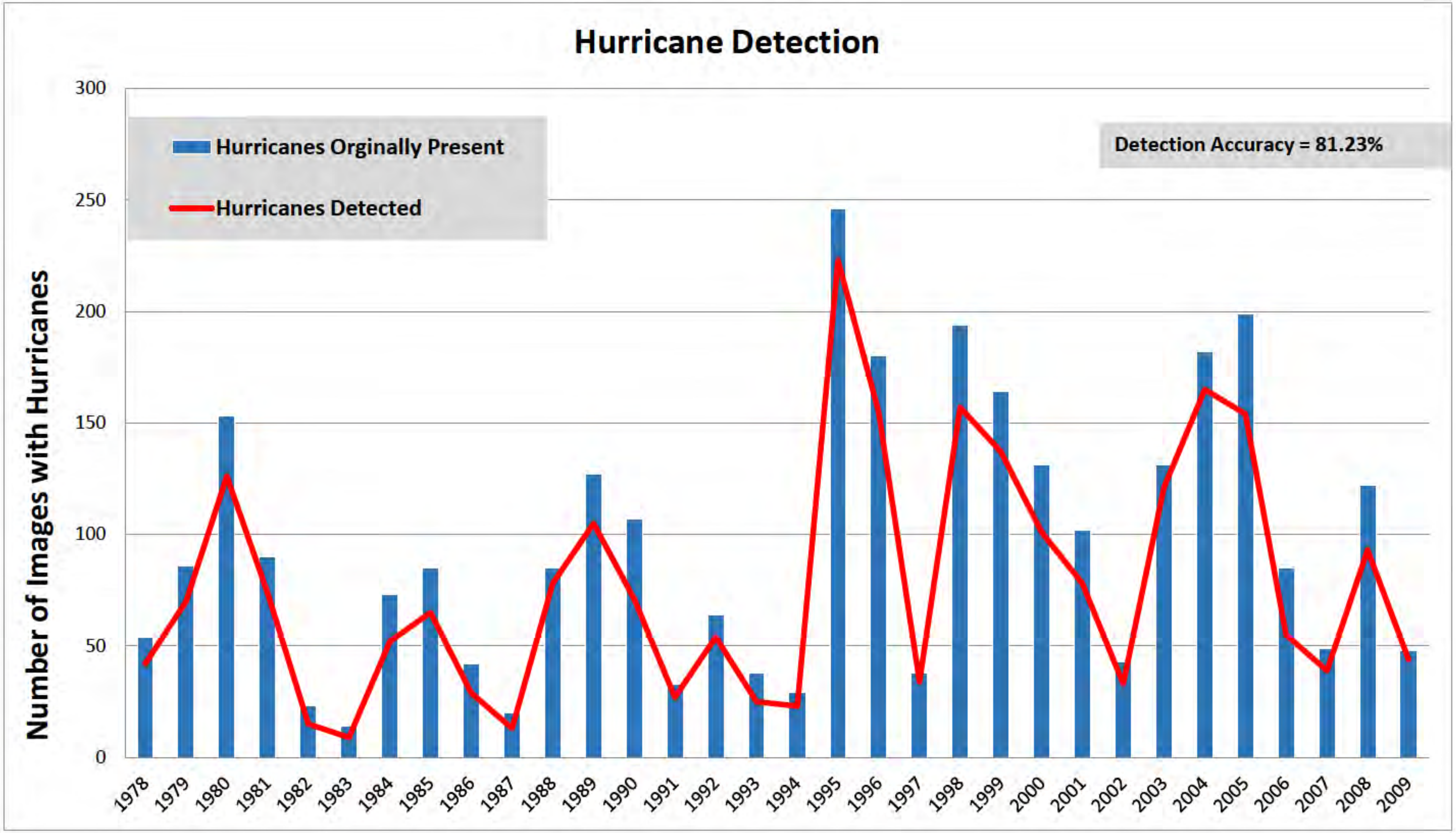

Figure 6.5: A graph showing accuracy of hurricane detection yearly

The system also indicated an accuracy of 73.38% in recognising the storms before they reach their hurricane intensity as compared to an average pre hurricane stage detection accuracy of 70% achieved by published research (Pal et al., 2006; Talukder et al., 2008; You et al., 1999; Wei and Jing, 2010; Khalid et al., 2003; Theilen-Willige, 2009). This creates huge potential for any early warning system.

Table 6.3: Error Matrix for hurricane detection

	Hurricane Present Number of images (%)	Hurricane Absent Number of images (%)
	Total = 3037	Total = 8680
PR Module Detected	2467 (81.23%)	646 (7.44%)
PR Module Undetected	570 (18.77%)	8034 (92.56%)

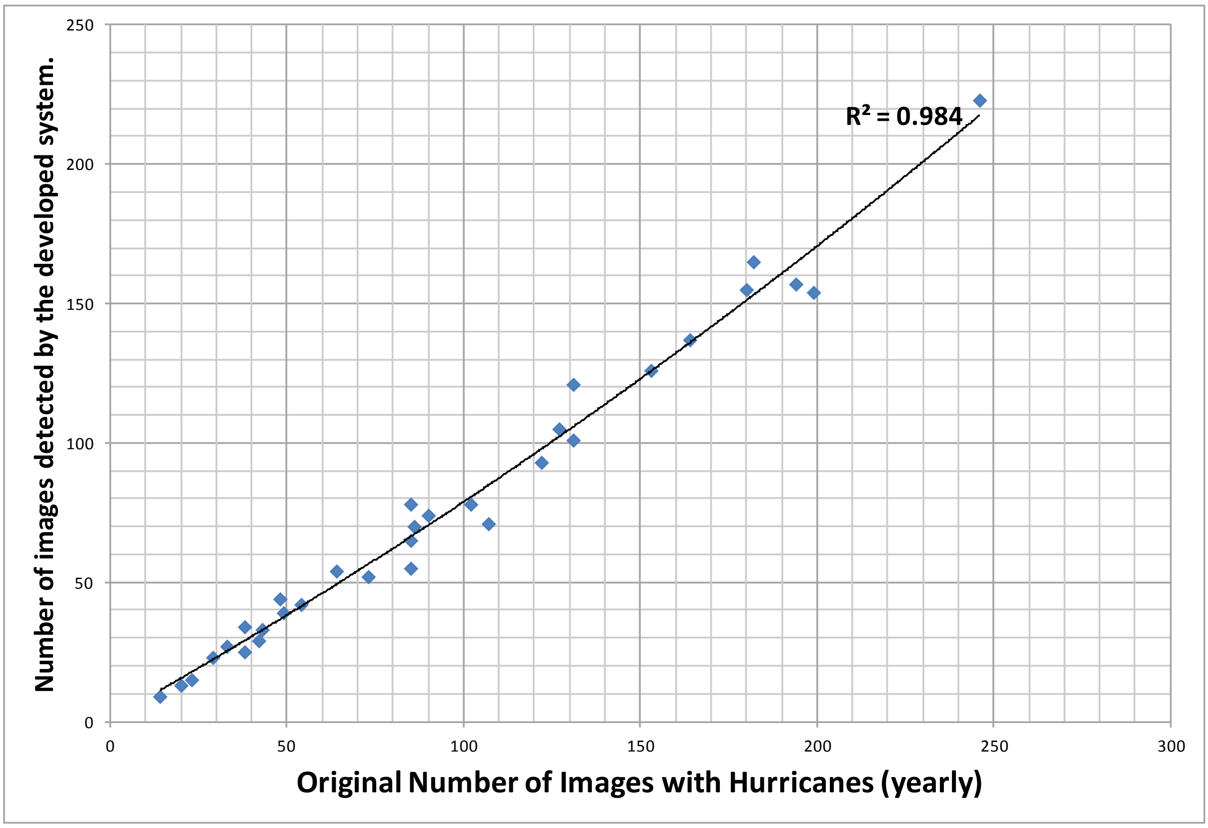

Figure 6.6: Correlation of hurricane detected with the original occurrences.

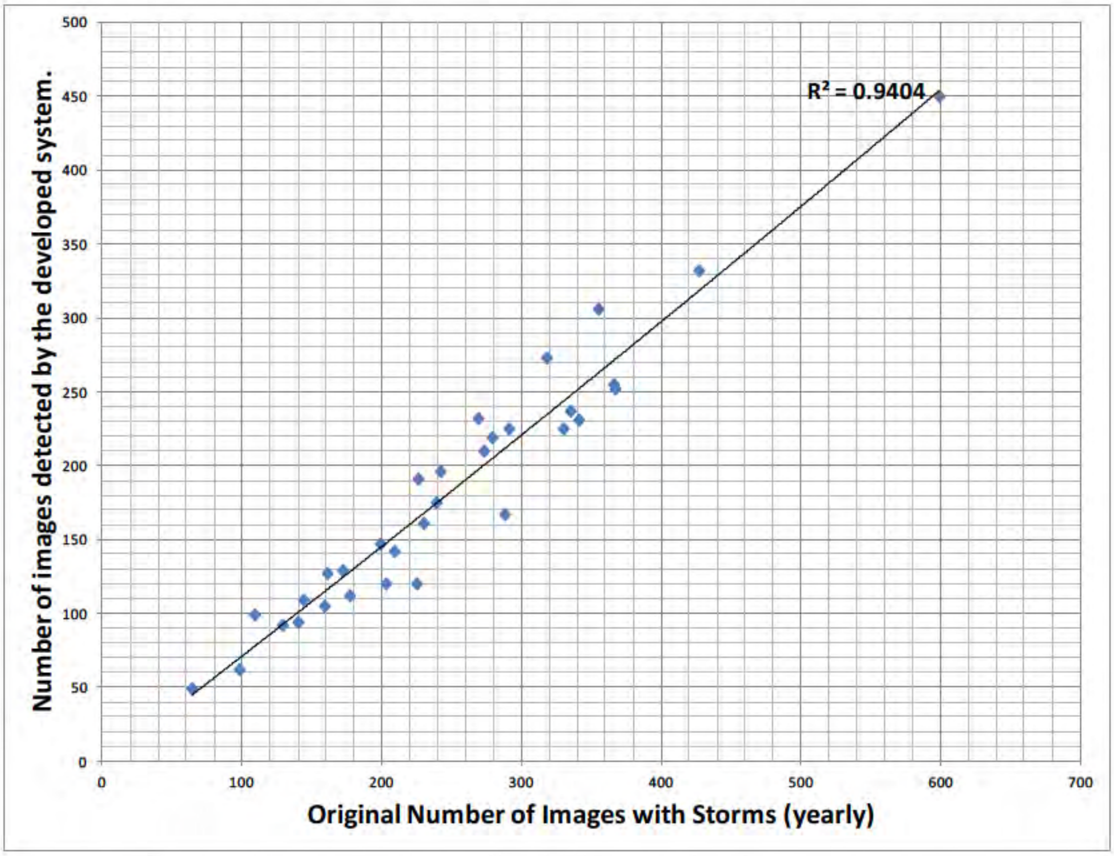

Figure 6.7: Correlation of storms detected with the original occurrences.

6.4.2 Storm Centre

Simply identifying a storm on an image is not the milestone in pattern detection. It is also extremely necessary that the characteristics of the recognised article are true to their original form and shape. For this purpose centre of the storm needs to be accurate for precise path tracking and intensity monitoring. NHC and NOAA with the help of Hurricane Reconnaissance unit, produce the best storm track records that represent the true location of the storm. Comparative analyses were performed on the centre coordinates extracted from the developed system and the reconnaissance data. An RMSE was calculated to estimate the trend in the shift of the centres from the original locations. As compared to the official records the RMSE calculated was 0.854 when all the centre points were used; the unit for the RMSE was degrees. After calculating the RMSE, it was decided to analyse the predicted storm centre spatial distribution as compared to the original storm centres. ArcGIS was used to estimate the true geographic coordinates of detected storm. This was done in ArcGIS due to the incapability of the developed system to incorporate spatial data. Figures 6.7 and 6.8

show the correlation graphs between the original coordinates compared with the estimated values.

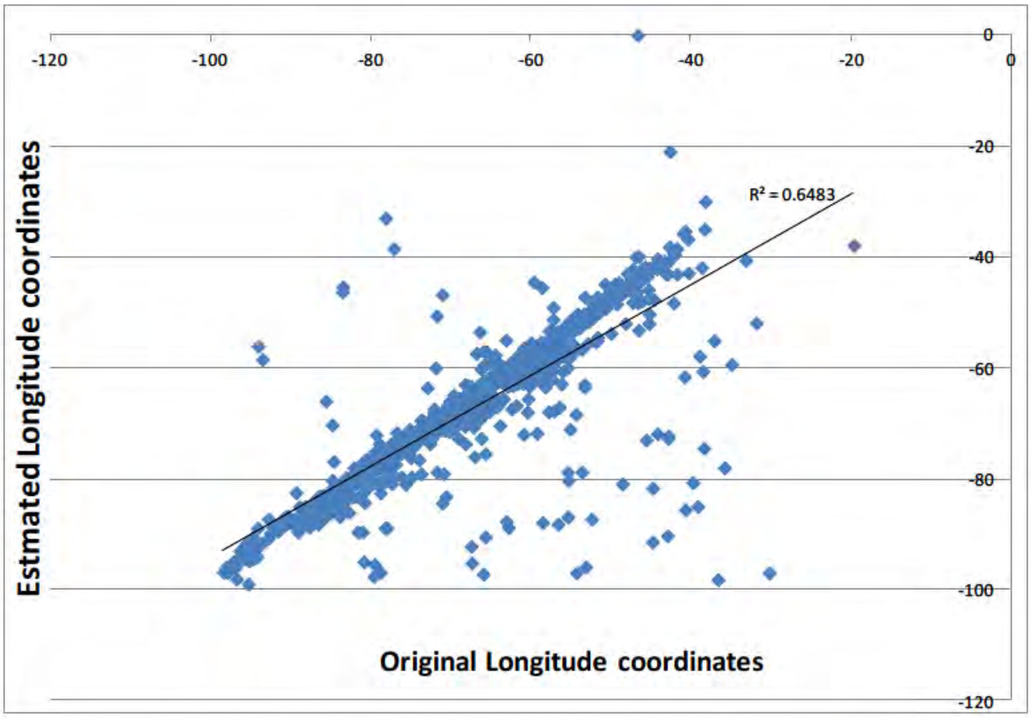

Figure 6.8: A correlation graphs showing a shift away from the plotted trend in the X direction.

Figure 6.9: A graphs showing a strong correlation with the plotted trend in the Y direction. Wrong geographic referencing of the images have caused some clusters, in red, to shift from the norm.

It is very clear from the resulting data that the errors in estimating the centre of the storm were introduced mainly due to the storm fluctuating over the X coordinates. This is anomalously caused by a small number of centre locations being extremely far from the original centre of the storm. After examining the images it was noted that some of them lost their georeferenced coordinate system and ArcGIS misrecognised the world file attached. At places the distance was unacceptably large. Considering it was the error introduced outside the realm of the algorithm, its removal caused the RMSE to shift from 0.85 to 0.55. Figure 6.8 provides an example of such a case. The figure displays the storm features detected by the system, with the estimated and original track. Estimated centres are show as black dots while the official track locations are displayed as larger circular dots. The colours in the circular dots represent the intensity estimated by the system. It is clearly seen that the cyclone detected by the system is not a false detection but erroneous input. The graph embedded in the figure shows the life span of the hurricane, with green area showing the official figures of intensity, while blue and red represent the estimated fuzzy low and fuzzy high membership values, respectively.

In summary the PR module showed higher accuracies than current research in the field (Herndon et al., 2010; Landsea et al., 2012; Olander and Velden, 2011; Velden et al., 1998a). Different algorithms and detection systems use different accuracy references. Certain algorithms will use spatial deviation from the storm centre, while others use maximum sustained wind speeds as a reference. In both cases the developed system performed better than current algorithms in practice. The developed system logged an average spatial deviation of 19km as compared to recorded average accuracies of 50km for storm track centres. The intensity accuracies are documented in section 6.5. Not many researcher have approached the process of tropical cyclone detection and classification with ease. Many tend to focus on central feature measurements or the spiral band and their precipitation ratios, and often they use numerical prediction models to estimate the intensity (Wei et al., 2011; In-Hyuk and Hyeong-Bin, 2010; Lajoie and Walsh, 2010).

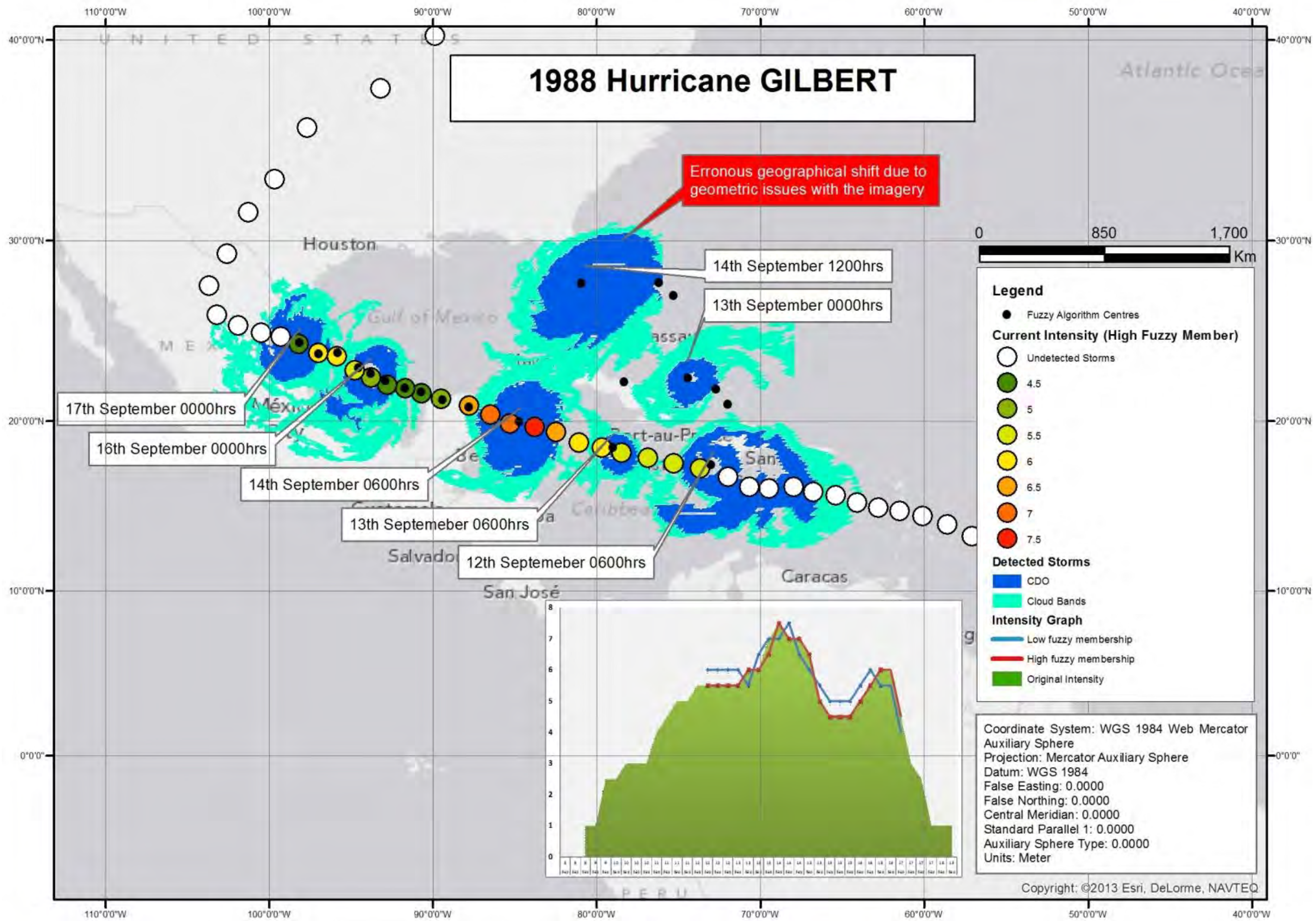

Figure 6.10: Map of hurricane GILBERT 1988, showing erroneous input data.

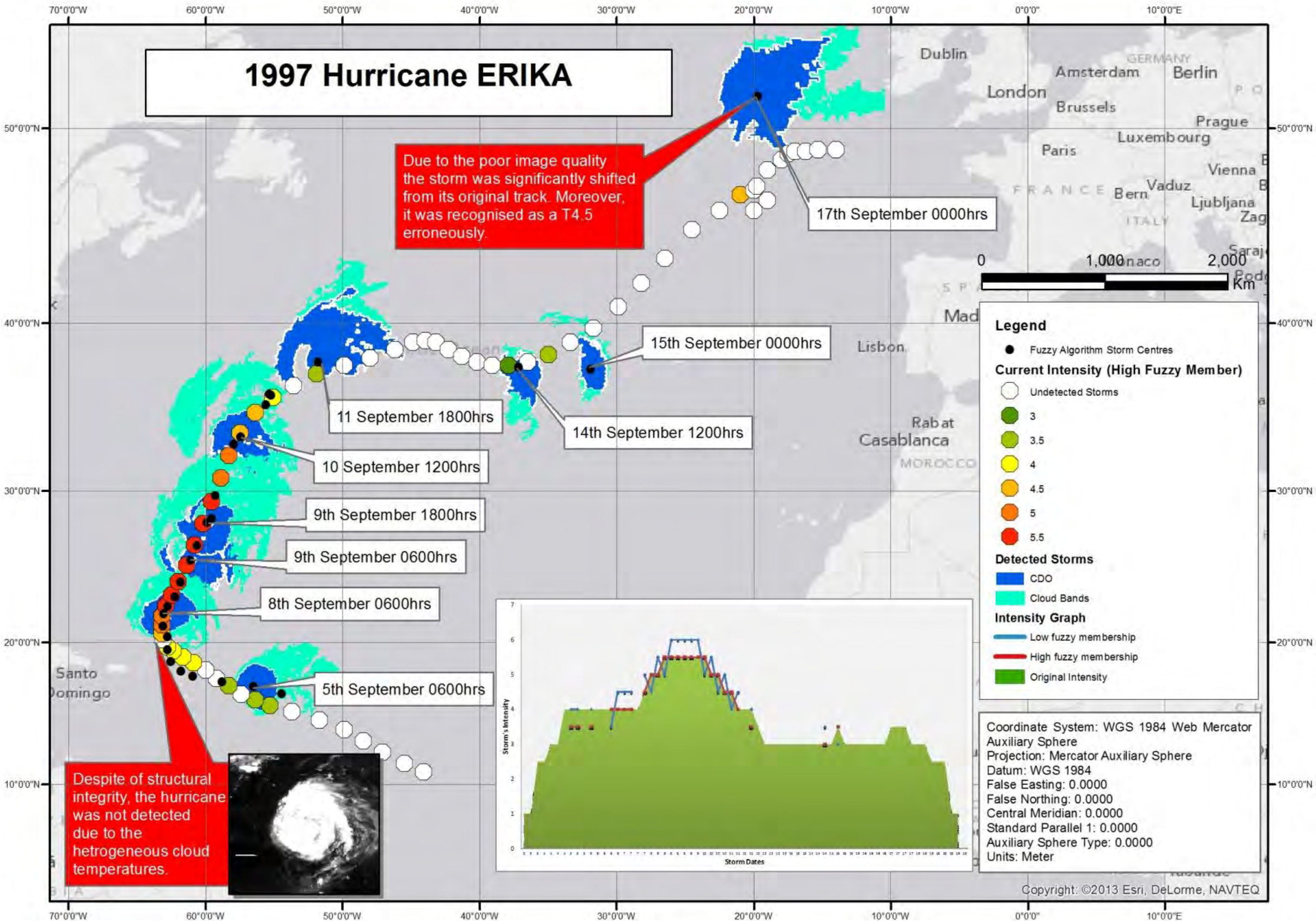

Figure 6.11:Hurricane ERICA also showing shifted centre because of image mis-registration.

6.5 Intensity Classifier (IC)

Once a storm was detected by the PR module, its major geometric properties would be stored in the database and then passed on to the Intensity Classifier for further processing. The IC thoroughly utilised the fuzzy membership functions and the knowledge base/ rule base to estimate the intensity of the detected storm. Based on the fuzzy values and rule base, IC generated a high membership value and a low membership value. It was necessary to choose the high membership value to trust the model. However in the following section even the low fuzzy membership values were validated for accuracy. For each storm detected two fuzzy values were identified, and a T number with the stronger membership value was allocated to the results. The number of occasions the lower fuzzy membership value provided the better results than the high fuzzy value was also assessed. This would suggest that the algorithm was over estimating the intensity. However, it was only applicable to a small number of cases, 3.4% of the images. As one would imagine, some intensity cyclones were easier to detect than the others. Figure 6. 10 show the Intensity accuracy per T class.

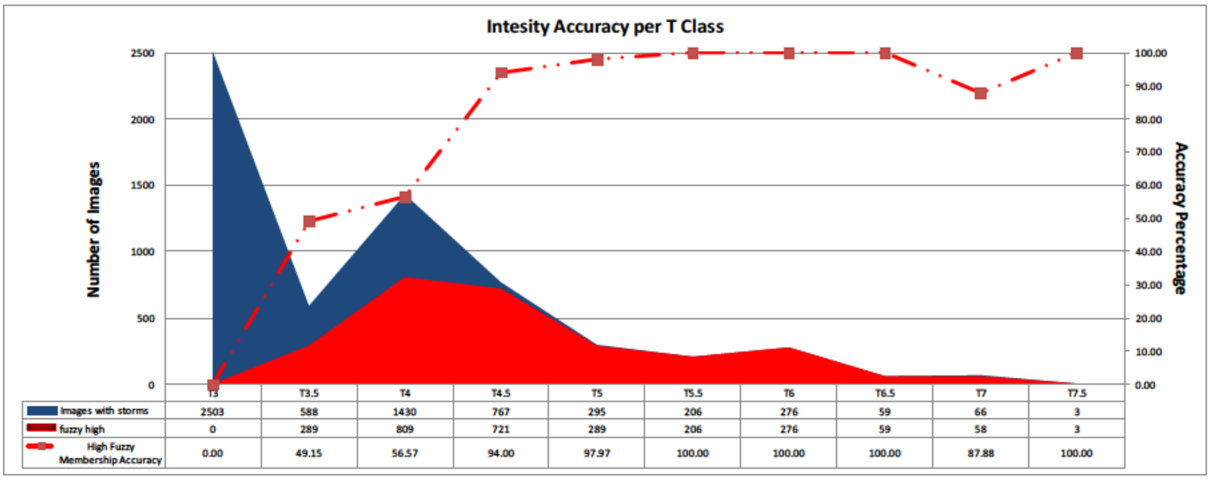

	T3	T3.5	T4	T4.5	T5	T5.5	T6	T6.5	T7	T7.5
Images with storms	2503	588	1430	767	295	206	276	59	66	3
fuzzy high	0	289	809	721	289	206	276	59	58	3
High Fuzzy Membership Accuracy	0.00	49.15	56.57	94.00	97.97	100.00	100.00	100.00	87.88	100.00

Figure 6.12: Intensity accuracy per T number

Overall IC managed to identify 78.04% of the images with the correct intensity as the high fuzzy membership function. If the low fuzzy membership function is included in the accuracy calculation, i.e. either one of the low or high membership values was true to the original value, the accuracy soared to over 90%. It is obvious from figure 6.10 that the later the stage of the cyclone development, the better it is for accurate assessment. It is the early storms that are difficult to identify. Figure 6.12 - 6.22, show a set of graphs indicating detection accuracy for different T classes, mapped over the year.

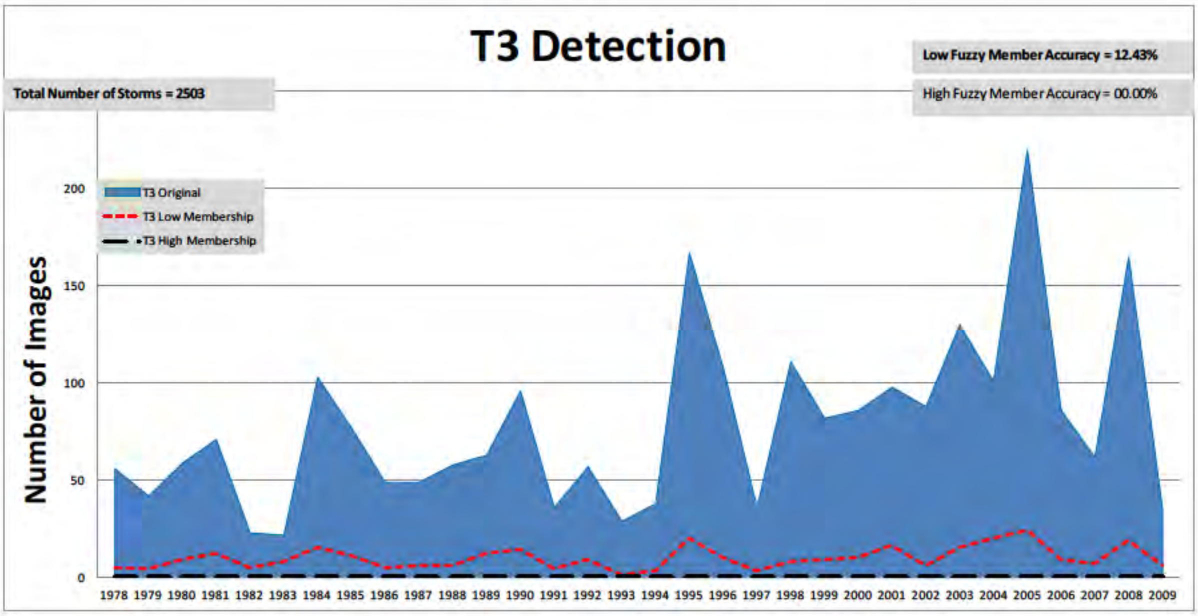

Figure 6.13: Fuzzy membership classification for T3 estimates

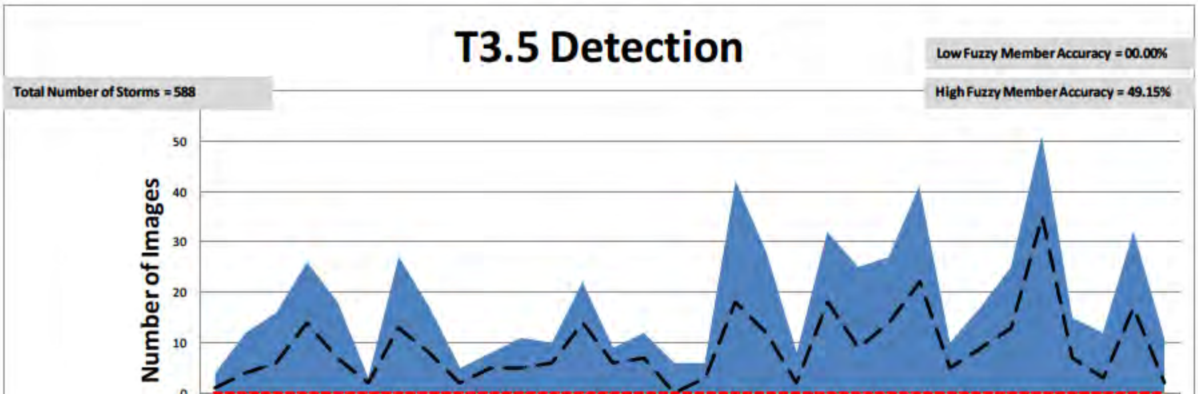

	1978	1979	1980	1981	1982	1983	1984	1985	1986	1987	1988	1989	1990	1991	1992	1993	1994	1995	1996	1997	1998	1999	2000	2001	2002	2003	2004	2005	2006	2007	2008	2009
T3.5 Original	4	12	16	26	18	3	27	17	5	8	11	10	22	9	12	6	6	42	28	8	32	25	27	41	10	17	25	51	15	12	32	11
T3.5 Low Membership	0	0	0	0	0	0	0	0	0	0	0	0	0	0	0	0	0	0	0	0	0	0	0	0	0	0	0	0	0	0	0	0
T3.5 High Membership	1	4	6	14	7	2	13	8	2	5	5	6	14	6	7	0	3	18	12	2	18	9	14	22	5	9	13	35	7	3	17	2

Figure 6.14: Fuzzy membership classification for T3.5 estimates

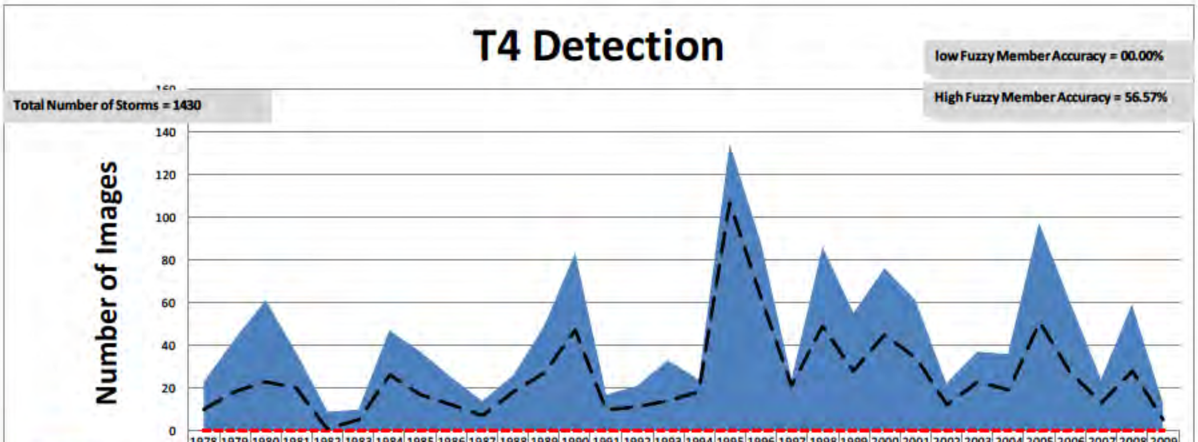

	1978	1979	1980	1981	1982	1983	1984	1985	1986	1987	1988	1989	1990	1991	1992	1993
T4 Original	23	43	61	36	9	10	47	37	25	14	26	49	83	17	21	33
T4 Low Membership	0	0	0	0	0	0	0	0	0	0	0	0	0	0	0	0
T4 High Membership	10	18	23	20	1	5	26	17	12	7	18	27	47	10	11	14

	1994	1995	1996	1997	1998	1999	2000	2001	2002	2003	2004	2005	2006	2007	2008	2009
T4 Original	24	134	88	24	86	55	76	61	22	37	36	97	60	24	59	13
T4 Low Membership	0	0	0	0	0	0	0	0	0	0	0	0	0	0	0	0
T4 High Membership	18	107	63	21	49	28	45	34	12	23	19	51	27	13	28	5

Figure 6.15: Fuzzy membership classification for T4 estimates

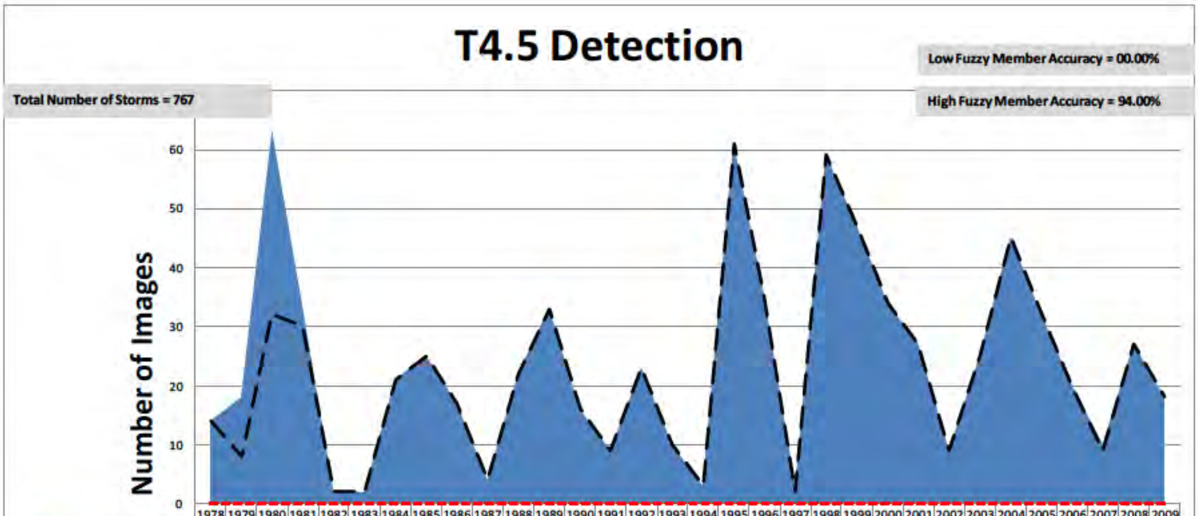

	1978	1979	1980	1981	1982	1983	1984	1985	1986	1987	1988	1989	1990	1991	1992	1993
T4.5 Original	14	18	63	33	2	2	21	25	17	4	22	33	16	9	23	10
T4.5 Low Membership	0	0	0	0	0	0	0	0	0	0	0	0	0	0	0	0
T4.5 High Membership	14	8	32	30	2	2	21	25	17	4	22	33	16	9	23	10

	1994	1995	1996	1997	1998	1999	2000	2001	2002	2003	2004	2005	2006	2007	2008	2009
T4.5 Original	3	61	35	3	59	47	34	27	9	25	45	32	20	10	27	18
T4.5 Low Membership	0	0	0	0	0	0	0	0	0	0	0	0	0	0	0	0
T4.5 High Membership	3	61	35	2	59	47	34	27	9	25	45	32	20	9	27	18

Figure 6.16: Fuzzy membership classification for T4.5 estimates

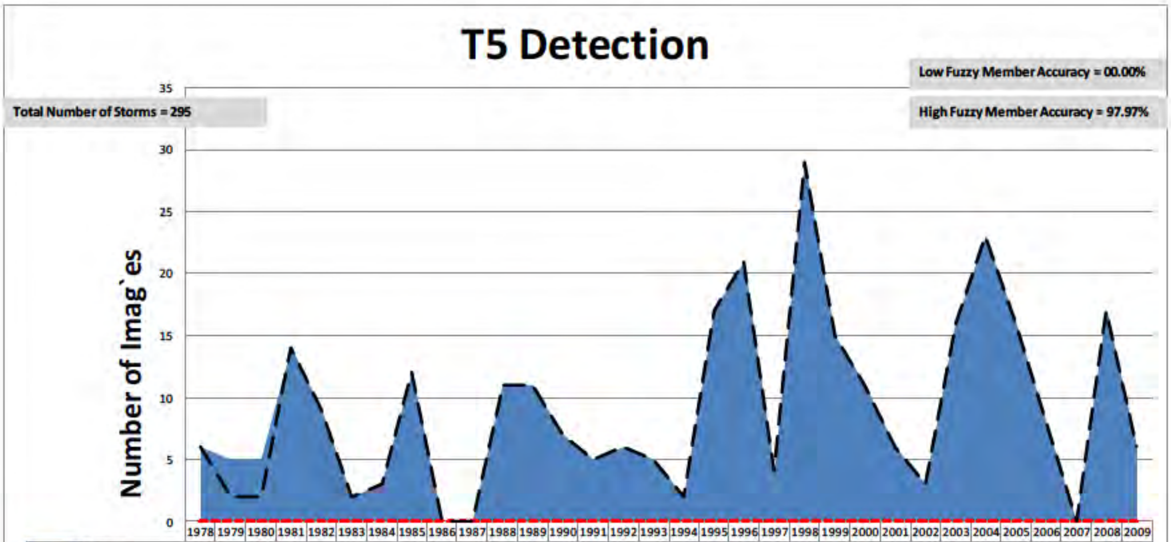

	1978	1979	1980	1981	1982	1983	1984	1985	1986	1987	1988	1989	1990	1991	1992	1993	1994	1995	1996	1997	1998	1999	2000	2001	2002	2003	2004	2005	2006	2007	2008	2009
T5 Original	6	5	5	14	9	2	3	12	0	0	11	11	7	5	6	5	2	17	21	4	29	15	11	6	3	16	23	16	8	0	17	6
T5 Low Membership	0	0	0	0	0	0	0	0	0	0	0	0	0	0	0	0	0	0	0	0	0	0	0	0	0	0	0	0	0	0	0	0
•T5 High Membership	6	2	2	14	9	2	3	12	0	0	11	11	7	5	6	5	2	17	21	4	29	15	11	6	3	16	23	16	8	0	17	6

Figure 6.17: Fuzzy membership classification for T5 estimates

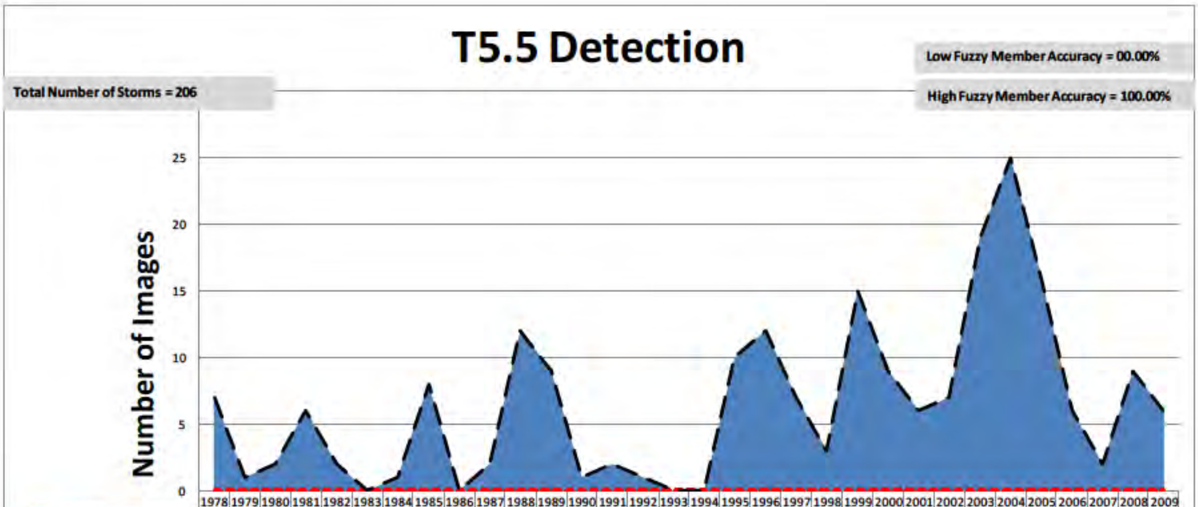

	1978	1979	1980	1981	1982	1983	1984	1985	1986	1987	1988	1989	1990	1991	1992	1993	1994	1995	1996	1997	1998	1999	2000	2001	2002	2003	2004	2005	2006	2007	2008	2009
T5.5 Original	7	1	2	6	2	0	1	8	0	2	12	9	1	2	1	0	0	10	12	7	3	15	9	6	7	19	25	16	6	2	9	6
T5.5 Low Membership	0	0	0	0	0	0	0	0	0	0	0	0	0	0	0	0	0	0	0	0	0	0	0	0	0	0	0	0	0	0	0	0
•T5.5 High Membership	7	1	2	6	2	0	1	8	0	2	12	9	1	2	1	0	0	10	12	7	3	15	9	6	7	19	25	16	6	2	9	6

Figure 6.18: Fuzzy membership classification for T5.5 estimates

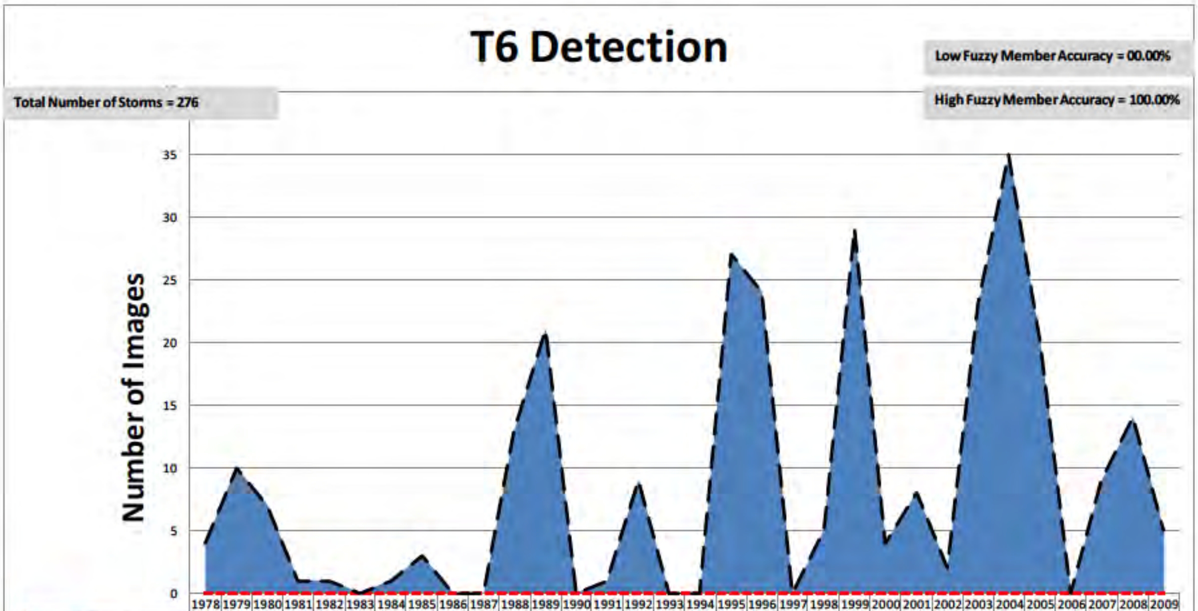

	1978	1979	1980	1981	1982	1983	1984	1985	1986	1987	1988	1989	1990	1991	1992	1993	1994	1995	1996	1997	1998	1999	2000	2001	2002	2003	2004	2005	2006	2007	2008	2009
T6 Original	4	10	7	1	1	0	1	3	0	0	13	21	0	1	9	0	0	27	24	0	5	29	4	8	2	23	35	20	0	9	14	5
T6 Low Membership	0	0	0	0	0	0	0	0	0	0	0	0	0	0	0	0	0	0	0	0	0	0	0	0	0	0	0	0	0	0	0	0
T6 High Membership	4	10	7	1	1	0	1	3	0	0	13	21	0	1	9	0	0	27	24	0	5	29	4	8	2	23	35	20	0	9	14	5

Figure 6.19: Fuzzy membership classification for T6 estimates

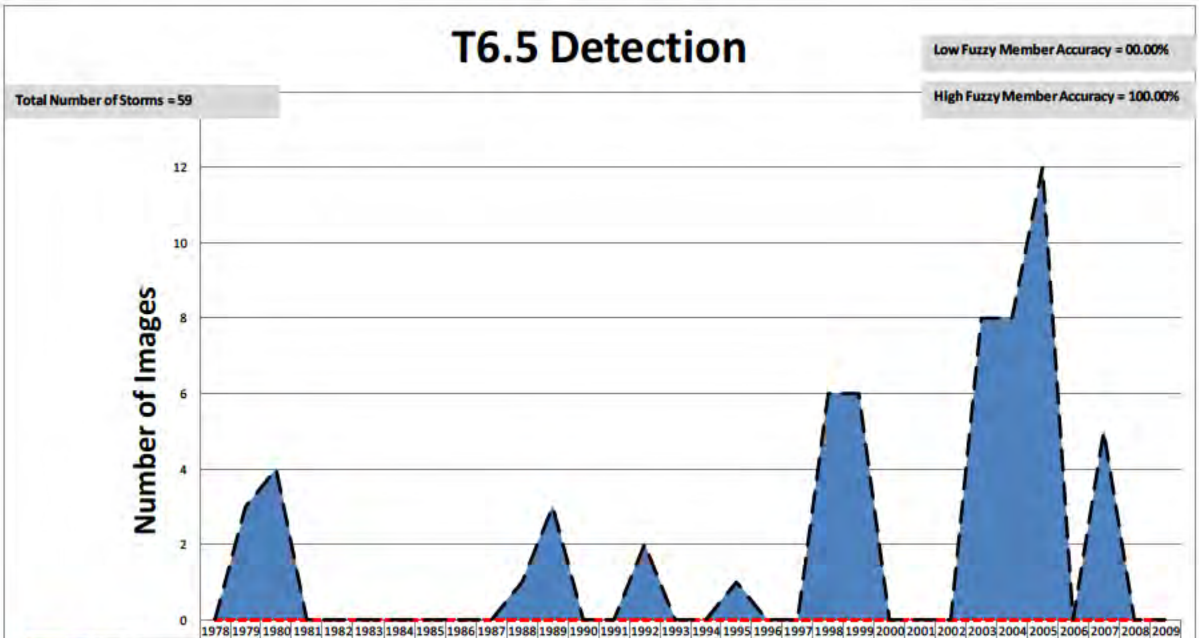

	1978	1979	1980	1981	1982	1983	1984	1985	1986	1987	1988	1989	1990	1991	1992	1993	1994	1995	1996	1997	1998	1999	2000	2001	2002	2003	2004	2005	2006	2007	2008	2009
T6.5 Original	0	3	4	0	0	0	0	0	0	0	1	3	0	0	2	0	0	1	0	0	6	6	0	0	0	8	8	12	0	5	0	0
T6.5 Low Membership	0	0	0	0	0	0	0	0	0	0	0	0	0	0	0	0	0	0	0	0	0	0	0	0	0	0	0	0	0	0	0	0
T6.5 High Membership	0	3	4	0	0	0	0	0	0	0	1	3	0	0	2	0	0	1	0	0	6	6	0	0	0	8	8	12	0	5	0	0

Figure 6.20: Fuzzy membership classification for T6.5 estimates

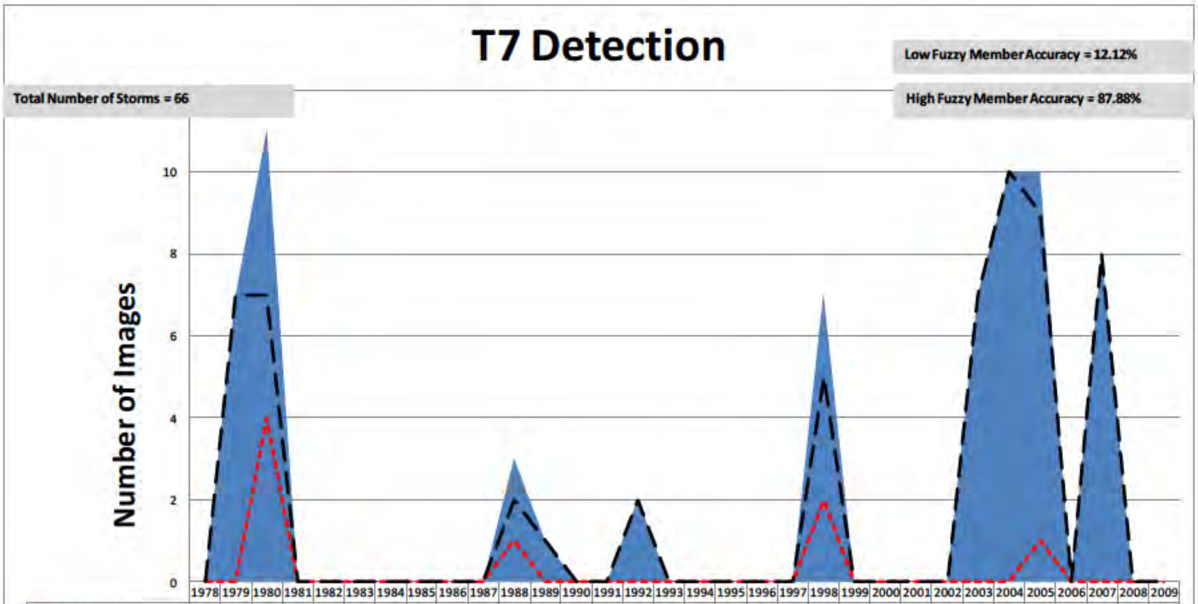

	1978	1979	1980	1981	1982	1983	1984	1985	1986	1987	1988	1989	1990	1991	1992	1993	1994	1995	1996	1997	1998	1999	2000	2001	2002	2003	2004	2005	2006	2007	2008	2009
T7 Original	0	7	11	0	0	0	0	0	0	0	3	1	0	0	2	0	0	0	0	0	7	0	0	0	0	7	10	10	0	8	0	0
T7 Low Membership	0	0	4	0	0	0	0	0	0	0	1	0	0	0	0	0	0	0	0	0	2	0	0	0	0	0	0	1	0	0	0	0
T7 High Membership	0	7	7	0	0	0	0	0	0	0	2	1	0	0	2	0	0	0	0	0	5	0	0	0	0	7	10	9	0	8	0	0

Figure 6.21: Fuzzy membership classification for T7 estimates

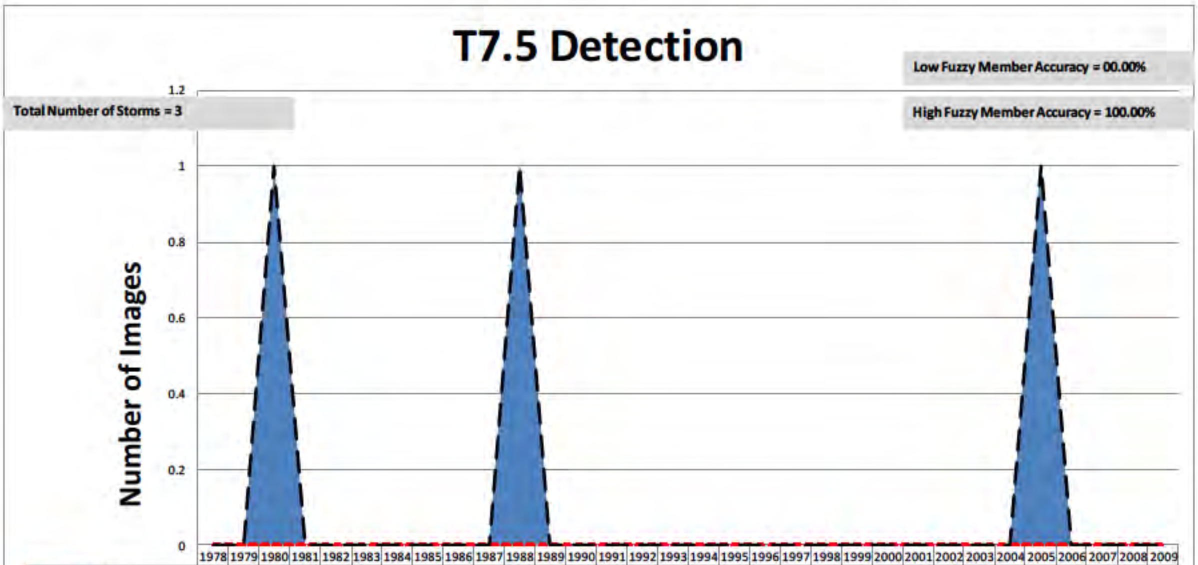

	1978	1979	1980	1981	1982	1983	1984	1985	1986	1987	1988	1989	1990	1991	1992	1993	1994	1995	1996	1997	1998	1999	2000	2001	2002	2003	2004	2005	2006	2007	2008	2009
T7.5 Original	0	0	1	0	0	0	0	0	0	0	1	0	0	0	0	0	0	0	0	0	0	0	0	0	0	0	0	1	0	0	0	0
T7.5 Low Membership	0	0	0	0	0	0	0	0	0	0	0	0	0	0	0	0	0	0	0	0	0	0	0	0	0	0	0	0	0	0	0	0
T7.5 High Membership	0	0	1	0	0	0	0	0	0	0	1	0	0	0	0	0	0	0	0	0	0	0	0	0	0	0	0	1	0	0	0	0

Figure 6.22: Fuzzy membership classification for T7.5 estimates

It is important to note that even though the overall accuracy for intensity classification was merely 78.04%, the final percentage was skewed because of the lower T numbers. If the accuracy is calculated based on a T estimation of T4.5 and above, the accuracy goes up to

97.12%. T4.5 in the Saffir-Simpson Scale is a category 1 hurricane. This suggests that the system is highly accurate even from the stage of origin of the storm. Nonetheless, low pressure systems and extratropical storms do find it difficult to get classified accurately; the system produces a 73.38% accuracy for juvenile storms. In order to develop confidence in the produced results it is important to study the fuzzy membership values that were used to classify the cyclone's intensity. One must note that the higher the fuzzy membership value, the stronger the confidence in it being the correct choice. Figure 6.21 shows the average fuzzy values for each class that was recognised. Both the low membership value and high membership value averages are noted.

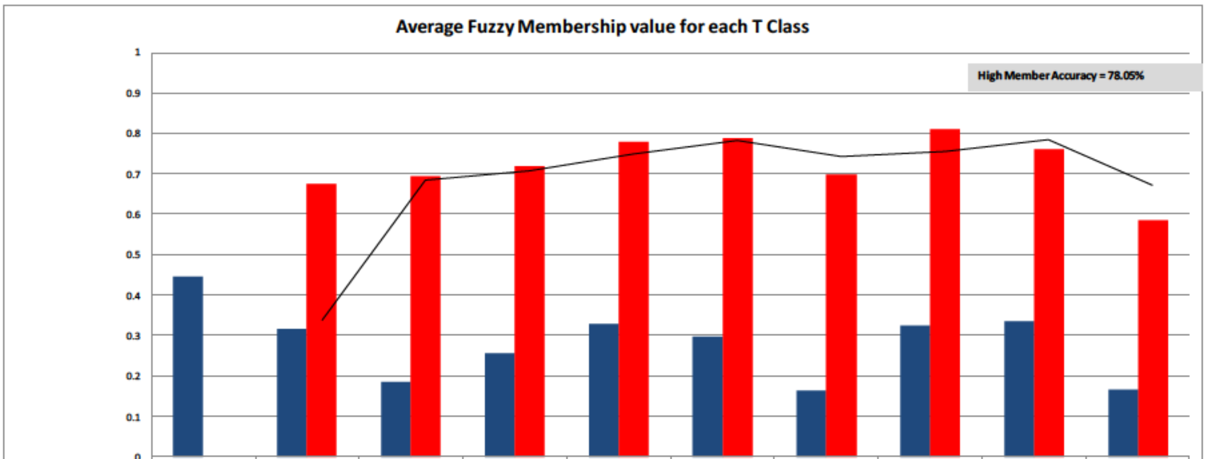

	T3	T3.5	T4	T4.5	T5	T5.5	T6	T6.5	T7	T7.5
Avg Low Membership Confidence	0.444444444	0.317073171	0.185762534	0.256586282	0.328563566	0.298206829	0.164089307	0.325040307	0.334367246	0.165260546
Avg High Membership Confidence	0	0.67564589	0.694367442	0.718254056	0.779900707	0.786407767	0.698389789	0.81029106	0.759482759	0.584149184

Figure 6.23 Average fuzzy membership value for confidence of results.

This is the area that requires improvement in this research. With an overall average high membership value of 0.72, the confidence in making a judgment call is always difficult. On a positive note, the changes in the difference between the low fuzzy value and the high fuzzy value are significant very well correlated, providing confidence in results.

As part of the validation process, maps were produced to ensure that the results from the system can be incorporated into a generic GIS. Apart from a few minor glitches in the coordinate system files, the system produced files in usable standards which allowed GIS software such as ArcGIS to utilise the data and integrate it into other projects seamlessly. Each map aims to show the processed image files, stored as GeoTiff, in its correct geographic context. Moreover centre of the storms detected by the PR module were displayed as black dots. These centres were allocated either from measurements of eye, CDO or spiral bands.

The official track information is also displayed for visual comparison. These are shown as white circles, which display fuzzy intensity estimated by the developed system. It was interesting matching the official records with estimated figures, since it provides an exciting appeal to the data visualisation. Furthermore a graph is also presented with the complete estimated/detected and original lifespan of the cyclone, as shown in figure 6.23. As suggested before the data on the graph of GLORIA's map hints at over estimation.

More of the maps are displayed in the appendix together with intensity graphs showing hurricane life span.

6.6 Summary of validation

The validation process was broken in to two phases; the Pattern Recognition Module phase and the Intensity Classifier phase. The Pattern Recognition Module's accuracy figures and Intensity Classifier's validation figures are summarises in table 6.4.

Table 6.4: PRM and IC validation results.

PRM Validation Process	Value	IC Validation Process	Value
Images processed	11717	Intensity Classification Accuracy	78.05%
Storm processed	375	Intensity Classification Accuracy (> T4)	91.02%
Storm Detection Accuracy	75.50%	Intensity Classification Accuracy (> T4 .5)	97.12%
Hurricane Detection Accuracy	81.23%	Intensity Classification Accuracy (< T4)	73.38%
Pre Storm Detection Accuracy	73.38%	Average High Membership Fuzzy Value (Confidence)	0.72
False Negative Detection	93%		
False Positive Detection	7.44%		
Storm Centre RMSE	0.85		
Corrected Storm Centre RMSE	0.55		

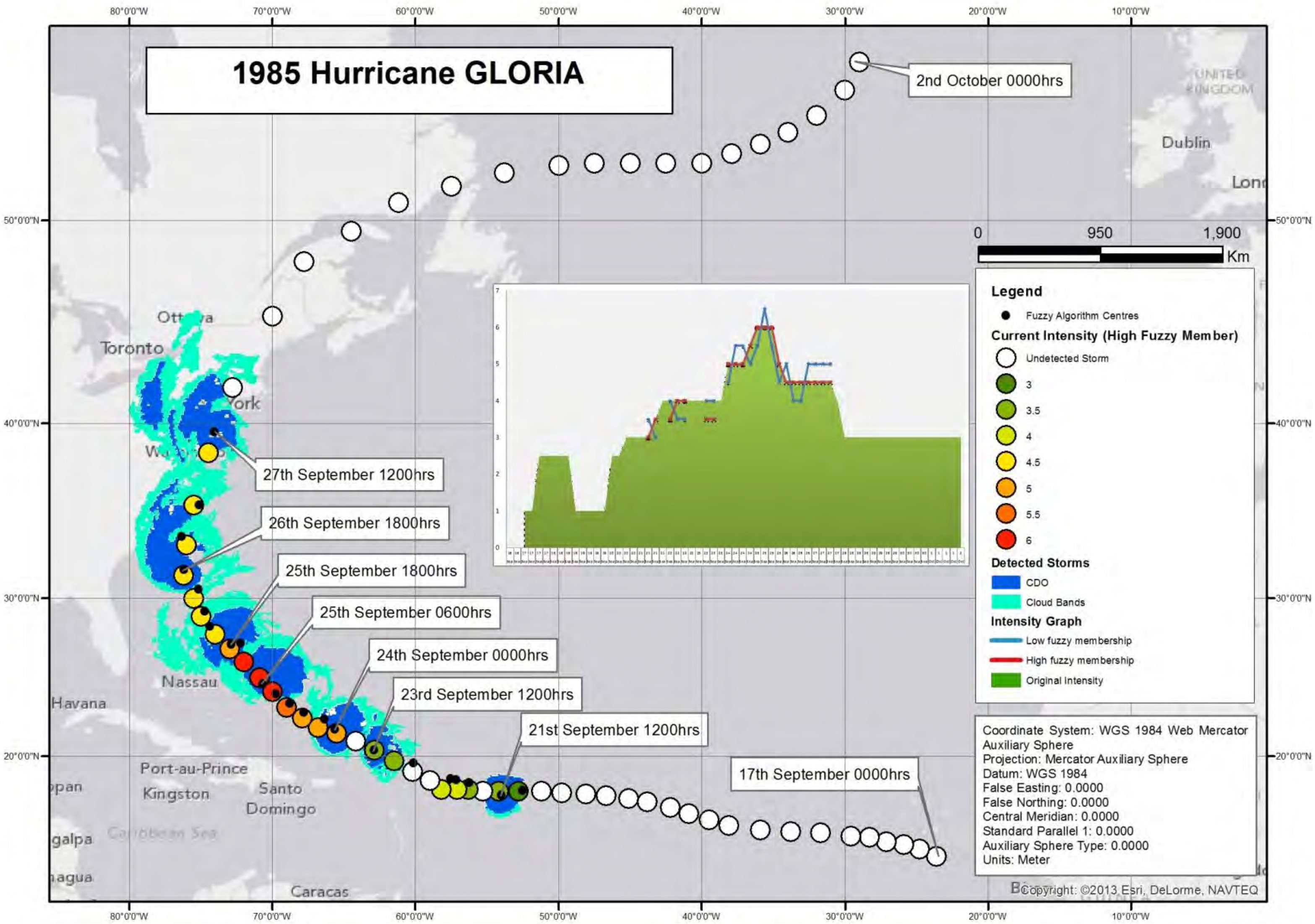

Figure 6.24: Hurricane GLORIA

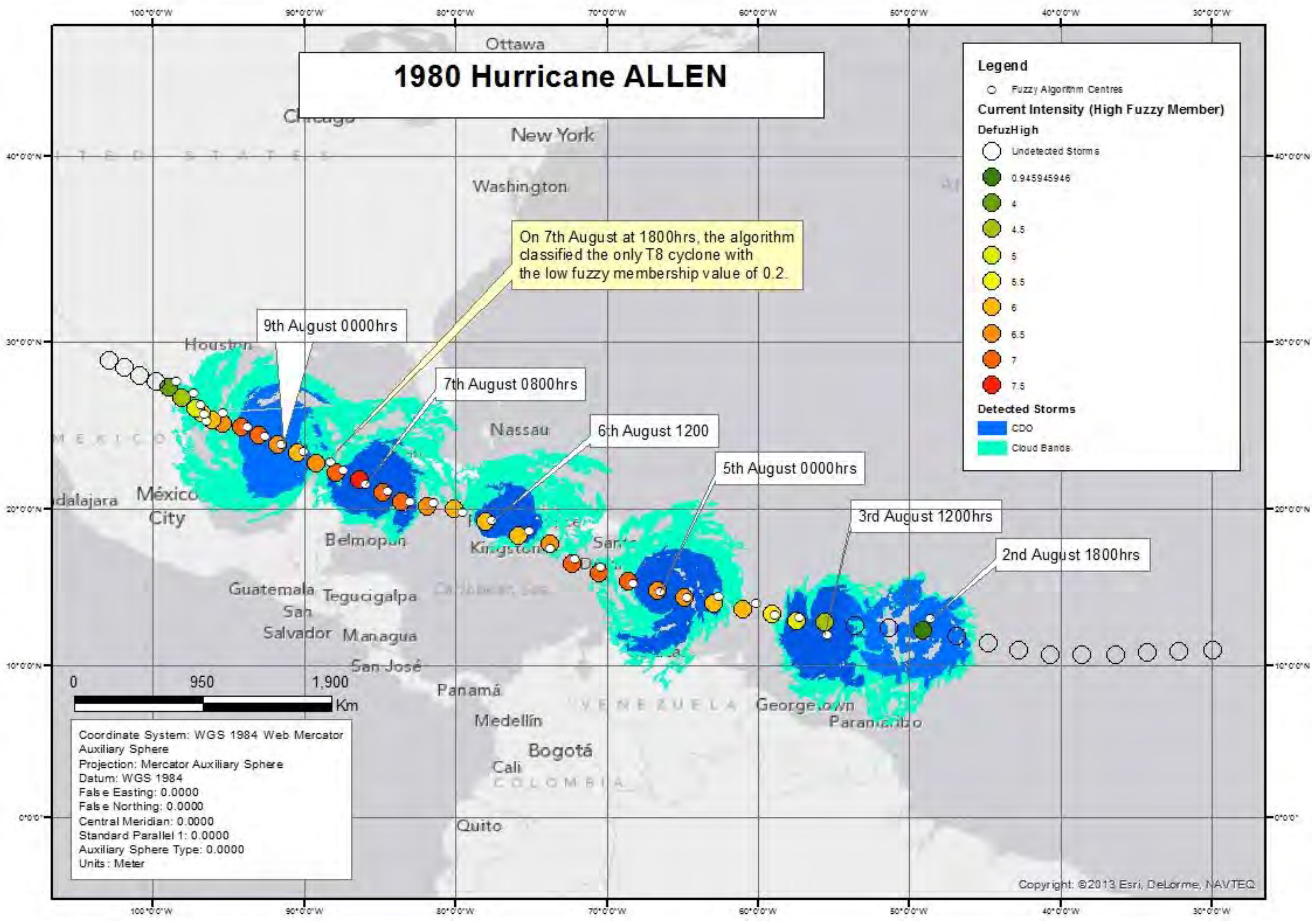

Figure 6.25: Hurricane ALLEN

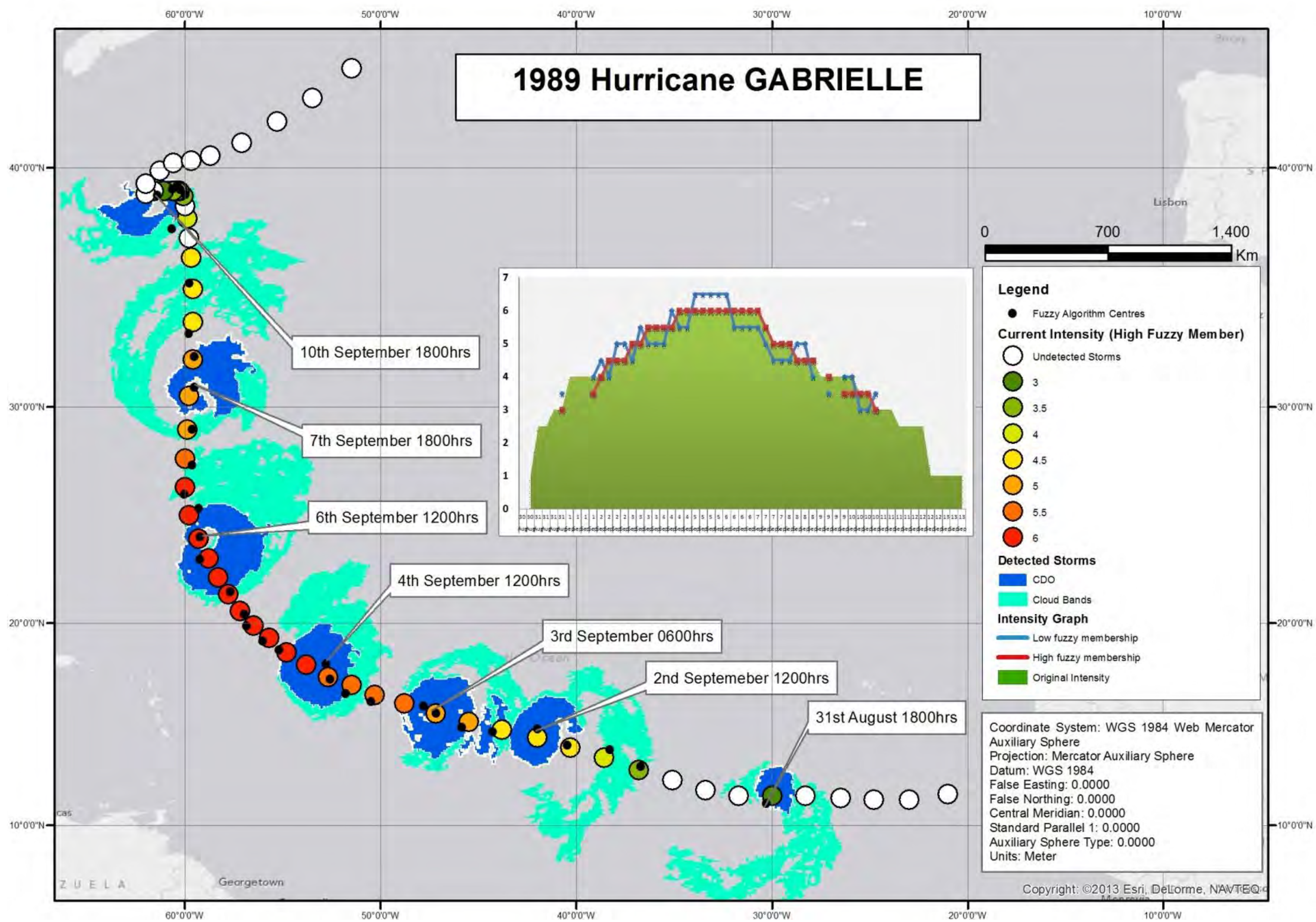

Figure 6.26: Hurricane GABRIELLE with a perfectly tracked path.

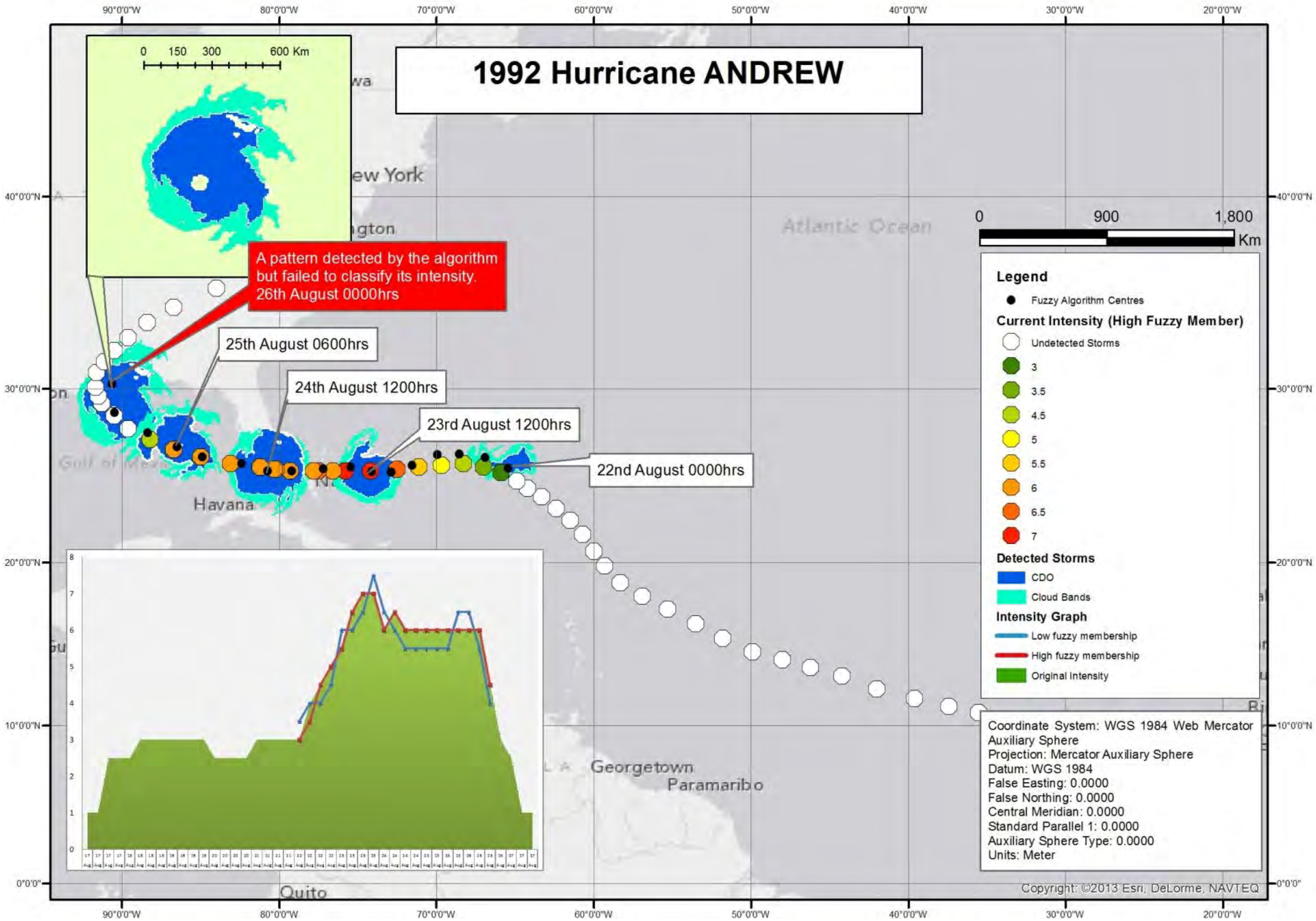

Figure 6.27: Hurricane ANDREW displaying certain problems with the algorithm

6.7 System Limitations

During the training and testing of the software, there were a few issues that required tackling. This section lists and discusses the issues highlighted

6.7.1 Software

The software utilising the developed algorithms was developed in-house from scratch. It was developed in 2005 using Visual C ++. Since then, other productive tools have appeared on the market and the software requires updating. The C algorithm requires an MFC 2005 compiler to compile and execute it, which is also obsolete and Microsoft does not support it anymore. Overall, this is a big drawback as the algorithms need updating now and then, and working with an obsolete software makes the work harder than it really is. Moreover, rewriting the algorithm in a GIS friendly environment will make its integration with the rest of the spatial world a lot easier. For example, the software could be reprogrammed in a .NET environment and compiled as an Addin to the suite of ESRI ArcGIS programmes. One of the issues that later created a hindrance was Visual C 2005's lack of support for geographic and projected coordinate systems.

6.7.2 Perforated Clouds - Pattern Recognition

It was noticed after examining the results that at times the software will detect an elliptical perforated cloud as a hurricane due to its similar context to a tropical cyclone, i.e. a warm eye with a colder cloud around it, especially when it was about to go over land or already had made landfall. Moreover, there were two instances in 11711 images, where a perfectly well recognised cyclone couldn't get an intensity classification. These issues can be ironed out with additional rules in the PR modules. The perforated clouds making landfall can be removed from being detected by looking at temporal record of the hurricane, e.g. if the hurricane has not been detected previously in the area and the centre of the storm is closer to land then it is very unlikely that it will be a hurricane.

6.7.3 Fuzzy Membership Values

Although the issue about fuzzy membership value is not urgent, it was noted that even though the correct classification is being suggested by the fuzzy membership function, the confidence in the suggestion is low. This issue can be resolved easily by referring back to the fuzzy function and rules. In addition, it was prominent that IC was exaggerating the final fuzzy value especially for stronger cyclones. The exaggeration in the fuzzy membership functions was never more than T0.5 either way. It even once classified a storm as a T8, when there has never been a T8 cyclone in the North Atlantic Basin; it was originally a T7.5.

6.8 Summary

The developed fuzzy rule based pattern recognition system and intensity classifier has been evaluated in this chapter. The PR module was validated against a full record of satellite imagery, HURSAT, while the IC module's estimated intensity was validated with the best storm track data acquired from NOAA. The validation process showed that the developed system can be used effectively for automated hurricane detection and intensity classification. This ensures that the system meets the last criteria listed in section 1.6. One of the unique advantages of this system over others is that it seamlessly integrates the complete process of classifying the meteorological imagery, detecting hurricanes, if present, and then classifying to an exceptional accuracy. Systems such as this have huge potential to be used in advanced real time monitoring of meteorological patterns.

CHAPTER 7. CONCLUSION

7.1 Introduction

The literature suggests that tropical cyclones and hurricanes are amongst the most devastating meteorological natural disasters. Major efforts are put in to correctly forecast these meteorological giants. However, this always requires expert knowledge in the form of people, who in turn bring subjectivity into the process. Many efforts have been made to automate at least part of the process of hurricane forecasting; it won't be long in the future before we have a system that doesn't require any subjective opinion on a physical phenomenon, but we are not there yet. Billions of US dollars are spent on disaster mitigation and post disaster management when these cloud engines make landfall. Hence there is a strong need for a holistic approach to cyclone detection and its processing. Chapter 2 highlighted the gaps in literature where either little effort has been made or, in the case of ongoing research it does not tackle the wholesome nature of the tropical cyclone analyses. Automated algorithms in the market typically are extremely focused on one aspect of the hurricane or its intensity; with questionable accuracies and validation.

The developed system aimed to fill the gap of the holistic study of tropical cyclones and hurricanes and achieved it. The modular approach to the system enables future modification possible for algorithm optimisation or parameter change. Expert knowledge, if administered personally, can lead to subjective results, nonetheless expert knowledge is one of the most crucial aspects of the research. To eliminate the personal subjectivity of expert knowledge system, a fuzzy rule based approach was implemented which allows the expert knowledge to be transferred through various modules of the program without personal input. The introduction of fuzzy logic in pattern recognition and intensity estimation enabled the system to deal with uncertainty and vagueness. This was apparent in the validation process when ragged edged polygons were being classified as 'elliptical'.

7.2 Summary of Research

The developed system works interactively in a modular form. The images are passed on to the system where it classifies them to remove unwanted data. After classification, depending on if it is a visible image or TIR, it highlights boundary regions and identifies elliptical patterns using various fuzzy algorithms. Once the ellipses are identified, they are vectorised and spatial statistics are calculated. Once the system recognises elliptical and spiral pattern associated with a prospective storm, it uses linguistic rules with help of a grammar to sort the cyclone primitives into knowledgeable patterns. These patterns then are recognised as hurricanes or tropical cyclones by the linguistic algorithm. Once a tropical cyclone is detected it is then passed swiftly on to another module where its intensity will be estimated. The intensity estimation is performed by applying a series of fuzzy membership algorithms, 31 in total. Then out of a possible 673, appropriate rules are applied to the data to produce fuzzy membership intensity estimates (Chapter 5).

The development system was validated using official hurricane records and satellite imagery of the last 30 years (Chapter 6). The validation process produced on overall accuracy of 81.23% for cyclone detection, with 78.04% accuracy for intensity classification. The intensity classification accuracy jumps to 97.12% if very early pre-hurricane storms are removed from the validation. For simply low pressure systems with some visible cloud formation or circulation, the pattern recognition module produced an accuracy of 73.38%. Overall the system has some limitations, mainly the development platform that it used. Nonetheless, the algorithms in the developed system are robust and perform at the highest of standards.

7.3 Research Contribution

This research makes several contributions in the field of tropical cyclone and hurricane monitoring and forecasting. The following is a summarised list of the contributions:

- ❖ An automated pattern recognition system - This is a bespoke pattern recognition system especially calibrated for the application of meteorology. The use of this system could feed in to real time early hazard warning systems where an automated procedure tracks required data through the cluster of datasets.
- ❖ Versatile algorithms - due to the nature of cyclones and their structural characteristics, many other objects following natural growth share their structure. There has always been a need for automated algorithms to identify spiral galaxies, which are not dissimilar from cyclone shapes. The algorithms can be easily modified to detect spiral galaxies in remote sensed astronomical datasets. Moreover, because the system was

designed and built over a modular approach it is relatively easy to integrate new systems.

- The unique holistic approach of this system allows the meteorological organisation to utilise these algorithms at varying hierarchical levels. The use of a fuzzy logic approach to detect uncertain shapes in the clouds and then using a linguistic logical approach to bind the primitives together make this system unique.
- The developed system has been presented twice at two international conferences; one of them winning the best paper prize. One journal paper article is near to competition where the editor of International journal of remote sensing has requested some edits.

7.4 Recommendations and Future Research

Based on the research and development of the system, the following recommendations are proposed for improvement and sustainability of accuracy in the results. These recommendations will lead to future research highlighted in section 7.4.2.

7.4.1 Recommendations

One of the major concerns in the developed system is the stability and sustainability of the programmed code. Due to the original development of the algorithms in Visual C++, it was decided not to change the development platform during the research, even though a much more stable development environment became available. The algorithms are robust but produce strain on the memory with the number of images processed. It is now recommended that the code is ported to a much stable development environment, especially one with recognition of geographic and projected coordinate systems. A recommended platform is ESRI's integration of their GIS software with Microsoft .Net development platform. This has been tested to be a much sustainable route than a standalone application which will require updating frequently.

During the detection of the storm primitives, CDO and the eye had the highest detection rate as compared to the spiral curves. The developed system detected and matched the spiral cloud band if there was only one spiral in question. In the case of multiple spirals with the same origin, the developed system failed to detect all but one with the highest match. This had a repercussion on the intensity classification of the storm. It is recommended that the algorithm should be modified to detect multiple spirals instead of one. This is achievable with relative ease, due to the fact that the individual spiral algorithm works well. The algorithm can learn to remember the detected spiral, remove it from the image segments and search for more spirals until none are found. Literature also suggests that due to a storm's natural growth, many cyclones follow the pattern of a Golden Spiral instead of the 10^{o} pitch logarithmic spiral utilised in the system. Future development can incorporate various spiral equations to detect different categories of spirals in the image.

In addition to spirals, at a very early stage in the cyclogenesis of storms, thunderstorms can form in the shape of a 'comma'. Some researchers consider this comma shape to be a subset of the spiral formation; however, a controlled algorithm to detect the comma shape in storm will result in an early detection of the storms.

Due to the heterogeneous nature of pixel values in meteorological data, a noise removal algorithm can enhance the detection rate of the storms. It is essential that either systematic, radiometric, or transmission noise does not progress through the results.

7.4.2 Areas of Future Research

The recommendations above form the basis of future research; however these recommendations are not the sole source of proposed research areas.

Improvement of the developed algorithm to incorporate multiple spiral detection will not only benefit tropical cyclone detection, but other fields of study. Detecting natural objects with multiple spirals can also lead into automated detection of spiral galaxies from Hubble telescope data (Davis and Hayes, 2012; S. C. Odewahn, 2002; Paul et al., 2002; Martinez-Valpuesta et al., 2007; Mashchenko, 1999; Elfattah et al., 2012). There is also a research gap in the field of astronomy where automated spiral recognition in extraterrestrial objects is needed. Recent studies have shown weather patterns in other possible habitable planets (Hollingsworth and Kahre, 2010), moreover, spiral features have been found on Mars attributed to unacknowledged lava flow (Geographic, 2012; Jet Propultion Laboratory, 2012). The existence of spiral features representing natural growth can be identified automatically using remotely sensed data.

Addition of Artificial Neural Networks (ANN) to the fuzzy logic algorithm will introduce a self-learning mechanism for the developed system. Currently the reliance on the training data is limiting the system's abililty to recognise all types of storm. ANNs have the ability to learn with new patterns emerging in the satellite imagery, improving the chances of an early storm detection. It is highly recommended that the fusion of ANNs and the fuzzy logic algorithm for tropical cyclone detection is further investigated.

REFERENCES

Abebe, A. J., Solomatine, D. P. & Venneker, R. G. W. 2000. Application of adaptive fuzzy rule-based models for reconstruction of missing precipitation events. *Hydrological Sciences Journal,* 45**,** 425-436.

Aberson, S. D. 1998. Five day tropical cyclone track forecasts in the North Atlantic basin. *Weather Forecasting,* 13**,** 1005 - 1015.

Ahmed, M. N., Yamany, S. M., Mohamed, N., Farag, A. A. & Moriarty, T. 2002. A modified fuzzy c-means algorithm for bias field estimation and segmentation of MRI data. *Medical Imaging, IEEE Transactions on,* 21**,** 193-199.

Ahrens, C. D., Jackson, P. L. & Jackson, C. E. O. 2011. *Meteorology Today - An introduction to weather, climate and the environment*, Cengage Learning.

Alcalá, R., Casillas, J., Cordón, O., Herrera, F. & Zwir, I. 1999. Techniques for learning and tuning fuzzy rule-based systems for linguistic modeling and their applications. *Knowledge Engineering Systems, Techniques and Applications,* 3**,** 889-941.

Ambroise, C., Sèze, G., Badran, F. & Thiria, S. 2000. Heirarchical clustering of self-organizing maps for cloud classification. *Neurocomputing,* 30**,** 47-52.

Anderson, M. 2011. *Investigating Earths Weather*, Rosen Education Service.

Anderson, R. 1971. *An Introduction to Linguistic Pattern Recognition*, RAND.

Andras, K. 2008. Linguistic pattern recognition. *Mathematical Linguistics.* Springer London.

Annadurai, S. 2007. *Fundamentals of Image Processing*, Dorling Kindersley.

Annonymous 1899. The Pearling Disaster 1899: A Memorial. The Outridge Company.

Anthes, R. 1982a. *Tropical Cyclones: Their Evolution, Structure and Effects (Meteological Monographs)*, Americal Meteorological Society.

Anthes, R. A. 1982b. *Tropical Cyclones: Their evolution, structure and effects*, Americal Meteorological Society.

Arnold, C. 1977. Tropical cyclone cloud and intensity relationships. *Atmospheric Science* 154.

Aziz, R., Aliev, O. & Aliev, R. R. 2001. *Soft Computing and its Applications*, World Scientific Publishing Co.

Ballard, D. & Brown, C. 1982. *Computer Vision*, Prentice Hall.

Bankert, R. & Tag, P. 2002a. An automated method to estimate tropical cyclone intensity using SSM/I imagery. *Journal of applied meteorology and climatology,* 41**,** 461-472.

Bankert, R. L. & Tag, P. M. 2002b. An Automated Method to Estimate Tropical Cyclone Intensity Using SSM/I Imagery. *Journal of Applied Meteorology,* 41**,** 461-472.

Bardossy, A., Duckstein, L. & Bogardi, I. 1995. Fuzzy rule-based classification of atmospheric circulation patterns. *International Journal of Climatology,* 15**,** 1087-1097.

Barnes, C. J. & Chang, D. 1968. Accurate cloud cover determination and its effect on albedo computations. Allied Research Association.

Barrett, C. & Curtis, F. 1999. *Introduction to Environmental Remote Sensing*, Stanley Thornes.

Baum, B. A., Tovinkere, V., Titlow, J. & Welch, R. M. 1997. Automated cloud classification of gloval AVHRR data using fuzzy logic approach. *Journal of applied meteorology and climatology,* 36.

Baum, B. A., Uttal, T., Poellot, M., Ackerman, T. P., Alvarez, J. M., Intrieri, J., Starr, D., Titlow, J., Tovinkere, V. & Clothiaux, E. 1995. Satellite remote sensing of mulitple cloud layers. *Journal of atmospheric sciences,* 52.

Belanger, J. I., Webster, P. J., Curry, J. A. & Jelinek, M. T. 2012. Extended Prediction of North Indian Ocean Tropical Cyclones. *Weather and Forecasting,* 27**,** 757-769.

Bellman, R., Kalaba, R. & Zadeh, L. 1966. Abstraction and pattern classification. *Journal of Math. Anal. Appl,* 13**,** 1-7.

Bendix, J., Rollenbeck, R. & Palacios, W. E. 2004. Cloud detection in the Tropics--a suitable tool for climate-ecological studies in the high mountains of Ecuador. *International Journal of Remote Sensing,* 25**,** 4521-4540.

Bentley, P. 2000. Evolving Fuzzy Detectives: An Investigation into the Evolution of Fuzzy Rules. *In:* Suzuki, Y., Ovaska, S., Furuhashi, T., Roy, R. & Dote, Y. (eds.) *Soft Computing in Industrial Applications.* Springer London.

Berger, J. 1985. *Statistical Decision Theory and Bayesian Analysis*, Springer.

Berglee, R. 2012. World Regional Geography: People, Place and Glocalization. Flat World Knowlege.

Berry, F. A., Bollay, E. & Beers, N. R. 1945. *Handbook of Meteorology*, McGraw Hill

Bezdek, J. 1981. *Pattern Recognition with Fuzzy Objective Function Algorithms*

Bezdek, J. C. 1998. some new indexes of cluster validity. *Part B: Cybernetics, IEEE transaction on System, Man and Cybernetics, ,* 28**,** 301-315.

Bezdek, J. C. & Castelaz, P. 1977. Prototype classification and feature selection with fuzzy sets. *IEEE Transactions on Systems, Man and Cybernetics,* 7**,** 87–92.

Bezdek, J. C., Keller, J., Krisnapuram, R. & Pal, N. 2005. *Fuzzy models and algorithms for pattern recognition and image processing*, Springer.

Bezdek, J. C. & Pal, S. K. 1992. *Fuzzy Models for Pattern Recognition*, IEEE Press.

Biederman, I. 1987. Recognition by components: theory of human image understanding. *Psychological Review,* 94**,** 115-147.

Biello, D. 2007. Stronger link found between hurricanes and global warming. *Scientific American* [Online]. Available: http://www.scientificamerican.com/article.cfm?id=stronger-link-found-between-hurricanes-global-warming [Accessed 10 July 2011].

Bishop, C. M. 1995. Statistical Pattern Recognition. *Neural Network for Pattern Recognition.* Oxford University Press.

Bishop, C. M. 2006. *Pattern Recognition and Machine Learning*, Springer.

Black, M. 1937. Vagueness: An exercise in logical analysis. *Philosophy of Science,* 4**,** 427-455.

Blankenship, J. R. 1962. An approach to objective nephanalysis from an earth oriented satellite. *Journal of Applied Meteorology,* 2**,** 809.

Bom, B. O. M. 2008. *About Tropical Cyclones* [Online]. Available: http://www.bom.gov.au/cyclone/about [Accessed 20/06/2010 2010].

Bom, B. O. M. 2009. *Storm surge preparedness and safety* [Online]. Available: http://www.bom.gov.au/info/cyclone/storm_surge/storm_surge.shtml 2011].

Bom, B. O. M. 2013a. *A look inside the structure of a tropical cyclone* [Online]. Bureau of Meteorology, Australian Government. Available: http://www.bom.gov.au/social/2012/11/structure-of-a-tropical-cyclone/ 2013].

Bom, B. O. M. 2013b. *Satellite data in tropical cyclone analyis* [Online]. Available: http://www.virtuallab.bom.gov.au/training/satellite-data-tropical-cyclone-analysis/ [Accessed May 2013 2013].

Bongirwar, V., Rakesh, V., Kishtawal, C. & Joshi, P. 2011. Impact of satellite observed microwave SST on the simulation of tropical cyclones. *Natural Hazards,* 58**,** 929-944.

Brennan, M. J. & Majumdar, S. J. 2011. An Examination of Model Track Forecast Errors for Hurricane Ike (2008) in the Gulf of Mexico. *Weather and Forecasting,* 26**,** 848-867.

Britannica 2013. Hurricane: life cycle of a North Atlantic hurricane. *Encyclopedia Britannica, Inc.*

Businger, S. & Reed, R. J. 1989. Cyclogenesis in cold air masses. *Weather Forecast,* 4**,** 133-156.

Camargo, S. J. & Zebiak, S. E. 2002. Improving the Detection and Tracking of Tropical Cyclones in Atmospheric General Circulation Models. *Weather and Forecasting,* 17**,** 1152 - 1162.

Carleton, A. 1991. *Satellite remote sensing in climatology,* London, Belhaven Press.

Charles, S. P. 1878. How to make our ideas clear. *Popular Science Monthly***,** 286-302.

Chi, Z., Yan, H. & Pham, T. 1996. *Fuzzy Algorithms: with application to image processing and pattern recognition*, World Scientific.

Chiu, S. L. 1994. Fuzzy model identification based on cluster estimation. *Journal of Intelligent and Fuzzy System,* 2**,** 267-278.

Chiu, S. L. 1997. Extracting fuzzy rules from data for function approximation and pattern classification. *In:* Dubois, D., Prade, H. & Yager, R. R. (eds.) *Fuzzy Information Engineering: A guided tour of applications.* John Wiley & Sons.

Chomsky, N. 1956a. *Syntactic Structures*, Mouton.

Chomsky, N. 1956b. Three models for the description of languages. *IRE Transactions on Information Theory,* 2**,** 113-124.

Chuai-Aree, S., Jäger, W., Bock, H. G., Krömker, S., Kanbua, W. & Siripant, S. 2008. 3D Cloud and Storm Reconstruction from Satellite Image

Modeling, Simulation and Optimization of Complex Processes. *In:* Bock, H. G., Kostina, E., Phu, H. X. & Rannacher, R. (eds.). Springer Berlin Heidelberg.

Coburn, A. R. 1971. Improved three-dimensional nephanalysis model. . Air Force Global Weather Center.

College, L. S. 2010. *Vertical cross section of the hurricane circulation* [Online]. Lyndon State College. Available: http://apollo.lsc.vsc.edu/classes/met130/notes/chapter15/vertical_circ.html 2011].

Conover, J. H. 1962. Cloud interpretation from satellite altitudes. *Research***,** 19.

Conover, J. H. 1963. Interpretation of cloud and mesoscale cloud patterns as seen from satellite altitudes. *Rocket and Satellite Meteorology***,** 388-392.

Cordón, O., Del Jesus, M. J. & Herrera, F. 1999. A proposal on reasoning methods in fuzzy rule-based classification systems. *International Journal of Approximate Reasoning,* 20**,** 21-45.

Cossuth, J. H., Knabb, R. D., Brown, D. P. & Hart, R. E. 2012. Tropical Cyclone Formation Guidance Using Pregenesis Dvorak Climatology. Part I: Operational Forecasting and Predictive Potential. *Weather and Forecasting,* 28**,** 100-118.

Cox, E. 1992. *Fuzzy Fundamentals*, IEEE.

Daff, D. O. A., Fisheries and Forecty, Australian Government. 2012. *Research Strategy - July 2012 to June 2017* [Online]. Available: http://www.daff.gov.au/climatechange/carbonfarmingfutures/ftrg/filling-the-research-gap-july-2012-to-june-2017 [Accessed January 2013.

Daily, J. 2012. Analysis of critical speed yaw scuffs using spiral curves. *SAE 2012 World Congress & Exhibition.* Detroit, Michigan.

Data, A. C. C. M. F. R. L. U. P. I. H. R. R. S. 1982. A contextual classification method for recognizing land use patterns in high resolution remotely sensed data. *Pattern Recognition,* 15**,** 317-324.

Davis, D. R. & Hayes, W. B. Automated quantitative description of spiral galaxy arm-segment structure. Computer Vision and Pattern Recognition (CVPR), 2012 IEEE Conference on, 16-21 June 2012 2012. 1138-1145.

Davolio, S. M., M. M. ; Moscatello, A. ; Pacifico, F. ; Buzzi, A. ; Rotunno, R. 2009. Numerical forecast and analysis of a tropical-like cyclone in the Ionian Sea. *Natural Hazard and Earth System Sciences,* 9**,** 551-562.

Dehzangi, O., Zolghadri, M. J., Taheri, S. & Fakhrahmad, S. M. Efficient Fuzzy Rule Generation: A New Approach Using Data Mining Principles and Rule Weighting. Fuzzy Systems and Knowledge Discovery, 2007. FSKD 2007. Fourth International Conference on, 24-27 Aug. 2007 2007. 134-139.

Delaware, S. G. 2009. *Coastal processes* [Online]. Available: http://www.deseagrant.org/outreach/coastal-processes-faq-difference-between-storm-tide-and-surge.

Demaria, M. 2005. Further Improvements to the Statistical Hurricane Intensity Prediction Scheme (SHIPS). *Weather and Forecasting,* 20**,** 531-543.

Demirci, O., Ritchie, E. A., Tyo, J. S. & Ieee 2004. *Application of spatiotemporal pattern recognition techniques on predicting extratropical transition (and reintensification) of tropical cyclones,* New York, Ieee.

Desbois, M., Seze, G. & Szejwach, G. 1982. Automatic classiŽ cation of clouds onMETEOSAT imagery: application to high level clouds. *Journal of Applied Meteorology,* 21**,** 401-412.

Devroye, L. 1996. *A Probabilistic Theory of Pattern Recognition*, Springer.

Dommin, S. 2010. *A hurricane hunter's photo album* [Online]. Available: http://www.pbase.com/sdommin/hurricanes 2011].

Dubois, D. & Prade, H. 2005. Fuzzy intervals versus fuzzy numbers: is there a missing concept in fuzzy set theory? . *26th Linz seminar on fuzzy set theory.* Linz Austria.

Duda, R., Hart, P. & Stork, D. 2001. *Pattern Classification*, John Wiley & Sons.

Dunn, G. E. 1964. The hurricane season of 1963. *Monthly Weather Review,* 92**,** 128.

Dunn, G. E. & Miller, B. I. 1964. *Atlantic Hurricane*, Louisiana State University Press.

Duong, T., Nguyen, D., Nguyen, S. & Hoang, M. 2013. An Adaptive Neuro-Fuzzy Inference System for Seasonal Forecasting of Tropical Cyclones Making Landfall along the Vietnam Coast. *In:* Nguyen, N. T., Do, T. & Thi, H. A. (eds.) *Advanced Computational Methods for Knowledge Engineering.* Springer International Publishing.

Dvorak, V. 1975. Tropical cyclone intensity analysis and forecasting from satellite imagery. . *Monthly Weather Review,* 103**,** 420-430.

Dvorak, V. 1984. Tropical cyclone intensity analysis using satellite data. *NOAA Technical Report. NESDIS11.*

Dvorak, V. F., Smigielski, F. J. & United, S. 1990. *A workbook on tropical clouds and cloud systems observed in satellite imagery,* [Rockville, Md.?], U.S. Dept. of Commerce, National Oceanic and Atmospheric Administration, National Environmental Satellite, Data, and Information Service [and] National Weather Service.

Eagleman, J. R. 1990. *Severe and Unusual Weather*, Trimedia Publishing Company.

Elfattah, M., Elsoud, M. A., Hassanien, A. & Kim, T.-H. 2012. Automated Classification of Galaxies Using Invariant Moments. *In:* Kim, T.-H., Lee, Y.-H. & Fang, W.-C. (eds.) *Future Generation Information Technology.* Springer Berlin Heidelberg.

Elsberry, R. L. 1985. Observation and Analysis of Tropical Cyclones. *In:* Elsberry, R. L. (ed.) *Global View of Tropical Cyclones.*

Elsner, J. B., Niu, X. & Tsonis, A. A. 1998. Multi-year prediction model of North Atlantic hurricane activity. *Meteorology and Atmospheric Physics,* 68**,** 43-51.

Emanuel, K. 2005. *Divine Wind: The history and science of hurricanes*, Oxford University Press.

Eugene, S. 2012. *Global Tropical Cyclogenesis*, Springer.

Eumetsat, E. O. F. T. E. O. M. S. 2013. *Monitoring weather and climate from Space - Meteosat* [Online]. Available:

http://www.eumetsat.int/website/home/Satellites/CurrentSatellites/Meteosat/index.html [Accessed June 2013.

Evan, A. T. & Camargo, S. 2011. A Climatology of Arabian Sea Cyclonic Storms. *Journal of Climate,* 24**,** 14-158.

Evans, T. G. 1971. Grammatical inference techniques in pattern analysis. *Software Engineering,* 2.

Finn, G. D. 1999. Learning Fuzzy Rules from Data. *Neural Computing & Applications,* 8**,** 9-24.

Fitzpatrick, P. J. 1997. Understanding and Forecasting Tropical Cyclone Intensity Change with the Typhoon Intensity Prediction Scheme (TIPS). *Weather and Forecasting,* 12**,** 828 - 846.

Fms, F. M. S. R. N. T. C. C. 2013. *Tropical cyclone forecast track map - tropical cyclone Sandra* [Online]. Available: http://www.met.gov.fj/aifs_prods/65661.html.

Forbes, C. & Rhome, J. An automated operational storm surge prediction system for the National Hurricane Center. *In:* Spaulding, M. L., ed. International Conference on Estuarine and Coastal Modelling, 7-9th November 2011 2012 Florida, USA. American Society of Civil Engineers.

Forrester, F. 1982. Winds of the World. *Weatherwise,* 35.

Freeman, H. 1974. Computer Processing of Line-Drawing Images. *ACM Comput. Surv.,* 6**,** 57-97.

Fukunaga, K. 1972. *Introduction to Statistical Pattern Recognition*, New York: Academic,.

Funtowicz, S. O. & Ravetz, J. R. 1990. *Uncertainty and Quality in Science for Policy*, Kluwer Academic Publisher.

Galarneau, T. J. & Davis, C. A. 2012. Diagnosing Forecast Errors in Tropical Cyclone Motion. *Monthly Weather Review,* 141**,** 405-430.

Geographic, N. 2012. *Huge Spirals Found on Mars—Evidence of New Lava Type?* [Online]. Available: http://news.nationalgeographic.co.uk/news/2012/04/120426-mars-new-lava-coils-volcanoes-ice-life-space-science/ 2013].

Ghosh, S. & Ghosh, A. 2002. Image ambiguity optimisation for object extraction; A soft computing approach. *International Journal of Fuzzy Systems,* 4**,** 673-679.

Gibilisco, S. 1984. *Violent Weather: Hurricanes, Tornadoes and Storms*, TAB Books Inc.

Goerss, J. S. 2000. Tropical Cyclone Track Forecasts Using an Ensemble of Dynamical Models. *Monthly Weather Review,* 128**,** 1187-1193.

Goerss, J. S. & Jeffries, R. A. 1994. Assimilation of synthetic tropical cyclone observations into the Navy Operational Global Atmospheric Prediction System. *Weather and Forecasting,* 9**,** 557 - 576.

Gombos, D., Hoffman, R. N. & Hansen, J. A. 2012. Ensemble Statistics for Diagnosing Dynamics: Tropical Cyclone Track Forecast Sensitivities Revealed by Ensemble Regression. *Monthly Weather Review,* 140**,** 2647-2669.

Goni, G., Demaria, M., Knaff, J., Sampson, C., Ginis, I., Bringas, F., Mavume, A., Lauer, C., Lin, M, A. M., Sandery, P., Buarque, S. R., Kang, K., Mehra, A., Chassignet, E. & Halliwell, G. 2009. Applications of Satellite-Derived Ocean Measurements to Tropical Cyclone Intensity Forecasting. *Oceanography,* 22**,** 190-197.

Gonzalez, R. C. & Wintz, P. A. 1987. *Digital Image Processing* Addison Wesley.

Goodchild, M. & Zhang, J. 2002. *Uncertainty in Geographical Informatoin*, CRC Press.

Gray, W. M. 1968. Global view of the origin of tropical disturbances and storms. *Monthly Weather Review,* 96**,** 669-700.

Gray, W. M. 1979. *Hurricanes: Their formation, structure and likely role in the general circulation. Meteorology Over the Tropical Oceans*, Royal Meteorological Society.

Greaves, J. & Chang, D. 1970. Technique development to permit optimum use of satellite radiation data.

Gsfc, G. S. F. C. 2009. *The Bermuda High, navigator of hurricanes* [Online]. Available: http://www.wunderground.com/.

Han, S.-R., Guikema, S. D. & Quiring, S. M. 2009. Improving the Predictive Accuracy of Hurricane Power Outage Forecasts Using Generalized Additive Models. *International Journal of Rish Analysis,* 29**,** 1443-1453.

Harris, L. 1963. Characteristics of Hurricane Storm Surge. *US Department of Commerce Weather Bereau Techincal Paper Series,* 48.

Harrison, M. A. 1978. *Introduction to Formal Language Theory*, Addison-Wesley Longman Publishing Co., Inc.

Herndon, D., Velden, C. S., Hawkins, J., Olander, T. & Wimmers, A. The CIMSS SATellite CONsensus (SATCON) tropical cyclone intensity algorithm. 29th Conference on Hurricanes and Tropical Meteorology, 11-14 May 2010 2010 Tucson, AZ.

Hha, H. H. A. 2011. *Hurricane Hunter Association* [Online]. Available: http://www.hurricanehunters.com/index.html 2011].

Higuera, C. D. L. 2010. *Grammatical Inference*, Cambridge University Press.

Hirth, F. 1880. The Word 'Typhoon'. Its History and Origin. *Journal of the Royal Geographical Society of London,* 50**,** 260-267.

Ho, L. T. K., Yamaguchi, Y. & Umitsu, M. 2012. Rule-Based Landform Classification by Combining Multi-Spectral/Temporal Satellite Data and the SRTM DEM. *International Journal of Geoinformatics,* 8.

Ho, S.-S. & Talukder, A. 2008. Automated Cyclone Discovery and Tracking using Multiple Heterogeneous Satellite Data. *Proc. 14th ACM SIGKDD Int. Conf. on Knowledge Discovery and Data Mining.* Las Vegas.

Hollingsworth, J. L. & Kahre, M. A. 2010. Extratropical cyclones, frontal waves, and Mars dust: Modeling and considerations. *Geophysical Research Letters,* 37**,** L22202.

Hong, F. T. 2013. The role of pattern recognition in creative problem solving: A case study in search of new mathematics for biology. *Progress in Biophysics and Molecular Biology*.

Hossain, M. I., Liu, J. & You, J. Tropical cyclone pattern recognition for intensity and forecasting analysis from satellite imagery. International conference on systems, man and cybernetics, 1999 Tokyo.

Houze, R. A. 1993. *Cloud Dynamics*, Academic Press, Inc.

Iman, R. L., Johnson, M. E. & Schroeder, T. A. 2002. Assessing hurricane effects. Part 2. Uncertainty analysis. *Reliability Engineering & System Safety,* 78**,** 147-155.

Imd. 2005. Cyclone Warning Services. Available: http://www.imd.ernet.in/services/cyclone/cyclone-warning-services.htm [Accessed 5th July 2005].

In-Hyuk, K. & Hyeong-Bin, C. 2010. Tropical Cyclone Initialization with a Spherical High-Order Filter and an Idealized Three-Dimensional Bogus Vortex. *Monthly Weather Review,* 138**,** 1344-1367.

Ishibuchi, H. & Nakashima, T. 2001. Effect of rule weights in fuzzy rule-based classification systems. *Fuzzy Systems, IEEE Transactions on,* 9**,** 506-515.

Jain, A. K., Duin, R. P. & Mao, J. 2000. Statistical pattern recognition: a review. *IEEE Transactions on Pattern Analysis and Machine Intelligence,* 22**,** 4-37.

Jesan, J. P. 2004. The neural approach to pattern recognition. *Ubiquity,* 2004.

Jet Propultion Laboratory, J. 2012. *10 Years on Mars: Science* [Online]. Available: http://www.jpl.nasa.gov/video/.

Johnson, M. E. & Watson, C. C. 2011. Statistical Aspects of Hurricane Modeling and Forecasting

International Encyclopedia of Statistical Science. *In:* Lovric, M. (ed.). Springer Berlin Heidelberg.

Johnston, R. J. 1945. *Geograpy & Geographers: Anglo-American Human Georaphy since 1945*, Arnold Publisher.

Jovanovic, V. 2011. Evaluating Hurricane Intensity Prediction Techniques in Real Time. *2011 IEEE 11th International Conference on Data Mining Workshops (ICDMW).* Vancouver, BC.

Kamat, S. P. Fuzzy logic based pattern recognition technique for non-intrusive load monitoring. TENCON 2004. 2004 IEEE Region 10 Conference, 24-24 Nov. 2004 2004. 528-530 Vol. 3.

Kerlin, J. 1979. Performance test of the movable area fine mesh model in the Western Pacific. *Office Note 194.* National Weather Service, NOAA.

Key, J. R., Maslanik, J. A. & Barry, R. G. 1989. Cloud classification from satellite data using a fuzzy sets algorithm: A polar example. *International Journal of Remote Sensing,* 10**,** 1823-1842.

Khalid, F., Power, C. & Shehab, E. Development of a fuzzy rule based pattern detection system for tropical cyclone canopy classification. Remote Sensing and Photogrammetry Society Annual Conference, September 2003 Nottingham.

Khalid, F., Power, C. & Shehab, E. Evaluation of a fuzzy pattern recognition algorithm for tropical cyclone monitoring and assessment. Remote Sensing and Photogrammetry Society Annual Conference, September 2005 Portsmouth.

Kim, H.-S., Kim, J.-H., Ho, C.-H. & Chu, P.-S. 2010. Pattern Classification of Typhoon Tracks Using the Fuzzy c-Means Clustering Method. *Journal of Climate,* 24**,** 488-508.

Kitler, J. & Pairman, D. 1985. Contextual pattern recognition applied to cloud detection and identification. *IEEE Transactions on geoscience and remote sensing,* 23**,** 855-863.

Klir, G. & Yuan, B. 1995. *Fuzzy Sets and Fuzzy Logic*, Prentice Hall.

Knaff, J. A., Brown, D. P., Gallina, J. L. & Beven, J. L. 2010. An evaluation of Dvorak technique-based tropical cyclone intensity estimates. *Weather Forecasting,* 25**,** 1362-1379.

Knapp, K. R. 2008. Calibration Assessment of ISCCP Geostationary Infrared Observations Using HIRS. *Journal of Atmospheric and Oceanic Technology,* 25**,** 183-195.

Knapp, K. R. & Kossin, J. P. 2007. New global tropical cyclone data set from ISCCP B1 geostationary satellite observations. *Journal of Applied Remote Sensing,* 1**,** 013505-013505.

Knapp, K. R., Kruk, M. C., Levinson, D. H., Diamond, H. J. & Newmann, C. J. 2010. The International Best Track Archive for Climate Stewardship (IBTrACS) unifying tropical cyclone data. *Bulletin of Americal Meteorological Society,* 91.

Kohavi, R. The Power of Decision Tables. European Conference on Machine Learning, 1995. Springer Verlag, 174-189.

Kousky, C. 2012. Informing Climate Adaptation: A Review of the Economic Costs of Natural Disasters, Their Determinants, and Risk Reduction Options. *Resources for the Future Discussion*, 12-28

Kovacs, T. 2011. Genetics-based Machine Learning. *In:* Rozenberg, G. & Thomas (eds.) *Handbook of Natural Computing: Theory, Experiments and Applications.* Springer-Verlag.

Kovordányi, R. & Roy, C. 2009. Cyclone track forecasting based on satellite images using artificial neural networks. *ISPRS Journal of Photogrammetry and Remote Sensing,* 64**,** 513-521.

Kuan, D. T., Sawchuk, A. A., Strand, T. C. & Chavel, P. 1985. Adaptive Noise Smoothing Filter for Images with Signal-Dependent Noise. *Pattern Analysis and Machine Intelligence, IEEE Transactions on,* PAMI-7**,** 165-177.

Kuciauskas, A. P., Brody, L. R., Hadjimichael, M., Bankert, R. L., Tag, P. M. & Peak, J. E. 1998. A fuzzy expert system to assist in the prediction of hazardous wind conditions within the Mediterranean basin. *Meteorological Applications,* 5**,** 307-320.

Kurihara, Y. & Bender, M. A. 1980. Use of movable nested mesh model for tracking a small vorted. *Monthly Weather Review,* 108**,** 1972 - 1809.

Laface, P. & De-Mori, R. (eds.) 1992. *Speech Recognition and Understanding. Recent Advances, Trends, and Applications*.

Laha, A. & Das, J. 2011. Fuzzy Rules and Evidence Theory for Satellite Image Analysis. *Computer Vision and Pattern Recognition*.

Laing, A. & Evans, J.-L. 2011. Introduction to Tropical Meteorology. 2nd ed.: University Corporation for Atmospheric Research.

Lajoie, F. & Walsh, K. 2010. A Diagnostic Study of the Intensity of Three Tropical Cyclones in the Australian Region. Part I: A Synopsis of Observed Features of Tropical Cyclone Kathy (1984). *Monthly Weather Review,* 138**,** 3-21.

Landsea, C., Glenn, D. A., Bredemeyer, W., Chenoweth, M., Ellis, R., Gamache, J., Hufstetler, L., Mock, C., Perez, R., Prieto, R., Sánchez-Sesma, J., Thomas, D. & Woolcock, L. 2008. A Reanalysis of the 1911-20 Atlantic Hurricane Database. *Journal of Climate,* 21**,** 2138-2168.

Landsea, C. & Goldenberg, S. 2011. Hurricanes, Typhoons, And Tropical Cyclones. Available: http://www.aoml.noaa.gov/hrd/tcfaq/tcfaqHED.html [Accessed 10 August 2011].

Landsea, C. W., Anderson, C., Charles, N., Clark, G., Dunion, J., Fernandez-Partagas, J., Hungerford, P., Neumann, C. & M. Zimmer 2004a. The Atlantic hurricane database re-analysis project: Documentation for the 1851-1910 alterations and additions to the HURDAT database. *In:* Murnane, R. & Liu, K.-B. (eds.) *Hurricanes and Typhoons: Past, Present and Future.* Cambridge University Press.

Landsea, C. W., Feuer, S., Hagen, A., Glenn, D. A., Sims, J., Perez, R., Chenoweth, M. & Anderson, N. 2012. A Reanalysis of the 1921–30 Atlantic Hurricane Database*. *Journal of Climate,* 25, 865-885.

Landsea, C. W., Franklin, J. L., Mcadie, C. J., Beven, J. L., Gross, J. M., Jarvinen, B. R., Pasch, R. J., Rappaport, E. N., Dunion, J. P. & Dodge, P. P. 2004b. A Reanalysis of Hurricane Andrew's Intensity. *Bulletin of the American Meteorological Society,* 85, 1699-1712.

Le Marshall, J. F., Leslie, L. M., Abbey Jr, R. F. & Qi, L. 2002. Tropical cyclone track and intensity prediction: The generation and assimilation of high-density, satellite-derived data. *Meteorology and Atmospheric Physics,* 80, 43-57.

Lee, R. S. T. & Liu, J. 2001. An elastic contour matching model for tropical cyclone pattern recognition. *IEEE transactions on systems, man and cybernetics, Part B: Cybernetics,* 31.

Lehmiller, G. S., Kimberlain, T. B. & Elsner, J. B. 1997. Seasonal prediction models for north atlantic basin hurricane location. *Monthly Weather Review,* 125, 1780–1791.

Lemons, J. 1996. *Scientific Uncertainty and Its Implications for Environmental Problem Solving*, Wiley.

Leslie, L. M., Abbey, R. F. & Holland, G. J. 1998. Tropical cyclone track predictability. *Meteorology and Atmospheric Physics,* 65, 223-231.

Lewis, W., Madison, W. I., Tripoli, G. J. & Hashino, T. 2010. High resolution satellite data assimilation and its role in tropical cyclone prediction. *29th Conference on Hurricane and Tropical Meteorology.* Arizona.

Li, S. & Jain, A. 2011. *Handbook of Face Recognition*, Springer-Verlag London.

Li, S. Z. 1995. *Markov Random Field Modeling in Computer Vision*, Springer-Verlag New York, Inc.

Li, X. Q., Zhao, Z. W., Cheng, H. D., Huang, C. M. & Harris, R. W. A fuzzy logic approach to image segmentation. Pattern Recognition, 1994. Vol. 1 - Conference A: Computer Vision & Image Processing., Proceedings of the 12th IAPR International Conference on, 9-13 Oct 1994 1994. 337-341 vol.1.

Liu, J. G. 2000. Smoothing Filter-based Intensity Modulation: A spectral preserve image fusion technique for improving spatial details. *International Journal of Remote Sensing,* 21, 3461-3472.

Liu, J. N. K., Shiu, S. C. K. & You, J. 2009. Tropical Cyclone Forecaster Integrated with Case-Based Reasoning

Proceedings of the European Computing Conference. *In:* Mastorakis, N., Mladenov, V. & Kontargyri, V. T. (eds.). Springer US.

Liu, L., Sun, X., Chen, F., Zhao, S. & Gao, T. 2011. Cloud Classification Based on Structure Features of Infrared Images. *Journal of atmospheric and oceanic technology,* 28**,** 410-417.

Lizarazo, I. & Elsner, P. 2009. Fuzzy segmentation for object-based image classification. *International Journal of Remote Sensing,* 30**,** 1643-1649.

Ludlum, D. 1963. *Early American Hurricanes 1492-1870*, American Meteorological Society.

Mallinson, H. & Bentley, P. 1999. Evolving Fuzzy Rules for Pattern Classification. *In:* Mohammadian, M. (ed.) *Computational Integration for Modelling, Control and Automation '99.* Hotel Marriott, Vienna, Austria: IOS Press.

Marr, D. 1982. *Vision: A Computational Investigation into the Human Representation*

and Processing of Visual Information, San Francisco: Freeman.

Martinez-Valpuesta, I., Knapen, J. H. & Buta, R. 2007. A Morphological and Statistical Analysis of Ansae in Barred Galaxies. *The Astronomical Journal,* 134**,** 1863.

Mashchenko, S. Y., Thilker, D. A., & Braun, R. 1999. Automated supershell recognition in spiral galaxies employing hydrodynamic simulations. *Astronomy and Astrophysics,,* 343**,** 352-366.

Maykut, E. S. 1964. An experiment in objective nephanalysis using proposed HRIR satellite infrared radiation data. *Journal of Applied Meteorology,* 3**,** 215-225.

Mcdonald, W. F. 1935. The hurricane of August 31 to September 6, 1935. *Monthly Weather Review,* 63.

Mcdonald, W. F. 1942. On a hypothesis regarding normal development and decay of tropical hurricanes. *Bulletin of the American Meteorological Society,* 23**,** 117-121.

Melin, P. 2012. Image Processing and Pattern Recognition with Mamdani Interval Type-2 Fuzzy Inference Systems. *In:* Trillas, E., Bonissone, P. P., Magdalena, L. & Kacprzyk, J. (eds.) *Combining Experimentation and Theory.* Springer Berlin Heidelberg.

Melin, P. & Castillo, O. 2013. Type-2 Fuzzy Logic in Image Analysis and Pattern Recognition. *In:* Sadeghian, A., Mendel, J. M. & Tahayori, H. (eds.) *Advances in Type-2 Fuzzy Sets and Systems.* Springer New York.

Melin, P., Mendoza, O. & Castillo, O. 2011. Face Recognition With an Improved Interval Type-2 Fuzzy Logic Sugeno Integral and Modular Neural Networks. *Systems, Man and Cybernetics, Part A: Systems and Humans, IEEE Transactions on,* 41**,** 1001-1012.

Merrill, R. 1985. Environmental Influences on Hurricane Intensification. *Journal of Atmospheric Sciences,* 45**,** 1678-1687.

Metoffice. 2011. *Tropical Cyclones* [Online]. Available: http://www.metoffice.gov.uk/weather/tropicalcyclone [Accessed 02/11/2011 2011].

Miller, D. B. Automated production of global cloud climatology based on satellite data. 6th Automated Weather Supp. Technical Exchange Conference 1971 US Naval Academy. USAF Tech.

Moore, P. L. & Davis, W. R. 1951. A preseason hurricane of subtropical origin. *Monthly Weather Review,* 79**,** 189-195.

Murthy, C. R., Sinha, P. C., Rao, Y. R., Mohanty, U. C. & Gupta, A. 2008. Deterministic Methods for Prediction of Tropical Cyclone Tracks

Modelling and Monitoring of Coastal Marine Processes. Springer Netherlands.

Musk, L. F. 1988. *Weather System*, Cambridge University Press.

Myagmarbayar, N., Nevrez Imamoglu, Yuki Yoshida, Jose Gonzalez, Masashi Sekine, Kazuya Kawamura & Yu, W. 2013. Human behavior recognition by a mobile robot following human subjects. *Communications in computer and informatoin science,* 362**,** 159-172.

Nafarieh, A. & Keller, J. M. 1991. A fuzzy logic rule-based automatic target recognizer. *International Journal of Intelligent Systems,* 6**,** 295-312.

Nagalakshmi, G. & Jyothi, S. 2013. A survey on pattern recognition using fuzzy clustering approaches. *international refereed journal of engineering and science,* 2**,** 24-31.

Nasa, N. a. a. S. A. 1975. Image Data Processing System (IDAPS) user manual.

Nasa, N. a. a. S. A. 2010. *GOES POES Programs: GOES project home* [Online]. Available: http://goespoes.gsfc.nasa.gov/goes/index.html 2011].

National History Museum. 2011. Mesopotamia. 2011. Available: http://www.mesopotamia.co.uk/ [Accessed 20th August 2011].

Neumann, C. J. 1972. An alternative to the HURRAN (Hurricane Analog) tropical cyclone forecast system. *NOAA, National Oceanic and Atmospheric Administration Technical Memo.* National Hurricane Centre, NOAA.

Neumann, C. J. 1993. Global Guide to Tropical Cyclone Forecasting, WMO/TC=No. 560 Report Np. RCP-31. *In:* Holland, G. J. (ed.). World Meteorological Organisation.

Neumann, C. J., Jarvinen, B. R., J., M. C. & Elms, J. D. 1993. Tropical Cyclones of the North Atlantic Ocean, 1871-1992. *Historical Climatology Series,* 6.

Ngia, N. G. I. A. 2012. South Atlantic Ocean and Indian Ocean - Sailing directions. *In:* Agency, N. G. I. (ed.) Tenth edition ed. Springfield, Virginia.

Nhc, N. H. C. 2009. Techincal Summary of the National Hurricane Center Track and Intensity Models. Available: http://www.nhc.noaa.gov/pdf/model_summary_20090724.pdf [Accessed 5th July 2010].

Nhc, N. H. C. 2011. *NHC Tropical Cyclone Forecast Verification* [Online]. Available: http://www.nhc.noaa.gov/verification/verify5.shtml 2012].

Nhc, N. H. C. 2012. *2012 Tropical cyclone advisory archive* [Online]. NOAA. Available: http://www.nhc.noaa.gov/archive/2012/ERNESTO_graphics.shtml [Accessed 20th August 2012.

Noaa. 2008a. The worst natural disaster by death toll. Available: http://docs.lib.noaa.gov/noaa_documents/NOAA_related_docs/death_toll_natural_disasters.pdf [Accessed 10 March 2013].

Noaa, N. O. a. a. A. 1999. Hurricane basics.

Noaa, N. O. a. a. A. 2008b. Worst Natural Disaster by Death Toll. Available: http://docs.lib.noaa.gov/noaa_documents/NOAA_related_docs/death_toll_natural_disasters.pdf [Accessed 15 August 2010].

Noaa, N. O. a. a. A. 2009. *NCDC: Hurricane Georges - Satellite images* [Online]. Available: http://www.ncdc.noaa.gov/oa/reports/georges/georges.html#IMAGES [Accessed May 2013 2013].

Noaa, N. O. a. a. A. 2010. *Hurricane FAQs* [Online]. Hurricane Research Division. Available: http://www.aoml.noaa.gov/hrd/tcfaq/tcfaqHED.html.

Noaa, N. O. a. a. A. 2011. *NOAA Photo Library* [Online]. Available: http://www.photolib.noaa.gov/brs/spind1.htm 2011].

Noaa, N. O. a. a. A. 2012. Saffire-Simpson Hurrican Wind Scale.

Norton, G. 1952. Hurricanes of 1951. *Monthly Weather Review,* 80**,** 1-4.

Nott, J. & Hayne, M. 2000. How high was the storm surge from Tropical Cyclone Mahina? North Queensland, 1899. *Australian Journal of Emergency Management*.

Nozaki, K., Ishibuchi, H. & Tanaka, H. 1996. Adaptive Fuzzy Rule-Based Classification Systems. *IEEe Transactions on Fuzzy Systems,* 4**,** 238-250.

Nrl, N. R. L., Marine Meteorology Division. 2011. *The Automated Tropical Cyclone Forecasting System (ATCF tm)* [Online]. Available: http://www.nrlmry.navy.mil/atcf_web/ [Accessed June 2013.

Nws, N. W. S. 2009. *Hurricane Fredric* [Online]. National Oceanic and Atmospheric Administration. Available: http://www.srh.noaa.gov/mob/?n=frederic 2011].

O'hare, G., Sweeney, J. & Wilby, R. L. 2005. *Weather, Climate and Climate Change: Human Perspective*, Pearson Education.

Ohring, G. 1973. Meteorological fields from remote infrared sensing. *Surveys in Geophysics,* 1**,** 163-193.

Olander, T. & Velden, C. 2007. The Advanced Dvorak Technique: Continued Development of an Objective Scheme to Estimate Tropical Cyclone Intensity Using Geostationary Infrared Satellite Imagery. *Weather and Forecasting,* 22**,** 287-298.

Olander, T. L. & Velden, C. S. 2011. ADT - Advanced Dvorak Technique USERS' GUIDE (McIDAS version 8.1.3). The Cooperative Institute for Meteorological Satellite Studies, Space Science and Engineering Center, University of Wisconsin-Madison.

Olander, T. L., Velden, C. S. & Turk, M. A. Development of the advanced objective Dvorak technique (AODT) - current progress and future directions. 25th Conference on Hurricanes and Tropical Meteorology, 2002 San Diego. American Meteorology Society, 585-586.

Opricovic, S. & Tzeng, G.-H. 2003. DEFUZZIFICATION WITHIN A MULTICRITERIA DECISION MODEL. *International Journal of Uncertainty, Fuzziness and Knowledge-Based Systems,* 11**,** 635-652.

Ospo, T. O. O. S. a. P. O., Noaa. 2013. *Geostationary Operational Environmental Satellites (GOES)* [Online]. Available: http://www.ospo.noaa.gov/Operations/GOES/index.html 2013].

Pal, N. R., Mandal, A. K., Pal, S., Das, J. & Lakshmanan, V. 2006. Fuzzy Rule–Based Approach for Detection of Bounded Weak-Echo Regions in Radar Images. *Journal of Applied Meteorology and Climatology,* 45**,** 1304-1312.

Pal, S. 1992. Fuzzy set theoretic measures for automatic feature evaluation: II. *information Sciences,* 64.

Pal, S. 2003. Soft Computing Pattern Recognition: Principles, Integrations and Data Mining. *In:* Inuiguchi, M., Hirano, S. & Tsumoto, S. (eds.) *Rough Set Theory and Granular Computing.* Springer.

Pal, S. & Chakraborty, B. 1986. Fuzzy set theoretic measures for automatic feature evaluation. *IEEE Transactions on Systems, Man and Cybernetics,* 16**,** 754-760.

Pal, S., Dutta-Mazumder, D. & Majumder, D. D. 1986. *Fuzzy Mathematical Approach to Pattern Recognition*, Halsted Pr.

Pal, S. & Mitra, S. 1999. *Neuro-fuzzy pattern recognition: methods in soft computing*.

Pal, S. & Pal, A. 2001. *Pattern recognition: from classical to modern approaches*, World scientific Publishing Co.

Palmen, E. 1948. On the formation and structure of tropical cyclones. *Geophysica,* 3**,** 26-38.

Pathak, A. & Pal, S. 1987. On the convergence of "A self-supervised vowel recognition system. *Pattern Recognition,* 20**,** 237-244.

Pathak, A. & Pal, S. K. 1986. Fuzzy Grammars in Syntactic Recognition of Skeletal Maturity from X-Rays. *Systems, Man and Cybernetics, IEEE Transactions on,* 16**,** 657-667.

Pathak, A., Sankar, P. & King, R. A. 1984. Syntactic recognition of skeletal maturity. *Pattern Recognition Letters,* 2**,** 193-197.

Pattanaik, D. & Rama Rao, Y. 2009. Track prediction of very severe cyclone 'Nargis' using high resolution weather research forecasting (WRF) model. *Journal of Earth System Science,* 118**,** 309-329.

Paul, B. E., Jay, A. F., Richard, W. P., Alice, C. Q., Andreas, A. B., Roger, L. D., Depoy, D. L., Karoline, M. G., Mark, L. H., Leslie, E. K., Solange, V. R., Sellgren, K., Amelia, S., Donald, M. T. & Glenn, P. T. 2002. Near-Infrared and Optical Morphology of Spiral Galaxies. *The Astrophysical Journal Supplement Series,* 143**,** 73.

Pedrycz, W. 1990. Fuzzy sets in pattern recognition: Methodology and methods. *Pattern Recognition,* 23**,** 121-146.

Peeva, K. & Kyosev, Y. 2004. *Fuzzy relational calculus: Theory, applications and software*, World Scientific Publising Co.

Peters, J., Skowron, A., Marek, V., Orlowska, E., Slowinski, R. & Ziarko, W. 2007. *Transactions on Rough Sets VII: Commenting the life and work of Zdzislaw Pawlak*, Springer.

Pielke, R. A. 1990. *The Hurricane*, Routledge.

Pielke, R. A. & Pielke, R. A. 1997. *Hurricanes: Their Nature and Impacts on Society,* New York, John Wiley and Sons.

Pietz, D. A. 2002. *Engineering the State: The Huai River and Reconstruction in Nationalist China, 1927-1937*.

Poroseva, S. V., Letschert, J. & Yousuff Hussaini, M. 2007. Application of evidence theory to quantify unvertainty in hurricane/typhoon track forecasts. *Meteorology and Atmospheric Physics,* 97**,** 149-169.

Potter, C., Tan, P.-N., Kumar, V., Kucharik, C., Klooster, S., Genovese, V., Cohen, W. & Healey, S. 2005. Recent History of Large-Scale Ecosystem Disturbances in North America Derived from the AVHRR Satellite Record. *Ecosystems,* 8**,** 808-824.

Power, C. 1989. *Rainfall estimation from tropical cyclones detected using satellite imagery (confirm the title).* PhD, University of Bristol.

Prasad, K. 2006. Further experiments on cyclone track prediction with a quasi-Lagrangian limited area model. *Meteorology and Atmospheric Physics,* 91**,** 183-199.

Raju, P., Potty, J. & Mohanty, U. 2011a. Prediction of severe tropical cyclones over the Bay of Bengal during 2007–2010 using high-resolution mesoscale model. *Natural Hazards***,** 1-14.

Raju, P., Potty, J. & Mohanty, U. 2011b. Sensitivity of physical parameterizations on prediction of tropical cyclone Nargis over the Bay of Bengal using WRF model. *Meteorology and Atmospheric Physics,* 113**,** 125-137.

Rappaport, E. N., Franklin, J. L., Avila, L. A., Baig, S. R., Beven, J. L., Blake, E. S., Burr, C. A., Jiing, J.-G., Juckins, C. A., Knabb, R. D., Landsea, C. W., Mainelli, M., Mayfield, M., Mcadie, C. J., Pasch, R. J., Sisko, C., Stewart, S. R. & Tribble, A. N. 2009. Advances and Challenges at the National Hurricane Center. *Weather and Forecasting,* 24**,** 395-419.

Rath, R. & Pradhan, S. 2011. Wireless sensor network for super cyclone prediction using artificial neural network. *Asian Journal Of Computer Science And Information Technology,* 1**,** 30 - 33.

Reilly, B. 2009. *Disaster and human history: case studies in nature, society and catastrophe*, McFarland & Co Inc.

Reynolds, D. W. & Haar, T. H. V. 1977. A bi-spectral method for cloud parameter determination. *Monthly Weather Review,* 105**,** 446-457.

Reynolds, K. & Ogley, B. 1989. *Eye on the Hurricane: Eastern Counties*, Froglets.

Riehl, H. 1954. *Tropical Meteorology*, McGrawHill.

Robert, T. & Tourneret, J. Y. Continuously evolving classification of signals corrupted by an abrupt change. IEEE-IMS Workshop on Information Theory and Statistics, 27-29 Oct 1994 1994 Alexandria, VA.

Rodionov, S. & Martin, J. 1996. A knowledge based system for the diagnosis and prediction of short term climate changes in the North Atlantic. *Journal of Climate,* 9**,** 1816-1823.

Rosenfeld, A. & Kak, A. 1982. *Digital picture processing*, Academic Press.

Ross, T. 2009. *Fuzzy Logic with Engineering Application*, John Wiley.

Rutkowska, D. 2002. *Neuro-Fuzzy architectures and hybrid learning,* Germany, Physica-Verlag.

S. C. Odewahn, S. H. C., R. A. Windhorst, and Ninan Sajeeth Philip 2002. Automated Galaxy Morphology: A Fourier Approach. *The Astrophysical Journal,* 568.

Sampson, C. R. & Schrader, A. J. 2000a. The automated Tropical Cyclone Forecasting System (ATCF) version 3.2. *Bulletin of Americal Meteorological Society,* 81**,** 1231-1240.

Sampson, C. R. & Schrader, A. J. 2000b. The Automated Tropical Cyclone Forecasting System (Version 3.2). *Bulletin of the American Meteorological Society,* 81**,** 1231-1240.

Sampson, C. R., Schumacher, A. B., Knaff, J. A., Demaria, M., Fukada, E. M., Sisko, C. A., Roberts, D. P., Winters, K. A. & Wilson, H. M. 2012. Objective Guidance for Use in Setting Tropical Cyclone Conditions of Readiness. *Weather and Forecasting,* 27**,** 1052-1060.

Sanford, T. B., Price, J. F., Girton, J. B. & Webb, D. C. 2007. Highly resolved observations and simulations of the ocean response to a hurricane. *Geophysical Research Letters,* 34.

Sankar, P. 1996. Soft Computing: Goal, Tools and Feasibility. *Journal of the institution of electronics and telecommunication engineers,* 42**,** 195-204.

Schalkoff 1992. *Pattern recognition: statistical, structural, and neural approaches*, J. Wiley.

Schmalzel, J. L. & Johnson, J. F. Pattern recognition based on fuzzy logic. Instrumentation and Measurement Technology Conference, 1993. IMTC/93. Conference Record., IEEE, 18-20 May 1993 1993. 681-684.

Schwarzbach, M. 1963. *Climates of the Past*.

Shafer, G. 1976. *A Mathematical Theory of Evidence*, Princeton University Press.

Shah, H., Jaafar, J., Ibrahim, R., Saima, H. & Maymunah, H. A hybrid system using Possibilistic fuzzy C-mean and Interval type-2 Fuzzy logic for forecasting: A review. Computer & Information Science (ICCIS), 2012 International Conference on, 12-14 June 2012 2012. 532-537.

Sheets, R. C. 1981. Tropical cyclone modification: The Project STORMFURY Hypothesis. *NOAA Technical Report.* NOAA.

Shenk, W. E., Holub, R. J. & Neff, R. A., 1976 1976. A multispectral cloud type identification method developed for tropical ocean areas with Nimbus 3 MRIR measurements. *Monthly Weather Review,* 104**,** 284-291.

Simpson, R. 1971. The decision process in hurricane forecasting. *NOAA Technical Memo,* NWS SR-53.

Skidmore, A. 2002. *Environmental Modelling with GIS and Remote Sensing*, Taylor & Francis.

Sorenson, J. H. 2000. Hazard Warning Systems: Review of 20 Years of Progress. *Natural Hazard Review,* 1.

Spencer, R. & Christry, J. 1990. Precise monitoring of global temperature trends from satellites. *Science* 247**,** 1558 - 1562.

Sternberg, R. 2006. *Cognitive Psychology*, Thomson Wadsworth.

Talbot, L. M., Talbot, B. G., Peterson, R. E., Tolly, H. D. & Mecham, H. D. 1999. Application of fuzzy grade-of-membership clustering to analysis of remote sensing data. *Journal of climate,* 12**,** 200-219.

Talukder, A., Ho, S.-S., Liu, T., Tang, W., Bingham, A. & Rigor, E. 2008. Global Cyclone Detection and Tracking using Multiple Remote Satellite Data. *NASA Earth Science Technology Conference.* Aldephi, Maryland.

Theilen-Willige, B. P.-C., George 2009. Natural hazard assessment of sw myanmar - A contribution of remote sensing and gis methods to the detection of areas vulnerable to earthquakes and tsunami / cyclone flooding. *Science of Tsunami Hazards,* 28**,** 108.

Thies, B., Turek, A., Nauss, T. & Bendix, J. 2010. Weather type dependent quality assessment of a satellite-based rainfall detection scheme for the mid-latitudes. *Meteorology and Atmospheric Physics,* 107**,** 81-89.

Toldalagi, P. M. & Lebow, W. M. 1982. Survey and Analysis of Satellite Cloud Classification Research Techniques,. Naval Environmental Prediction Research Facility, Monterey, CA.,.

Torn, R. D. & Snyder, C. 2012. Uncertainty of Tropical Cyclone Best-Track Information. *Weather and Forecasting,* 27**,** 715-729.

Tou, J. & Gonzalez, R. 1974. *Pattern Recognition Principles*, Addison Wesley.

Tsai, H.-C. & Elsberry, R. L. 2012. Opportunities and challenges for extended-range predictions of tropical cyclone impacts on hydrological predictions. *Journal of Hydrology*.

Uhr, L. 1971. Flexible linguistic pattern recognition. *Pattern Recognition,* 3**,** 363-383.

Upgren, A. & Stock, J. 2000. *Weather: How it Works and Why it Matters*, Perseus Books.

Van Asselt, M. B. A. 2000. *Perspectives on Uncertainty and Risk*, Springer.

Vega, A. J. 1991. Temporal variation of tropical cycloens in the North Atlantic Basin. *Geo Journal* 23**,** 311-322.

Velden, C. S., Olander, T. L. & Zehr, R. 1998a. Development of an objective scheme to estimate tropical cyclone intensity from digital geostationary satellite infrared imagery. *Weather and Forecasting,* 13**,** 172-186.

Velden, C. S., Olander, T. L. & Zehr, R. M. 1998b. Development of an objective scheme to estimate tropical cyclone intensity from digital geostationary satellite infrared imagery. *Forecasting,* 13**,** 172-186.

Vidale, P. L., Roberts, M., Hodges, K., Strachan, J., Demory, M. E. & Slingo, J. 2010. Tropical Cyclones in a Hieararchy of Climate Models of Increasing Resolution

Indian Ocean Tropical Cyclones and Climate Change. *In:* Charabi, Y. (ed.). Springer Netherlands.

Vigh, J. 2000. A fuzzy logic system for predicting hurricane intensity in the Eastern North Pacific.

Vines, R. B. 1898. Cyclonic Ciculation and the Translatory Movement of West Indian Hurricanes. Available: http://www.aoml.noaa.gov/general/lib/CREWS/Cleo/St.%20Croix/salt_river187.pdf [Accessed 23 August 2005].

Wadhawan, S., Goel, G. & Kaushik, S. 2013. Data driven fuzzy modelling for sugeno and mamdani type fuzzy model using memetic algorithm. *International Journal of Information Technology and Computer SCience,* 8**,** 24-37.

Wang, L.-X. & Mendel, J. M. 1991. Generating fuzzy rules from numerical data, with applications.: Signal and Image Processing Institute, University of Southern California, Department of Electrical Engineering Systems.

Wang, L.-X. & Mendel, J. M. 1992. Generating fuzzy rules by learning from examples. *IEEE Transactions on Systems, Man and Cybernetics,* 22**,** 1414-1427.

Weatherford, C. & Gray, W. M. 1988. Typhoon structure as revealed by aircraft reconnaissance. Part II: Structural variability. *Monthly Weather Review,* 116**,** 1044-1056.

Wehner, M. F., Bala, G., Duffy, P., Mirin, A. A. & Romano, R. 2010. Towards Direct Simulation of Future Tropical Cyclone Statistics in a High-Resolution Global Atmospheric Model. *Advances in Meteorology,* 2010**,** 1-14.

Wei, C.-C., Chen, L. & Hsu, H.-H. 2012. Neural-Based Decision Trees Classification Techniques: A Case Study in Water Resources Management. *In:* Qian, Z., Cao, L., Su, W., Wang, T. & Yang, H. (eds.) *Recent Advances in Computer Science and Information Engineering.* Springer Berlin Heidelberg.

Wei, K. & Jing, Z.-L. 2010. Spiral band model optimization by chaos immune evolutionary algorithm for locating tropical cyclones. *Atmospheric Research,* 97**,** 266-277.

Wei, K., Jing, Z.-L., Li, Y.-X. & Liu, S.-L. 2011. Spiral band model for locating Tropical Cyclone centers. *Pattern Recognition Letters,* 32**,** 761-770.

Weinkle, J., Maue, R. & Jr., R. P. 2012. Historic Global Tropical Cyclone Landfalls. *Journal of Climate,* 25**,** 4729-4735.

Whittingham, H. E. 1958. The Bathurst Bay Hurricane and Associated Storm Surge. *Australian Meteorological Magazine.*

Wimmers, A. & Velden, C. S. Satellite based center fixing of TCs: New automated approaches. Conference on Hurricaes and Tropical Meteorology, 2004 Miami, FL. American Meteorological Society.

Witlox, F., Borgers, A. & Timmermans, H. 2004. Modelling locational decision making of firms using multidimensional fuzzy decisoin tables: An illustration. *Solstice: An electronic journal of geography and mathematics,* 15.

Wong, K. Y. & Yip, C. L. 2009. Identifying centers of circulating and spiraling vector field patterns and its applications. *Pattern Recognition,* 42**,** 1371-1387.

Woodbury, G. & Mccormick, M. 1986. Zonal and geographical distribution of cirrus clouds determined from SAGE data. *Journal of Geophysical Research,* 91**,** 388 - 408.

World Meteorological Organisation 1976. Lectures on forecasting of tropical weather, including tropical cyclones, with particular relevance to Africa. Secretariat of the World Meteorological Organisation, Geneva, Switzerland.

World Meteorological Organisation 1983. Global guide to tropical cyclone forecasting.

Wu, B. & Sun, C.-M. 1996. Fuzzy statistics and computation on the lexical semantics: How much do you think? and how many? *Langage, Information and Computation,* 11**,** 337-346.

Wu, T.-P. & Chen, S.-M. 1999. A new method for constructing membership functions and fuzzy rules from training examples. *IEEE Transactions on Systems, Man and Cybernetics-Part B: Cybertenics,* 29**,** 25-40.

Wylie, P. & Menzel, P. 1989. Two years of cloud cover statistics using VAS. *Journal of Climate,* 2**,** 380-390.

Yingying, C., Renmao, T., Yuquan, Z., Zhenteng, Y., Yuchun, X. & Dejun, L. 2011. Interpretation of cloud classification using the color image composed by three channel data. *Journal of applied meteorological science,* 22**,** 691-697.

Yip, C. & Wong, K. 2004. Efficient and Effective Tropical Cyclone Eye Fix Using Genetic Algorithms

Knowledge-Based Intelligent Information and Engineering Systems. *In:* Negoita, M., Howlett, R. & Jain, L. (eds.). Springer Berlin / Heidelberg.

You, J., Liu, J. & Lee, R. 1999. *An image matching approach to tropical cyclone pattern recognition,* Athens, C S R E a Press.

Yu, H., Chen, P., Li, Q. & Tang, B. 2012. Current Capability of Operational Numerical Models in Predicting Tropical Cyclone Intensity in the Western North Pacific. *Weather and Forecasting,* 28**,** 353-367.

Zadeh, L. 1965. Fuzzy Sets. *Information and Control,* 8**,** 338-353.

Zadeh, L. Fuzzy Logic and Soft Computing. IEEE International Workshop on Neuro Fuzzy Control., 1993 Muroran, Japan.

Zadeh, L. 1996a. *Fuzzy Sets, Fuzzy Logic, and Fuzzy Systems*, World Scientific.

Zadeh, L. The Role of Soft Computing and Fuzzy Logic in the Conception, Design, Development of Intelligent Systems. IEEE International Workshop on Soft Computing Industry, 1996b Muroran, Japan.

Zadeh, L. 1997. *What is Soft Computing*, Springer-Verlag Germany/USA.

Zehr, R. 1989. Improving objective satellite estimates of tropical cyclone intensity. *18th Conference on Hurricanes and Tropical Meteorology.* San Diego: American Meteorological Society.

Zhang, Q., Lai, L. & Sun, W. 2006. Location of Tropical Cyclone Center with Intelligent Image Processing Technique

Advances in Machine Learning and Cybernetics. *In:* Yeung, D., Liu, Z.-Q., Wang, X.-Z. & Yan, H. (eds.). Springer Berlin / Heidelberg.

Zhang, T. Y. & Suen, C. Y. 1984. A fast parallel algorithm for thinning digital patterns. *Commun. ACM,* 27**,** 236-239.

Zhao, H., Wu, L. & Zhou, W. 2011. Interannual Changes of Tropical Cyclone Intensity in the Western North Pacific. *Journal of the Meteorological Society of Japan,* 89**,** 243-253.

APPENDIX I - Hurricane life span intensity graphs

1978 Hurricane CORA

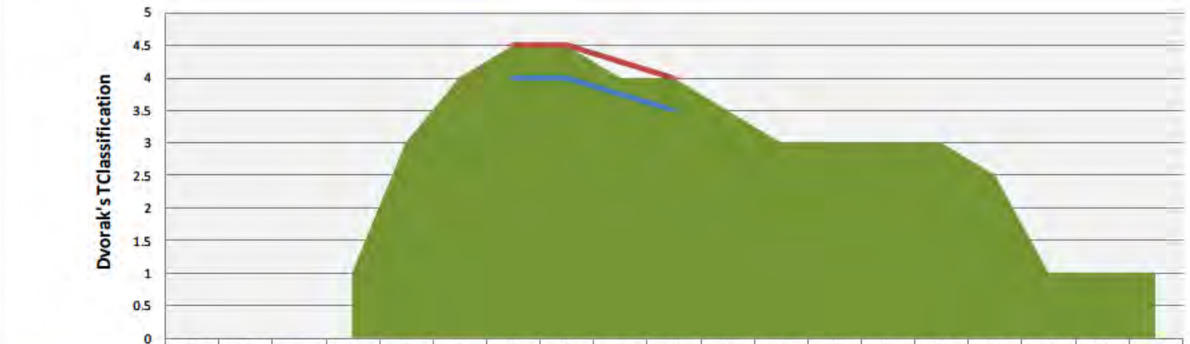

	7 Aug	7 Aug	8 Aug	8 Aug	8 Aug	8 Aug	9 Aug	9 Aug	9 Aug	9 Aug	10 Aug	10 Aug	10 Aug	10 Aug	11 Aug	11 Aug	11 Aug	11 Aug	12 Aug
WMO T Class				1	3	4	4.5	4.5	4	4	3.5	3	3	3	3	2.5	1	1	1
Defuzzified Lower Probability							4	4		3.5									
Defuzzified Higher Probability							4.5	4.5		4									

1978 Hurricane ELLA

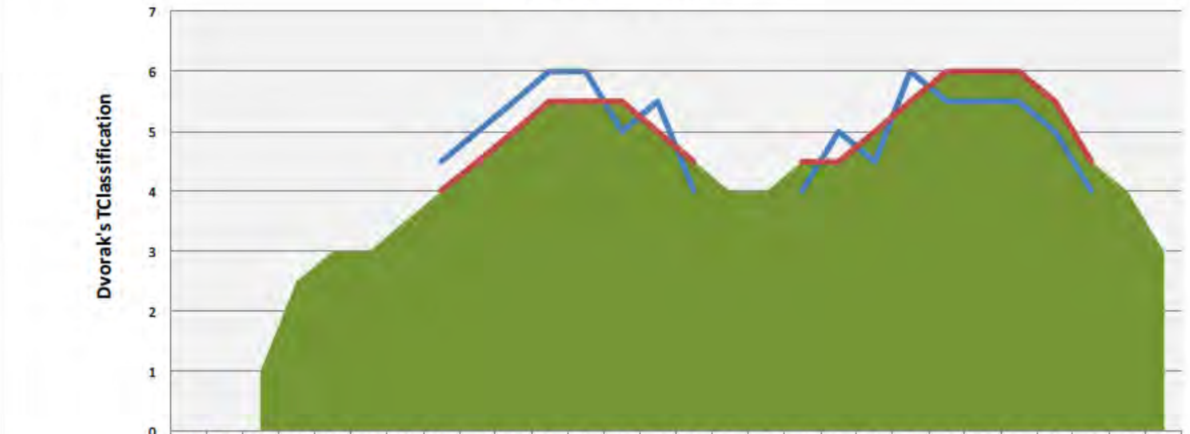

	30 Aug	30 Aug	30 Aug	30 Aug	31 Aug	31 Aug	31 Aug	31 Aug	1 Sep	1 Sep	1 Sep	1 Sep	2 Sep	2 Sep	2 Sep	2 Sep	3 Sep	3 Sep	3 Sep	3 Sep	4 Sep	4 Sep	4 Sep	4 Sep	5 Sep	5 Sep	5 Sep	5 Sep
WMO T Class			1	2.5	3	3	3.5	4	4.5	5	5.5	5.5	5.5	5	4.5	4	4	4.5	4.5	5	5.5	6	6	6	5.5	4.5	4	3
Defuzzified Lower Probability								4.5	5	5.5	6	6	5	5.5	4			4	5	4.5	6	5.5	5.5	5.5	5	4		
Defuzzified Higher Probability								4	4.5	5	5.5	5.5	5.5	5	4.5			4.5	4.5	5	5.5	6	6	6	5.5	4.5		

1978 Hurricane FLOSSIE

	4 Sep	4 Sep	4 Sep	4 Sep	5 Sep	5 Sep	5 Sep	5 Sep	6 Sep	6 Sep	6 Sep	6 Sep	7 Sep	7 Sep	7 Sep	7 Sep	8 Sep	8 Sep	8 Sep	8 Sep	9 Sep	9 Sep	9 Sep	9 Sep	10 Sep
WMO T Class		1	2.5	2.5	2.5	2.5	2.5	2.5	2.5	2.5	2.5	2.5	2.5	2.5	2.5	2.5	2.5	2.5	2.5	1	1				
Defuzzified Lower Probability																									
Defuzzified Higher Probability																									

	10 Sep	10 Sep	10 Sep	11 Sep	11 Sep	11 Sep	11 Sep	12 Sep	12 Sep	12 Sep	12 Sep	13 Sep	13 Sep	13 Sep	13 Sep	14 Sep	14 Sep	14 Sep	14 Sep	15 Sep	15 Sep	15 Sep	15 Sep	16 Sep	16 Sep
WMO T Class	1	1	1	2.5	3	3	3	3.5	4	4	4.5	4.5	4.5	4.5	4	4	4	4	4	4	4	3	3	3	3
Defuzzified Lower Probability						3		4		4.5	4	5	5	5				4.5		4.5	3.5	3			
Defuzzified Higher Probability						3.5		3.5		4	4.5	4.5	4.5	4.5				4		4	4	3.5			

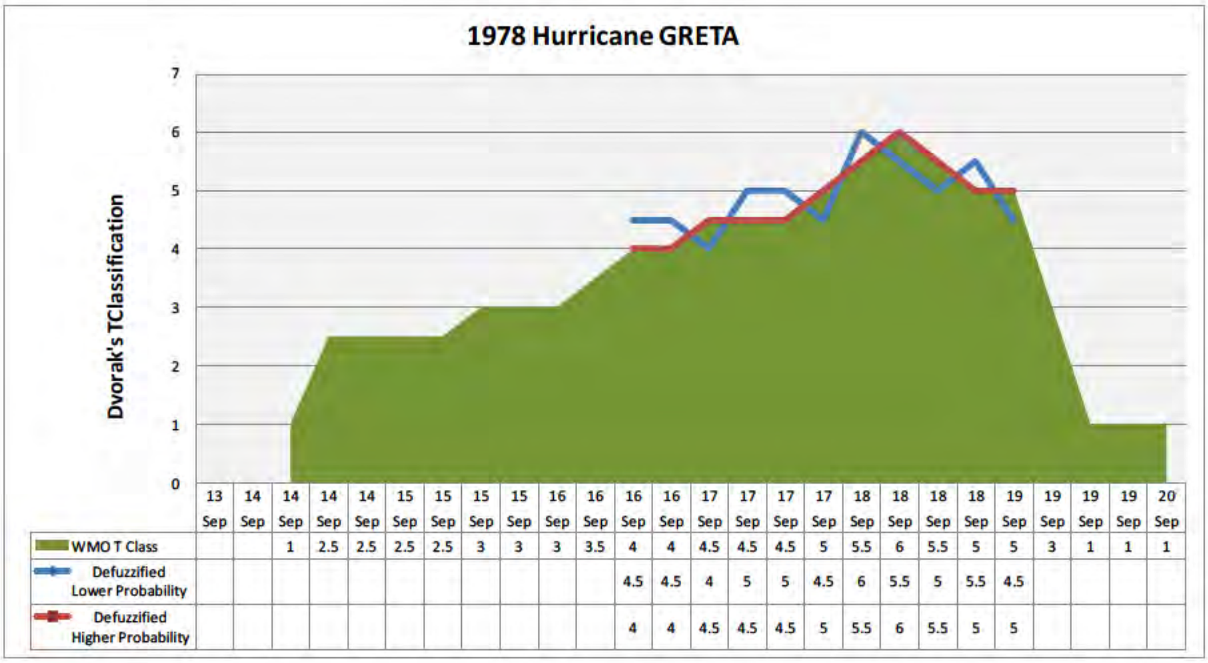
1978 Hurricane GRETA
Dvorak's TClassification
7
6
5
4
3
2
1
0
13 Sep | 14 Sep | 14 Sep | 14 Sep | 14 Sep | 15 Sep | 15 Sep | 15 Sep | 15 Sep | 16 Sep | 16 Sep | 16 Sep | 16 Sep | 17 Sep | 17 Sep | 17 Sep | 17 Sep | 18 Sep | 18 Sep | 18 Sep | 18 Sep | 19 Sep | 19 Sep | 19 Sep | 19 Sep | 20 Sep
WMO T Class | | | 1 | 2.5 | 2.5 | 2.5 | 2.5 | 3 | 3 | 3 | 3.5 | 4 | 4 | 4.5 | 4.5 | 4.5 | 5 | 5.5 | 6 | 5.5 | 5 | 5 | 3 | 1 | 1 | 1
Defuzzified Lower Probability | 4.5 | 4.5 | 4 | 5 | 5 | 4.5 | 6 | 5.5 | 5 | 5.5 | 4.5
Defuzzified Higher Probability | 4 | 4 | 4.5 | 4.5 | 4.5 | 5 | 5.5 | 6 | 5.5 | 5 | 5

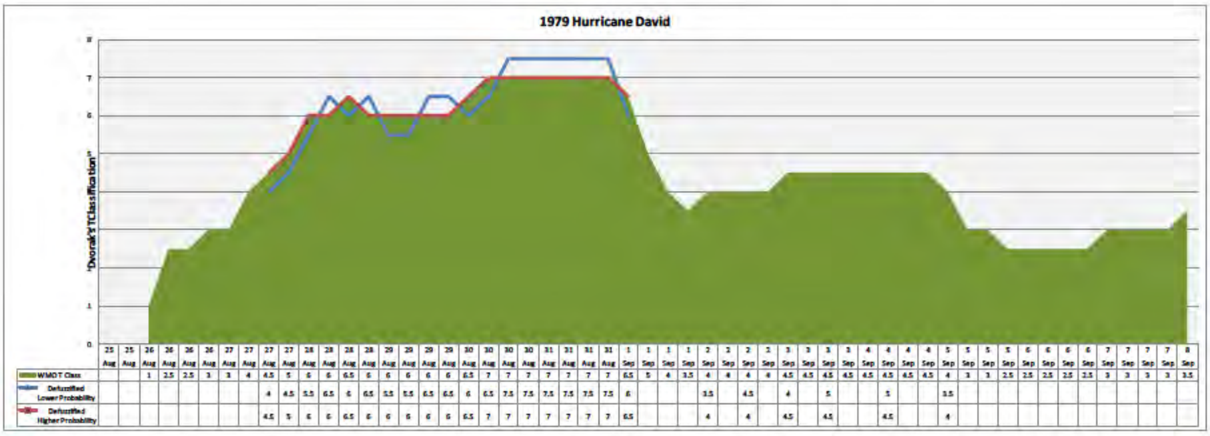
1979 Hurricane David

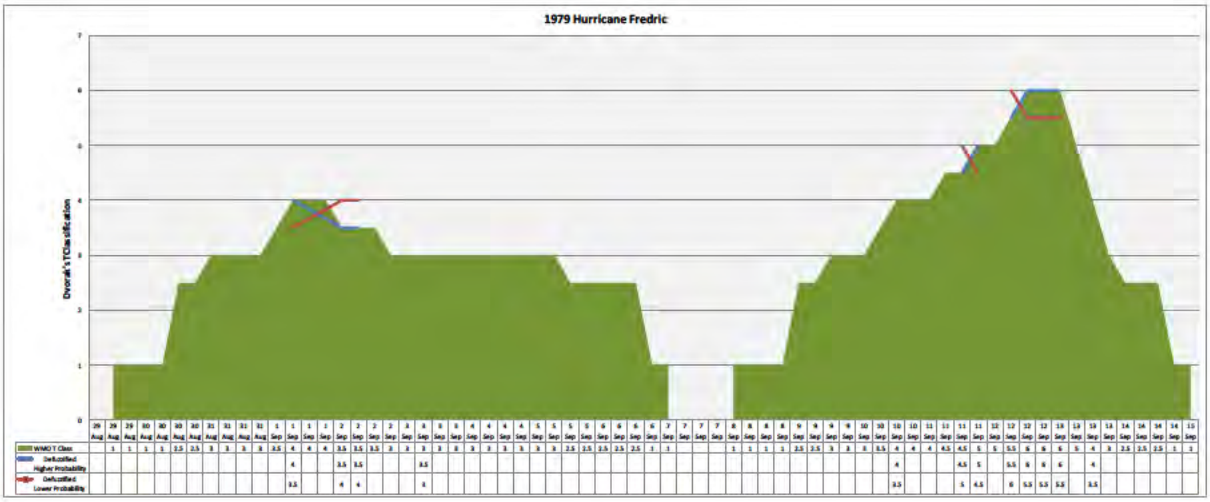
1979 Hurricane Fredric
Dvorak's TC classification
WMO T Class
Defuzzified Higher Probability
Defuzzified Lower Probability

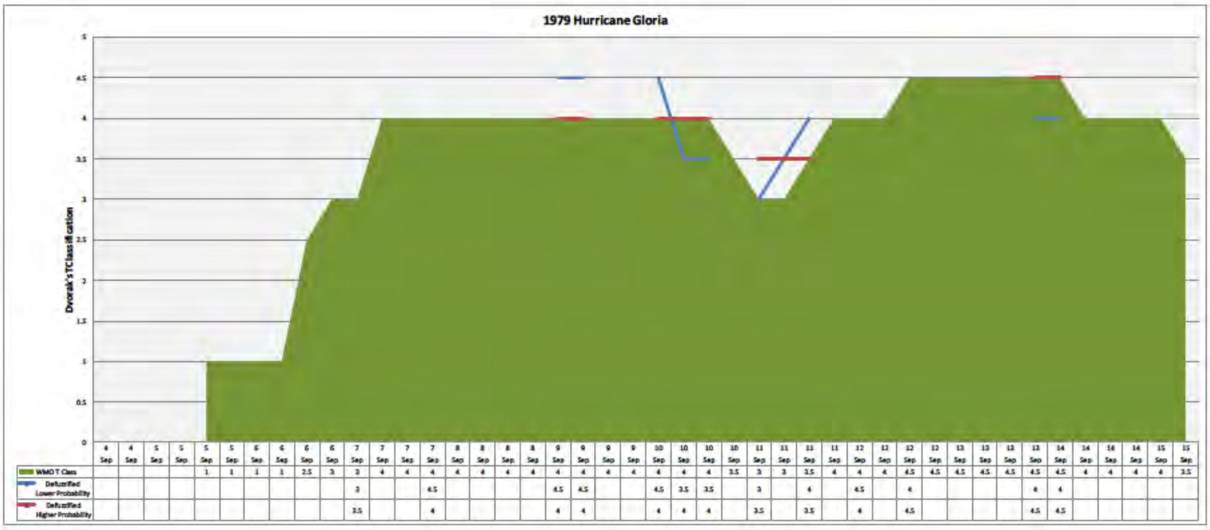
1979 Hurricane Gloria
Dvorak's TC classification
WMO T Class
Defuzzified Lower Probability
Defuzzified Higher Probability

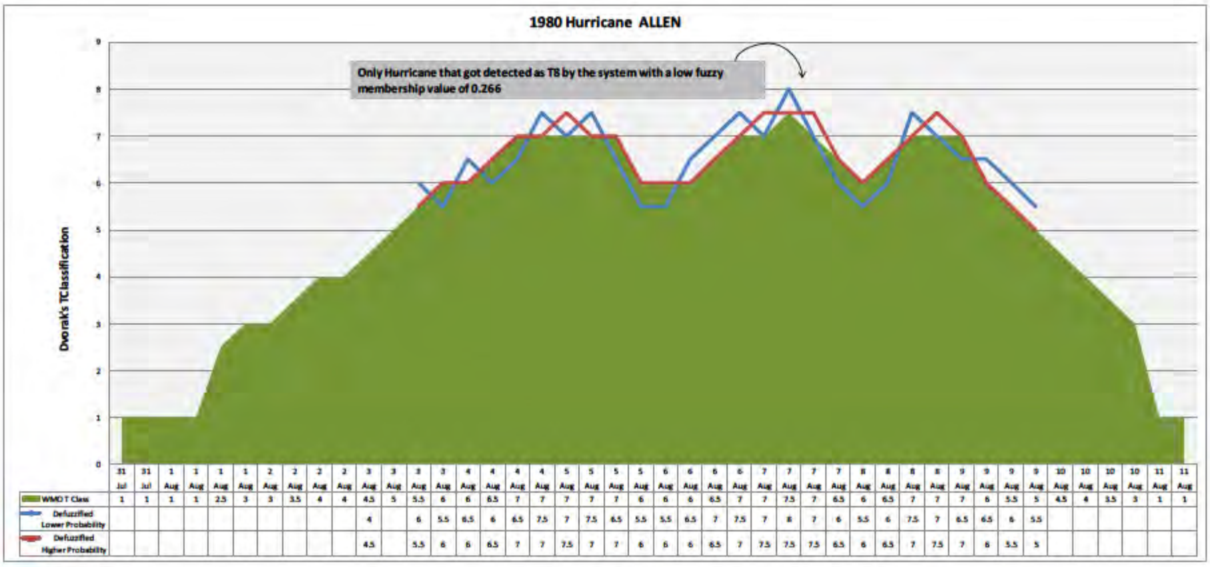
1980 Hurricane ALLEN
Only Hurricane that got detected as T8 by the system with a low fuzzy membership value of 0.266
Dvorak's TC classification
WMO T Class
Defuzzified Lower Probability
Defuzzified Higher Probability

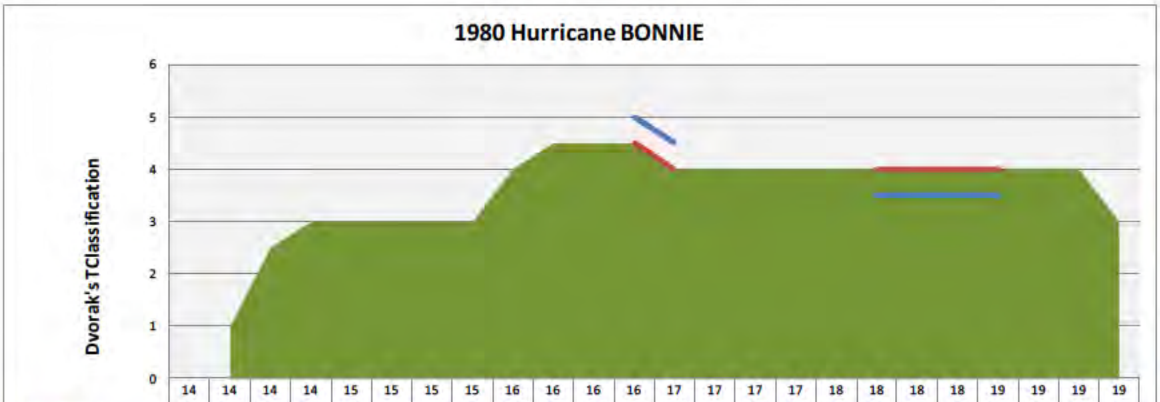

	14 Aug	14 Aug	14 Aug	14 Aug	15 Aug	15 Aug	15 Aug	15 Aug	16 Aug	16 Aug	16 Aug	16 Aug	17 Aug	17 Aug	17 Aug	17 Aug	18 Aug	18 Aug	18 Aug	18 Aug	19 Aug	19 Aug	19 Aug	19 Aug
WMO T Class		1	2.5	3	3	3	3	3	4	4.5	4.5	4.5	4	4	4	4	4	4	4	4	4	4	4	3
Defuzzified Lower Probability												5	4.5		3.5			3.5	3.5	3.5	3.5			
Defuzzified Higher Probability												4.5	4		4			4	4	4	4			

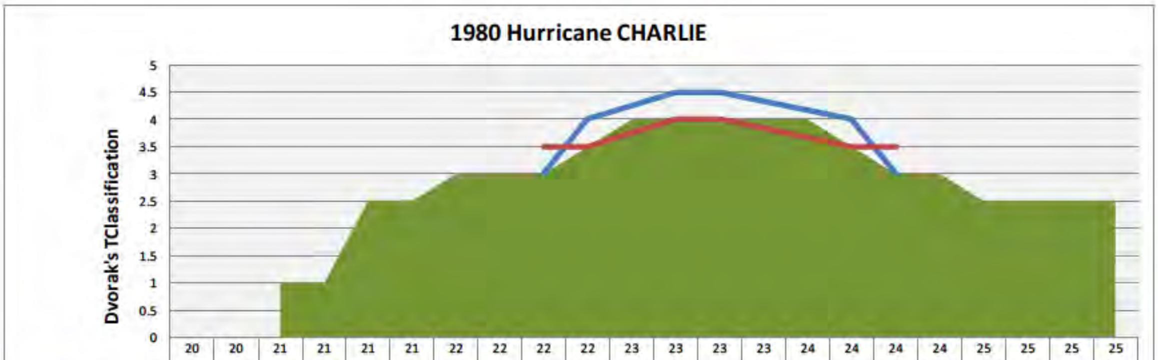

	20 Aug	20 Aug	21 Aug	21 Aug	21 Aug	21 Aug	22 Aug	22 Aug	22 Aug	22 Aug	23 Aug	23 Aug	23 Aug	23 Aug	24 Aug	24 Aug	24 Aug	24 Aug	25 Aug	25 Aug	25 Aug	25 Aug
WMO T Class			1	1	2.5	2.5	3	3	3	3.5	4	4	4	4	4	3.5	3	3	2.5	2.5	2.5	2.5
Defuzzified Lower Probability									3	4		4.5	4.5			4	3					
Defuzzified Higher Probability									3.5	3.5		4	4			3.5	3.5					

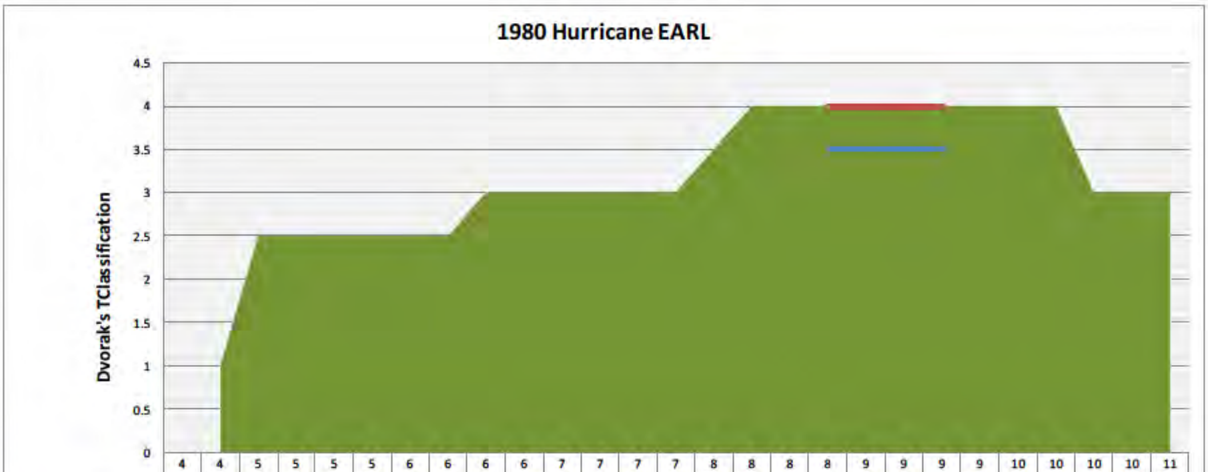

	4 Sep	4 Sep	5 Sep	5 Sep	5 Sep	5 Sep	6 Sep	6 Sep	6 Sep	6 Sep	7 Sep	7 Sep	7 Sep	7 Sep	8 Sep	8 Sep	8 Sep	8 Sep	9 Sep	9 Sep	9 Sep	9 Sep	10 Sep	10 Sep	10 Sep	10 Sep	11 Sep
WMO T Class		1	2.5	2.5	2.5	2.5	2.5	2.5	3	3	3	3	3	3	3.5	4	4	4	4	4	4	4	4	4	3	3	3
Defuzzified Lower Probability																		3.5			3.5		3.5				
Defuzzified Higher Probability																		4			4		4				

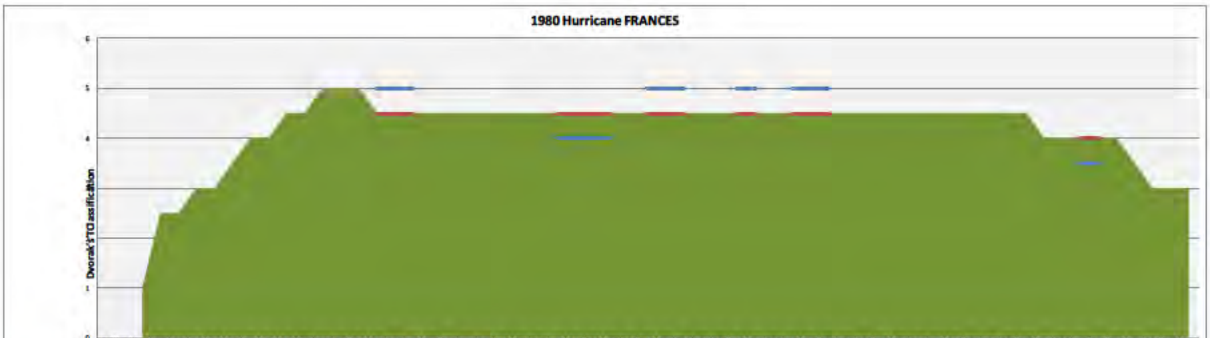

	6 Sep	6 Sep	6 Sep	6 Sep	7 Sep	7 Sep	7 Sep	7 Sep	8 Sep	8 Sep	8 Sep	8 Sep	9 Sep	9 Sep	9 Sep	9 Sep	10 Sep	10 Sep	10 Sep	10 Sep	11 Sep	11 Sep	11 Sep	11 Sep	12 Sep	12 Sep	12 Sep	12 Sep	13 Sep	13 Sep	13 Sep	13 Sep	14 Sep	14 Sep	14 Sep	14 Sep	15 Sep	15 Sep	15 Sep	15 Sep	16 Sep	16 Sep	16 Sep	16 Sep	17 Sep	17 Sep	17 Sep	17 Sep	18 Sep	18 Sep	18 Sep	18 Sep	19 Sep	19 Sep	19 Sep	19 Sep	20 Sep	20 Sep	20 Sep	20 Sep	21 Sep
WMOT Class			1	2.5	2.5	3	3	3.5	4	4	4.5	4.5	5	5	5	4.5	4.5	4.5	4.5	4.5	4.5	4.5	4.5	4.5	4.5	4.5	4.5	4.5	4.5	4.5	4.5	4.5	4.5	4.5	4.5	4.5	4.5	4.5	4.5	4.5	4.5	4.5	4.5	4.5	4.5	4.5	4.5	4.5	4.5	4.5	4.5	4.5	4	4	4	4	4	3.5	3	3	3
Defuzzified Lower Probability										4.5			5.5			5	5	5		4			5			4	4	4	4		5	5	5			5	5		5	5	5				5						4				3.5	3.5			3		
Defuzzified Higher Probability										4			5			4.5	4.5	4.5		4.5			4.5			4.5	4.5	4.5	4.5		4.5	4.5	4.5			4.5	4.5		4.5	4.5	4.5				4.5						4.5				4	4			3.5		

APPENDIX II - Maps of detected hurricanes.

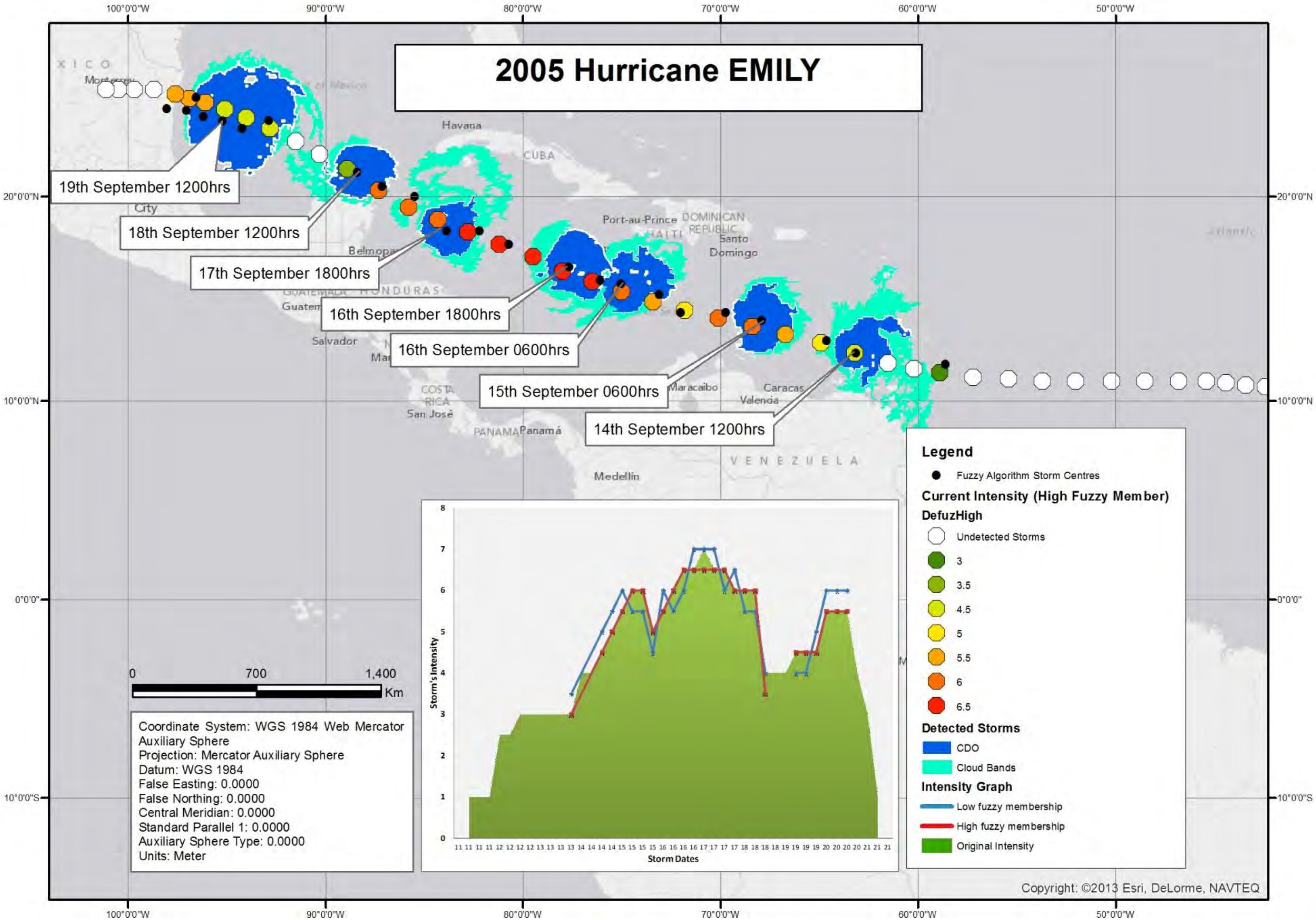

2005 Hurricane EMILY
19th September 1200hrs
18th September 1200hrs
17th September 1800hrs
16th September 1800hrs
16th September 0600hrs
15th September 0600hrs
14th September 1200hrs
Legend
Fuzzy Algorithm Storm Centres
Current Intensity (High Fuzzy Member)
DefuzHigh
Undetected Storms
3
3.5
4.5
5
5.5
6
6.5
Detected Storms
CDO
Cloud Bands
Intensity Graph
Low fuzzy membership
High fuzzy membership
Original Intensity
Storm's Intensity
Storm Dates
0
700
1,400
Km
Coordinate System: WGS 1984 Web Mercator Auxiliary Sphere
Projection: Mercator Auxiliary Sphere
Datum: WGS 1984
False Easting: 0.0000
False Northing: 0.0000
Central Meridian: 0.0000
Standard Parallel 1: 0.0000
Auxiliary Sphere Type: 0.0000
Units: Meter
Copyright: ©2013 Esri, DeLorme, NAVTEQ

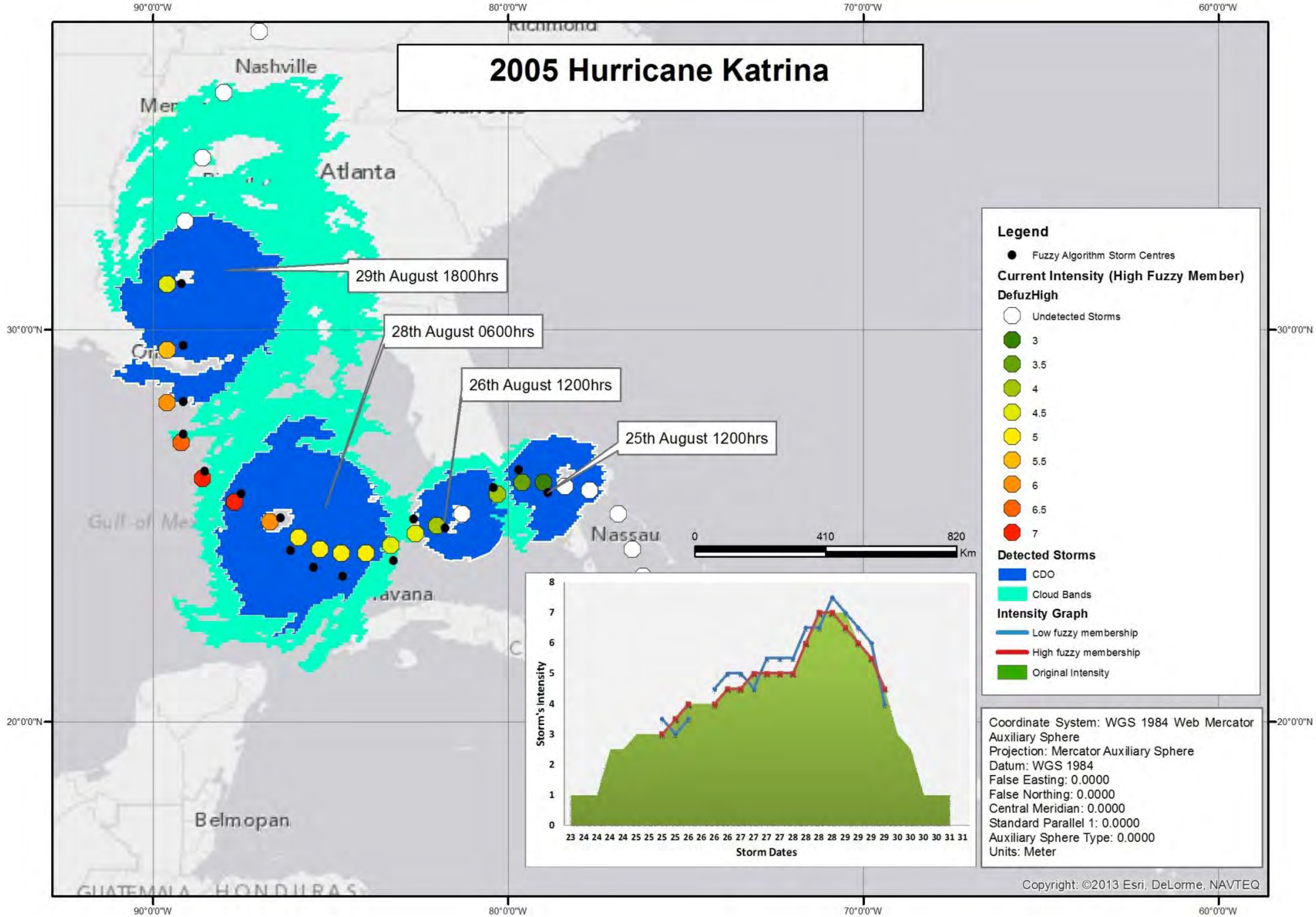
2005 Hurricane Katrina
Nashville
Atlanta
Nassau
Belmopan
29th August 1800hrs
28th August 0600hrs
26th August 1200hrs
25th August 1200hrs
90°0'0"W
80°0'0"W
70°0'0"W
60°0'0"W
30°0'0"N
20°0'0"N
0
410
820
Km
Legend
Fuzzy Algorithm Storm Centres
Current Intensity (High Fuzzy Member)
DefuzHigh
Undetected Storms
3
3.5
4
4.5
5
5.5
6
6.5
7
Detected Storms
CDO
Cloud Bands
Intensity Graph
Low fuzzy membership
High fuzzy membership
Original Intensity
Storm's Intensity
Storm Dates
Coordinate System: WGS 1984 Web Mercator Auxiliary Sphere
Projection: Mercator Auxiliary Sphere
Datum: WGS 1984
False Easting: 0.0000
False Northing: 0.0000
Central Meridian: 0.0000
Standard Parallel 1: 0.0000
Auxiliary Sphere Type: 0.0000
Units: Meter
Copyright: ©2013 Esri, DeLorme, NAVTEQ

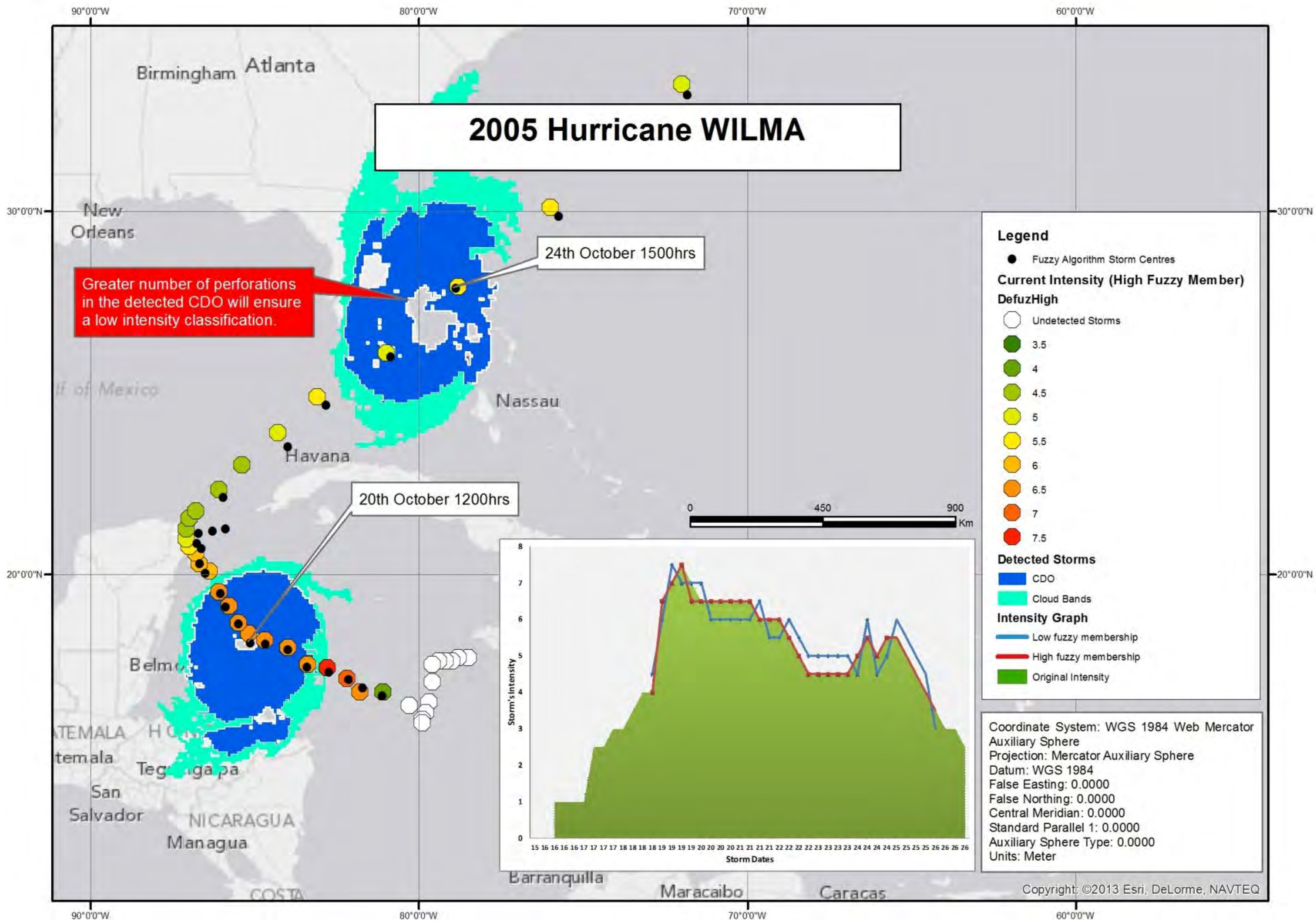

2005 Hurricane WILMA
24th October 1500hrs
Greater number of perforations in the detected CDO will ensure a low intensity classification.
20th October 1200hrs
Legend
Fuzzy Algorithm Storm Centres
Current Intensity (High Fuzzy Member)
DefuzHigh
Undetected Storms
3.5
4
4.5
5
5.5
6
6.5
7
7.5
Detected Storms
CDO
Cloud Bands
Intensity Graph
Low fuzzy membership
High fuzzy membership
Original Intensity
Coordinate System: WGS 1984 Web Mercator Auxiliary Sphere
Projection: Mercator Auxiliary Sphere
Datum: WGS 1984
False Easting: 0.0000
False Northing: 0.0000
Central Meridian: 0.0000
Standard Parallel 1: 0.0000
Auxiliary Sphere Type: 0.0000
Units: Meter
Copyright: ©2013 Esri, DeLorme, NAVTEQ
Storm's Intensity
Storm Dates
0
450
900
Km
90°0'0"W
80°0'0"W
70°0'0"W
60°0'0"W
30°0'0"N
20°0'0"N
Birmingham
Atlanta
New Orleans
Nassau
Havana
Belmo
Teg ga pa
San Salvador
NICARAGUA
Managua
Barranquilla
Maracaibo
Caracas

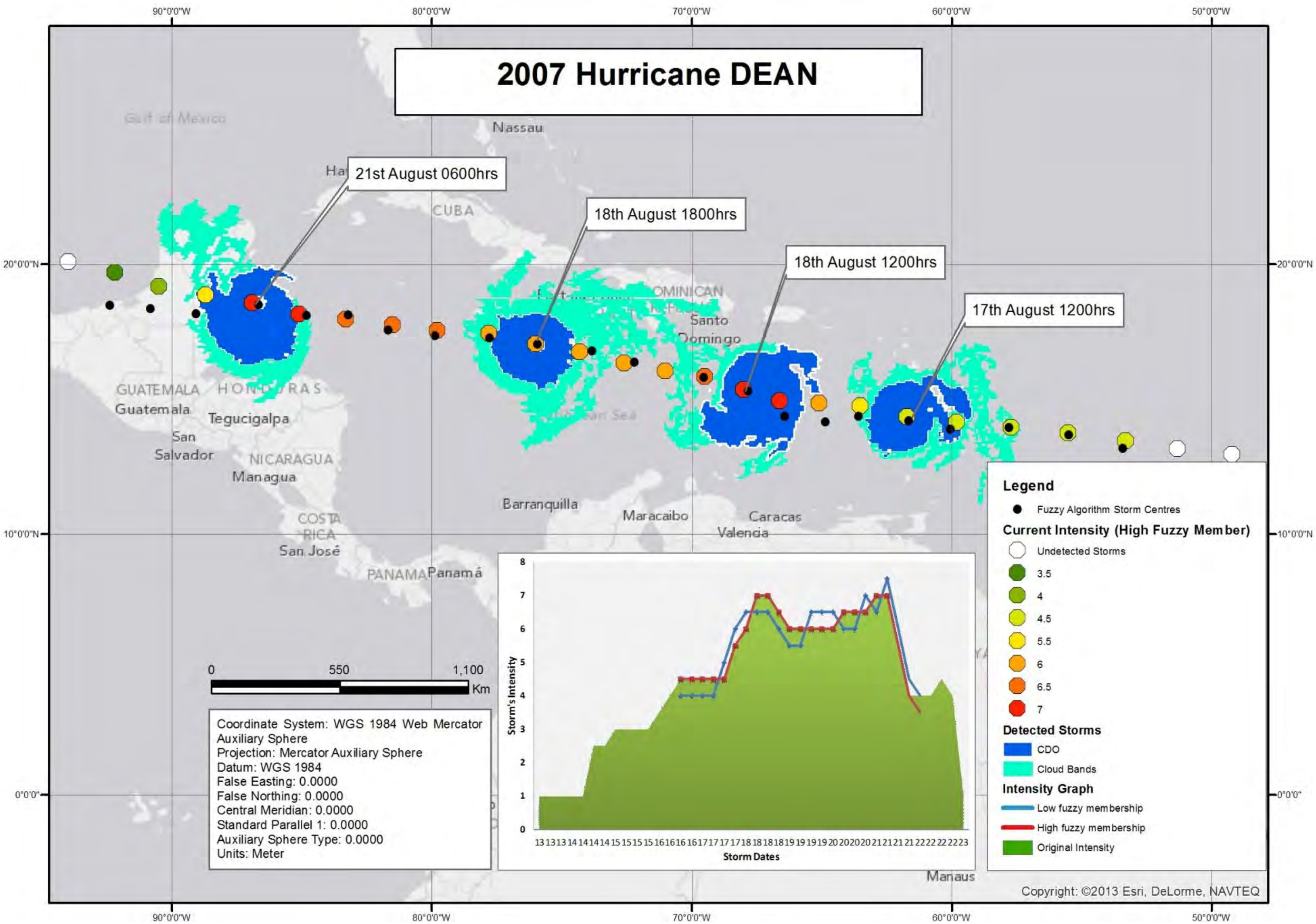
2007 Hurricane DEAN
21st August 0600hrs
18th August 1800hrs
18th August 1200hrs
17th August 1200hrs
Nassau
CUBA
Santo
Domingo
GUATEMALA
HONDURAS
Guatemala
Tegucigalpa
San
Salvador
NICARAGUA
Managua
COSTA
RICA
San José
PANAMA
Panamá
Barranquilla
Maracaibo
Caracas
Valencia
Manaus
90°0'0"W
80°0'0"W
70°0'0"W
60°0'0"W
50°0'0"W
20°0'0"N
10°0'0"N
0°0'0"
0
550
1,100
Km
Coordinate System: WGS 1984 Web Mercator Auxiliary Sphere
Projection: Mercator Auxiliary Sphere
Datum: WGS 1984
False Easting: 0.0000
False Northing: 0.0000
Central Meridian: 0.0000
Standard Parallel 1: 0.0000
Auxiliary Sphere Type: 0.0000
Units: Meter
Storm's Intensity
Storm Dates
Legend
Fuzzy Algorithm Storm Centres
Current Intensity (High Fuzzy Member)
Undetected Storms
3.5
4
4.5
5.5
6
6.5
7
Detected Storms
CDO
Cloud Bands
Intensity Graph
Low fuzzy membership
High fuzzy membership
Original Intensity
Copyright: ©2013 Esri, DeLorme, NAVTEQ

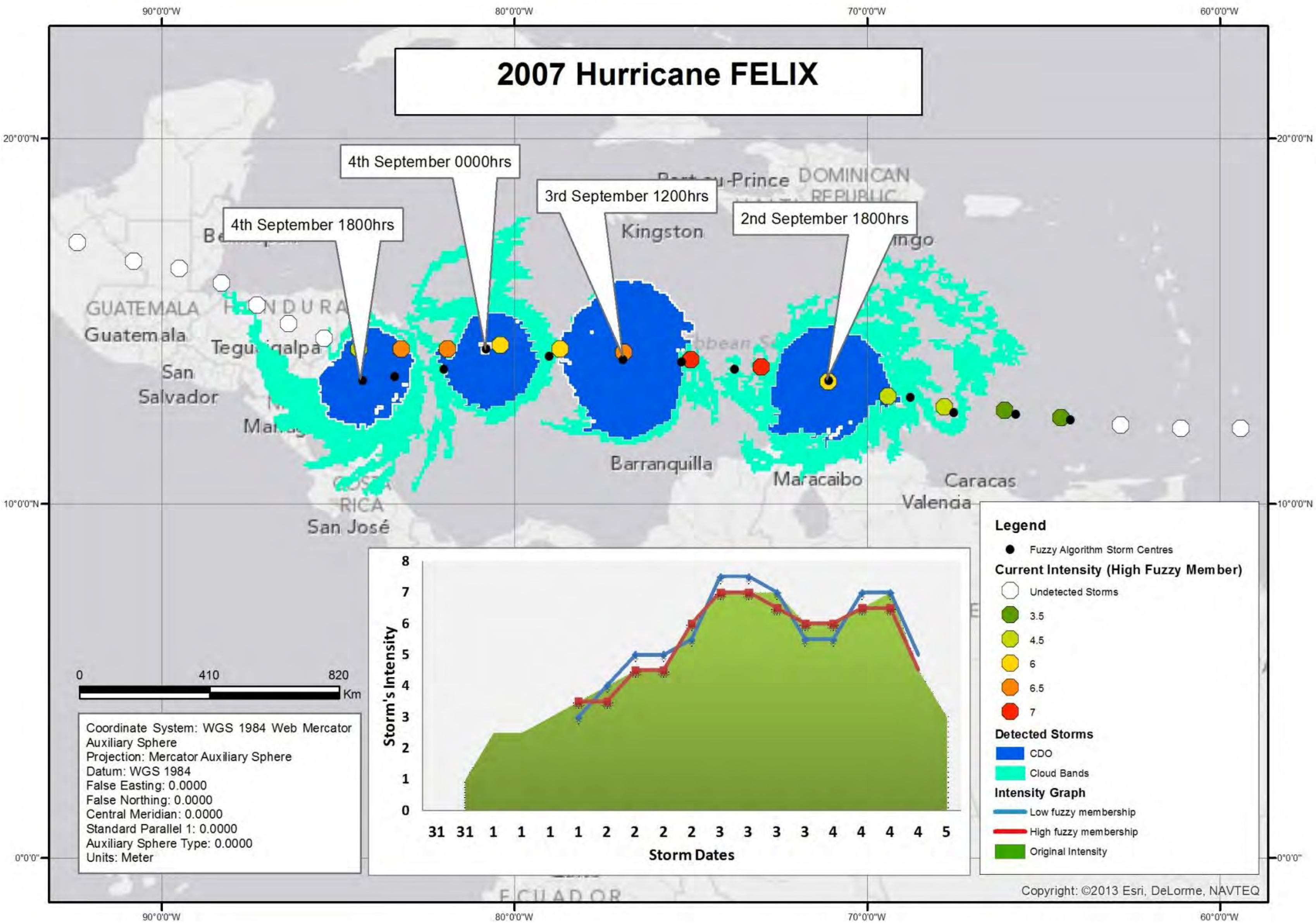

2007 Hurricane FELIX
4th September 0000hrs
3rd September 1200hrs
4th September 1800hrs
2nd September 1800hrs
GUATEMALA
Guatemala
Tegucigalpa
San Salvador
San José
Kingston
Barranquilla
Maracaibo
Caracas
Valencia
DOMINICAN REPUBLIC
ECUADOR
90°0'0"W
80°0'0"W
70°0'0"W
60°0'0"W
20°0'0"N
10°0'0"N
0°0'0"
0
410
820
Km
Coordinate System: WGS 1984 Web Mercator Auxiliary Sphere
Projection: Mercator Auxiliary Sphere
Datum: WGS 1984
False Easting: 0.0000
False Northing: 0.0000
Central Meridian: 0.0000
Standard Parallel 1: 0.0000
Auxiliary Sphere Type: 0.0000
Units: Meter
Storm's Intensity
8
7
6
5
4
3
2
1
0
31 31 1 1 1 1 2 2 2 2 3 3 3 3 4 4 4 4 5
Storm Dates
Legend
Fuzzy Algorithm Storm Centres
Current Intensity (High Fuzzy Member)
Undetected Storms
3.5
4.5
6
6.5
7
Detected Storms
CDO
Cloud Bands
Intensity Graph
Low fuzzy membership
High fuzzy membership
Original Intensity
Copyright: ©2013 Esri, DeLorme, NAVTEQ

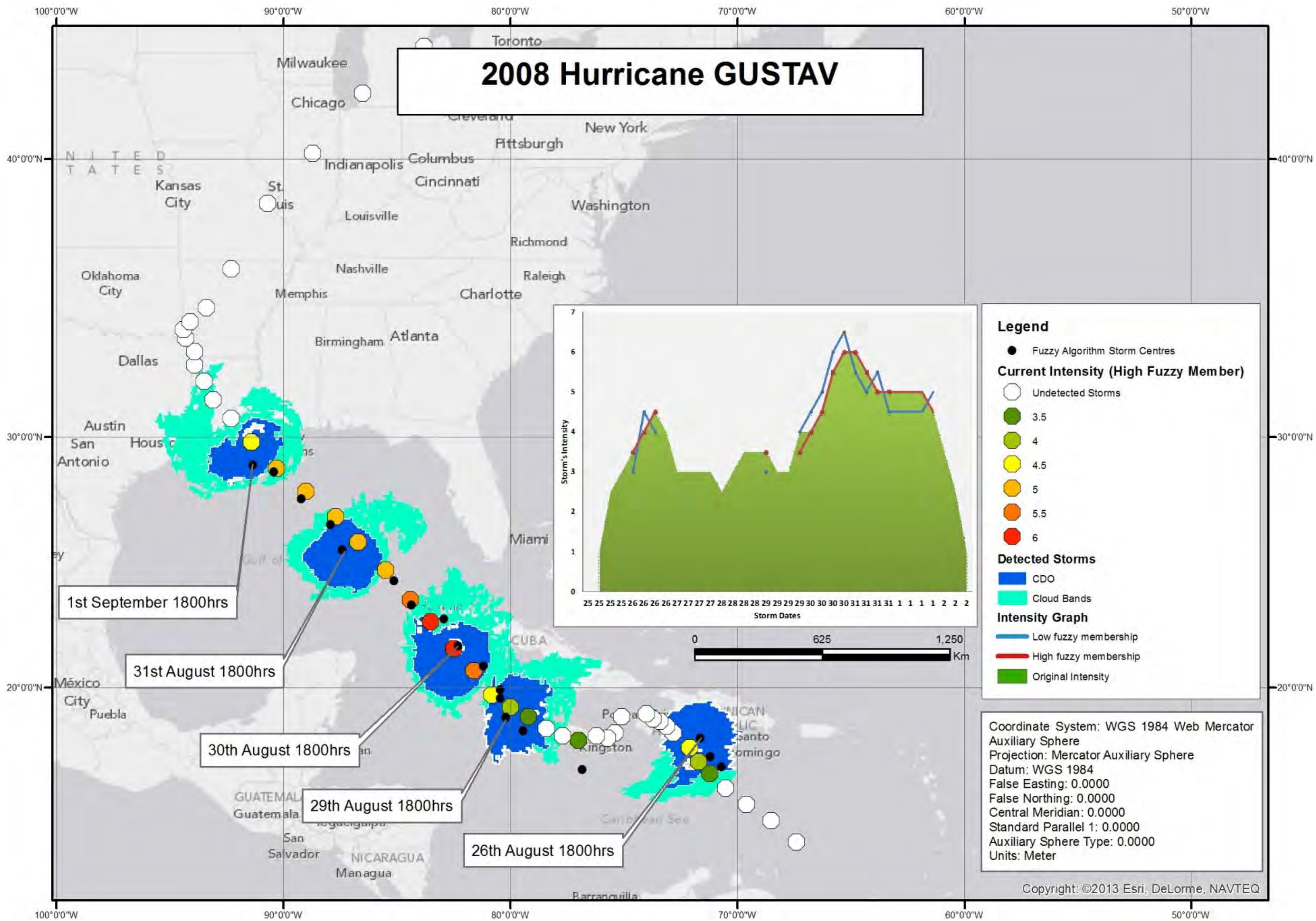
2008 Hurricane GUSTAV
1st September 1800hrs
31st August 1800hrs
30th August 1800hrs
29th August 1800hrs
26th August 1800hrs
Legend
Fuzzy Algorithm Storm Centres
Current Intensity (High Fuzzy Member)
Undetected Storms
3.5
4
4.5
5
5.5
6
Detected Storms
CDO
Cloud Bands
Intensity Graph
Low fuzzy membership
High fuzzy membership
Original Intensity
Storm's Intensity
Storm Dates
0 625 1,250 Km
Coordinate System: WGS 1984 Web Mercator Auxiliary Sphere
Projection: Mercator Auxiliary Sphere
Datum: WGS 1984
False Easting: 0.0000
False Northing: 0.0000
Central Meridian: 0.0000
Standard Parallel 1: 0.0000
Auxiliary Sphere Type: 0.0000
Units: Meter
Copyright: ©2013 Esri, DeLorme, NAVTEQ

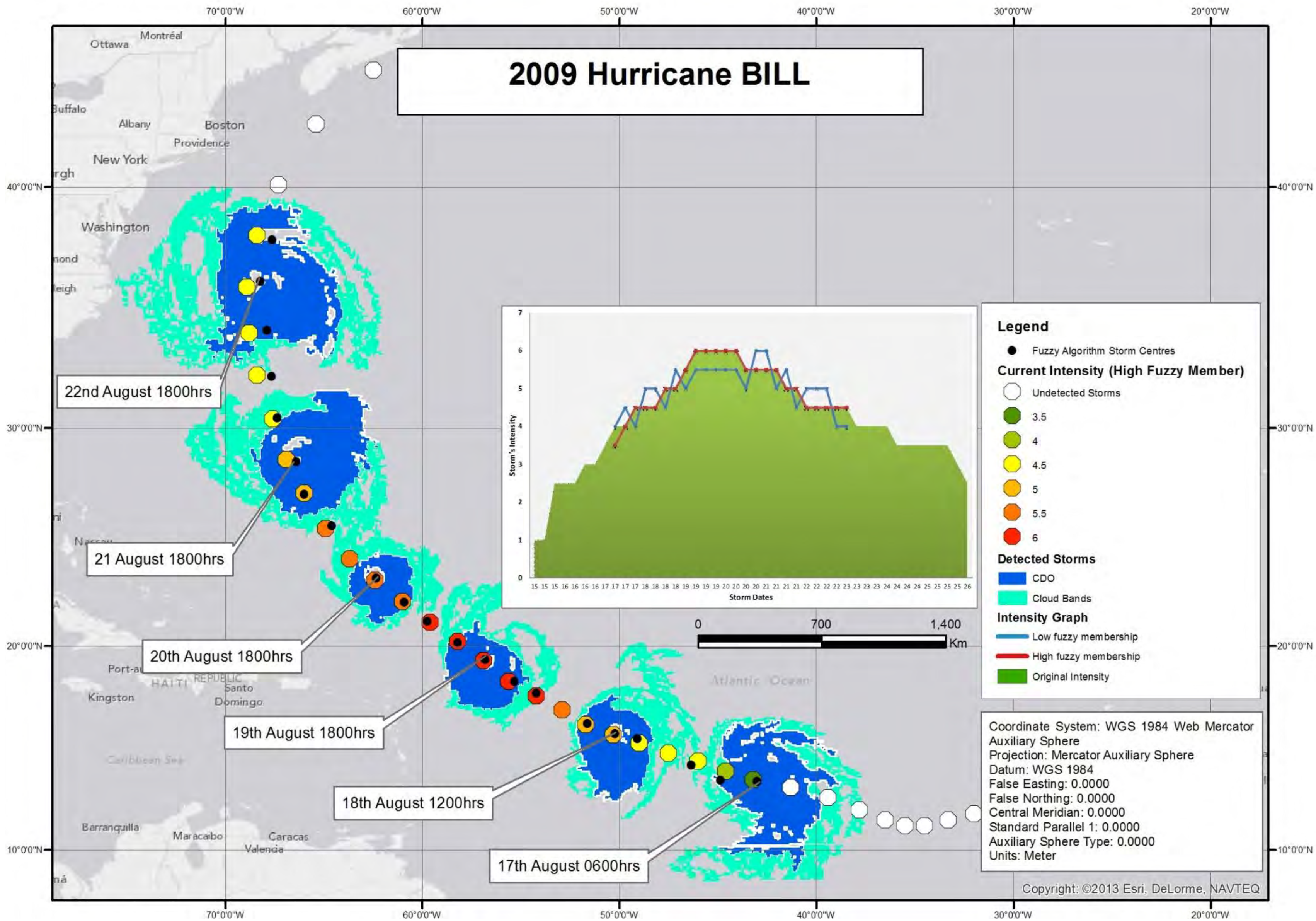
2009 Hurricane BILL
22nd August 1800hrs
21 August 1800hrs
20th August 1800hrs
19th August 1800hrs
18th August 1200hrs
17th August 0600hrs
Legend
Fuzzy Algorithm Storm Centres
Current Intensity (High Fuzzy Member)
Undetected Storms
3.5
4
4.5
5
5.5
6
Detected Storms
CDO
Cloud Bands
Intensity Graph
Low fuzzy membership
High fuzzy membership
Original Intensity
Storm's Intensity
Storm Dates
0
700
1,400
Km
Coordinate System: WGS 1984 Web Mercator Auxiliary Sphere
Projection: Mercator Auxiliary Sphere
Datum: WGS 1984
False Easting: 0.0000
False Northing: 0.0000
Central Meridian: 0.0000
Standard Parallel 1: 0.0000
Auxiliary Sphere Type: 0.0000
Units: Meter
Copyright: ©2013 Esri, DeLorme, NAVTEQ
Atlantic Ocean
70°0'0"W
60°0'0"W
50°0'0"W
40°0'0"W
30°0'0"W
20°0'0"W
40°0'0"N
30°0'0"N
20°0'0"N
10°0'0"N
Montréal
Ottawa
Buffalo
Albany
Boston
Providence
New York
Washington
Kingston
Santo Domingo
Barranquilla
Maracaibo
Caracas
Valencia

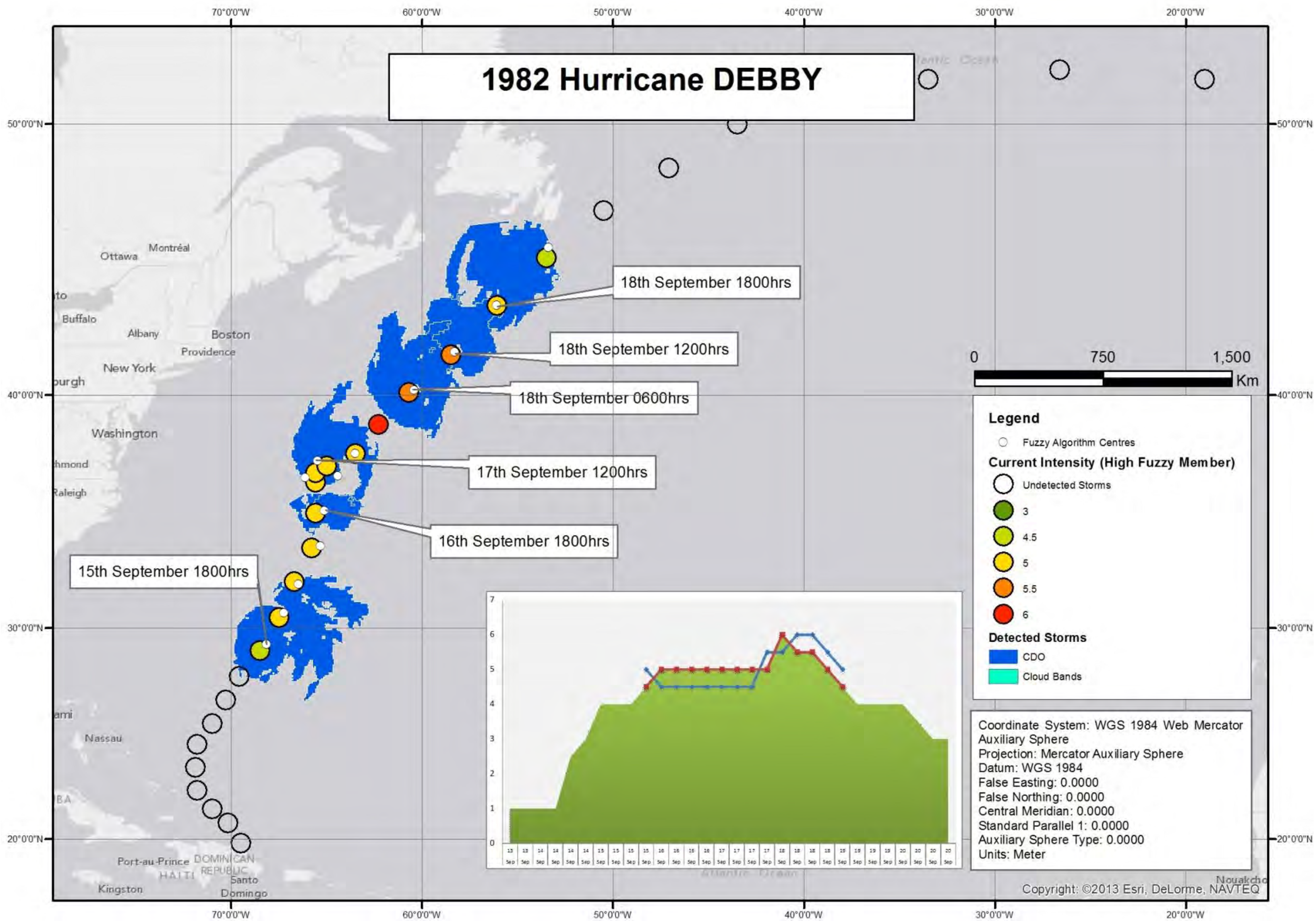
1982 Hurricane DEBBY
18th September 1800hrs
18th September 1200hrs
18th September 0600hrs
17th September 1200hrs
16th September 1800hrs
15th September 1800hrs
0
750
1,500
Km
Legend
Fuzzy Algorithm Centres
Current Intensity (High Fuzzy Member)
Undetected Storms
3
4.5
5
5.5
6
Detected Storms
CDO
Cloud Bands
Coordinate System: WGS 1984 Web Mercator Auxiliary Sphere
Projection: Mercator Auxiliary Sphere
Datum: WGS 1984
False Easting: 0.0000
False Northing: 0.0000
Central Meridian: 0.0000
Standard Parallel 1: 0.0000
Auxiliary Sphere Type: 0.0000
Units: Meter
Copyright: ©2013 Esri, DeLorme, NAVTEQ
70°0'0"W
60°0'0"W
50°0'0"W
40°0'0"W
30°0'0"W
20°0'0"W
50°0'0"N
40°0'0"N
30°0'0"N
20°0'0"N
Ottawa
Montréal
Buffalo
Albany
Boston
Providence
New York
Washington
Raleigh
Nassau
Port-au-Prince
HAITI
DOMINICAN REPUBLIC
Santo Domingo
Kingston

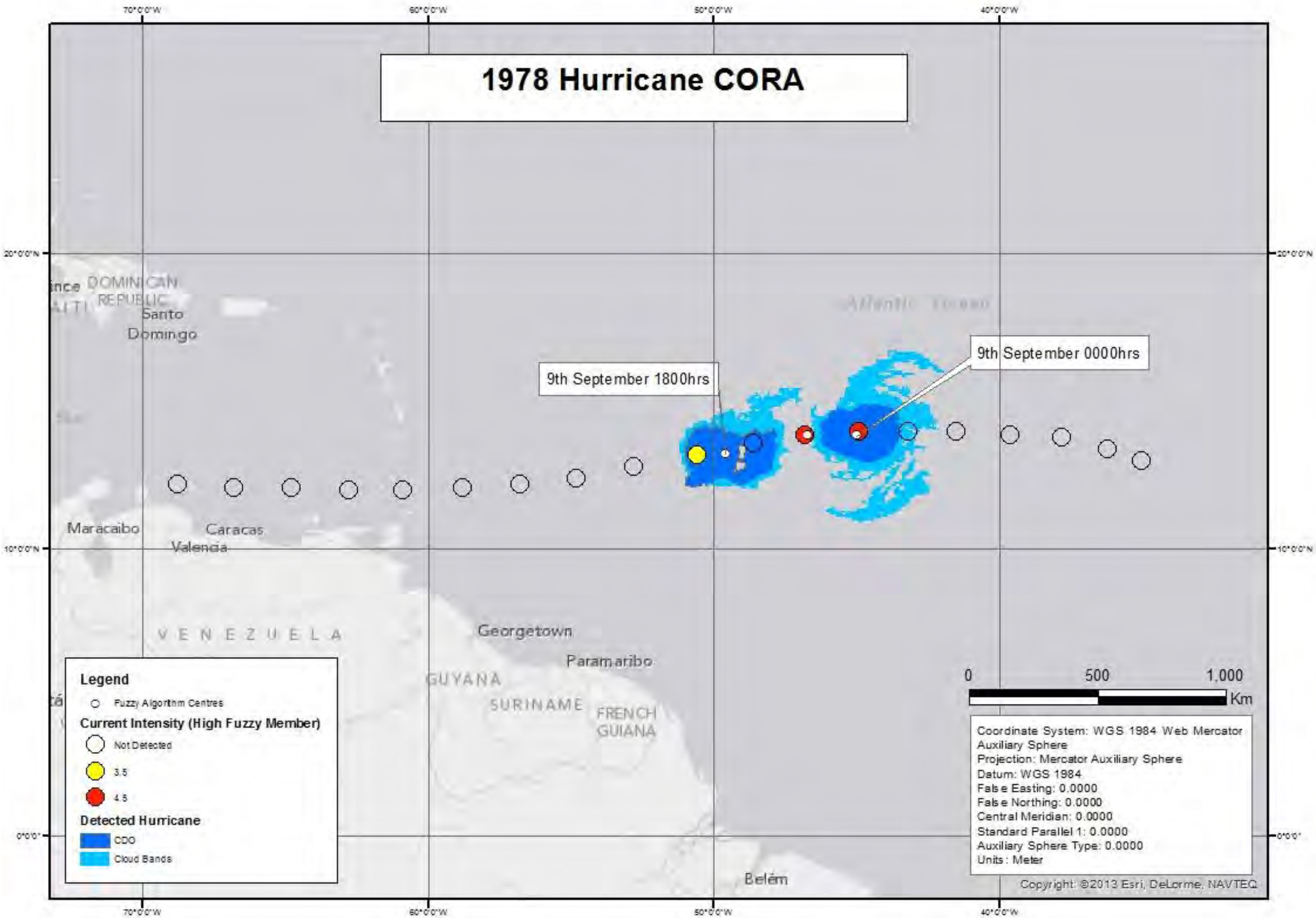

1978 Hurricane CORA
9th September 1800hrs
9th September 0000hrs
Atlantic Ocean
DOMINICAN
REPUBLIC
Santo
Domingo
Maracaibo
Caracas
Valencia
VENEZUELA
Georgetown
Paramaribo
GUYANA
SURINAME
FRENCH
GUIANA
Belém
Legend
Fuzzy Algorithm Centres
Current Intensity (High Fuzzy Member)
Not Detected
3.5
4.5
Detected Hurricane
CDO
Cloud Bands
0
500
1,000
Km
Coordinate System: WGS 1984 Web Mercator Auxiliary Sphere
Projection: Mercator Auxiliary Sphere
Datum: WGS 1984
False Easting: 0.0000
False Northing: 0.0000
Central Meridian: 0.0000
Standard Parallel 1: 0.0000
Auxiliary Sphere Type: 0.0000
Units: Meter
Copyright: ©2013 Esri, DeLorme, NAVTEQ

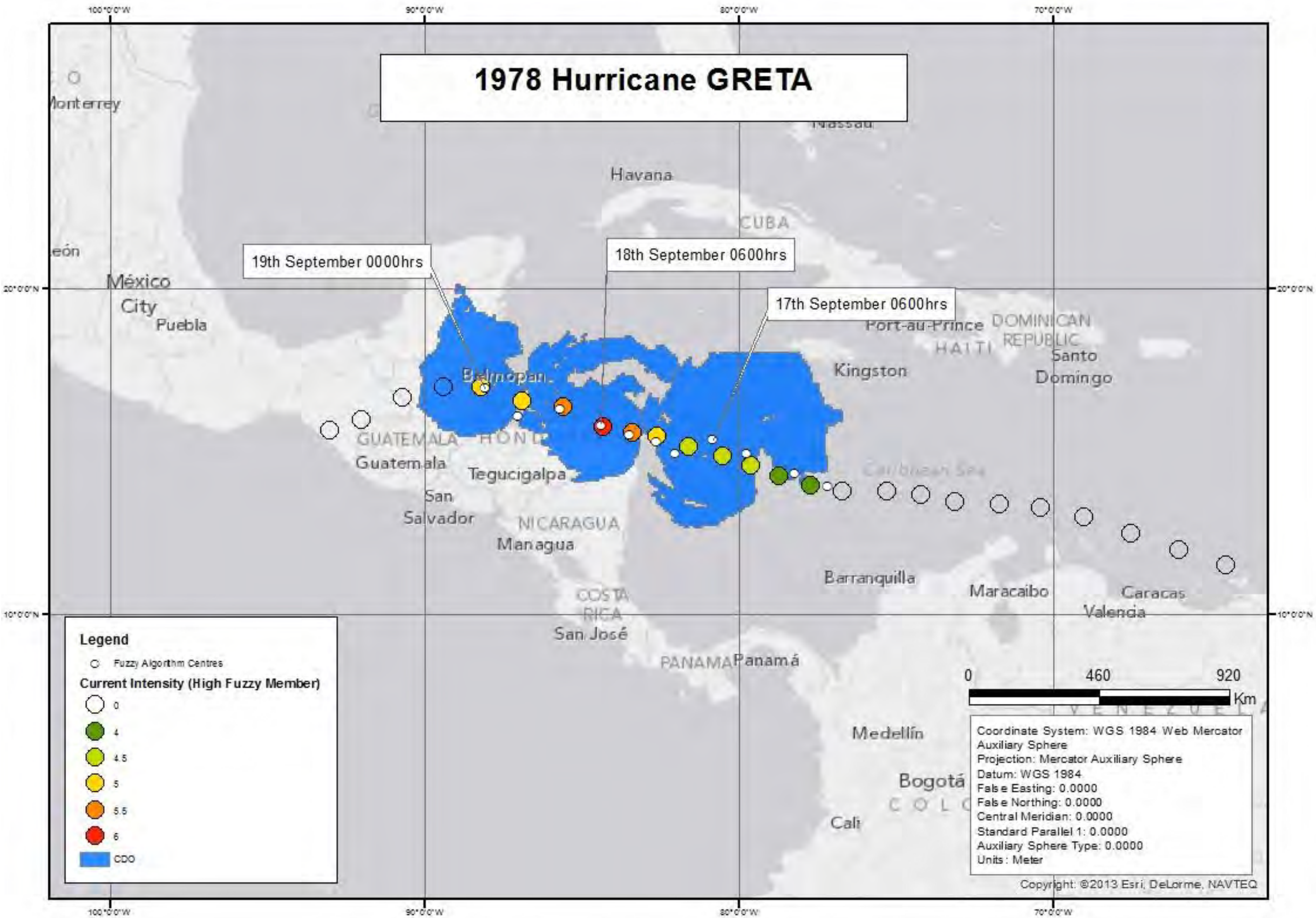
1978 Hurricane GRETA
19th September 0000hrs
18th September 0600hrs
17th September 0600hrs
Legend
Fuzzy Algorithm Centres
Current Intensity (High Fuzzy Member)
0
4
4.5
5
5.5
6
CDO
0
460
920
Km
Coordinate System: WGS 1984 Web Mercator Auxiliary Sphere
Projection: Mercator Auxiliary Sphere
Datum: WGS 1984
False Easting: 0.0000
False Northing: 0.0000
Central Meridian: 0.0000
Standard Parallel 1: 0.0000
Auxiliary Sphere Type: 0.0000
Units: Meter
Copyright: ©2013 Esri, DeLorme, NAVTEQ

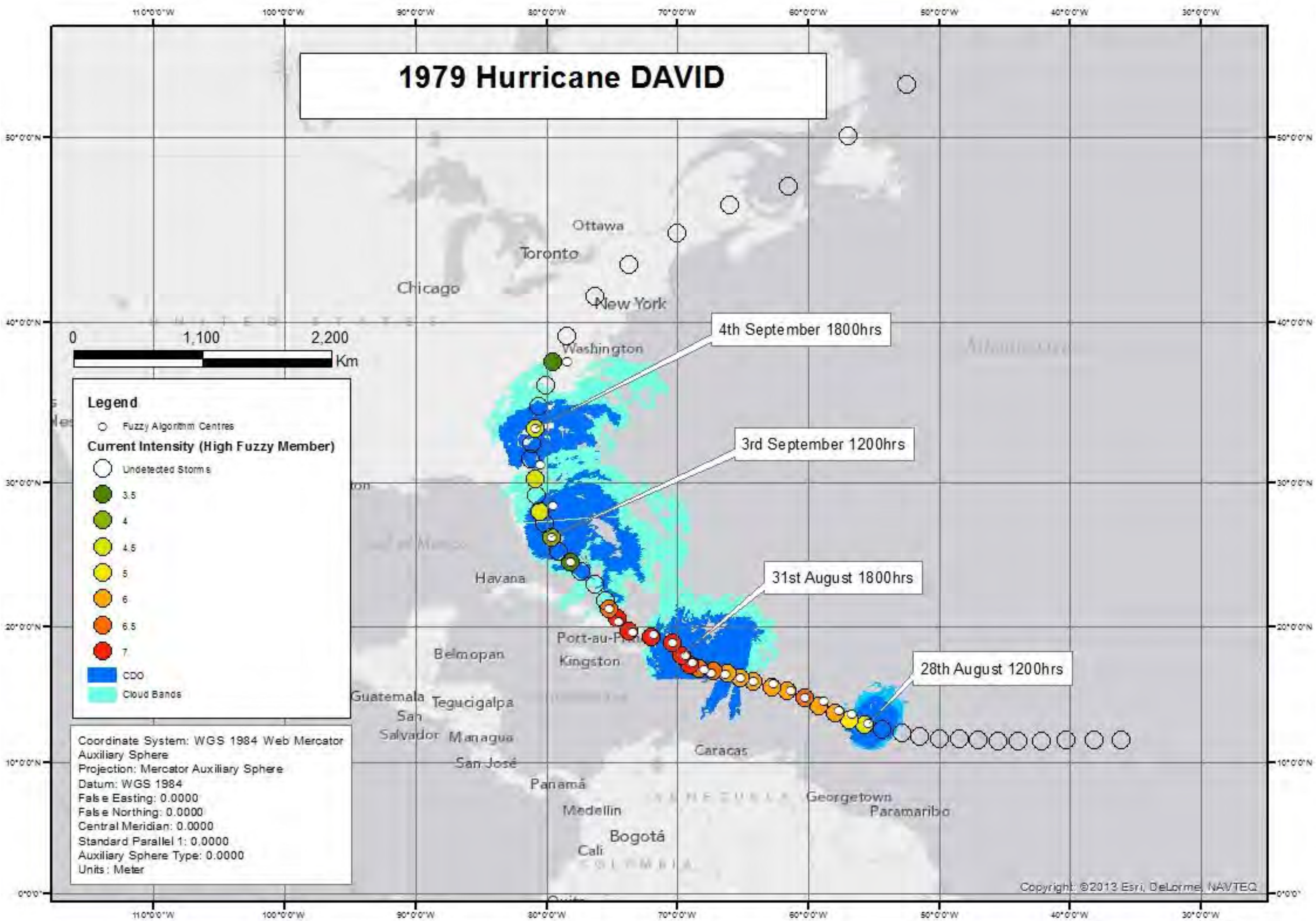
1979 Hurricane DAVID
4th September 1800hrs
3rd September 1200hrs
31st August 1800hrs
28th August 1200hrs
0
1,100
2,200
Km
Legend
Fuzzy Algorithm Centres
Current Intensity (High Fuzzy Member)
Undetected Storms
3.5
4
4.5
5
6
6.5
7
CDO
Cloud Bands
Coordinate System: WGS 1984 Web Mercator Auxiliary Sphere
Projection: Mercator Auxiliary Sphere
Datum: WGS 1984
False Easting: 0.0000
False Northing: 0.0000
Central Meridian: 0.0000
Standard Parallel 1: 0.0000
Auxiliary Sphere Type: 0.0000
Units: Meter
Copyright: ©2013 Esri, DeLorme, NAVTEQ
Ottawa
Toronto
Chicago
New York
Washington
Havana
Port-au-Prince
Kingston
Belmopan
Guatemala
Tegucigalpa
San Salvador
Managua
San José
Panamá
Caracas
Georgetown
Paramaribo
Medellín
Bogotá
Cali

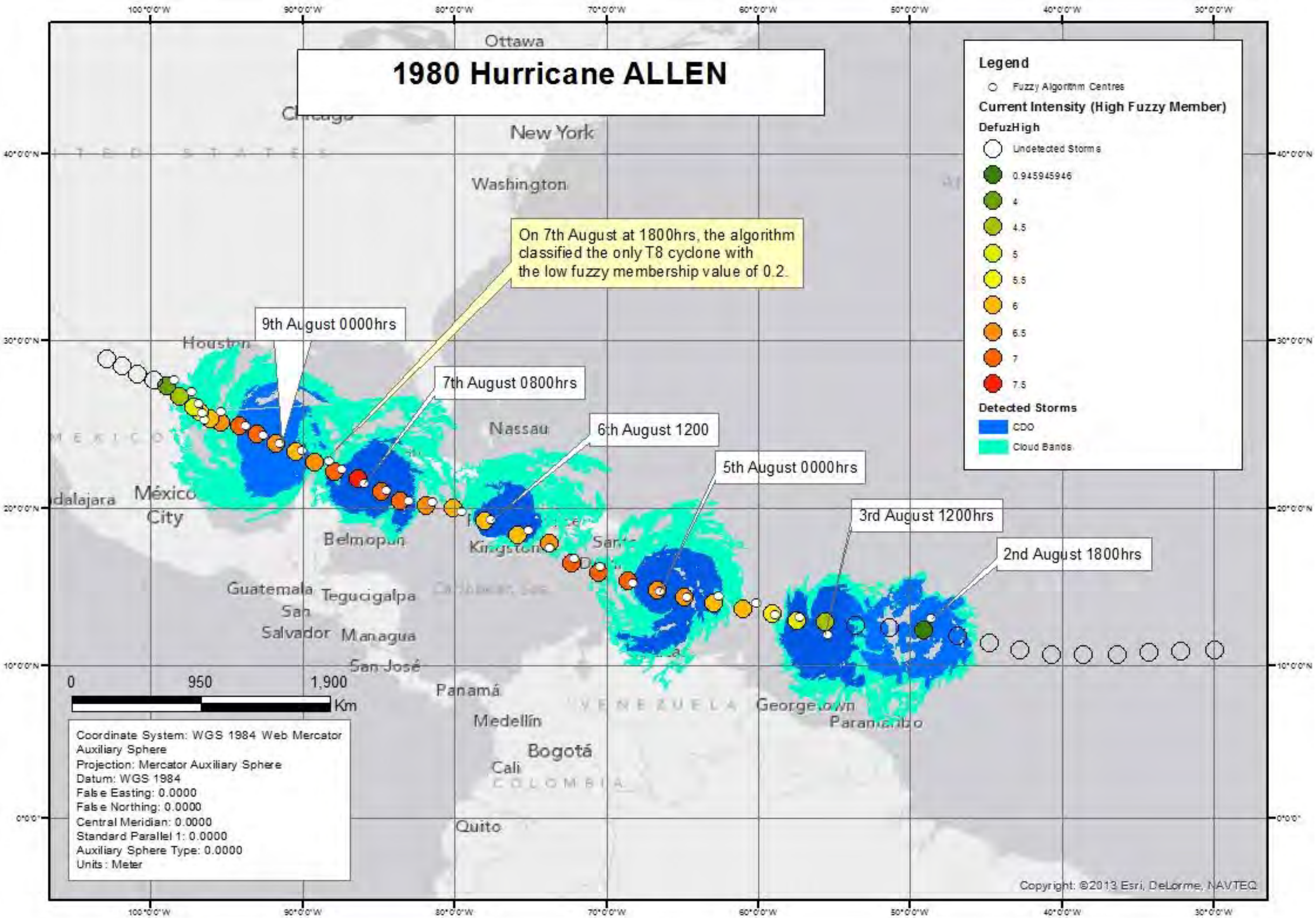
1980 Hurricane ALLEN
Legend
Fuzzy Algorithm Centres
Current Intensity (High Fuzzy Member)
DefuzHigh
Undetected Storms
0.945945946
4
4.5
5
5.5
6
6.5
7
7.5
Detected Storms
CDO
Cloud Bands
On 7th August at 1800hrs, the algorithm classified the only T8 cyclone with the low fuzzy membership value of 0.2.
9th August 0000hrs
7th August 0800hrs
6th August 1200
5th August 0000hrs
3rd August 1200hrs
2nd August 1800hrs
0
950
1,900
Km
Coordinate System: WGS 1984 Web Mercator Auxiliary Sphere
Projection: Mercator Auxiliary Sphere
Datum: WGS 1984
False Easting: 0.0000
False Northing: 0.0000
Central Meridian: 0.0000
Standard Parallel 1: 0.0000
Auxiliary Sphere Type: 0.0000
Units: Meter
Copyright: ©2013 Esri, DeLorme, NAVTEQ

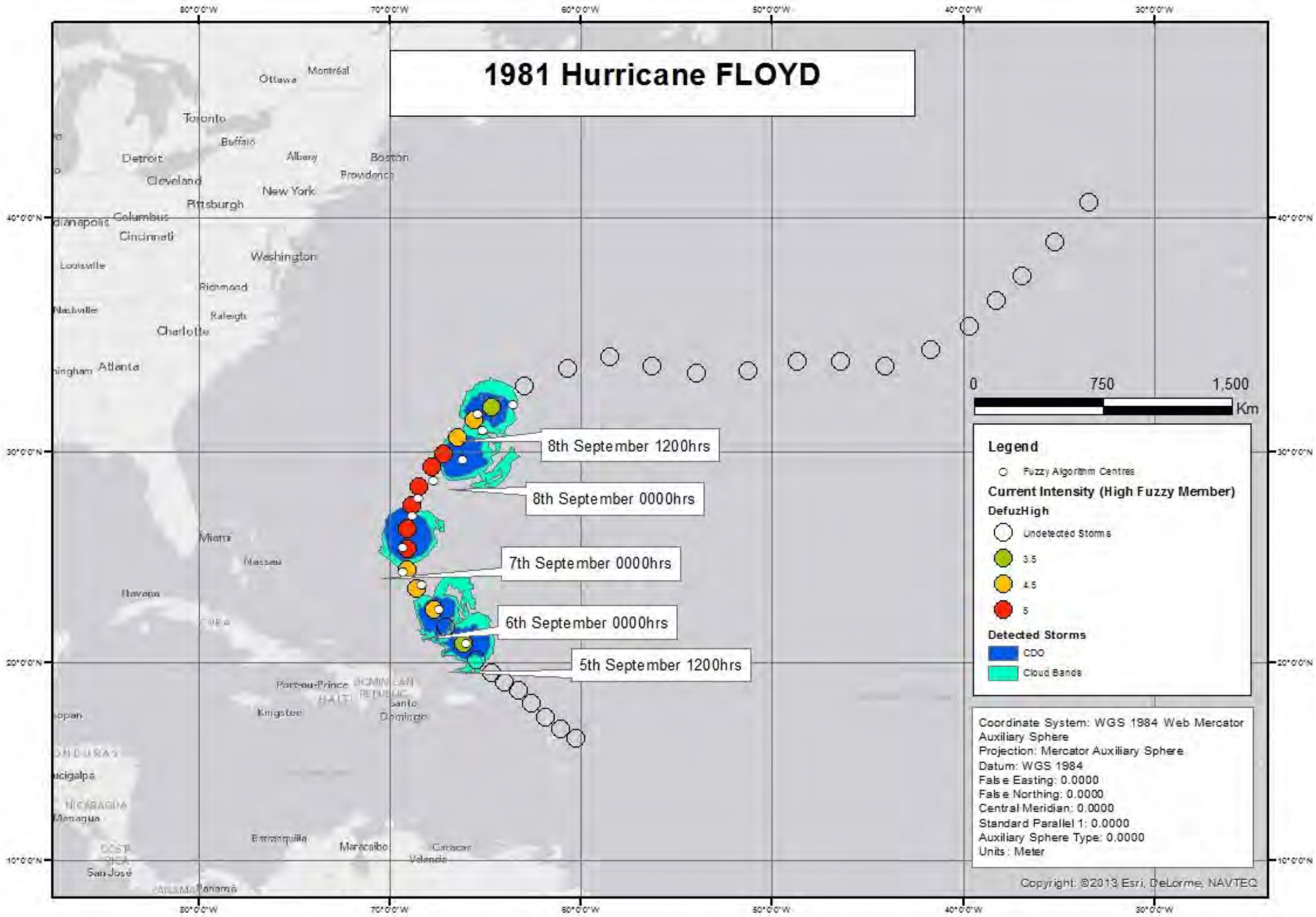

1981 Hurricane FLOYD
8th September 1200hrs
8th September 0000hrs
7th September 0000hrs
6th September 0000hrs
5th September 1200hrs
0
750
1,500
Km
Legend
Fuzzy Algorithm Centres
Current Intensity (High Fuzzy Member)
DefuzHigh
Undetected Storms
3.5
4.5
5
Detected Storms
CDO
Cloud Bands
Coordinate System: WGS 1984 Web Mercator Auxiliary Sphere
Projection: Mercator Auxiliary Sphere
Datum: WGS 1984
False Easting: 0.0000
False Northing: 0.0000
Central Meridian: 0.0000
Standard Parallel 1: 0.0000
Auxiliary Sphere Type: 0.0000
Units: Meter
Copyright: ©2013 Esri, DeLorme, NAVTEQ

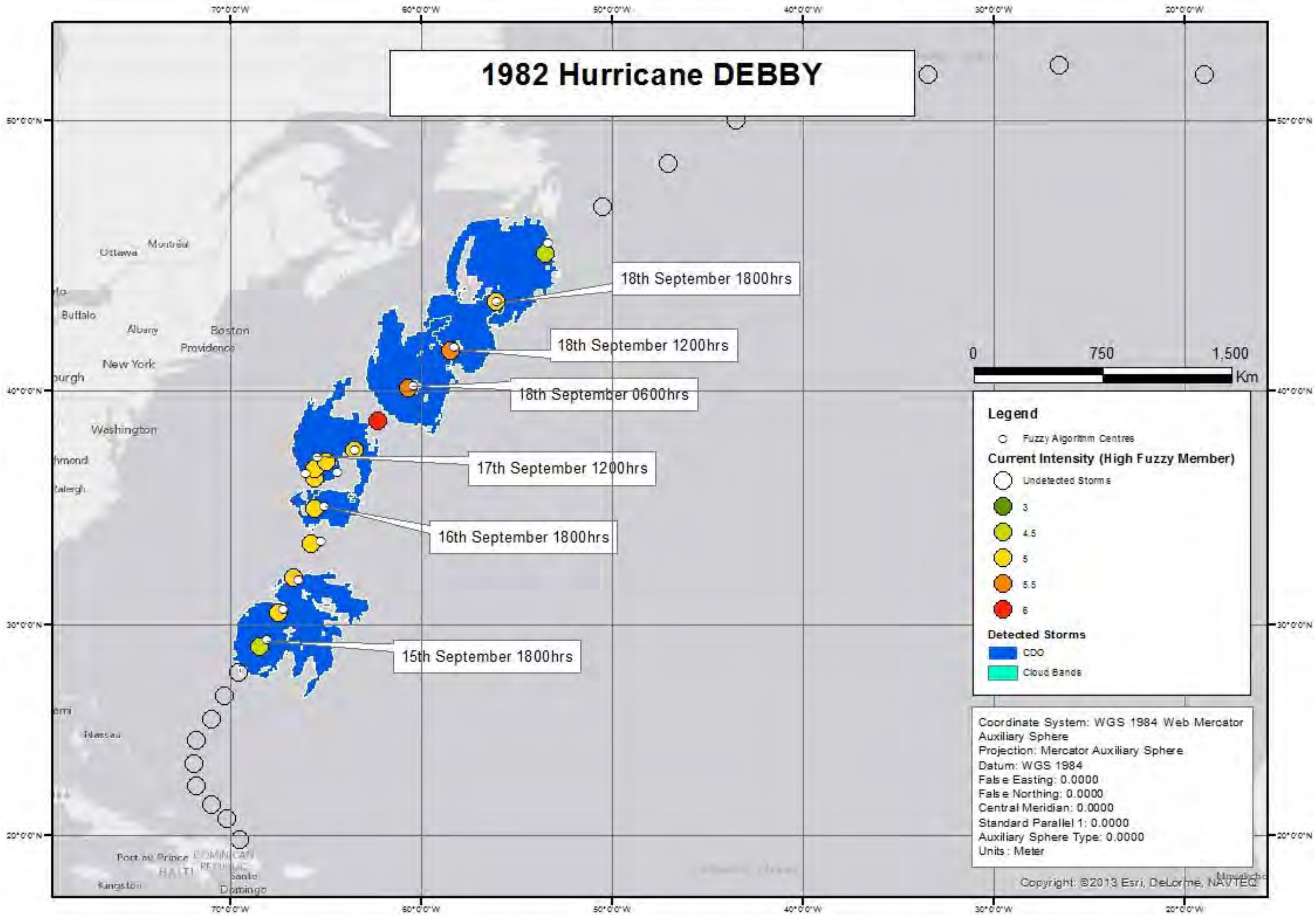
1982 Hurricane DEBBY
18th September 1800hrs
18th September 1200hrs
18th September 0600hrs
17th September 1200hrs
16th September 1800hrs
15th September 1800hrs
0
750
1,500
Km
Legend
Fuzzy Algorithm Centres
Current Intensity (High Fuzzy Member)
Undetected Storms
3
4.5
5
5.5
6
Detected Storms
CDO
Cloud Bands
Coordinate System: WGS 1984 Web Mercator Auxiliary Sphere
Projection: Mercator Auxiliary Sphere
Datum: WGS 1984
False Easting: 0.0000
False Northing: 0.0000
Central Meridian: 0.0000
Standard Parallel 1: 0.0000
Auxiliary Sphere Type: 0.0000
Units: Meter
Copyright: ©2013 Esri, DeLorme, NAVTEQ
Ottawa
Montreal
Buffalo
Albany
Boston
Providence
New York
Washington
Nassau
Port au Prince
Kingston

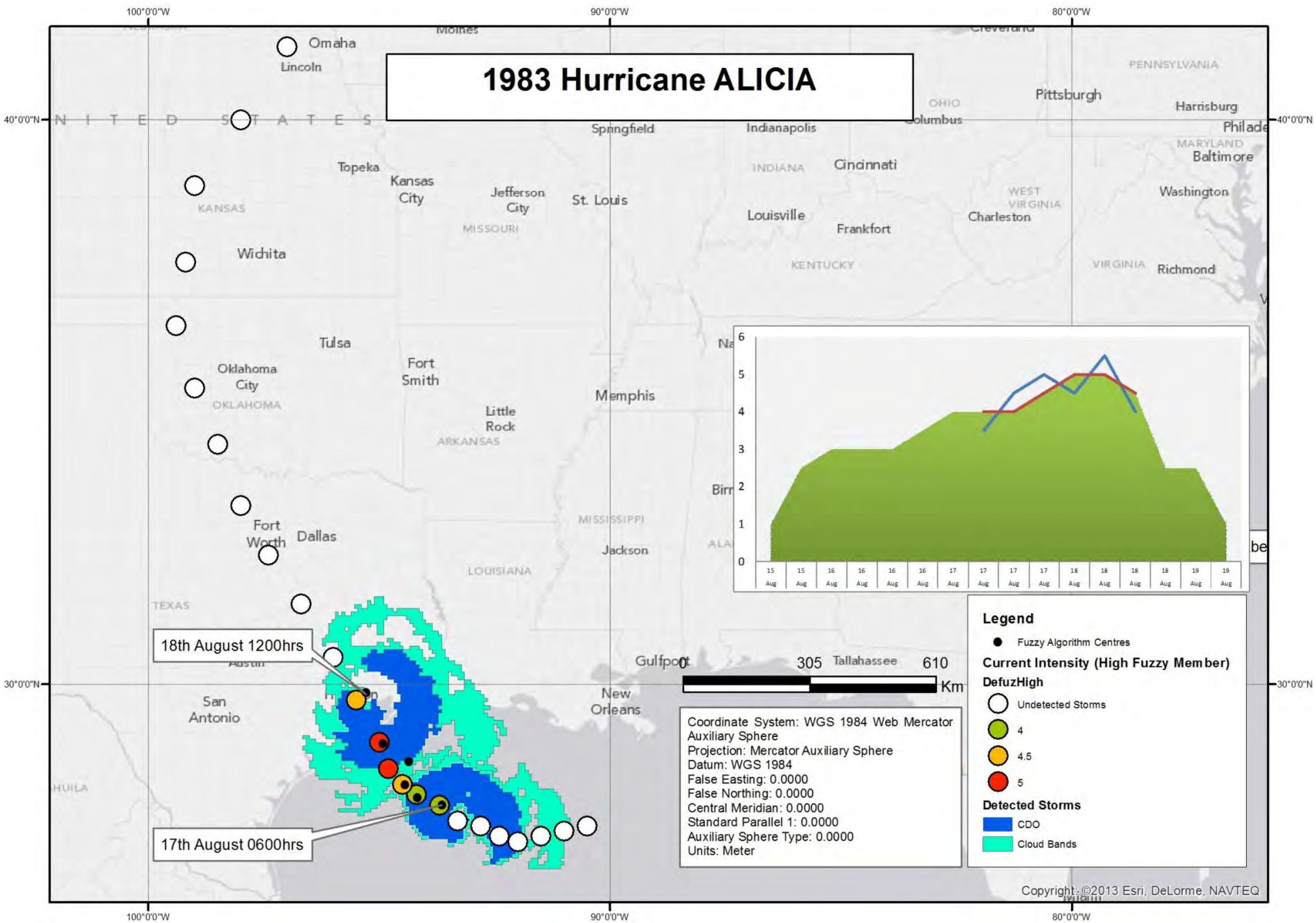
1983 Hurricane ALICIA
18th August 1200hrs
17th August 0600hrs
Legend
Fuzzy Algorithm Centres
Current Intensity (High Fuzzy Member)
DefuzHigh
Undetected Storms
4
4.5
5
Detected Storms
CDO
Cloud Bands
Coordinate System: WGS 1984 Web Mercator Auxiliary Sphere
Projection: Mercator Auxiliary Sphere
Datum: WGS 1984
False Easting: 0.0000
False Northing: 0.0000
Central Meridian: 0.0000
Standard Parallel 1: 0.0000
Auxiliary Sphere Type: 0.0000
Units: Meter
0 305 610 Km
Copyright: ©2013 Esri, DeLorme, NAVTEQ
100°0'0"W
90°0'0"W
80°0'0"W
40°0'0"N
30°0'0"N

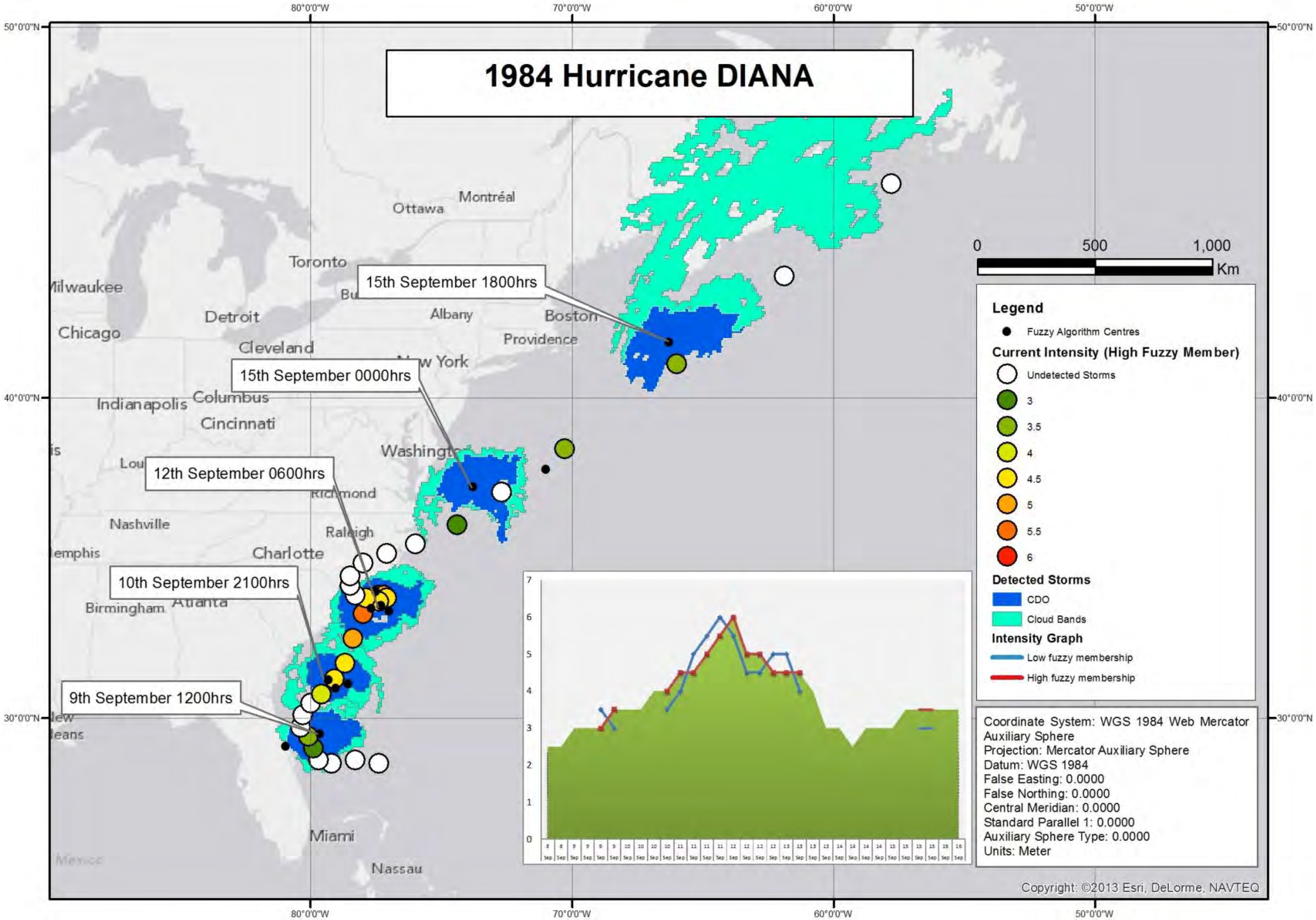

1984 Hurricane DIANA
15th September 1800hrs
15th September 0000hrs
12th September 0600hrs
10th September 2100hrs
9th September 1200hrs
Legend
Fuzzy Algorithm Centres
Current Intensity (High Fuzzy Member)
Undetected Storms
3
3.5
4
4.5
5
5.5
6
Detected Storms
CDO
Cloud Bands
Intensity Graph
Low fuzzy membership
High fuzzy membership
Coordinate System: WGS 1984 Web Mercator Auxiliary Sphere
Projection: Mercator Auxiliary Sphere
Datum: WGS 1984
False Easting: 0.0000
False Northing: 0.0000
Central Meridian: 0.0000
Standard Parallel 1: 0.0000
Auxiliary Sphere Type: 0.0000
Units: Meter
0
500
1,000
Km
Copyright: ©2013 Esri, DeLorme, NAVTEQ
80°0'0"W
70°0'0"W
60°0'0"W
50°0'0"W
50°0'0"N
40°0'0"N
30°0'0"N
Ottawa
Montréal
Toronto
Detroit
Chicago
Cleveland
Albany
Boston
Providence
Columbus
Indianapolis
Cincinnati
Washington
Richmond
Nashville
Raleigh
Charlotte
Atlanta
Birmingham
Miami
Nassau

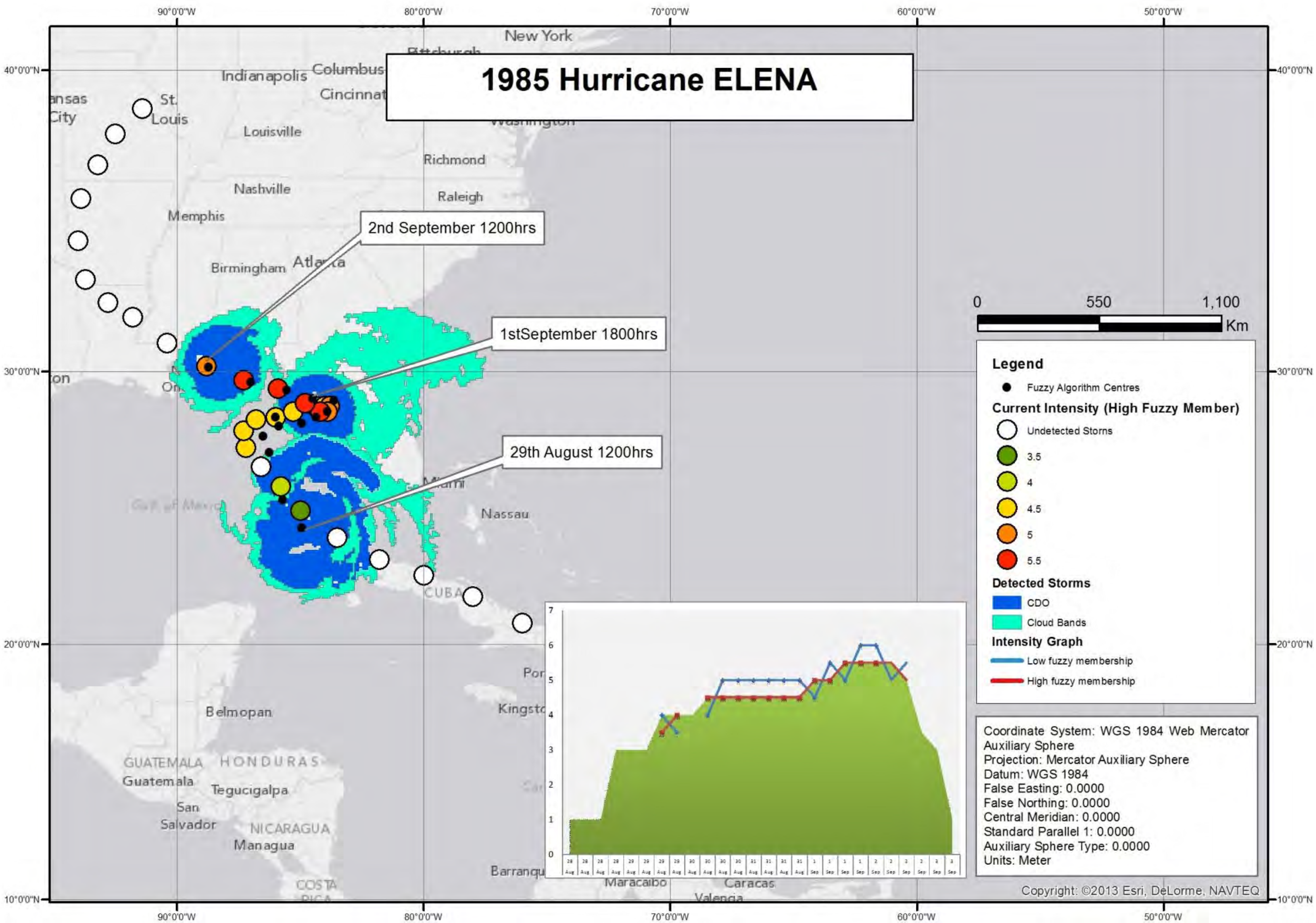
1985 Hurricane ELENA
2nd September 1200hrs
1stSeptember 1800hrs
29th August 1200hrs
0 550 1,100
Km
Legend
Fuzzy Algorithm Centres
Current Intensity (High Fuzzy Member)
Undetected Storms
3.5
4
4.5
5
5.5
Detected Storms
CDO
Cloud Bands
Intensity Graph
Low fuzzy membership
High fuzzy membership
Coordinate System: WGS 1984 Web Mercator Auxiliary Sphere
Projection: Mercator Auxiliary Sphere
Datum: WGS 1984
False Easting: 0.0000
False Northing: 0.0000
Central Meridian: 0.0000
Standard Parallel 1: 0.0000
Auxiliary Sphere Type: 0.0000
Units: Meter
Copyright: ©2013 Esri, DeLorme, NAVTEQ
90°0'0"W
80°0'0"W
70°0'0"W
60°0'0"W
50°0'0"W
40°0'0"N
30°0'0"N
20°0'0"N
10°0'0"N
New York
Indianapolis
Columbus
Cincinnati
St. Louis
Louisville
Richmond
Nashville
Raleigh
Memphis
Birmingham
Nassau
Belmopan
GUATEMALA
Guatemala
HONDURAS
Tegucigalpa
San Salvador
NICARAGUA
Managua
Maracaibo
Caracas

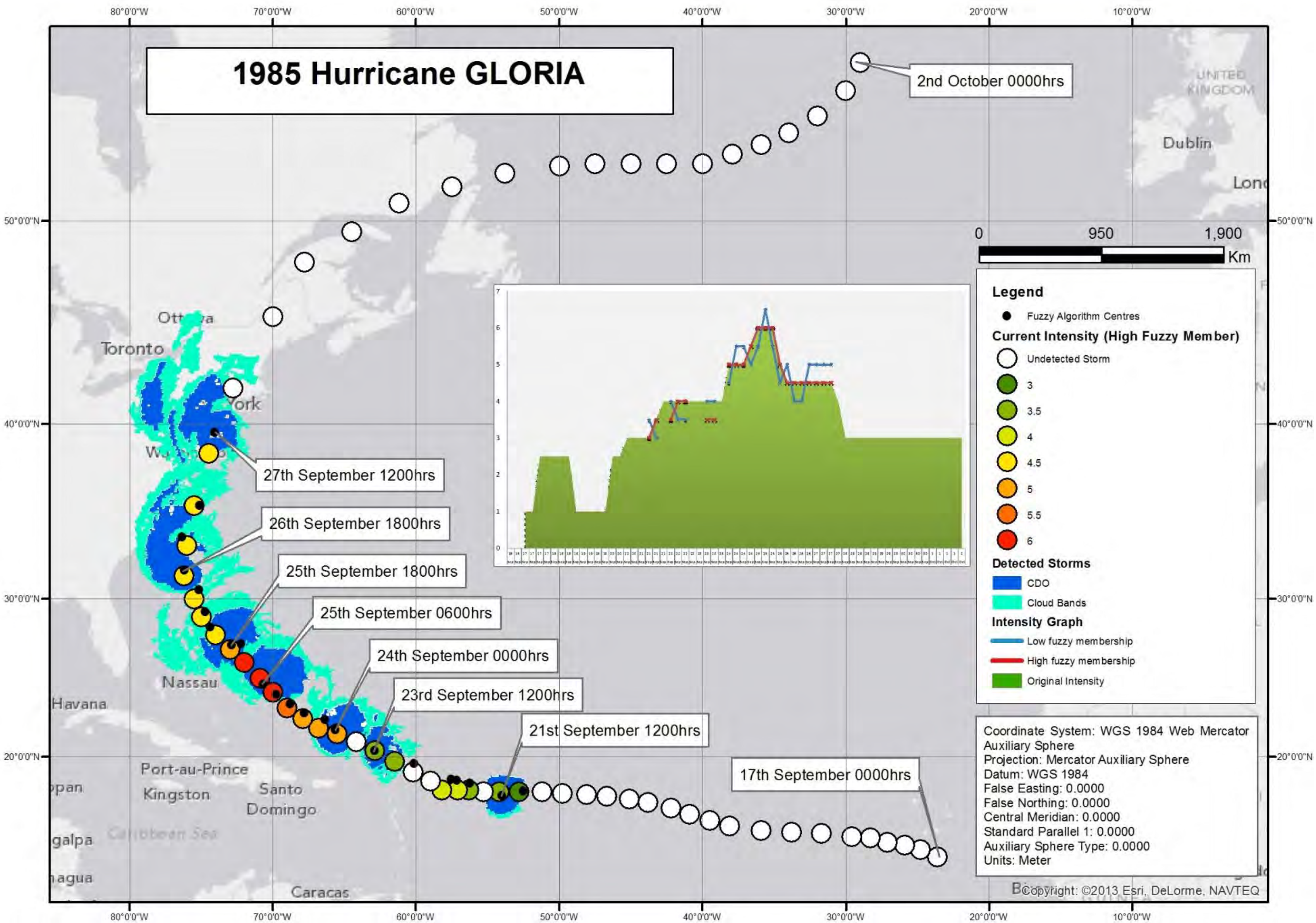
1985 Hurricane GLORIA
2nd October 0000hrs
27th September 1200hrs
26th September 1800hrs
25th September 1800hrs
25th September 0600hrs
24th September 0000hrs
23rd September 1200hrs
21st September 1200hrs
17th September 0000hrs
Legend
Fuzzy Algorithm Centres
Current Intensity (High Fuzzy Member)
Undetected Storm
3
3.5
4
4.5
5
5.5
6
Detected Storms
CDO
Cloud Bands
Intensity Graph
Low fuzzy membership
High fuzzy membership
Original Intensity
0
950
1,900
Km
Coordinate System: WGS 1984 Web Mercator Auxiliary Sphere
Projection: Mercator Auxiliary Sphere
Datum: WGS 1984
False Easting: 0.0000
False Northing: 0.0000
Central Meridian: 0.0000
Standard Parallel 1: 0.0000
Auxiliary Sphere Type: 0.0000
Units: Meter
Copyright: ©2013 Esri, DeLorme, NAVTEQ
Dublin
Toronto
Nassau
Havana
Port-au-Prince
Kingston
Santo Domingo
Caracas
80°0'0"W
70°0'0"W
60°0'0"W
50°0'0"W
40°0'0"W
30°0'0"W
20°0'0"W
10°0'0"W
50°0'0"N
40°0'0"N
30°0'0"N
20°0'0"N

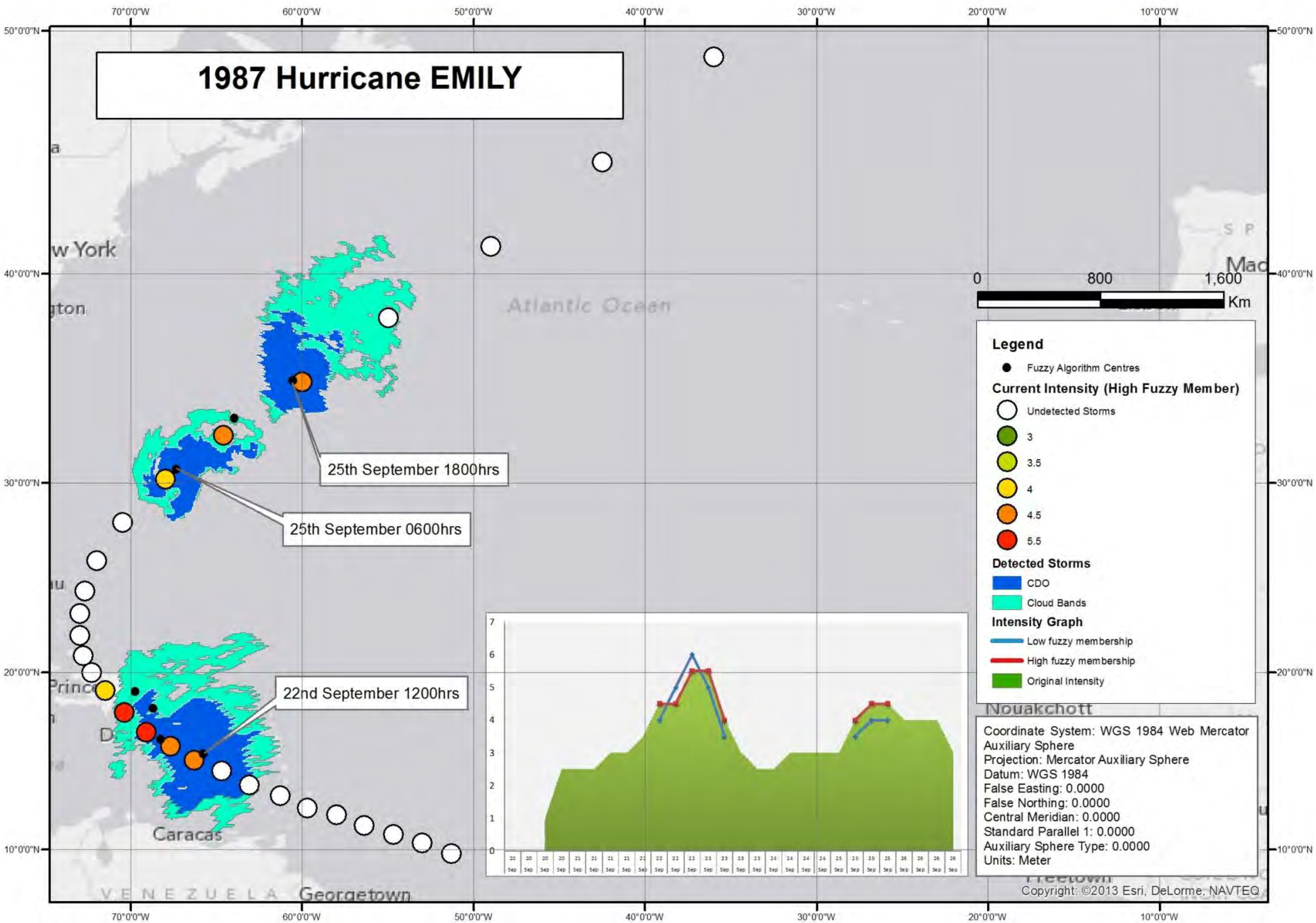
1987 Hurricane EMILY
25th September 1800hrs
25th September 0600hrs
22nd September 1200hrs
Atlantic Ocean
w York
Caracas
Georgetown
VENEZUELA
Nouakchott
0
800
1,600
Km
Legend
Fuzzy Algorithm Centres
Current Intensity (High Fuzzy Member)
Undetected Storms
3
3.5
4
4.5
5.5
Detected Storms
CDO
Cloud Bands
Intensity Graph
Low fuzzy membership
High fuzzy membership
Original Intensity
Coordinate System: WGS 1984 Web Mercator Auxiliary Sphere
Projection: Mercator Auxiliary Sphere
Datum: WGS 1984
False Easting: 0.0000
False Northing: 0.0000
Central Meridian: 0.0000
Standard Parallel 1: 0.0000
Auxiliary Sphere Type: 0.0000
Units: Meter
Copyright: ©2013 Esri, DeLorme, NAVTEQ
70°0'0"W
60°0'0"W
50°0'0"W
40°0'0"W
30°0'0"W
20°0'0"W
10°0'0"W
50°0'0"N
40°0'0"N
30°0'0"N
20°0'0"N
10°0'0"N

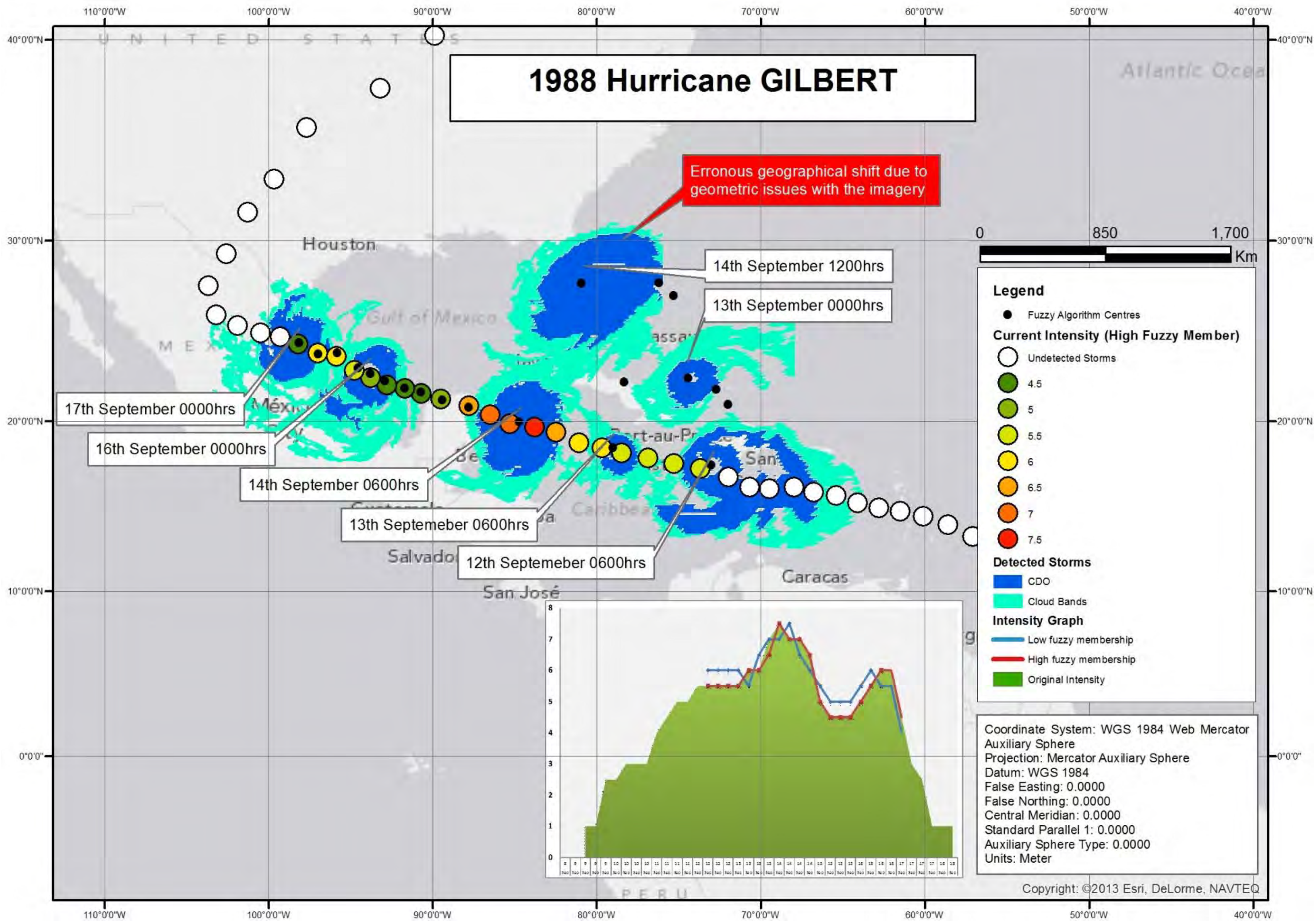

1988 Hurricane GILBERT
Erronous geographical shift due to geometric issues with the imagery
14th September 1200hrs
13th September 0000hrs
17th September 0000hrs
16th September 0000hrs
14th September 0600hrs
13th Septemeber 0600hrs
12th Septemeber 0600hrs
Houston
Gulf of Mexico
Caracas
San José
Atlantic Ocea
Legend
Fuzzy Algorithm Centres
Current Intensity (High Fuzzy Member)
Undetected Storms
4.5
5
5.5
6
6.5
7
7.5
Detected Storms
CDO
Cloud Bands
Intensity Graph
Low fuzzy membership
High fuzzy membership
Original Intensity
0 850 1,700 Km
Coordinate System: WGS 1984 Web Mercator Auxiliary Sphere
Projection: Mercator Auxiliary Sphere
Datum: WGS 1984
False Easting: 0.0000
False Northing: 0.0000
Central Meridian: 0.0000
Standard Parallel 1: 0.0000
Auxiliary Sphere Type: 0.0000
Units: Meter
Copyright: ©2013 Esri, DeLorme, NAVTEQ

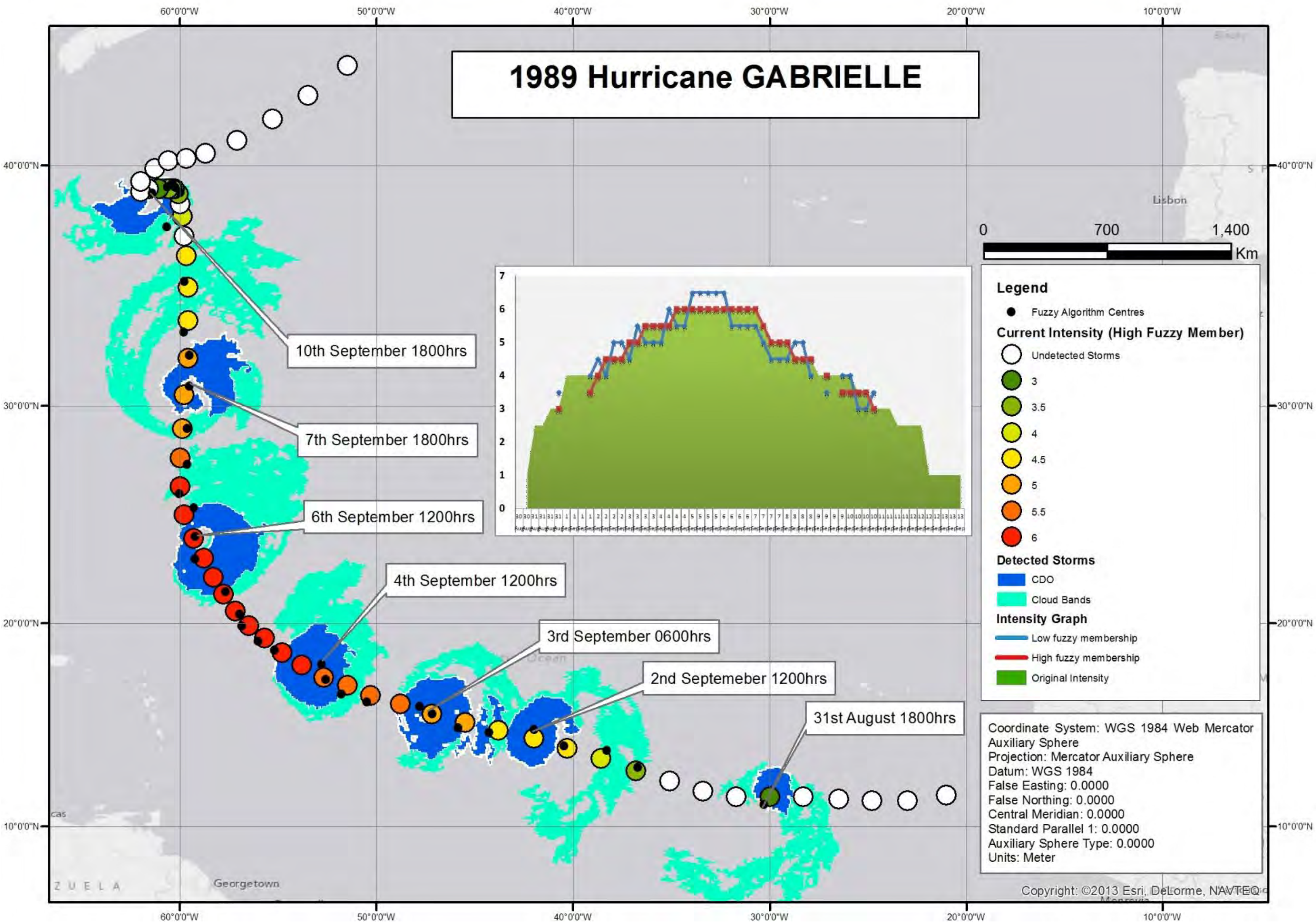

1989 Hurricane GABRIELLE
10th September 1800hrs
7th September 1800hrs
6th September 1200hrs
4th September 1200hrs
3rd September 0600hrs
2nd Septemeber 1200hrs
31st August 1800hrs
0 700 1,400 Km
Legend
Fuzzy Algorithm Centres
Current Intensity (High Fuzzy Member)
Undetected Storms
3
3.5
4
4.5
5
5.5
6
Detected Storms
CDO
Cloud Bands
Intensity Graph
Low fuzzy membership
High fuzzy membership
Original Intensity
Coordinate System: WGS 1984 Web Mercator Auxiliary Sphere
Projection: Mercator Auxiliary Sphere
Datum: WGS 1984
False Easting: 0.0000
False Northing: 0.0000
Central Meridian: 0.0000
Standard Parallel 1: 0.0000
Auxiliary Sphere Type: 0.0000
Units: Meter
Copyright: ©2013 Esri, DeLorme, NAVTEQ
60°0'0"W
50°0'0"W
40°0'0"W
30°0'0"W
20°0'0"W
10°0'0"W
40°0'0"N
30°0'0"N
20°0'0"N
10°0'0"N
Lisbon
Georgetown

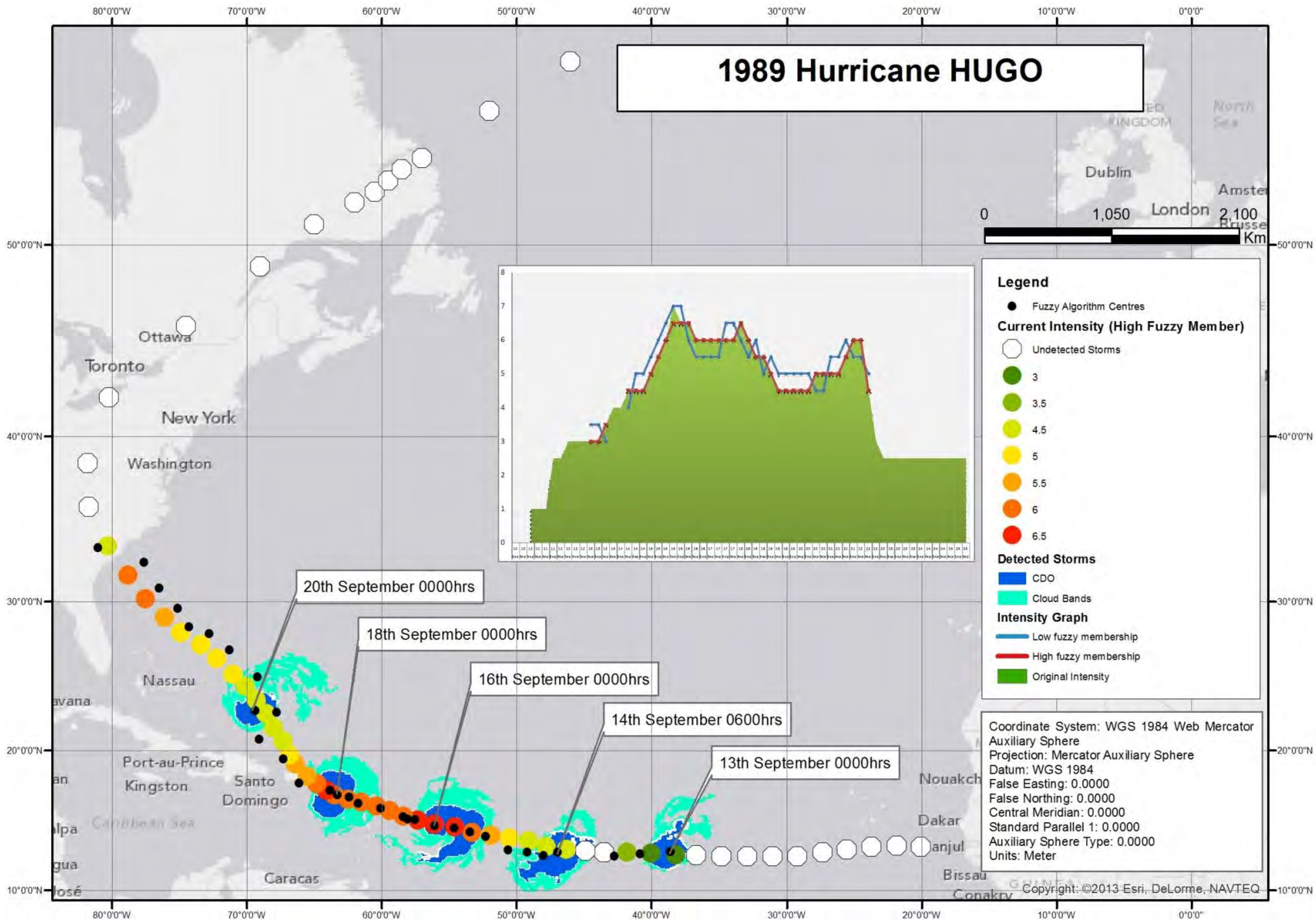
1989 Hurricane HUGO
Legend
Fuzzy Algorithm Centres
Current Intensity (High Fuzzy Member)
Undetected Storms
3
3.5
4.5
5
5.5
6
6.5
Detected Storms
CDO
Cloud Bands
Intensity Graph
Low fuzzy membership
High fuzzy membership
Original Intensity
20th September 0000hrs
18th September 0000hrs
16th September 0000hrs
14th September 0600hrs
13th September 0000hrs
0
1,050
2,100
Km
Coordinate System: WGS 1984 Web Mercator Auxiliary Sphere
Projection: Mercator Auxiliary Sphere
Datum: WGS 1984
False Easting: 0.0000
False Northing: 0.0000
Central Meridian: 0.0000
Standard Parallel 1: 0.0000
Auxiliary Sphere Type: 0.0000
Units: Meter
Copyright: ©2013 Esri, DeLorme, NAVTEQ

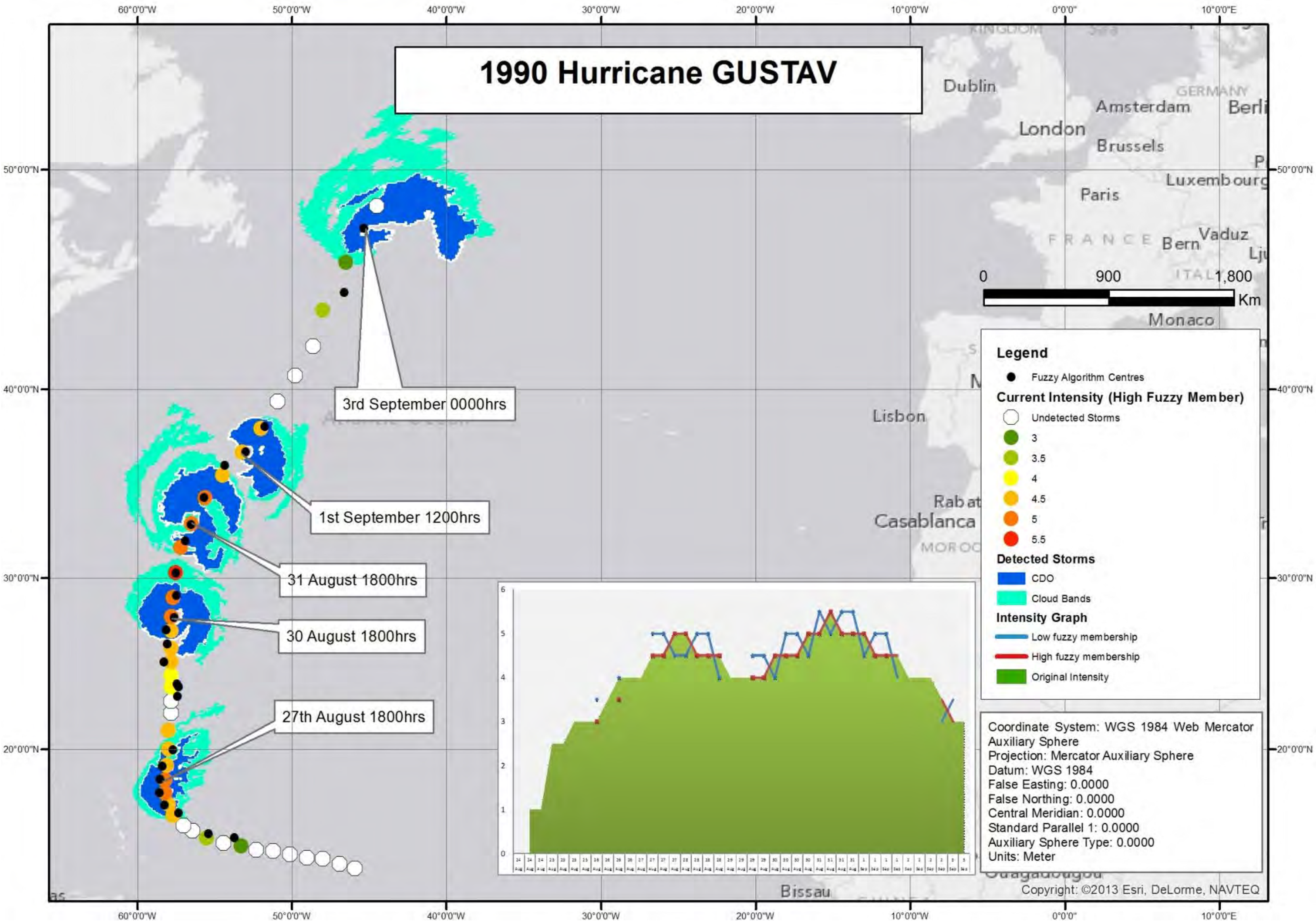

1990 Hurricane GUSTAV
3rd September 0000hrs
1st September 1200hrs
31 August 1800hrs
30 August 1800hrs
27th August 1800hrs
Dublin
London
Amsterdam
Brussels
Paris
Luxembourg
Bern
Vaduz
Monaco
Lisbon
Rabat
Casablanca
Bissau
0
900
1,800
Km
Legend
Fuzzy Algorithm Centres
Current Intensity (High Fuzzy Member)
Undetected Storms
3
3.5
4
4.5
5
5.5
Detected Storms
CDO
Cloud Bands
Intensity Graph
Low fuzzy membership
High fuzzy membership
Original Intensity
Coordinate System: WGS 1984 Web Mercator Auxiliary Sphere
Projection: Mercator Auxiliary Sphere
Datum: WGS 1984
False Easting: 0.0000
False Northing: 0.0000
Central Meridian: 0.0000
Standard Parallel 1: 0.0000
Auxiliary Sphere Type: 0.0000
Units: Meter
Copyright: ©2013 Esri, DeLorme, NAVTEQ
60°0'0"W
50°0'0"W
40°0'0"W
30°0'0"W
20°0'0"W
10°0'0"W
0°0'0"
10°0'0"E
50°0'0"N
40°0'0"N
30°0'0"N
20°0'0"N

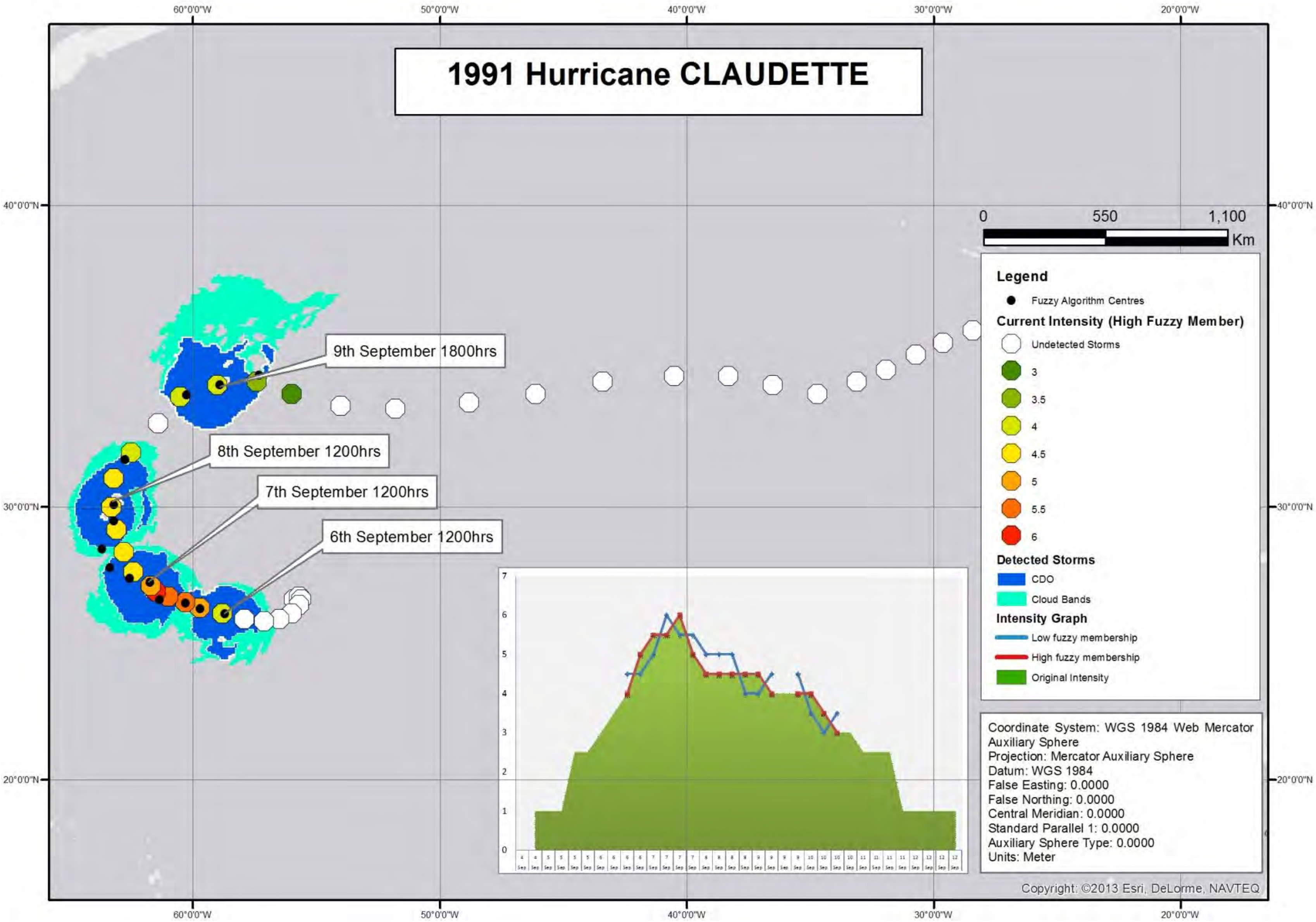
1991 Hurricane CLAUDETTE
60°0'0"W
50°0'0"W
40°0'0"W
30°0'0"W
20°0'0"W
40°0'0"N
30°0'0"N
20°0'0"N
9th September 1800hrs
8th September 1200hrs
7th September 1200hrs
6th September 1200hrs
0
550
1,100
Km
Legend
Fuzzy Algorithm Centres
Current Intensity (High Fuzzy Member)
Undetected Storms
3
3.5
4
4.5
5
5.5
6
Detected Storms
CDO
Cloud Bands
Intensity Graph
Low fuzzy membership
High fuzzy membership
Original Intensity
Coordinate System: WGS 1984 Web Mercator Auxiliary Sphere
Projection: Mercator Auxiliary Sphere
Datum: WGS 1984
False Easting: 0.0000
False Northing: 0.0000
Central Meridian: 0.0000
Standard Parallel 1: 0.0000
Auxiliary Sphere Type: 0.0000
Units: Meter
Copyright: ©2013 Esri, DeLorme, NAVTEQ

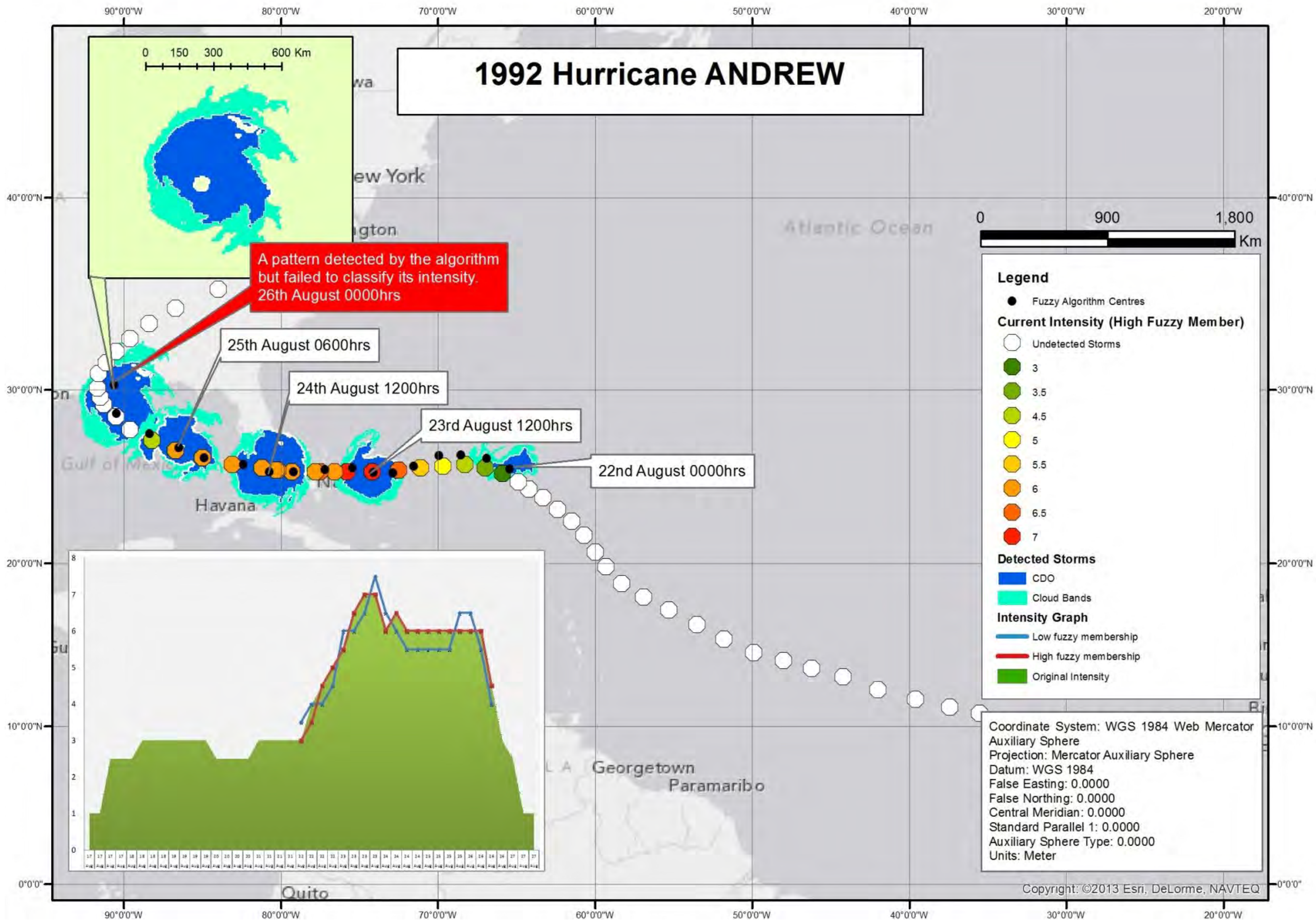

1992 Hurricane ANDREW
0 150 300 600 Km
A pattern detected by the algorithm but failed to classify its intensity. 26th August 0000hrs
25th August 0600hrs
24th August 1200hrs
23rd August 1200hrs
22nd August 0000hrs
Atlantic Ocean
New York
Havana
Gulf of Mexico
Georgetown
Paramaribo
Quito
0 900 1,800 Km
Legend
Fuzzy Algorithm Centres
Current Intensity (High Fuzzy Member)
Undetected Storms
3
3.5
4.5
5
5.5
6
6.5
7
Detected Storms
CDO
Cloud Bands
Intensity Graph
Low fuzzy membership
High fuzzy membership
Original Intensity
Coordinate System: WGS 1984 Web Mercator Auxiliary Sphere
Projection: Mercator Auxiliary Sphere
Datum: WGS 1984
False Easting: 0.0000
False Northing: 0.0000
Central Meridian: 0.0000
Standard Parallel 1: 0.0000
Auxiliary Sphere Type: 0.0000
Units: Meter
Copyright: ©2013 Esri, DeLorme, NAVTEQ
90°0'0"W
80°0'0"W
70°0'0"W
60°0'0"W
50°0'0"W
40°0'0"W
30°0'0"W
20°0'0"W
40°0'0"N
30°0'0"N
20°0'0"N
10°0'0"N
0°0'0"

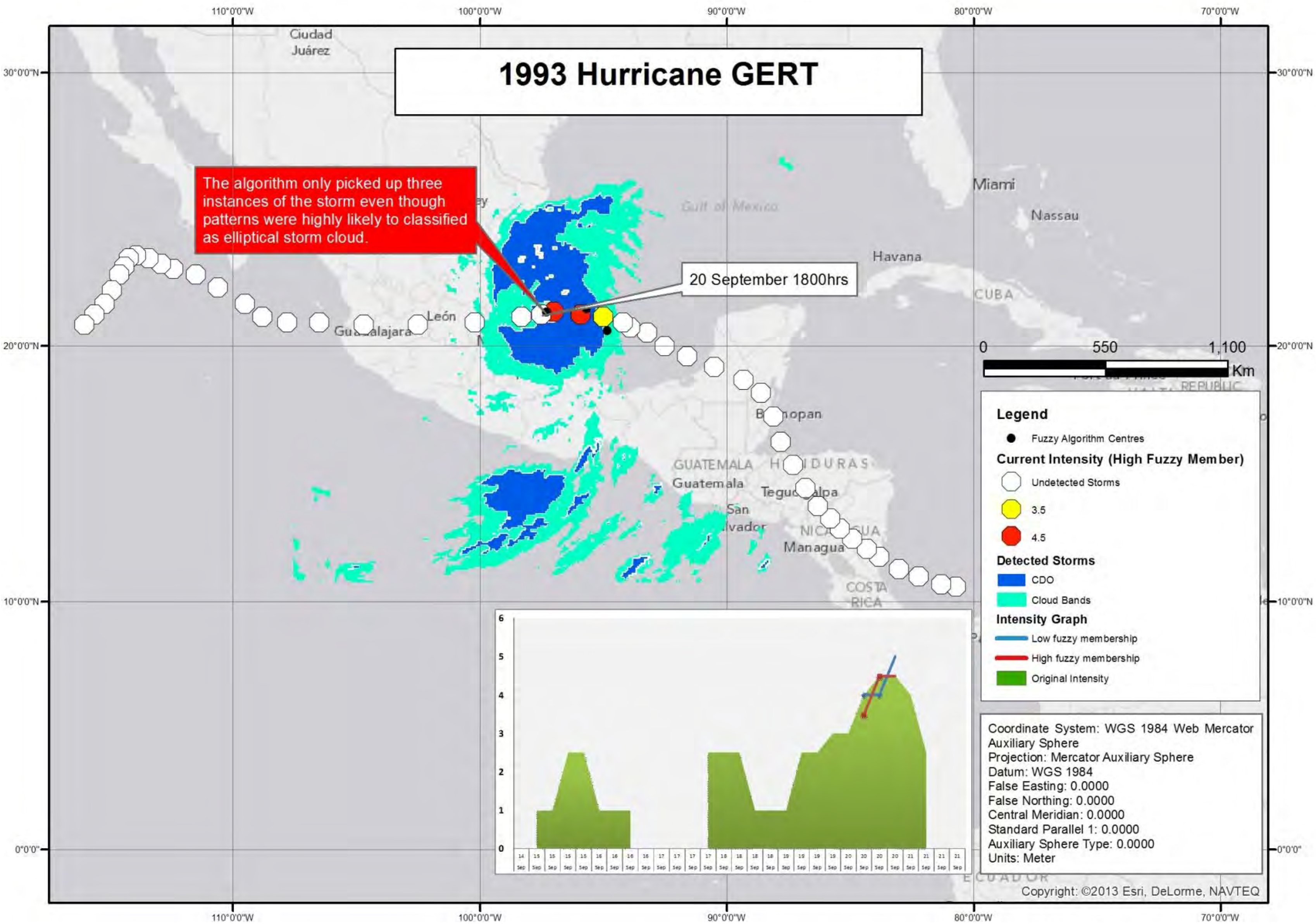

1993 Hurricane GERT
The algorithm only picked up three instances of the storm even though patterns were highly likely to classified as elliptical storm cloud.
20 September 1800hrs
Legend
Fuzzy Algorithm Centres
Current Intensity (High Fuzzy Member)
Undetected Storms
3.5
4.5
Detected Storms
CDO
Cloud Bands
Intensity Graph
Low fuzzy membership
High fuzzy membership
Original Intensity
Coordinate System: WGS 1984 Web Mercator Auxiliary Sphere
Projection: Mercator Auxiliary Sphere
Datum: WGS 1984
False Easting: 0.0000
False Northing: 0.0000
Central Meridian: 0.0000
Standard Parallel 1: 0.0000
Auxiliary Sphere Type: 0.0000
Units: Meter
Copyright: ©2013 Esri, DeLorme, NAVTEQ
0 550 1,100 Km

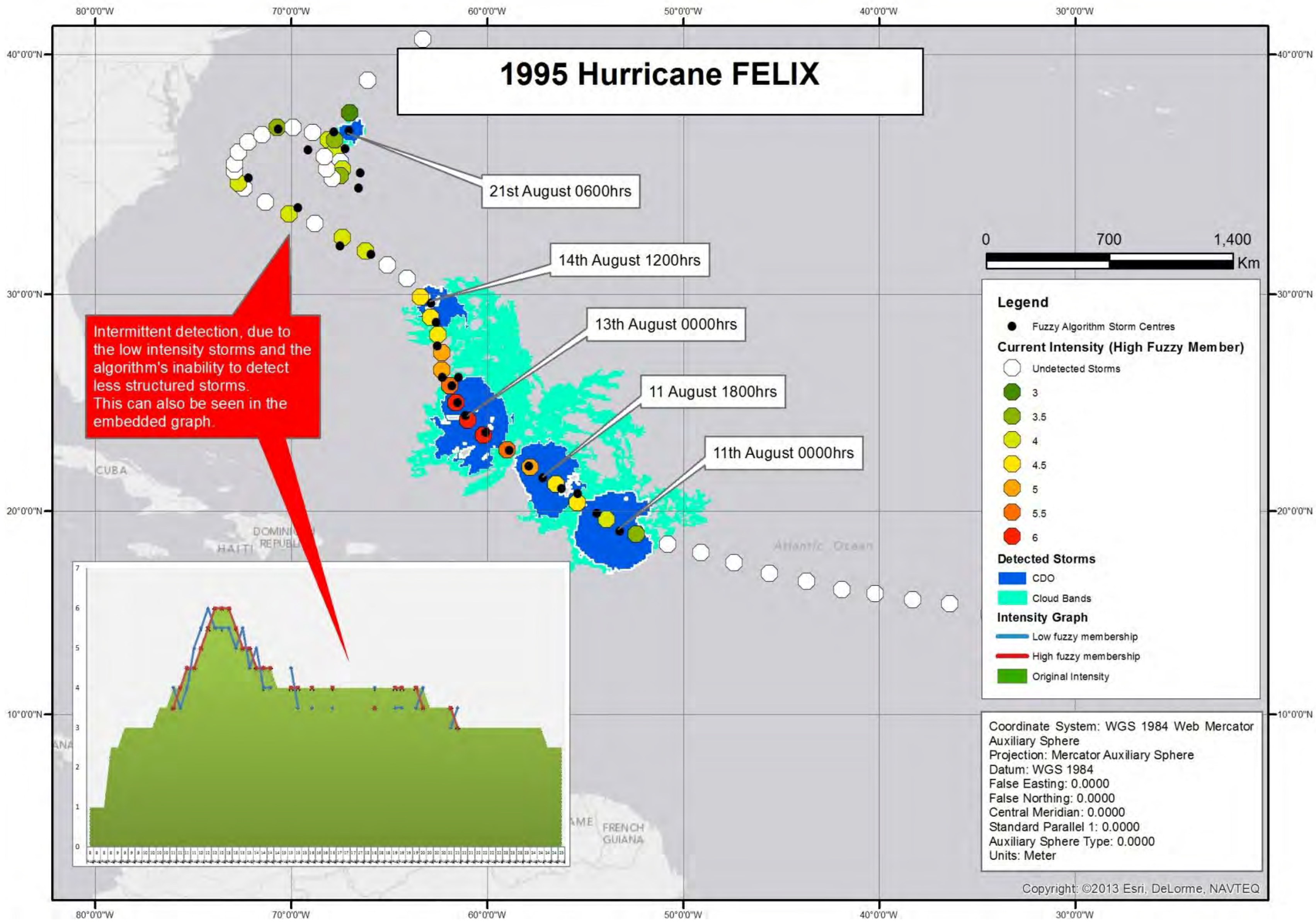
1995 Hurricane FELIX
21st August 0600hrs
14th August 1200hrs
13th August 0000hrs
11 August 1800hrs
11th August 0000hrs
Intermittent detection, due to the low intensity storms and the algorithm's inability to detect less structured storms.
This can also be seen in the embedded graph.
0
700
1,400
Km
Legend
Fuzzy Algorithm Storm Centres
Current Intensity (High Fuzzy Member)
Undetected Storms
3
3.5
4
4.5
5
5.5
6
Detected Storms
CDO
Cloud Bands
Intensity Graph
Low fuzzy membership
High fuzzy membership
Original Intensity
Coordinate System: WGS 1984 Web Mercator Auxiliary Sphere
Projection: Mercator Auxiliary Sphere
Datum: WGS 1984
False Easting: 0.0000
False Northing: 0.0000
Central Meridian: 0.0000
Standard Parallel 1: 0.0000
Auxiliary Sphere Type: 0.0000
Units: Meter
Copyright: ©2013 Esri, DeLorme, NAVTEQ
CUBA
HAITI
FRENCH GUIANA
Atlantic Ocean
80°0'0"W
70°0'0"W
60°0'0"W
50°0'0"W
40°0'0"W
30°0'0"W
40°0'0"N
30°0'0"N
20°0'0"N
10°0'0"N

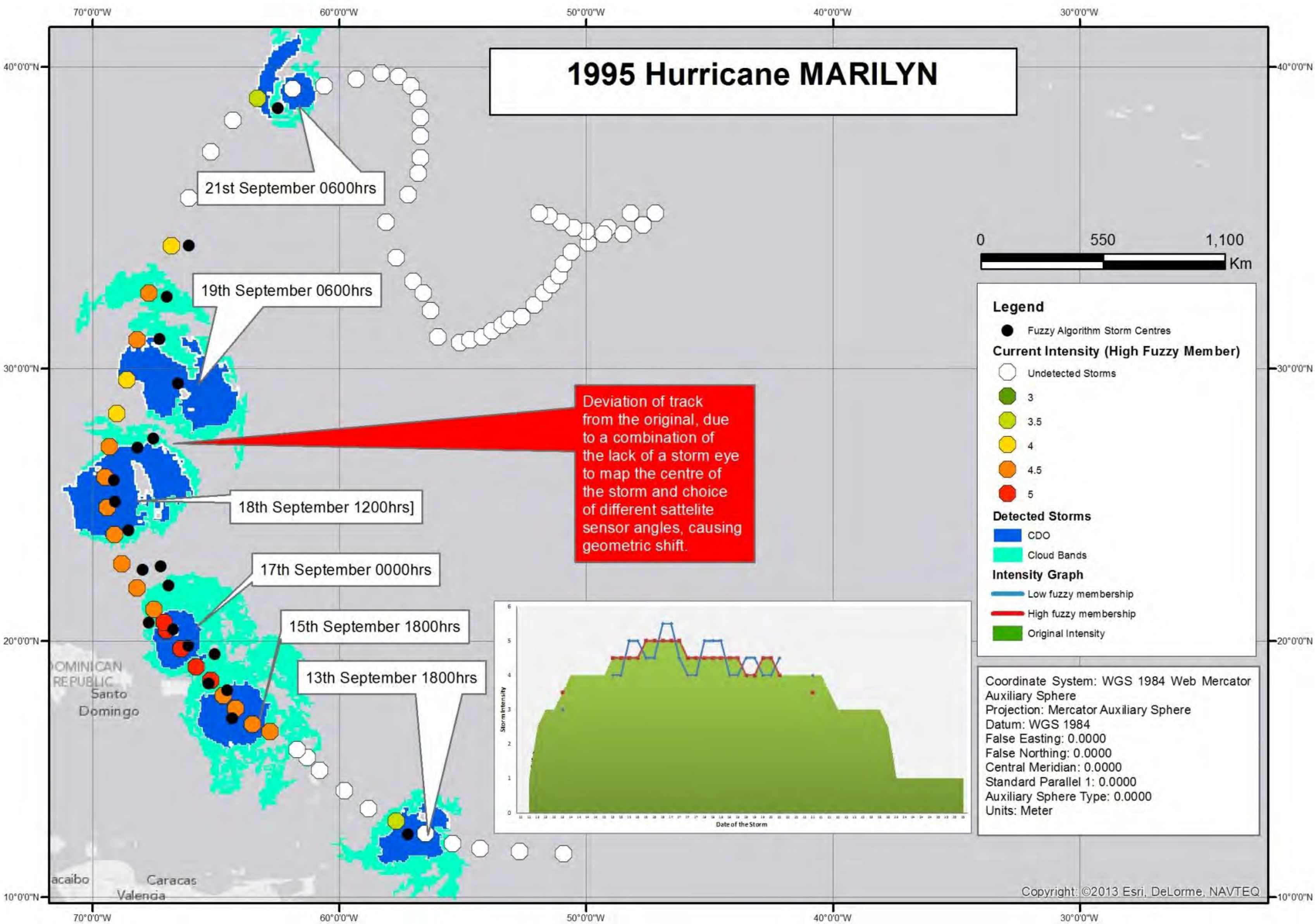
1995 Hurricane MARILYN
21st September 0600hrs
19th September 0600hrs
18th September 1200hrs]
17th September 0000hrs
15th September 1800hrs
13th September 1800hrs
Deviation of track from the original, due to a combination of the lack of a storm eye to map the centre of the storm and choice of different sattelite sensor angles, causing geometric shift.
0
550
1,100
Km
Legend
Fuzzy Algorithm Storm Centres
Current Intensity (High Fuzzy Member)
Undetected Storms
3
3.5
4
4.5
5
Detected Storms
CDO
Cloud Bands
Intensity Graph
Low fuzzy membership
High fuzzy membership
Original Intensity
Coordinate System: WGS 1984 Web Mercator Auxiliary Sphere
Projection: Mercator Auxiliary Sphere
Datum: WGS 1984
False Easting: 0.0000
False Northing: 0.0000
Central Meridian: 0.0000
Standard Parallel 1: 0.0000
Auxiliary Sphere Type: 0.0000
Units: Meter
Copyright: ©2013 Esri, DeLorme, NAVTEQ
70°0'0"W
60°0'0"W
50°0'0"W
40°0'0"W
30°0'0"W
40°0'0"N
30°0'0"N
20°0'0"N
10°0'0"N
DOMINICAN REPUBLIC
Santo Domingo
Caracas
Valencia
Storm Intensity
Date of the Storm

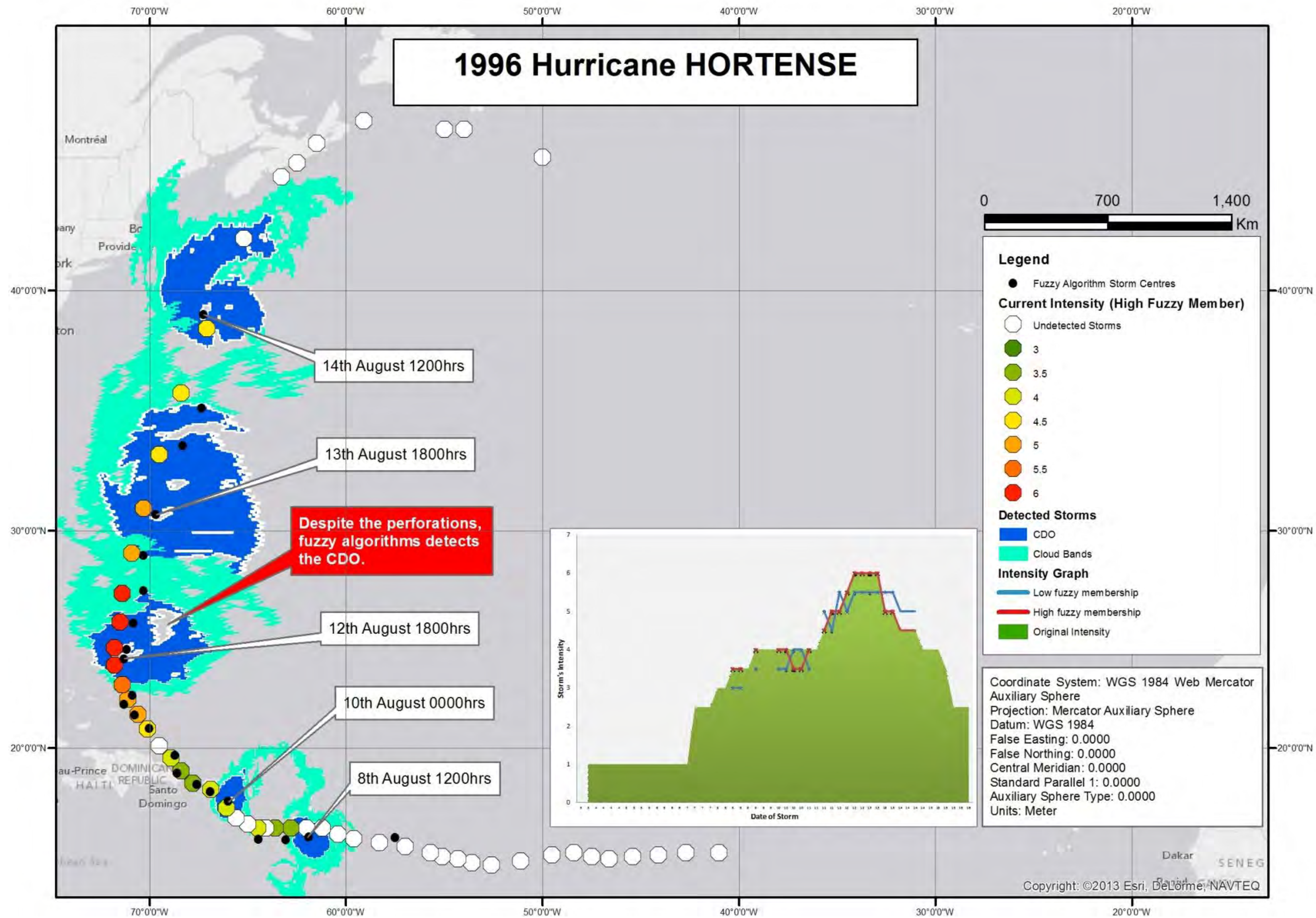

1996 Hurricane HORTENSE
14th August 1200hrs
13th August 1800hrs
Despite the perforations, fuzzy algorithms detects the CDO.
12th August 1800hrs
10th August 0000hrs
8th August 1200hrs
Montréal
Dakar
0
700
1,400
Km
Legend
Fuzzy Algorithm Storm Centres
Current Intensity (High Fuzzy Member)
Undetected Storms
3
3.5
4
4.5
5
5.5
6
Detected Storms
CDO
Cloud Bands
Intensity Graph
Low fuzzy membership
High fuzzy membership
Original Intensity
Storm's Intensity
Date of Storm
Coordinate System: WGS 1984 Web Mercator Auxiliary Sphere
Projection: Mercator Auxiliary Sphere
Datum: WGS 1984
False Easting: 0.0000
False Northing: 0.0000
Central Meridian: 0.0000
Standard Parallel 1: 0.0000
Auxiliary Sphere Type: 0.0000
Units: Meter
Copyright: ©2013 Esri, DeLorme, NAVTEQ
70°0'0"W
60°0'0"W
50°0'0"W
40°0'0"W
30°0'0"W
20°0'0"W
40°0'0"N
30°0'0"N
20°0'0"N

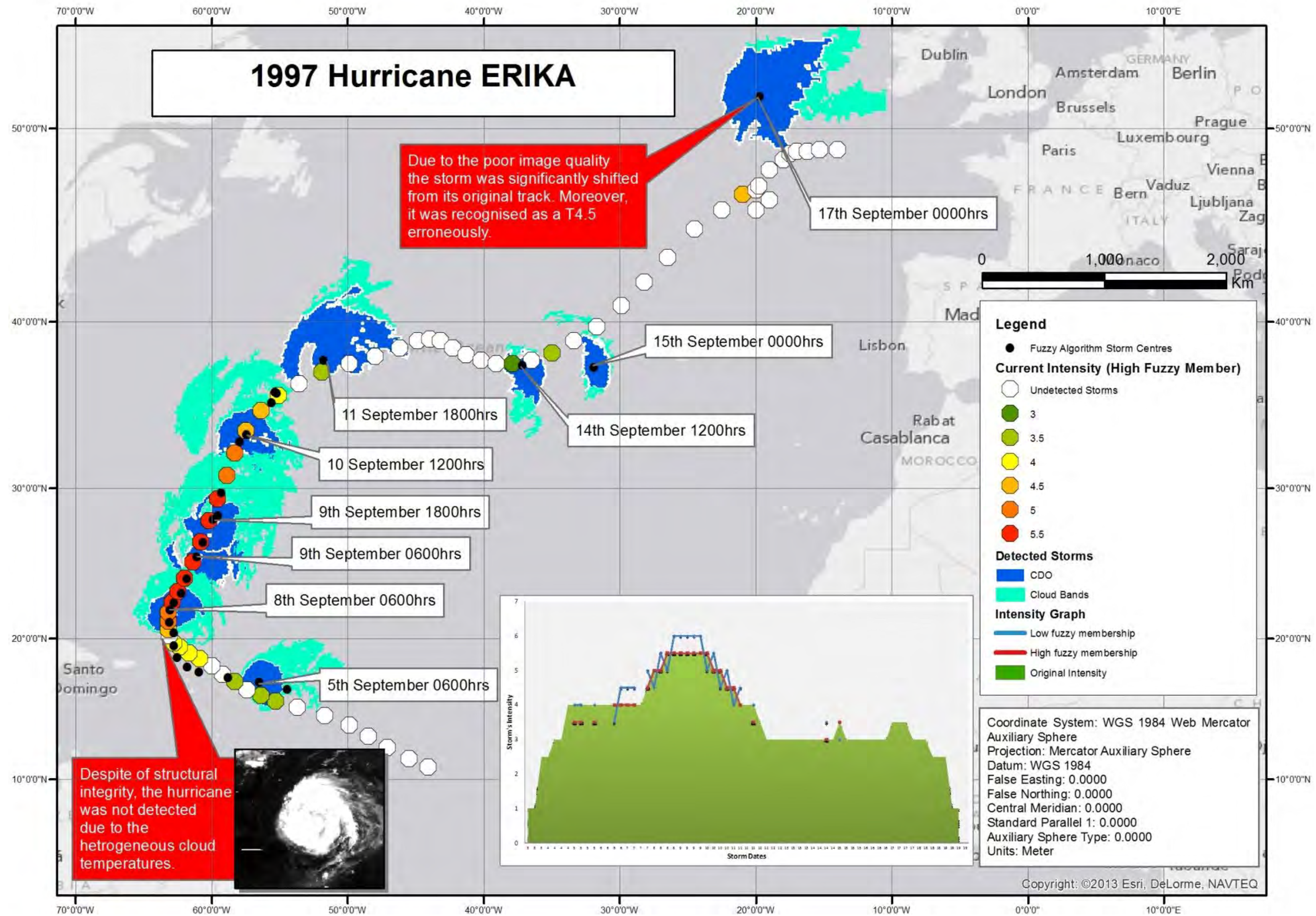

1997 Hurricane ERIKA
Due to the poor image quality the storm was significantly shifted from its original track. Moreover, it was recognised as a T4.5 erroneously.
17th September 0000hrs
15th September 0000hrs
14th September 1200hrs
11 September 1800hrs
10 September 1200hrs
9th September 1800hrs
9th September 0600hrs
8th September 0600hrs
5th September 0600hrs
Despite of structural integrity, the hurricane was not detected due to the hetrogeneous cloud temperatures.
Legend
Fuzzy Algorithm Storm Centres
Current Intensity (High Fuzzy Member)
Undetected Storms
3
3.5
4
4.5
5
5.5
Detected Storms
CDO
Cloud Bands
Intensity Graph
Low fuzzy membership
High fuzzy membership
Original Intensity
Storm's Intensity
Storm Dates
0
1,000
2,000
Km
Coordinate System: WGS 1984 Web Mercator Auxiliary Sphere
Projection: Mercator Auxiliary Sphere
Datum: WGS 1984
False Easting: 0.0000
False Northing: 0.0000
Central Meridian: 0.0000
Standard Parallel 1: 0.0000
Auxiliary Sphere Type: 0.0000
Units: Meter
Copyright: ©2013 Esri, DeLorme, NAVTEQ
Dublin
London
Amsterdam
Berlin
Brussels
Paris
Luxembourg
Prague
Vienna
Bern
Vaduz
Ljubljana
Lisbon
Rabat
Casablanca
MOROCCO
Santo Domingo
70°0'0"W
60°0'0"W
50°0'0"W
40°0'0"W
30°0'0"W
20°0'0"W
10°0'0"W
0°0'0"
10°0'0"E
50°0'0"N
40°0'0"N
30°0'0"N
20°0'0"N
10°0'0"N

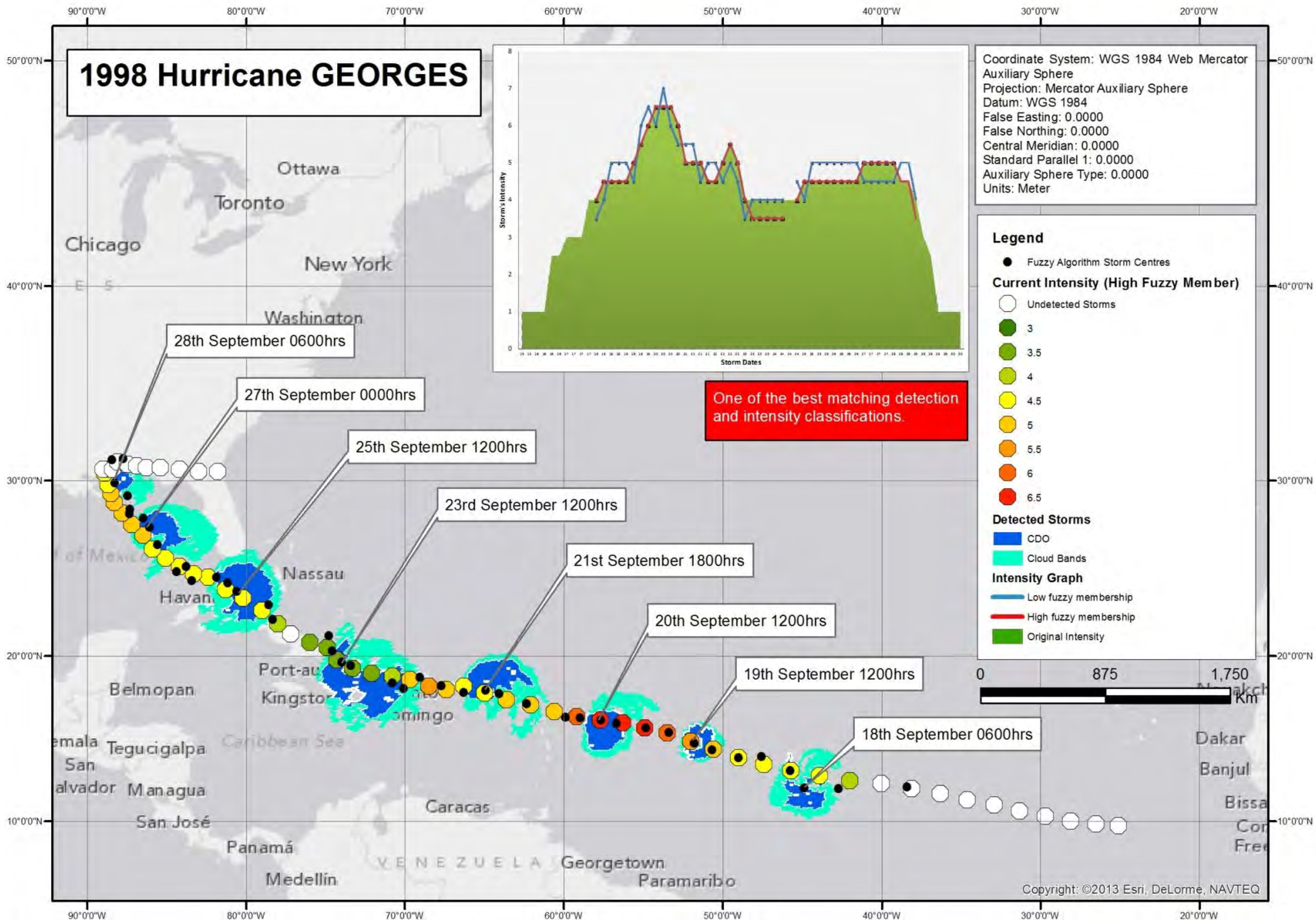

1998 Hurricane GEORGES
Coordinate System: WGS 1984 Web Mercator Auxiliary Sphere
Projection: Mercator Auxiliary Sphere
Datum: WGS 1984
False Easting: 0.0000
False Northing: 0.0000
Central Meridian: 0.0000
Standard Parallel 1: 0.0000
Auxiliary Sphere Type: 0.0000
Units: Meter
Legend
Fuzzy Algorithm Storm Centres
Current Intensity (High Fuzzy Member)
Undetected Storms
3
3.5
4
4.5
5
5.5
6
6.5
Detected Storms
CDO
Cloud Bands
Intensity Graph
Low fuzzy membership
High fuzzy membership
Original Intensity
Storm Dates
One of the best matching detection and intensity classifications.
28th September 0600hrs
27th September 0000hrs
25th September 1200hrs
23rd September 1200hrs
21st September 1800hrs
20th September 1200hrs
19th September 1200hrs
18th September 0600hrs
0
875
1,750
Km
Copyright: ©2013 Esri, DeLorme, NAVTEQ

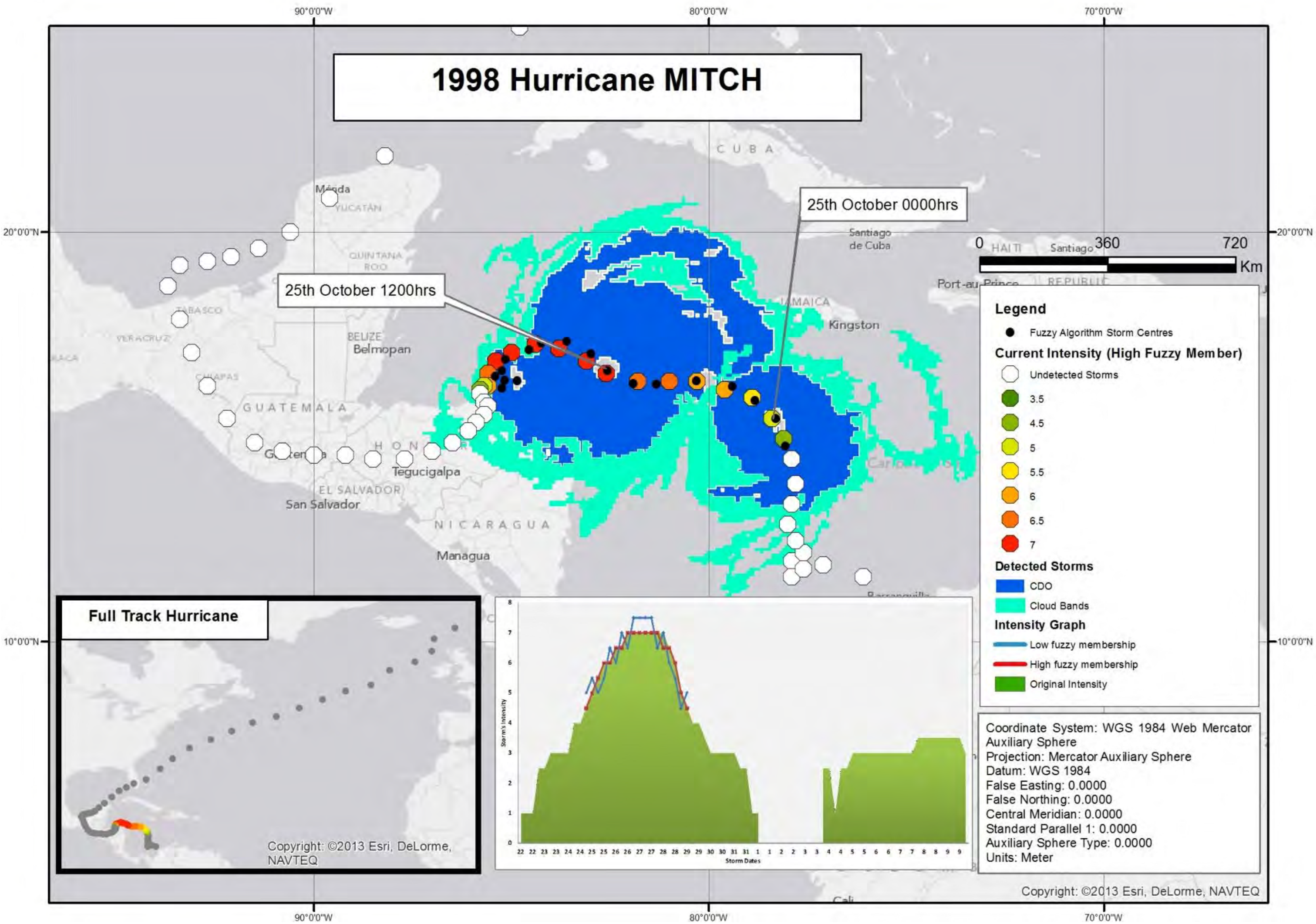

1998 Hurricane MITCH
25th October 0000hrs
25th October 1200hrs
0 360 720 Km
Legend
Fuzzy Algorithm Storm Centres
Current Intensity (High Fuzzy Member)
Undetected Storms
3.5
4.5
5
5.5
6
6.5
7
Detected Storms
CDO
Cloud Bands
Intensity Graph
Low fuzzy membership
High fuzzy membership
Original Intensity
Full Track Hurricane
Copyright: ©2013 Esri, DeLorme, NAVTEQ
Coordinate System: WGS 1984 Web Mercator Auxiliary Sphere
Projection: Mercator Auxiliary Sphere
Datum: WGS 1984
False Easting: 0.0000
False Northing: 0.0000
Central Meridian: 0.0000
Standard Parallel 1: 0.0000
Auxiliary Sphere Type: 0.0000
Units: Meter
Copyright: ©2013 Esri, DeLorme, NAVTEQ
90°0'0"W
80°0'0"W
70°0'0"W
20°0'0"N
10°0'0"N

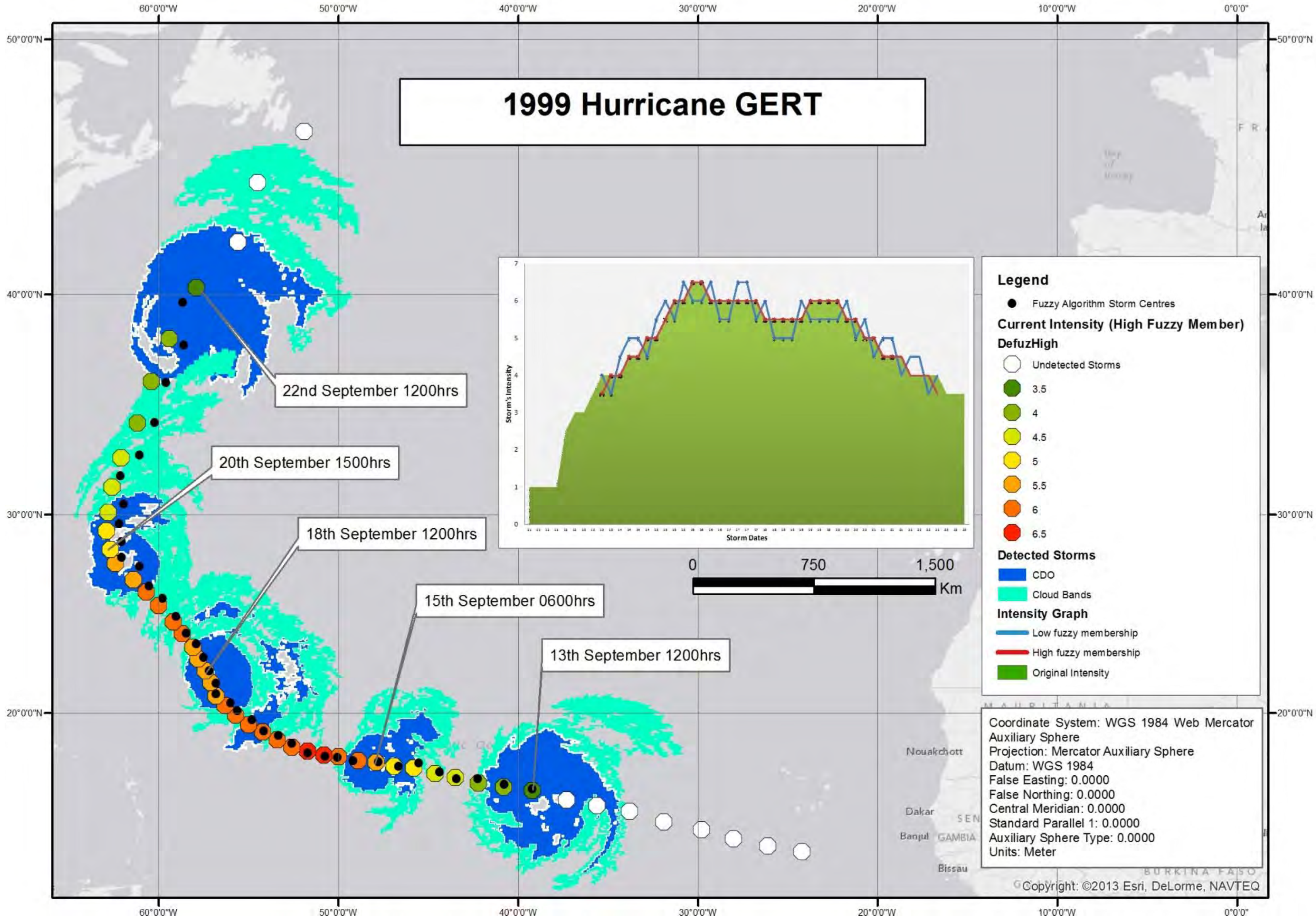

1999 Hurricane GERT
22nd September 1200hrs
20th September 1500hrs
18th September 1200hrs
15th September 0600hrs
13th September 1200hrs
Legend
Fuzzy Algorithm Storm Centres
Current Intensity (High Fuzzy Member)
DefuzHigh
Undetected Storms
3.5
4
4.5
5
5.5
6
6.5
Detected Storms
CDO
Cloud Bands
Intensity Graph
Low fuzzy membership
High fuzzy membership
Original Intensity
Storm's Intensity
Storm Dates
0
750
1,500
Km
Coordinate System: WGS 1984 Web Mercator Auxiliary Sphere
Projection: Mercator Auxiliary Sphere
Datum: WGS 1984
False Easting: 0.0000
False Northing: 0.0000
Central Meridian: 0.0000
Standard Parallel 1: 0.0000
Auxiliary Sphere Type: 0.0000
Units: Meter
Copyright: ©2013 Esri, DeLorme, NAVTEQ
Nouakchott
Dakar
Banjul
Bissau
60°0'0"W
50°0'0"W
40°0'0"W
30°0'0"W
20°0'0"W
10°0'0"W
0°0'0"
50°0'0"N
40°0'0"N
30°0'0"N
20°0'0"N

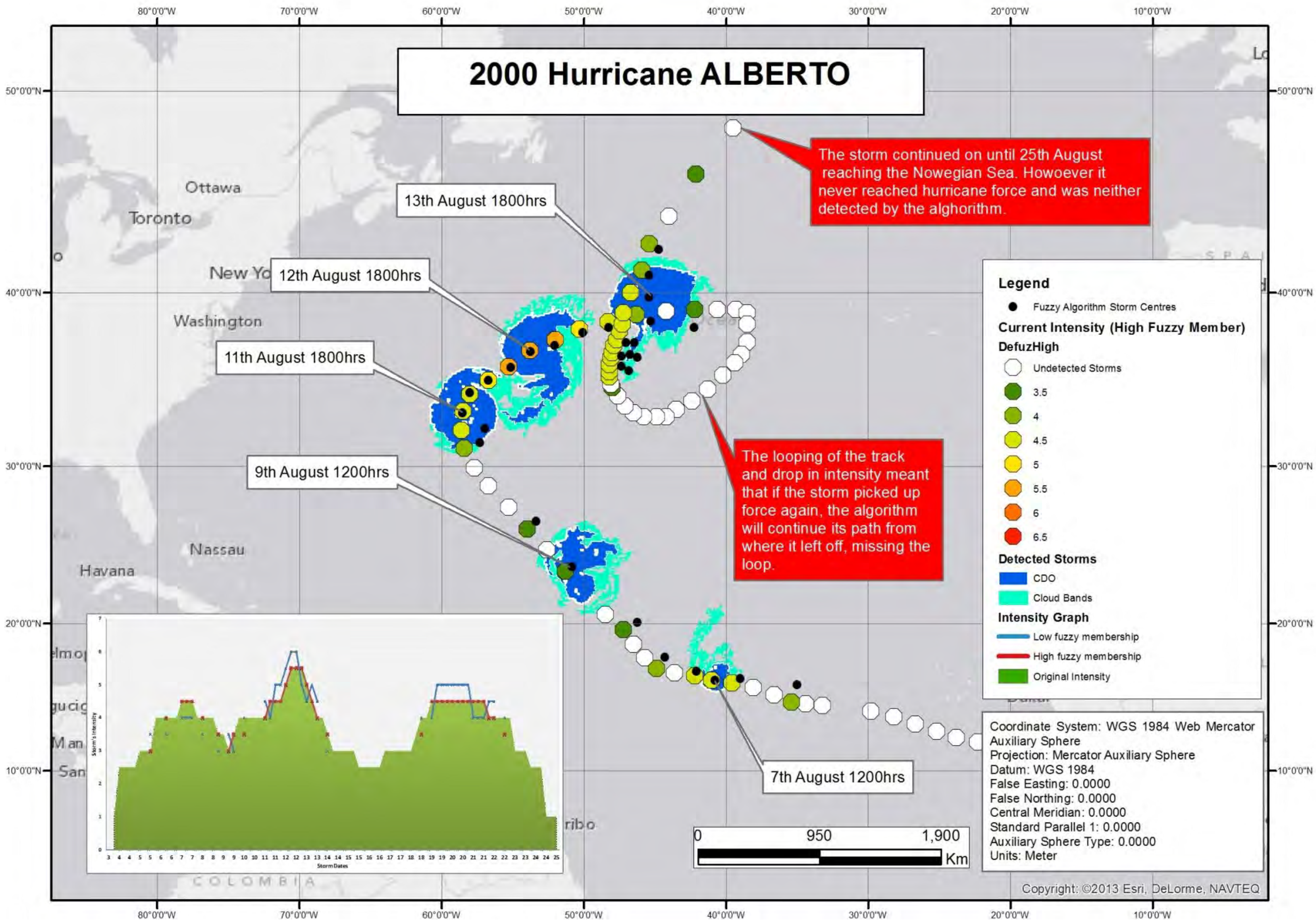
2000 Hurricane ALBERTO
The storm continued on until 25th August reaching the Nowegian Sea. Howoever it never reached hurricane force and was neither detected by the alghorithm.
13th August 1800hrs
12th August 1800hrs
11th August 1800hrs
9th August 1200hrs
7th August 1200hrs
The looping of the track and drop in intensity meant that if the storm picked up force again, the algorithm will continue its path from where it left off, missing the loop.
Ottawa
Toronto
Washington
Nassau
Havana
Legend
Fuzzy Algorithm Storm Centres
Current Intensity (High Fuzzy Member)
DefuzHigh
Undetected Storms
3.5
4
4.5
5
5.5
6
6.5
Detected Storms
CDO
Cloud Bands
Intensity Graph
Low fuzzy membership
High fuzzy membership
Original Intensity
Coordinate System: WGS 1984 Web Mercator Auxiliary Sphere
Projection: Mercator Auxiliary Sphere
Datum: WGS 1984
False Easting: 0.0000
False Northing: 0.0000
Central Meridian: 0.0000
Standard Parallel 1: 0.0000
Auxiliary Sphere Type: 0.0000
Units: Meter
0
950
1,900
Km
Copyright: ©2013 Esri, DeLorme, NAVTEQ

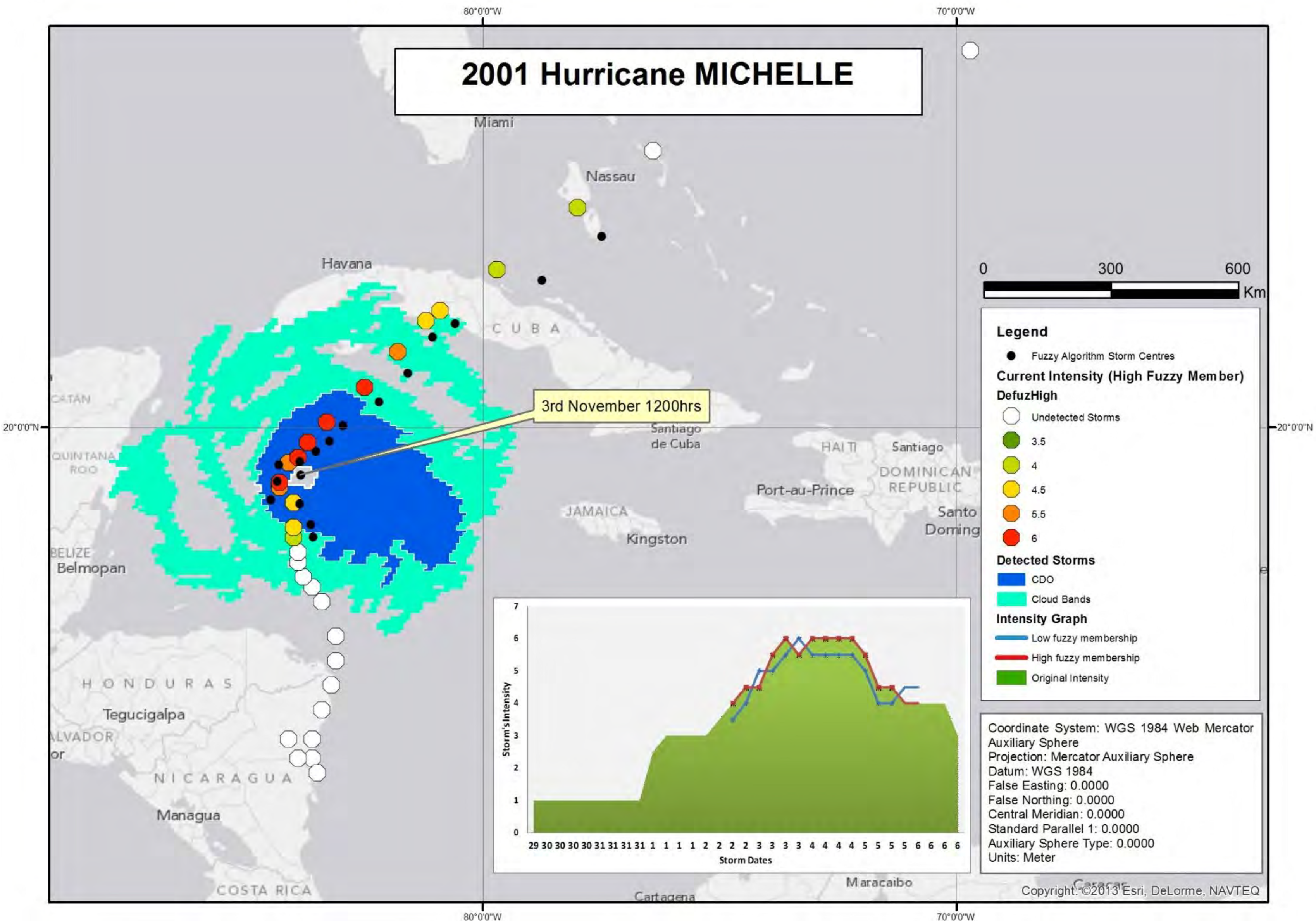

2001 Hurricane MICHELLE
80°0'0"W
70°0'0"W
20°0'0"N
Miami
Nassau
Havana
CUBA
Santiago de Cuba
HAITI
Santiago
DOMINICAN REPUBLIC
Port-au-Prince
Santo Doming
JAMAICA
Kingston
BELIZE
Belmopan
HONDURAS
Tegucigalpa
NICARAGUA
Managua
COSTA RICA
Cartagena
Maracaibo
3rd November 1200hrs
0 300 600 Km
Legend
Fuzzy Algorithm Storm Centres
Current Intensity (High Fuzzy Member)
DefuzHigh
Undetected Storms
3.5
4
4.5
5.5
6
Detected Storms
CDO
Cloud Bands
Intensity Graph
Low fuzzy membership
High fuzzy membership
Original Intensity
Storm's Intensity
Storm Dates
Coordinate System: WGS 1984 Web Mercator Auxiliary Sphere
Projection: Mercator Auxiliary Sphere
Datum: WGS 1984
False Easting: 0.0000
False Northing: 0.0000
Central Meridian: 0.0000
Standard Parallel 1: 0.0000
Auxiliary Sphere Type: 0.0000
Units: Meter
Copyright: ©2013 Esri, DeLorme, NAVTEQ

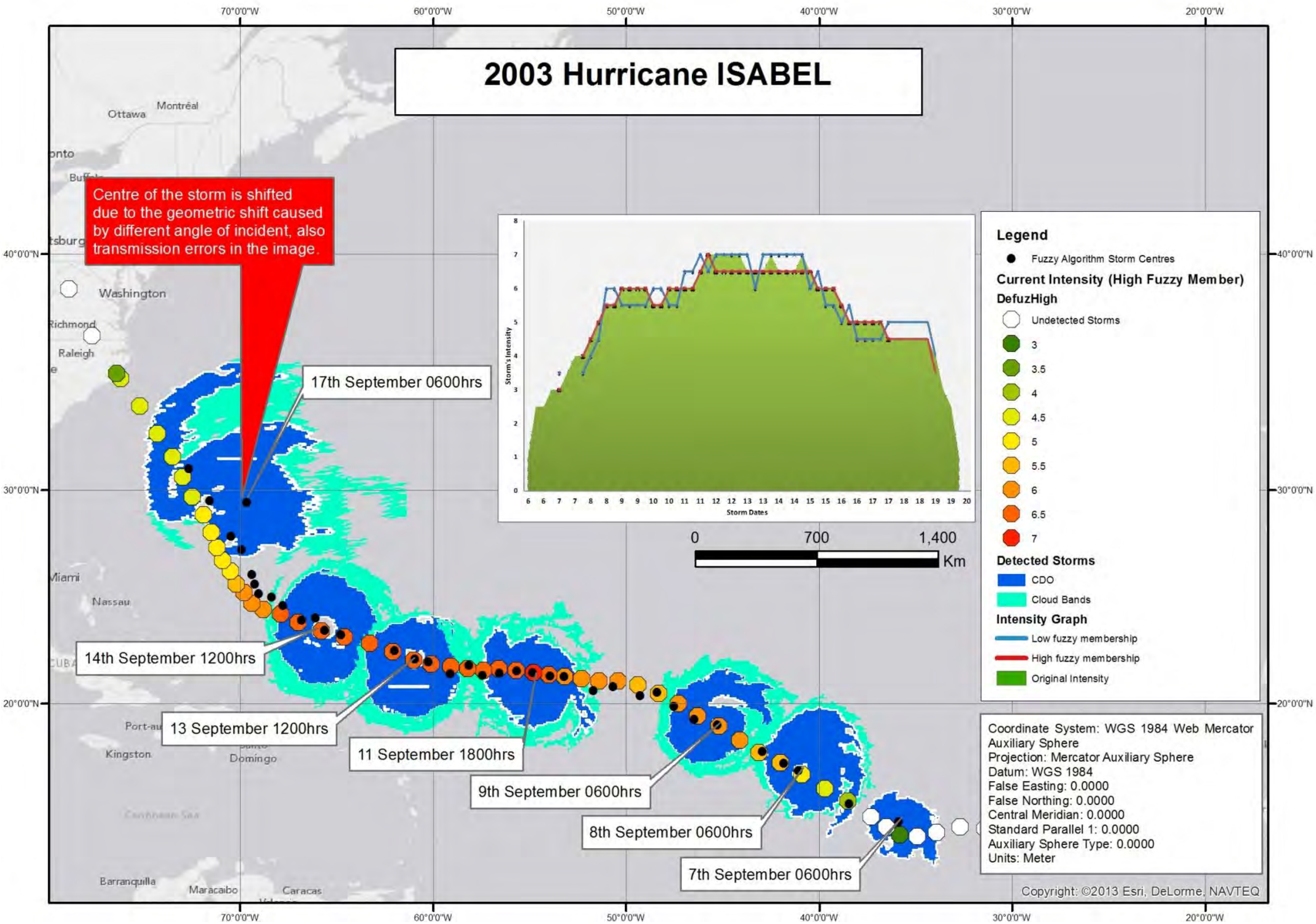

2003 Hurricane ISABEL
Centre of the storm is shifted due to the geometric shift caused by different angle of incident, also transmission errors in the image.
17th September 0600hrs
14th September 1200hrs
13 September 1200hrs
11 September 1800hrs
9th September 0600hrs
8th September 0600hrs
7th September 0600hrs
Storm Dates
0
700
1,400
Km
Legend
Fuzzy Algorithm Storm Centres
Current Intensity (High Fuzzy Member)
DefuzHigh
Undetected Storms
3
3.5
4
4.5
5
5.5
6
6.5
7
Detected Storms
CDO
Cloud Bands
Intensity Graph
Low fuzzy membership
High fuzzy membership
Original Intensity
Coordinate System: WGS 1984 Web Mercator Auxiliary Sphere
Projection: Mercator Auxiliary Sphere
Datum: WGS 1984
False Easting: 0.0000
False Northing: 0.0000
Central Meridian: 0.0000
Standard Parallel 1: 0.0000
Auxiliary Sphere Type: 0.0000
Units: Meter
Copyright: ©2013 Esri, DeLorme, NAVTEQ
70°0'0"W
60°0'0"W
50°0'0"W
40°0'0"W
30°0'0"W
20°0'0"W
40°0'0"N
30°0'0"N
20°0'0"N
Ottawa
Montréal
Washington
Richmond
Raleigh
Miami
Nassau
Kingston
Barranquilla
Maracaibo
Caracas

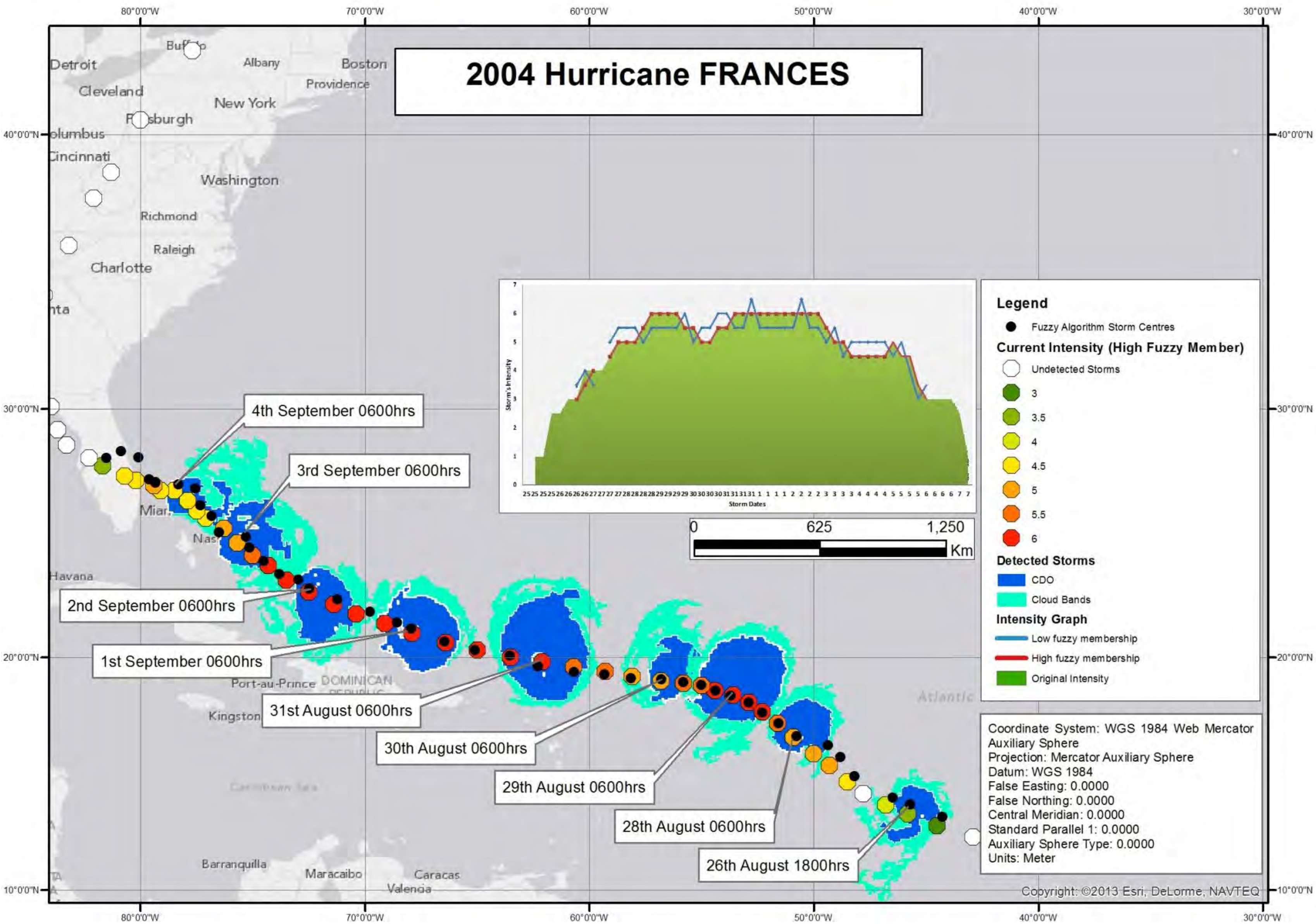

2004 Hurricane FRANCES
4th September 0600hrs
3rd September 0600hrs
2nd September 0600hrs
1st September 0600hrs
31st August 0600hrs
30th August 0600hrs
29th August 0600hrs
28th August 0600hrs
26th August 1800hrs
Legend
Fuzzy Algorithm Storm Centres
Current Intensity (High Fuzzy Member)
Undetected Storms
3
3.5
4
4.5
5
5.5
6
Detected Storms
CDO
Cloud Bands
Intensity Graph
Low fuzzy membership
High fuzzy membership
Original Intensity
Storm Dates
0
625
1,250
Km
Coordinate System: WGS 1984 Web Mercator Auxiliary Sphere
Projection: Mercator Auxiliary Sphere
Datum: WGS 1984
False Easting: 0.0000
False Northing: 0.0000
Central Meridian: 0.0000
Standard Parallel 1: 0.0000
Auxiliary Sphere Type: 0.0000
Units: Meter
Copyright: ©2013 Esri, DeLorme, NAVTEQ

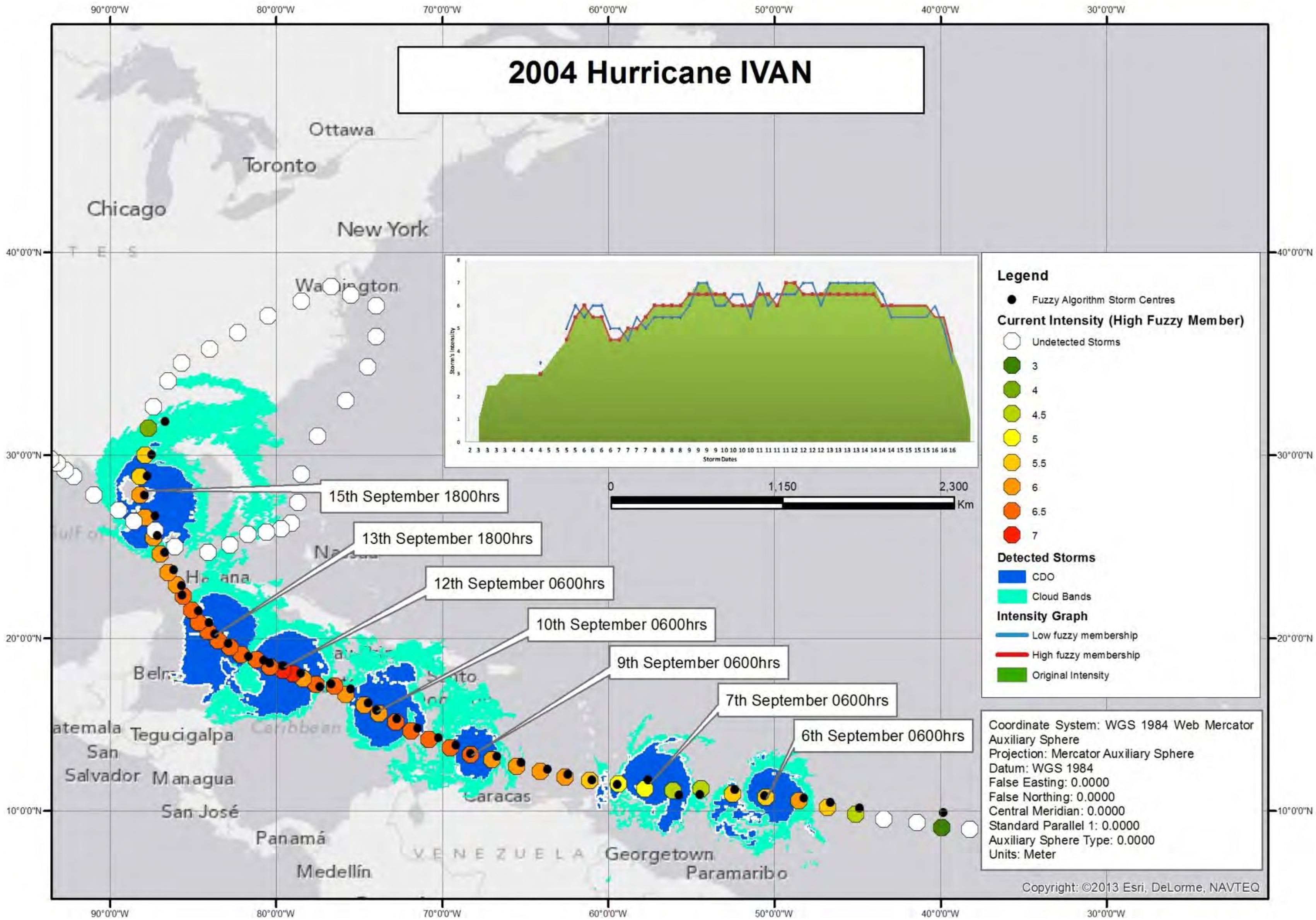
2004 Hurricane IVAN
15th September 1800hrs
13th September 1800hrs
12th September 0600hrs
10th September 0600hrs
9th September 0600hrs
7th September 0600hrs
6th September 0600hrs
Legend
Fuzzy Algorithm Storm Centres
Current Intensity (High Fuzzy Member)
Undetected Storms
3
4
4.5
5
5.5
6
6.5
7
Detected Storms
CDO
Cloud Bands
Intensity Graph
Low fuzzy membership
High fuzzy membership
Original Intensity
Coordinate System: WGS 1984 Web Mercator Auxiliary Sphere
Projection: Mercator Auxiliary Sphere
Datum: WGS 1984
False Easting: 0.0000
False Northing: 0.0000
Central Meridian: 0.0000
Standard Parallel 1: 0.0000
Auxiliary Sphere Type: 0.0000
Units: Meter
0
1,150
2,300
Km
Copyright: ©2013 Esri, DeLorme, NAVTEQ
Storm Dates
90°0'0"W
80°0'0"W
70°0'0"W
60°0'0"W
50°0'0"W
40°0'0"W
30°0'0"W
40°0'0"N
30°0'0"N
20°0'0"N
10°0'0"N

APPENDIX III – GLOSSARY

Term	Definition
Soft Computing	Soft computing is a field of computer science where, unlike hard computing, it can deal with uncertainties and inexact solutions to real world problems.
Fuzzy Logic	A form or mathematics and computer science, in which a classified object assumes a continuum of membership values between 0 and 1.
Tropical Cyclone	An intense low pressure system forming over tropical oceans with high sustained winds. Normally originates in the Indian ocean and Australasian waters.
Typhoon	An intense low pressure system forming over tropical oceans of Pacific ocean.
Hurricane	An intense low pressure system forming over Atlantic ocean.
Rule Based Approach	Logical programming paradigm consists of logical statements based of facts translated in form of conditional rules.
Linguistic Methods	A logical problem solving approach, which uses a combination of syntax and semantics to generate a language grammar.
Index of Goodness-of-fit	The goodness-of-fit is a statistical test to match the modelling results with the observational data.
Hedges	Hedge is a moderating word used to lessen the impact of statement.
Knowledge Base	A repository of data and facts that can be mined and processed.
Image Smoothing Filter	A statistical method and an approximation function that can extract principal patterns in the data by diluting the extreme pixel values.
Chain Coding	Chain coding is a compression algorithm based on hierarchical reasoning where data in the image

	can be reduced by defining boundaries in the data.
Density Slicing	An image classification algorithm that groups the data into classes by using a defined threshold interval.
Line Thinning Algorithm	A line thinning algorithm is a generalisation algorithm where a number of points/vertices on the lines are selected to be removed using a mathematical algorithm.
Commission Errors	A type of an error when a system recognises an object erroneously when it shouldn't have.
Omission Errors	A type of an error when a system fails to recognise an object, when it was clearly present.